National Library
of Canada

Acquisitions and
Bibliographic Services Branch

395 Wellington Street
Ottawa, Ontario
K1A 0N4

Bibliothèque nationale
du Canada

Direction des acquisitions et
des services bibliographiques

395, rue Wellington
Ottawa (Ontario)
K1A 0N4

Your file Votre reference

Our file Notre reference

NOTICE

The quality of this microform is heavily dependent upon the quality of the original thesis submitted for microfilming. Every effort has been made to ensure the highest quality of reproduction possible.

If pages are missing, contact the university which granted the degree.

Some pages may have indistinct print especially if the original pages were typed with a poor typewriter ribbon or if the university sent us an inferior photocopy.

Reproduction in full or in part of this microform is governed by the Canadian Copyright Act, R.S.C. 1970, c. C-30, and subsequent amendments.

AVIS

La qualité de cette microforme dépend grandement de la qualité de la thèse soumise au microfilmage. Nous avons tout fait pour assurer une qualité supérieure de reproduction.

S'il manque des pages, veuillez communiquer avec l'université qui a conféré le grade.

La qualité d'impression de certaines pages peut laisser à désirer, surtout si les pages originales ont été dactylographiées à l'aide d'un ruban usé ou si l'université nous a fait parvenir une photocopie de qualité inférieure.

La reproduction, même partielle, de cette microforme est soumise à la Loi canadienne sur le droit d'auteur, SRC 1970, c. C-30, et ses amendements subséquents.

Canada

GEOLOGY OF THE B-BASELINE ZONE, WALTON BA-CU-PB-ZN-AG DEPOSIT, NOVA SCOTIA

by

Martin David Burtt
(Ottawa-Carleton Geoscience Centre)

A thesis submitted to the School of Graduate Studies
in partial fulfillment of the requirements
for the degree of
Master of Science in Earth Sciences

University of Ottawa
Ottawa, Canada

ISBN 0-612-07839-6

UNIVERSITÉ D'OTTAWA
UNIVERSITY OF OTTAWA

Master of Science
(Earth Sciences)

University of Ottawa
Ottawa, Ontario

TITLE: Geology of the B-baseline zone, Walton Ba-Cu-Pb-Zn-Ag deposit, Nova Scotia

AUTHOR: MARTIN DAVID BURTT B.Sc. (Queen's University)

SUPERVISOR: Dr. D. F. Sangster

NUMBER OF PAGES: xv,116,A47

EXAMINING COMMITTEE: Dr. K. Hattori (Chair)
Dr. G. R. Dix
Dr. A. D. Fowler

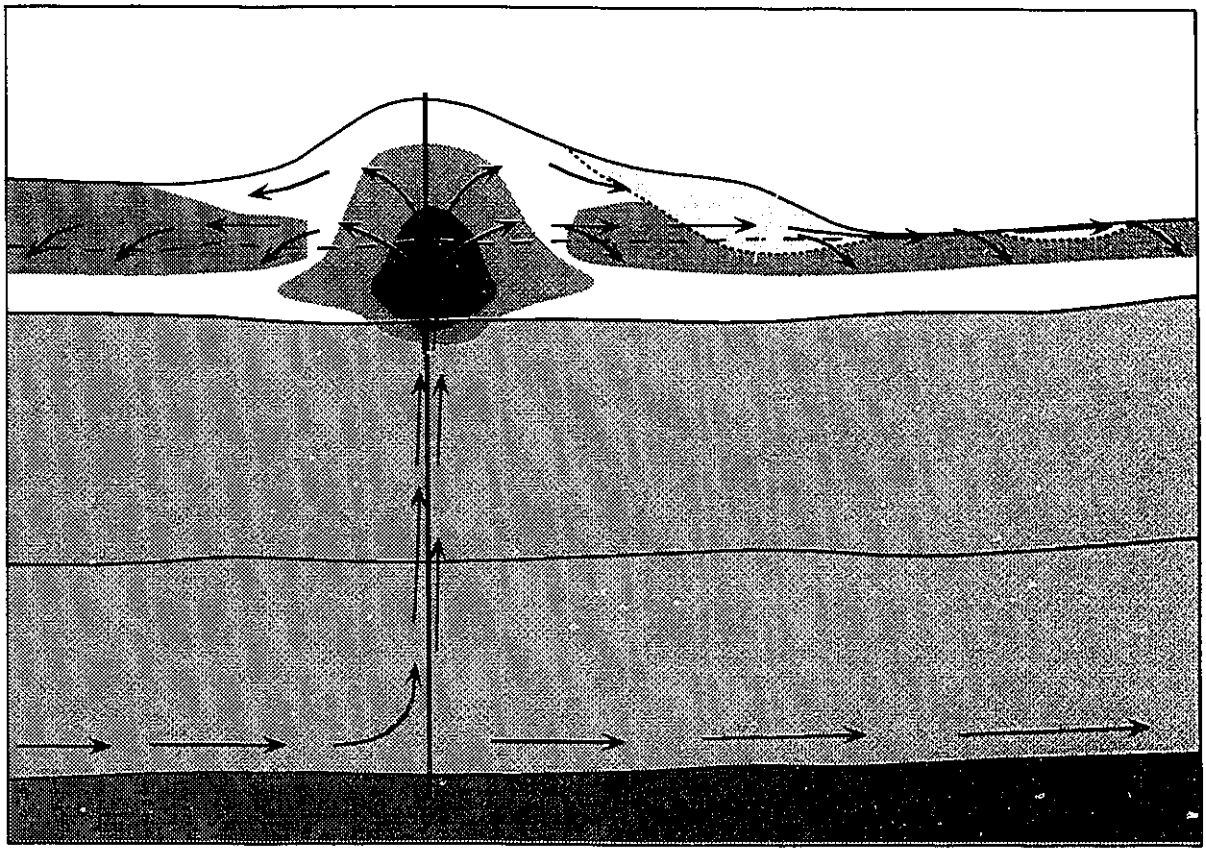

Schematic cross-section of the B-baseline showing proposed path of fluid flow and the relationship of the ore types. See Figure 7-6 for details.

ABSTRACT

The Walton Ba-Cu-Pb-Zn-Ag deposit, Nova Scotia (production 4.5 Mt >90% $BaSO_4$ and 412,850t @ 0.52% Cu, 4.28% Pb, 1.29% Zn, and 350g/t Ag), is hosted by Viséan-aged carbonate rocks of the Macumber Formation and its associated breccia. The Macumber Formation in the Walton area is divided into two units, the lower Macumber, a laminated carbonate 30-40' thick and the upper Macumber, a synsedimentary slump breccia that forms two mounds up to 70' thick.

Outside the immediate mine area the carbonate is either limestone or dolostone; the Macumber Formation surrounding the deposit has been altered by hydrothermal fluids to manganiferous siderite. In general the upper Macumber has lower $FeCO_3$:$MgCO_3$ ratios than the lower Macumber and a slightly higher manganese content. Although three textural types of siderite were recognized, little variation in composition is evident among them.

Mineralisation formed in the sequence: barite, pyrite/marcasite, sphalerite, galena, tennantite, chalcopyrite and (para)rammelsbergite followed by a second generation of siderite, barite, tennantite and chalcopyrite. Each mineral replaces earlier minerals to varying degrees.

Based on barite and metal content two main ore types were defined. Type I comprises barite and variable sulphide contents, whereas Type II comprises only sulphides. Further subdivision of both types can be made into Cu-rich ore and Pb-rich ore. Type I ore forms a stratiform sheet which straddles the upper Macumber/lower Macumber contact and contains lenses of Pb-rich and Cu-rich ore. Type II ore is most commonly associated with the upper Macumber mounds where it forms a large pod which cuts the Type I ore zone. Type II ore also occurs within the underlying Horton sandstones, but only below the upper Macumber mounds. Type I ore has a lower average copper content and higher average lead, zinc and silver contents than Type II ore. There is also a stratigraphic zonation in metal content

inasmuch as all metals are higher, on average, in the lower Macumber relative to the upper Macumber.

The host stratigraphy is presently steeply dipping and faulted, both of which are considered to be post-ore events. Karsting, which also post-dates mineralisation and probably folding, has removed portions of the stratigraphically upper parts of the deposit. The cavity produced by this process is now partially filled with sand and limestone breccia.

The Walton deposit probably formed when uplift of the Cobequid Highlands in the late Namurian initiated gravity-driven flow of basinal fluids through a basal aquifer within the Horton Bluff Formation. The hot fluids flowed south toward the basin margin and leached salts and metals from the aquifer. In the Walton area these fluids were released, along faults, into the overlying Macumber carbonate and synsedimentary carbonate breccia, replacing them initially with manganiferous siderite. Continued fluid flow was primarily laterally through the porous upper Macumber and from there downward into the lower Macumber. Barite replaced the siderite and was in turn replaced by pyrite, sphalerite, galena, tennantite and chalcopyrite, each of which replaced earlier phases. Near the faults, the barite sheet straddling the lower Macumber/upper Macumber contact was removed by the later fluids and replaced by a discordant copper-rich pod.

RÉSUMÉ

Le gisement Ba-Cu-Pb-Zn-Ag de Walton en Nouvelle-Écosse (production de 4,5 Mt >90% $BaSO_4$ et 412 850t à 0,525 Cu, 4,28% Pb, 1,29% Zn et 350g/t Ag), est situé dans les carbonates d'âge Viséen appartenant à la Formation de Macumber et par la brèche associée à celle-ci. Dans la région de Walton, la Formation de Macumber est divisée en deux unités: le Macumber inférieur, constitué de carbonates laminés de 30 à 40 pieds d'épaisseur, et le Macumber supérieur, constitué d'une brèche de glissement syn-sédimentaire formant deux monticules atteignant 70 pieds d'épaisseur.

A l'extérieur de l'environnement immédiat de la mine, les carbonates sont des calcaires et des dolomies; en périphérie du gisement, la Formation de Macumber a été altérée en sidérite manganésifère par des fluides hydrothermaux. En général, le Macumber supérieur possède un rapport Fe_2O_3:$MgCO_3$ moins élevé que le Macumber inférieur et une teneur en manganèse légèrement supérieure. Bien que trois types texturaux de sidérite aient été reconnus, la variation en composition entre eux est minimale.

La minéralisation a suivi la séquence suivante: barytine, pyrite/marcasite, sphalérite, galène, tennantite, chalcopyrite et (para)rammelsbergite, succédée par une seconde génération de sidérite, barytine, tennantite et chalcopyrite. Chaque minéral remplace les minéraux précédents à des degrés variables.

Deux types principaux de minerai ont été définis selon le contenu en barytine et en métaux: le Type I comprend de la barytine et des teneurs variables en sulfures, tandis que le Type II ne contient que des sulfures. Une subdivision supplémentaire peut être faite entre le minerai riche en Cu et celui riche en Pb. Le minerai de Type I forme une couche stratiforme qui chevauche le contact entre le Macumber supérieur et le Macumber inférieur et contient des masses lenticulaires de minerai riche en Pb et en Cu. Le minerai de Type II est le plus fréquemment associé aux monticules du Macumber supérieur où il forme une large masse minéralisée qui recoupe la zone de minerai de Type I. Le minerai de Type II se présente aussi

à l'intérieur des grès sous-jacents de la Formation Horton, mais seulement en-dessous des monticules du Macumber supérieur. Le minerai de Type I possède des teneurs moyennes en Cu moins élevées et des teneurs moyennes en Pb, Zn et Ag plus élevées que le minerai de Type II. Une zonalité stratigraphique en teneurs métalliques est aussi reconnue: toutes les teneurs en métaux sont plus élevées, en moyenne, dans le Macumber inférieur que dans le Macumber supérieur.

La sequence stratigraphique hôte est présentement fortement inclinée et faillée, ces deux caractéristiques étant considérées postérieur à la minéralisation. La karstification, qui a suivi la minéralisation et probablement la déformation, a éliminé des portions stratigraphiquement supérieures du gisement. La cavité produite par ce processus est maintentant partiellement remplie de sable et de brèche calcaire.

Le gisement de Walton a probablement été formé lors du soulèvement des Hautes-Terres Cobequid au Namurien tardif. Cet évènement a initié l'écoulement gravitationnel des fluides du bassin le long d'un aquifère basal dans la Formation Horton Bluff. Les fluides chauds se sont écoulés vers le sud et vers la marge du bassin, tout en lessivant les sels et les métaux de l'aquifère. Dans le région de Walton ces fluides se sont épanchés le long de failles, dans les carbonates Macumber et les brèches syn-sédimentaires sus-jacents, les remplaçant initialement par la sidérite manganésifère. L'écoulement de fluides a principalement procédé latéralement à travers les couches poreuses du Macumber supérieur et s'est poursuivi dans les strates sous-jacentes du Macumber inférieur. La barytine a remplaçé la sidérite qui a été à son tour remplacée par la pyrite, sphalérite, galène, tennantite et chalcopyrite, chaque minéral remplaçant des phases antérieures. A proximité des failles, la couche de barytine chevauchant le contact Macumber inférieur/Macumber supérieur a été lessivée par les fluides subséquents et remplacée par une masse minéralisée discordante riche en cuivre.

ACKNOWLEDGEMENTS

I would like to thank Don Sangster for inviting me to undertake this project, for freely sharing his knowledge and wisdom in economic geology and many other fields, for his red pen which greatly improved the text of this thesis, and for his patience and encouragement when it was needed.

Also from the GSC, I would like to thank John Stirling for his assistance with the microprobe analysis; Richard Lancaster for his assistance with sample preparation, photography, and microscopy; and François Robert for reviewing the French abstract.

A field trip in Nova Scotia, with Dan Kontak and Bob Boehner of the Nova Scotia Dept. of Natural Resources, Don Black, consulting geologist, Truro, Nova Scotia, Reg Moore of Acadia University and Denis Lavois of Centre Géoscientifique de Québec, greatly contributed to my understanding of Nova Scotia geology, as did discussions with Avarid Hudgins, consulting geologist, Truro, Nova Scotia. Jim Langille and the staff of the Nova Scotia Dept. of Natural Resources Drill Core Library in Stellarton were most helpful. Bruce Dunlop is thanked for permission to work on the Walton mine property. Bruce Hudgins of Hudgtec Consulting Ltd., Dartmouth, Nova Scotia produced the original contour maps of the Walton stratigraphy.

My friends from Queen's Geology were a great source of encouragement and provided welcome relief from the real world. In particular, I thank Anne Sherman for translating the abstract and Natalie Sweet for being in Ottawa.

This study was funded by a Canada-Nova Scotia Co-operation Agreement on Mineral Development.

Finally, I would like to thank my family for their continuing support, both moral and financial.

TABLE OF CONTENTS

CHAPTER 3

GEOLOGY OF THE B-BASELINE

CHAPTER 4

ORE PETROGRAPHY

CHAPTER 5

MINERAL CHEMISTRY

CHAPTER 6

ORE TYPE CLASSIFICATION

CHAPTER 7

DISCUSSION, GENESIS, AND EXPLORATION GUIDELINES

CHAPTER 8

SUMMARY AND CONCLUSIONS

LIST OF FIGURES

LIST OF TABLES

CHAPTER 1
INTRODUCTION TO THE WALTON DEPOSIT AND SCOPE OF PRESENT STUDY

INTRODUCTION

The Walton deposit is also known as the Magnet Cove Barium Corporation mine and quarry, or the Pembroke quarry, and is located in Hants County, Nova Scotia about 70km northwest of Halifax and 3.5km southwest of the town of Walton (Lat. 45°12'N, Long. 64°03'W; Figure 1-1). The abandoned mine site is accessible from Highway 215 between Walton and Cheverie, via a short private gravel road.

The deposit contains barite and base metal mineralisation hosted by sideritised Macumber Formation limestone. It was the largest producer of ground barite in Canada (Boyle and Jambor, 1966), producing approximately 4.5 million tonnes of >90% $BaSO_4$ between 1941 and 1978 (Patterson, 1987). The sulphide orebodies produced 412,850 tonnes of ore at a head grade of 0.52% Cu, 4.28% Pb, 1.29% Zn and 350 g/T Ag between 1961 and 1973 (Cranstone, 1982).

HISTORY

The Walton deposit was first noted as a small outcrop of impure barite breccia (Fletcher, 1894) only a square metre in size and was referred to by locals as "heavy marble". The outcrop was rediscovered in 1940 by Roscoe Hiltz, a local prospector. At the time, the Canadian Government had asked all gold mining companies to seek deposits of strategic minerals and metals to help the war effort. One of the companies, Springer Sturgeon Gold Mines Limited, sent prospectors to Nova Scotia to investigate the possibility of reviving the manganese mining industry that had existed on a small scale in earlier years

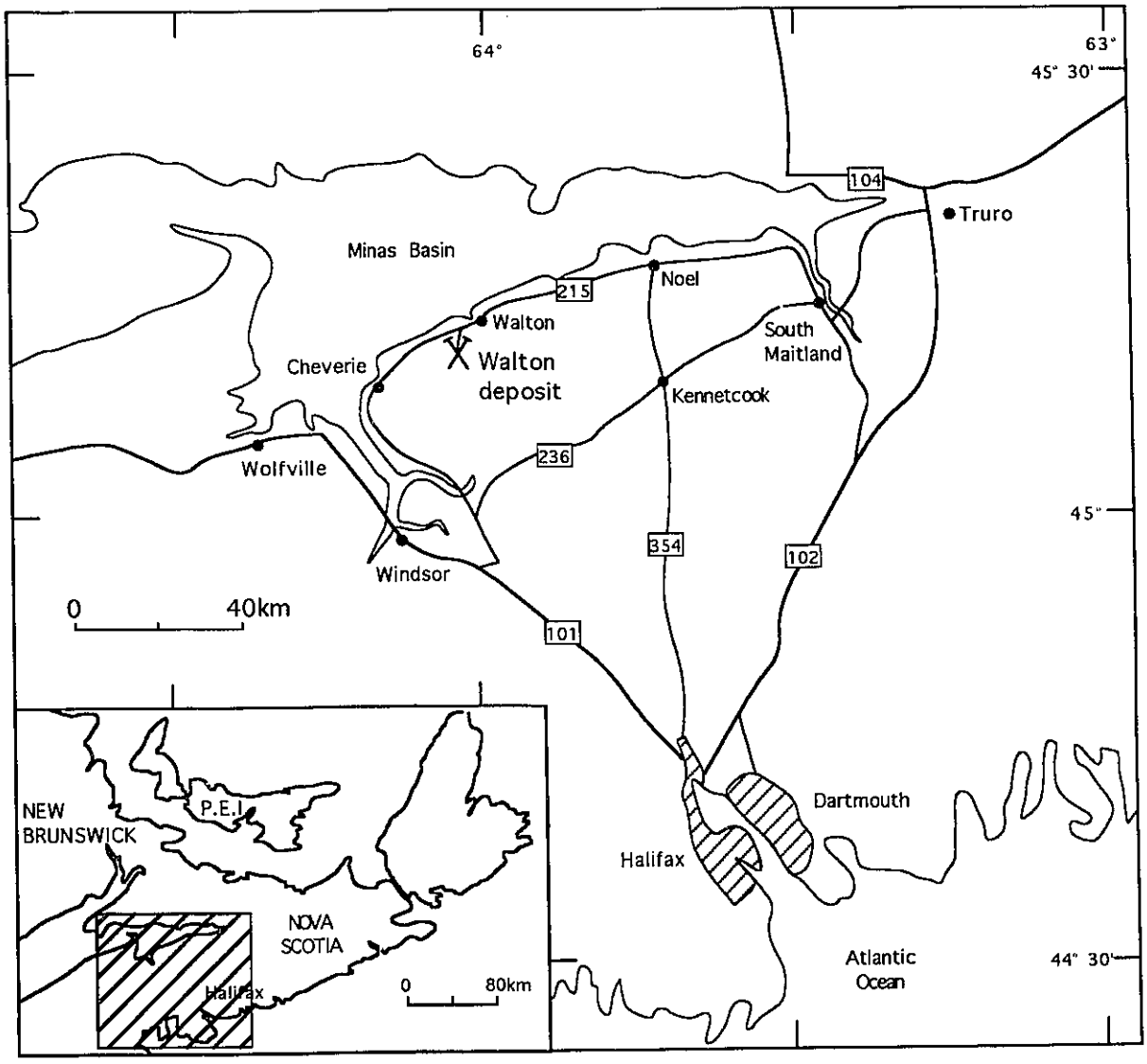

Figure 1-1. Location of the Walton deposit.

(Tenny, 1959). Hiltz brought the barite outcrop to the attention of C. W. McKee, a field engineer for Springer Sturgeon Gold Mines Limited. McKee recommended further exploration, and a drilling program in the fall and winter of 1940-1941 by a newly formed subsidiary company, Canadian Industrial Minerals Ltd., outlined the extent and grade of the orebody. A plant was set up to quarry, process and ship the barite and production began in the spring of 1942.

Mining began as an open pit operation but was soon found to be inadequate so underground development was initiated. A head frame was brought from a northern Ontario gold mine, a shaft was sunk and two levels were driven at 270' and 350' below surface. Underground development had progressed sufficiently by 1947 that about half of the ore was recovered by glory hole operation and half by conventional quarry methods. Ore was shipped by truck from the mine to the mill and dock at the town of Walton, 5km to the north.

In 1955 the property was leased to the Magnet Cove Barium Corporation, a subsidiary of Dresser Industries Inc., of Dallas, Texas. Small quantities of sulphides had been identified in drill core and geochemical surveys revealed that waters issuing from fractures around the quarry were high in zinc and copper content. Diamond drilling in 1956 by the Nova Scotia Department of Mines for Magnet Cove Barium Corporation identified a lead-zinc-silver-copper orebody below the main barite deposit. A mill was constructed at the mine site and production of sulphide concentrates began in 1961. Underground diamond drilling in the mid-1960's delineated a barite and sulphide orebody along the limb of a fold immediately south of the main barite pipe. About half of the base metals were mined from the sulphide zone under the barite pipe and the other half from the barite and sulphide zone south of the main pipe. Mining progressively expanded until 1978 when the mine was closed due to flooding as a result of breaking through the crown pillar.

OBJECTIVES

This study constitutes part of a larger study of Carboniferous-hosted mineralisation in Nova Scotia funded by a Canada-Nova Scotia Co-operation Agreement on Mineral Development (Sangster, 1994). The goal of the larger study is to determine the origin and nature of mineralising fluids in three Carboniferous sedimentary basins; the River Denys basin on Cape Breton Island; the Shubenacadie-Musquodoboit basin in central Nova Scotia; and the Kennetcook basin also in central Nova Scotia. Work in each basin is focused on the largest deposit in that basin; the Jubilee deposit in River Denys basin; the Gays River deposit in Shubenacadie-Musquodoboit basin; and the Walton deposit in Kennetcook basin. The nature of the mineralising fluids in each of the three deposits is being studied to determine if there is a genetic link between the three deposits.

Objectives of this study of the Walton deposit are:

1. To document the geology of the southern barite-sulphide zone, also known as the B-baseline. This includes petrological descriptions of the host rocks, petrographic descriptions of the ore mineral relationships, and metal zoning in the deposit.
2. To suggest a genetic model for the origin of the deposit.
3. To provide the geological groundwork by which the Walton deposit can be compared to deposits in the other two basins.
4. To suggest areas of exploration for further mineralisation of this type.

METHODOLOGY

Due to the flooding of the mine and the scarcity of outcrop in the mine area (less than 1%) this study has been based almost entirely on the study of drill core samples and company analyses. Two hundred and thirty-three underground diamond drill holes were drilled on three levels along the B-baseline, and the core for most of these holes is available at the Nova Scotia Department of Natural Resources Drill Core Library at Stellarton, Nova

Scotia. The logs for these holes are available in Nova Scotia Department of Natural Resources Assessment Report 21H/01D 06-I-51(42).

A suite of 290 samples was selected from the drill core at the Stellarton Drill Core Library. The samples were selected to be representative of each of the lithologies found in the mine and of the various styles of mineralisation. Sampling was difficult due to the intense weathering of the core. A rind of chocolate-coloured alteration products coats all of the core due to weathering of the manganese and iron-rich minerals in the 25-30 years since the holes were drilled. As a result it was necessary to rely on the drill logs to select lithologies in the core. Samples of interest were then sawed in half to reveal a fresh surface.

A total of 5 thin sections and 67 polished thin sections were prepared. A detailed petrographic study was carried out on the thin sections in order to understand the petrogenetic relationships of the minerals and to establish a paragenesis. Mineral chemistry was also determined for most minerals using an electron microprobe.

The second part of the study examined metal zoning in the deposit. Assessment reports contain more than 840 analyses of drill core samples for Cu, Pb, Zn, Ag and $BaSO_4$ content. The analyses and the sample locations were entered in a computer database for each drill hole. The data were then plotted on vertical sections in order to examine patterns in metal zoning and to define a number of ore types. All geological contacts and lithologies were also entered into a database. The geological data were sent to Bruce Hudgins of Hudgtec Consulting Ltd., Dartmouth, Nova Scotia who calculated the position of the lithological contacts above a reference plane in order to produce a series of contour maps showing the thickness of each lithological unit. These contour maps served as the basemaps on which this study was based.

CHAPTER 2
REGIONAL AND DEPOSIT GEOLOGY

REGIONAL GEOLOGY

General Geology of Central Nova Scotia

The stratigraphic succession of Central Nova Scotia represents three main periods of deposition, each followed by regional deformation and erosion.

During the pre-Carboniferous period, the Ordovician Meguma Group and Silurian-Devonian Cobequid complex were formed. The Meguma Group consists of a thick sequence of quartzites and slate folded into northeast-trending, upright structures and metamorphosed to greenschist-amphibolite facies. The Cobequid complex comprises slightly metamorphosed volcanic and sedimentary rocks. Both units were deformed during the mid-Devonian Acadian orogeny and intruded by granites.

Unconformably overlying the pre-Carboniferous rocks are Mississippian and Pennsylvanian sedimentary rocks (Fig. 2-1). Up to 12km of dominantly continental sediments were deposited in pull-apart basins formed by wrench faulting (Belt, 1968). A major marine transgression interrupted the continental sedimentation during the Mississippian and was followed by further continental deposition. These strata were folded during late Palaeozoic regional deformation.

Continental sandstones and conglomerates unconformably covered the Carboniferous sediments during the Late Triassic. These strata have been gently folded and partly eroded.

Little deposition has occurred since the Triassic. Glacial drift and outwash of Pleistocene age covers much of the area today.

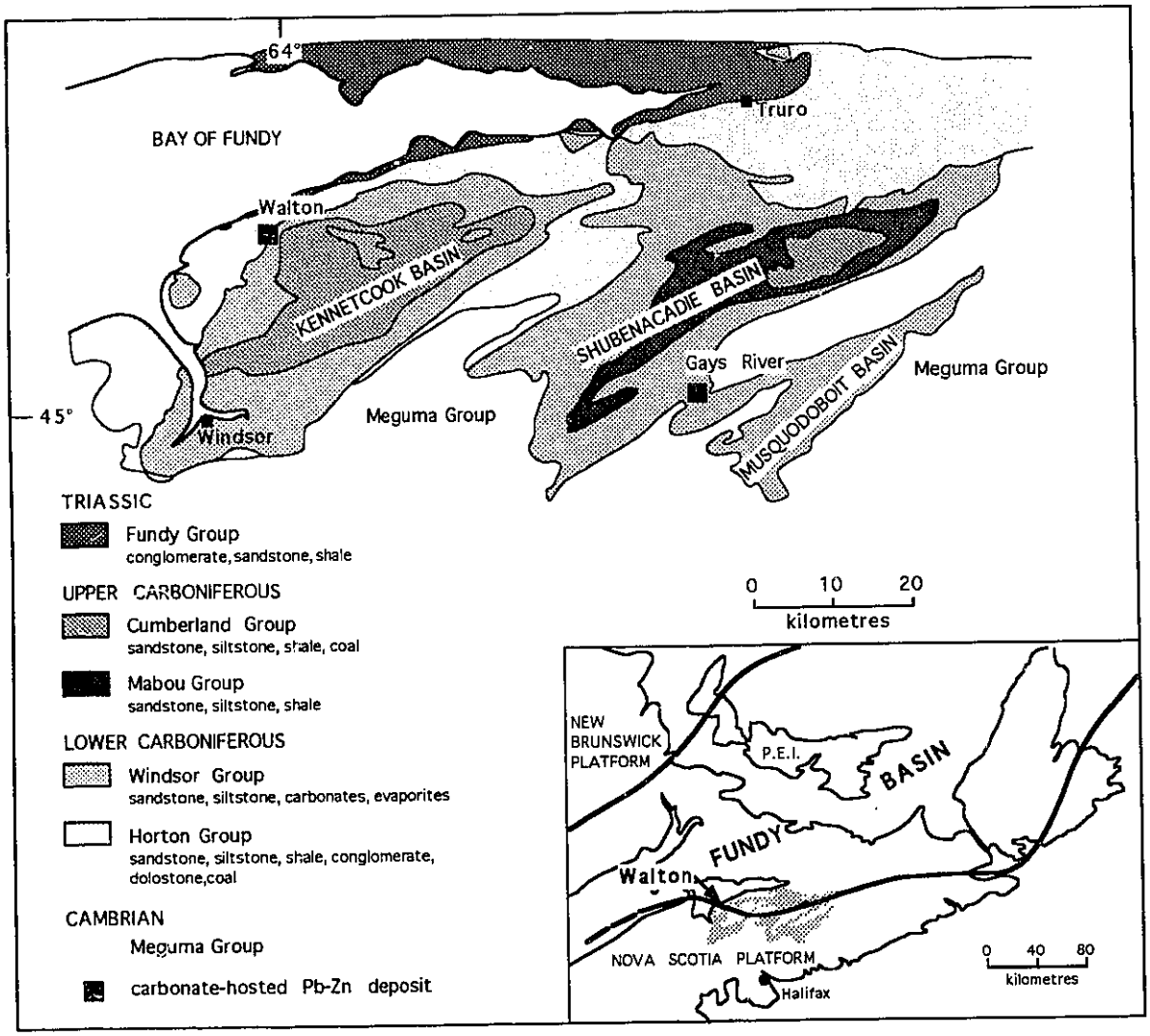

Figure 2-1. Geological map of Kennetcook, Shubenacadie and Musquodoboit basins showing the location of the Walton and Gays River deposits. The inset shows the location of the basins in relation to the Fundy basin. Modified from Kontak (1992).

Kennetcook Basin

The Kennetcook basin is one of several Carboniferous sedimentary basins in Nova Scotia at the southern margin of the large (≥250,000km^2) and deep (>10km) Maritimes (Fundy-Magdalen) Basin. The Kennetcook basin is bounded to the north by the Cobequid-Chedabucto fault system and the Fundy Rift and to the south by the Rawdon fault. The Cobequid-Chedabucto Fault System is an east-west trending dextral wrench fault that was particularly active following the Acadian orogeny (Ravenhurst et al., 1989). The wrench faulting resulted in a series of pull-apart basins that include the Kennetcook, Shubenacadie and Musquodoboit sub-basins. The Fundy Rift is a half-graben that superimposed Mesozoic rocks on the northern margin of the Kennetcook basin (Boehner, 1991). To the south the Kennetcook basin is bordered by the Rawdon Fault which faults rocks of the Meguma Group and, locally, Horton Group against the basin (Boehner, 1991).

Accumulations, up to 12km thick (prior to erosion), of terrestrial and shallow-marine sediment were deposited in the basins. The stratigraphic sequence of these rocks has been divided into the Horton, Windsor, Mabou (formerly Canso), Cumberland, and Pictou Groups (Bell, 1929; Ryan et al., 1991; Moore, 1994). The Mabou Group occurs in the Shubenacadie and Musquodoboit basins but is absent in the Kennetcook basin. Several stratigraphic schemes are presented in Figure 2-2. The sequence used by Boyle (1972) is derived from Weeks (1948) and is the sequence that has been used by most workers in the Walton area. Although Boyle's (1972) sequence has been used in this study it is recognised that the more recent work by Moore (1994) may supersede the earlier system. Lead-zinc and barite deposits in central Nova Scotia occur immediately above the Horton-Windsor contact.

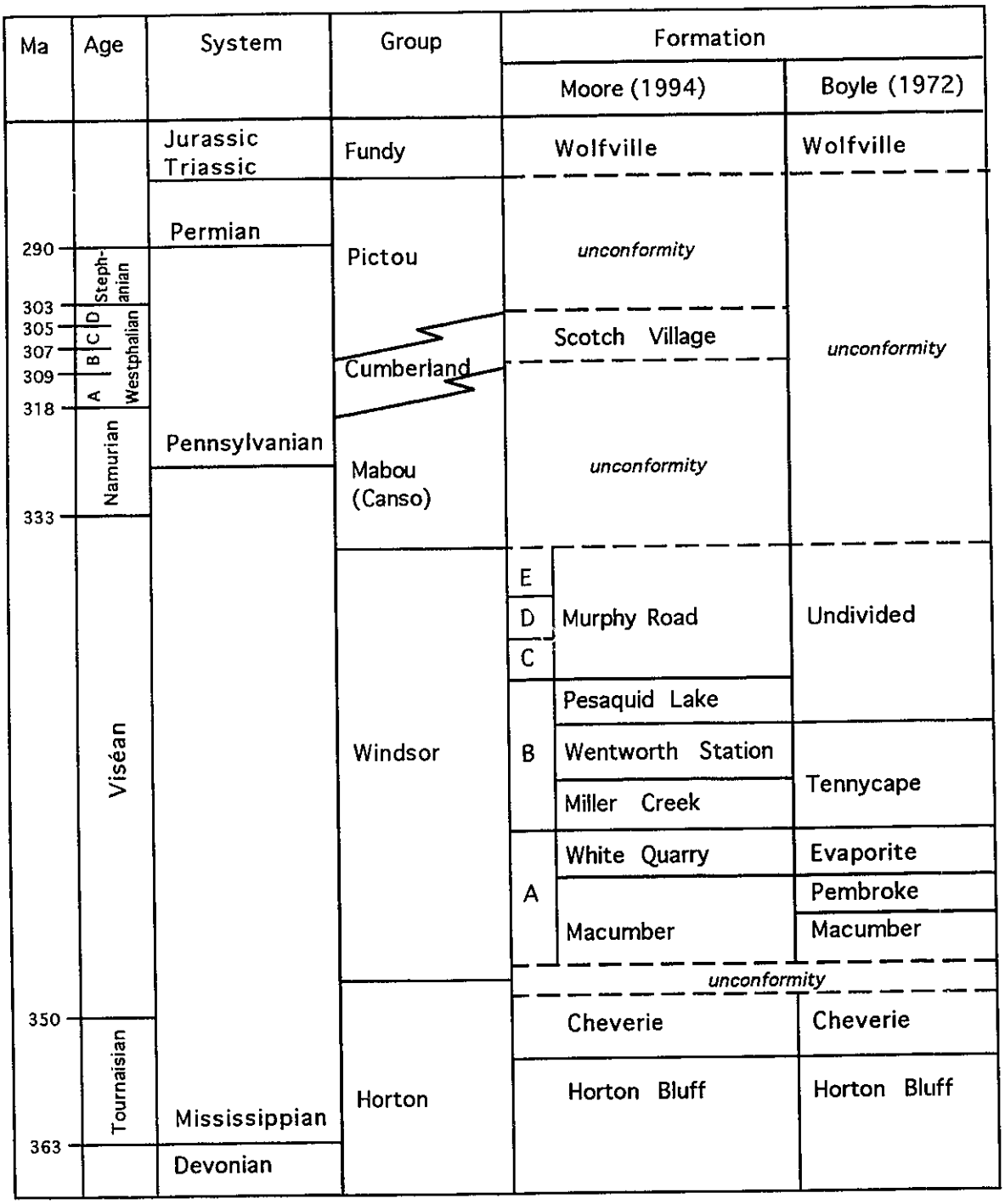

Figure 2-2. Stratigraphic sequences of Boyle (1972) and Moore (1994). Also shown are the Windsor sub-zones A-E of Bell (1929). Boundary ages are from Harland et al. (1990). (Not to scale)

Horton Group

The basal sedimentary unit, the Horton Group of Tournaisian age, overlies pre-Carboniferous basement with angular unconformity. The Horton Group consists of continental sediments that typically vary through fanglomerate, fluvial and estuarine (or lacustrine) facies, including non-marine limestone and evaporite. The thickness of the Horton Group has been estimated to be >4km in the deepest Magdalen Basin (Howie and Barss, 1975) and 1.4km in the Walton area (Moore, 1994). Bell (1929) divided the Horton Group into two formations in the Windsor type area. The lower Horton Bluff Formation, estimated to be 415m thick in the Walton area (Moore, 1994), is composed of argillaceous to arenaceous shales, quartzitic sandstone, quartzite, argillaceous dolomite and feldspathic conglomerate. The upper Cheverie Formation is composed of thick- and thin-bedded, crossbedded sandstones, grits and microconglomerates, interbedded with siltstones, mudstones and shales. The thickness of the Cheverie Formation is estimated to range from 375m near the town of Walton to 775m in the Goshen area (Moore, 1994). In the mine area, there is usually a 3m thick quartz arenite unit at or near the top of the Cheverie Formation (Moore, 1994). Workers in some areas have reported difficulty in distinguishing the two formations of the Horton Group based on lithological characteristics due to scarcity of outcrops and marker units (Weeks, 1948; Stevenson, 1959; Crosby, 1962).

The lower part of the Horton Group is interpreted to represent fluvial deposits accumulated in a humid climate (Bell, 1929; Crosby, 1962). The upper part of the Horton Group probably formed in a series of interconnected, block faulted, continental basins (Schenk, 1969, Kirkham, 1978). Conglomerates formed in proximal alluvial-colluvial fans as a result of high energy currents (Crosby, 1962; Kirkham, 1978) and fluvial deposits formed in more distal areas. The climate became progressively more arid resulting

in subaerial exposure and formation of evaporitic beds and lacustrine deposits (Crosby, 1962; Kirkham, 1978).

Windsor Group

The Windsor Group contains the only major marine sedimentary rocks in the Carboniferous sequence. The unit is typically composed of a 750m to 1000m thick succession of carbonates, evaporites and siltstones of Viséan age. The Macumber Formation is regionally unconformable with the Horton Group, although locally it may appear to be conformable to disconformable, or is unconformable with pre-Mississippian rocks. The Windsor Group has been divided into numerous sub-groups by various workers.

Bell (1929) identified two major zones, each consisting of a number of subzones with its own particular fauna. Subzones A and B are within the lower Windsor and subzones C, D, and E are within the upper Windsor. Weeks (1948) divided the lower Windsor into five formational units (from bottom to top): the Macumber Formation, the *Pembroke Formation*, the Lower Sulphate Bed, the Tennycape Formation and an upper formation (second sulphate bed). In some map areas the Windsor Group rocks above the *Pembroke Formation* are indivisible as mappable units (Stevenson, 1959; Crosby, 1962). Giles (1981) recognised five major cycles of marine transgression and regression in the Windsor Group, the lower boundaries of which coincide with the biostratigraphic subzones of Bell (1929).

Macumber Formation

The Macumber Formation marks the base of the Windsor Group and the first marine transgression into the Magdalen Basin. Lithologically the Macumber Formation is a very finely laminated limestone that is usually about 8m thick although it does range between 0m and 25m in thickness. The description of the Macumber Formation that follows is summarised from Schenk (1967).

A lower unit, Lithosome A, has characteristic laterally continuous, flat laminae, from 5mm to 10mm in thickness. The limestone is composed of small, oval, structureless, micritic pellets that range from 0.05mm to 0.4mm in diameter. Pellets increase in size upwards from the base of the unit as the groundmass changes from micrite to sparite. Individual pellets and groups of pellets are surrounded by thin, spherulitic, coatings up to 3mm thick of from one to four concentric layers. Ostracod carapaces and fragmented brachiopod valves are also present.

Lithosome B always lies immediately above Lithosome A and is a very finely laminated limestone that becomes more dolomitic upward. The laminations occur as couplets less than 5mm thick, each consisting of a thin basal layer and a thicker upper layer. The thin layer usually consists of a bituminous film overlain by dolomite micrite containing quartz silt. The thick layer consists of a medium-grained calcite spar that commonly shows a palisade structure. The lower part of Lithosome B may have a microbreccia texture as the calcite layer is commonly occupied by intraclasts of either eroded upper layers or less commonly Lithosome A. The upper third of Lithosome B is much more dolomitic as the calcite layers occur only as intraclasts.

Schenk (1967) concluded the Macumber Formation is a strandline deposit formed in a very shallow subtidal environment analogous to the modern strandline algal and related carbonates of the Persian Gulf. He suggested the Macumber Formation was the result of a sudden marine invasion followed by slow regression. The resulting shallow subtidal to supratidal carbonate, originally calcitic, was partly dolomitised by the passage of a hypersaline, supratidal environment over the site of deposition.

Geldsetzer (1978) proposed the Macumber Formation to be a cryptalgal laminate deposited in deep water with the scarcity of fauna attributed to hypersalinity that preceded a major evaporite cycle. He cited the widespread distribution, the absence of desiccation cracks, the laterally persistent lamination and the association with a subtidal and possibly

euryhaline fossil assemblage as evidence for subtidal deposition. von Bitter et al. (1990) proposed that the Macumber Formation may be a deep water bacteriolaminate. Moore (1994) also favours a mainly deep water origin with the ooids transported by downslope currents from shallower, higher energy environments. Lavoie and Sangster (1995) also suggest an environment below storm wave base.

Pembroke Breccia

Also occurring at this stratigraphic level is the *Pembroke Breccia*, a chaotic, unsorted mass of angular Macumber limestone fragments and slabs, in calcareous mudstones and sandstones, with scattered pebbles of granite and Horton Group clasts. Fragments of limestone range in size from a few millimetres to several metres. The breccia ranges from 0m to 30m in thickness and always disconformably overlies Macumber limestone. Weeks (1948) named the breccia and cavity fill the *Pembroke Formation*; however use of the term was pre-empted and it was recommended that the name be abandoned (Clifton, 1967). Although the terms *Pembroke Formation* and *Pembroke Breccia* were originally applied to the breccia found in the quarry at Walton, the name has since been applied to any breccia found at the same stratigraphic level in central and eastern Nova Scotia.

The origin of the *Pembroke Formation/Breccia* is controversial. It has been interpreted as a karstic collapse breccia (Clifton, 1967; Geldsetzer, 1977; Smith and Collins, 1979; Lavoie, 1994; Lavoie and Sangster, 1995); a solution collapse breccia (Smith and Collins, 1979); a coarse grained storm deposit (Schenk, 1969); a breccia formed by hydrofracturing during mineralisation (Ravenhurst et al., 1989); a tectonic breccia formed during low angle faulting (Lavoie, 1994; Lavoie and Sangster, 1995); and a synsedimentary slump breccia (Lavoie and Sangster, 1995). Although the term has been applied to breccias at the same stratigraphic interval in many parts of Nova Scotia, it is clear that the breccias may have formed by different mechanisms in different areas. Lavoie

(1994) recognised a karstic breccia overprinting an earlier tectonic breccia in his study of the *Pembroke Formation* at six locations in Nova Scotia.

At the Walton deposit the term *Pembroke Formation/Breccia* was applied by mine workers to both a mottled non-laminated carbonate and a petroliferous limestone breccia. While the petroliferous limestone breccia bears some resemblance to the karstic breccia elsewhere in the region, the mottled non-laminated unit has little resemblance to the *Pembroke Formation/Breccia* in other regions. Lavoie and Sangster (1995, p. 5) advocate a synsedimentary breccia origin for the mottled unit based on six points: "*1) the presence of discrete concave-up shear failure planes; 2) the lack of wave- or current-induced sedimentary structures; 3) the presence of a fine-grained matrix in part derived from background suspension sedimentation; 4) the rounding of clast margins reflecting remobilisation from gravity-driven movement of disrupted beds; 5) the nature of the cyclic succession hosting the breccia showing variable degrees of internal deformation; and 6) the preferred association to the Macumber platy lithofacies, that is deep-water microbial mats*". They suggest rotational sliding as a result of soft sediment slumping on a below wave base slope formed the breccia. Lavoie and Sangster (1995) recommend that the synsedimentary breccia be considered a Macumber breccia.

Evaporite

Where breccias do not occur, the Macumber Formation is conformably overlain by 38 metres of evaporite called the Lower Sulphate Bed (Weeks, 1948). The unit consists of anhydrite, gypsum and minor interbedded calcareous and petroliferous shales. Moore (1994) assigned the evaporite in the Walton area to the White Quarry Formation. The evaporite can also be correlated with the Vinland Formation (Moore and Ryan, 1976), Subzone A gypsum (Bell, 1929), and the Carrolls Corner Formation in the Shubenacadie and Musquodoboit basins (Giles, 1981). Geldsetzer (1978) proposed that stagnation of the

"Windsor Sea" led to extensive precipitation of gypsum, followed by halite and potash salts in some areas.

Tennycape Formation

Weeks (1948) named the soft, red, fine, sandy shales overlying the evaporites the Tennycape Formation. It rests on the evaporite or on the breccia where the evaporite is not present and is approximately 200m thick in the type locality (Weeks, 1948). Weeks (1948) reported that the Tennycape Formation was overlain by a second sulphate bed in its type area.

Moore (1994) reports that the Tennycape Formation is not present in the Walton area, and suggests that what Boyle (1972) shows as Tennycape Formation should be included in the Wentworth Station and/or Murphy Road Formation.

Undivided Windsor

In many map areas it is impossible to subdivide the Windsor Group strata above the Macumber Formation due to lack of outcrops and marker beds (Stevenson, 1959; Crosby, 1962, Boyle, 1972). Crosby (1962) estimated the thickness of the undivided Windsor Group to be 600m.

Post-Windsor Deposition

The Windsor Group rocks in the Kennetcook basin are overlain unconformably by feldspathic sandstones of the upper Carboniferous Scotch Village Formation. The Scotch Village Formation rests on isoclinally and recumbantly folded evaporites and Horton Group sediments with angular unconformity indicating the deformation event occurred between the late Viséan to early Namurian (youngest deformed strata) and late Westphalian B (oldest undeformed strata) (Boehner, 1991).

Triassic sandstones and conglomerates of the Wolfville Formation, Fundy Group overlie Carboniferous sediments with angular unconformity.

THE WALTON DEPOSIT

Previous Work

A number of workers have studied the Walton deposit in detail (Boyle and Jambor, 1966; Boyle, 1972; Boyle et al., 1976; Patterson, 1986, 1987, 1988a,b, 1989) in addition to work by mine staff. The most comprehensive study was conducted by R. W. Boyle whose field investigations of 1957, 1960 and 1961 and subsequent laboratory studies are presented in Boyle and Jambor (1966), Boyle (1972) and Boyle et al. (1976). Boyle's work on the Walton deposit was part of a more regional mineralogical and geochemical study of all mineral occurrences in the Walton-Cheverie area. As the largest deposit and the only operating mine in the study area, Walton was studied in greater detail than the other occurrences. Boyle's work at Walton concentrated on the massive barite pipe and the underlying sulphide zone. Boyle and Jambor (1966) and Boyle (1972) documented the ore mineralogy and geochemistry and suggested a paragenetic sequence and possible origin for the mineralisation.

Patterson (1986, 1987, 1988a,b, 1989) studied the potential for future exploitation of the deposit. Using the original drill core logs he reconstructed sections through the sulphide-rich areas of the deposit and contoured metal values. The remaining work on the deposit is in the form of company reports filed with the Nova Scotia Department of Natural Resources as assessment reports. These reports are generally concerned with the day-to-day operations of the mine but also include many of the original drill core logs.

Additional work on the Walton deposit, including studies of stable isotopes (Sangster et al., 1994), fluid inclusions (Kontak and Sangster, 1994), origin of the breccias (Lavoie and Sangster, 1995; Lavoie et al., 1994), and fluid migration (Sangster and Savard, 1994), is on-going as part of the larger study of which this thesis is a part.

Deposit Geology

The Walton deposit consists of a barite orebody near the surface with more sulphide-rich zones below and south of the main barite orebody. The work of Boyle (1972), Boyle and Jambor (1966), and Boyle et al. (1976) was focused on the main barite orebody and its underlying sulphide zone. The following description of the main zone is summarised from Boyle (1972).

In plan, the barite orebody is a pear-shaped lens at surface that becomes elongated and S-shaped at depth. In longitudinal E-W section it is a pipelike mass that rakes 35° east. In vertical sections the orebody has a lens-like shape, with interfingering extensions into the enclosing sediments. The barite pipe is localised by hanging-wall and footwall faults at the nose of an S-shaped fold. The footwall fault, strikes west and dips at 75°N while the hanging-wall fault, strikes northwest and dips at 70°NE. Both faults are marked by extensive brecciation over several tens of metres. Boyle (1972) states that the faults are pre-ore but provides no evidence to support this. He also notes that brecciation of barite and sulphides suggests post-ore movement of the faults. The sedimentary rocks have been highly contorted and dragged into a broken S-shaped fold creating a dilatant zone which was replaced and partly filled with barite. The replacement was most pervasive in the *Pembroke Formation* and to a lesser degree in the Macumber Formation. The sulphide body, which does not outcrop but comes within 250' of the surface, is an irregular lens that lies within the brecciated zone of footwall fault below the barite pipe and spreads along the southern limb of the fold. The sulphide body represents replacement and fracture filling of a dilatant zone in the Pembroke and Macumber Formations and underlying Cheverie clastic sediments. The carbonate host rocks in the deposit were replaced by siderite and barite in the earliest stages of the mineralising process. Siderite and barite were then replaced or veined by pyrite and marcasite followed by sphalerite, galena, chalcopyrite, tennantite,

proustite, pearceite and stromeyerite in approximately that order. Sulphur isotope investigations by Boyle et al. (1976) suggested that the massive cryptocrystalline body of the deposit formed by replacement of evaporites while the coarsely crystalline barite veins and pods and the sulphides were precipitated from deeply circulating brines.

Patterson (1986, 1987, 1988a,b, 1989) examined all of the available drill logs and other mine records in order to investigate the potential for further argentiferous base metal reserves at Walton. He constructed new geological plans, cross sections, and longitudinal sections. Patterson (1988) noted that most of the drillholes in the mine were situated along two main baselines: the D-baseline, which is located in the area immediately down plunge from the open pit and contains the deepest mine workings; and the B-baseline, which occurs to the south of the D-baseline and contains the barite-sulphide deposit which is the focus of this study (Fig. 2-3). Cross sections are spaced at 50' intervals with 17 along the D-baseline and 31 on the B-baseline[1]. The cross sections on the D-baseline show a massive barite zone at surface with an argentiferous sulphide zone in the footwall between depths of 270 feet and 1100 feet. The hanging-wall in this area is composed of shale and sandstone of the Tennycape Formation. Below 1100 feet the hanging wall is anhydrite and the barite zone gives way to the barite-sulphide zone located near the *Pembroke Formation*/evaporite contact. A composite cross section is shown in Figure 2-4. On the B-baseline there is a much greater strike length of mineralisation and the barite is much more intimately associated with the sulphides. Plotting of metal values by Patterson (1989) indicated several ore shoots within the mineralised body which plunge in a southwest direction slightly cross cutting the geology in the plane of the section. In

[1] Note: in all previous work mine distances have been measured in feet. This report will also use feet when dealing with distances in the mine, in order to allow comparison with previous work.

conclusion Patterson (1989) identified the up and down plunge extensions of the ore shoots as potential areas for further exploration.

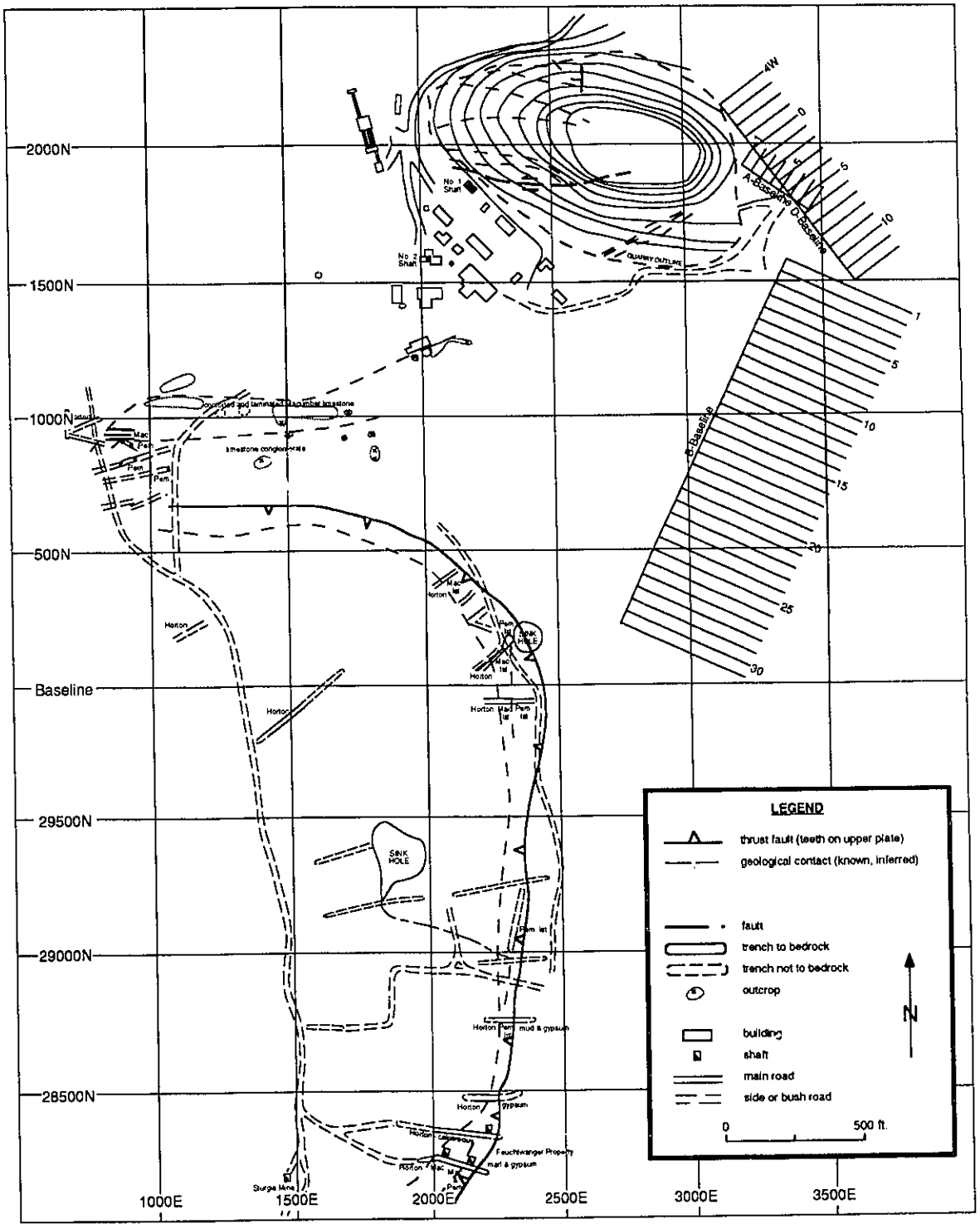

Figure 2-3. Map of the Walton mine site showing the open pit, mine buildings, geological contacts, and the location of the A-, B-, and D- baselines. Note the presence of a thrust fault, south of the quarry, which has overturned the stratigraphy. Modified from NSDME AR 21H/01D 06-I-51(00).

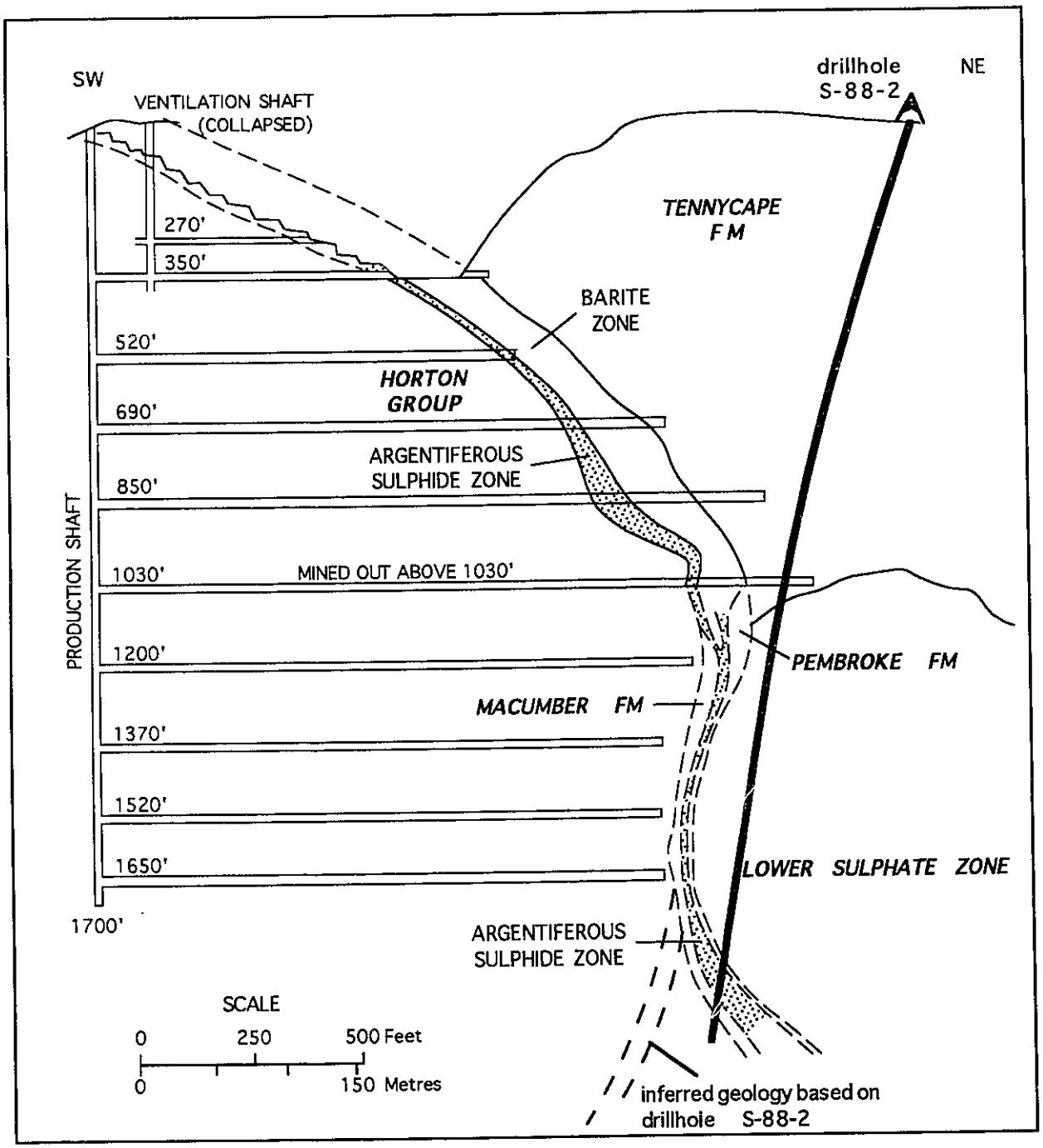

Figure 2-4. Composite cross-section of the main Walton deposit (Patterson, 1989) also showing drillhole S-88-2 and inferred geology (Boehner, 1991).

CHAPTER 3
GEOLOGY OF THE B-BASELINE

STRATIGRAPHY

The Walton B-baseline deposit, hosted mainly by carbonate rocks of the basal Windsor Group, lies immediately above the Horton Group/Windsor Group contact. Quartz arenites occuring at the top of the Cheverie Formation locally contain copper mineralisation. The carbonate host rocks have been divided into the Macumber Formation and the *Pembroke Formation* (Weeks, 1948), however, due to the confusion arising from the inconsistent use of the term *Pembroke*, in this study the carbonate rocks that host the mineralisation at Walton will all be termed Macumber. The laminated unit that was previously known as the Macumber Formation will be termed the lower Macumber and the non-laminated unit previously known as the *Pembroke Formation*, and interpreted by Lavoie and Sangster (1995) to be formed by synsedimentary slumping, will be called the upper Macumber. This terminology is only intended for use at the Walton deposit itself, as the upper Macumber as used here has not been recognised at any other locations in the Kennetcook basin. The evaporites which overlie the Macumber Formation are unmineralised in the B-baseline area.

A number of geological processes have acted upon the rocks in the Walton area since their deposition. These processes include folding and weathering and, depending on the timing of mineralisation, these processes may also have acted upon the Walton orebody. Unmineralised limestone breccias and sand occur stratigraphically above and within the Macumber Formation.

HOST ROCKS

Horton Group

Cheverie Formation rocks of the Horton Group underlie mineralisation at Walton and primarily comprise quartzitic sandstones. The sandstones are quite well sorted with equigranular, subrounded to angular grains of quartz and minor feldspar. Quartz grain size is consistent within each sample but varies from sample to sample. Coarser grained samples are usually clast supported whereas the finer grained samples are matrix supported. The matrix is composed of red-brown clays and plates of mica are not uncommon between quartz grains.

Lower Macumber

Contouring of the lower Macumber thickness reveals a relatively uniform unit of 30-40 feet thick (Fig. 3-1). The increased thickness of the lower Macumber on the 850 level between sections 1 and 8 may be more apparent than real. The drill holes upon which these are based were among the first to be drilled underground and it is believed that the core loggers may not have recognised the distinction between the upper and lower units. In addition, several of these holes did not cross the upper Macumber/lower Macumber contact.

The lower Macumber is usually laminated in either of two styles. The first lamination is defined by fine parallel wavy stylolites and occurs in samples from Schenk's (1967) Lithosome B, while the second is defined by distinct variations in colour in samples from Lithosome A.

In samples exhibiting the first style, the stylolites are variable in thickness from 0.01mm to 0.6mm and are spaced at intervals of between 0.5mm and 10mm, most commonly between 1mm and 3mm. The stylolites are generally dark in colour and contain variable amounts of residual materials such as quartz, pyrite, marcasite, mica, and bitumen. The quartz grains are fine-grained and are sub-angular to sub-rounded. Mica is

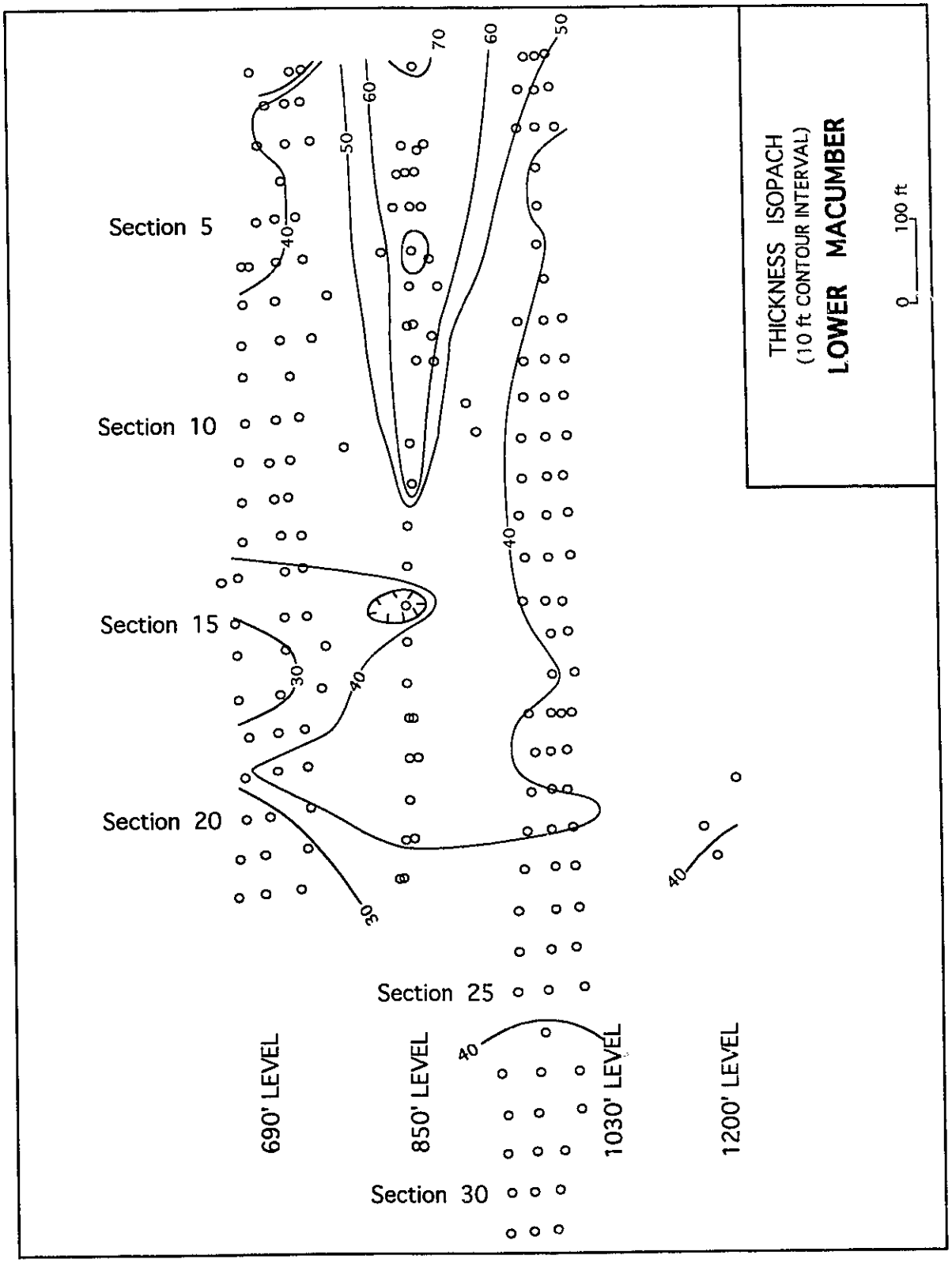

Figure 3-1. Contour map of lower Macumber thickness. Note that drill hole locations are their approximate intersection with the centre of the lower Macumber.

usually oriented with the long axis along the stylolites although there are exceptions. Pyrite and marcasite are most commonly in the form of very fine framboids or tubercles. Pyrite is most abundant in the darker stylolites.

The second style of lamination occurs most commonly in ooidiferous samples. The lamination is due to distinct changes in colour at intervals of approximately 10mm. The colour change is cyclical with the colour becoming gradually darker across the laminae and then abruptly changing to a lighter colour and then darkening again across the next laminae.

Ooids occur in lower Macumber samples with both styles of lamination although they are much more abundant in samples with the second style. In samples with stylolites the ooids only occur between widely spaced stylolites. The ooids range in size from 0.1mm to 2.0mm and are spherical. They commonly show a variation in colour between the core and the rim. In some cases the centre of the ooid may be open space or may be filled with barite, euhedral siderite or pyrite. Fractured brachiopod shells were observed in several samples.

Upper Macumber

Samples of upper Macumber are generally non-laminated and have a mottled appearance, although laminated samples and laminated fragments can be found in the upper Macumber. In many cases it is difficult to label a sample as upper or lower Macumber in core sample. In these cases it was necessary to classify the samples based on the original drill logs. It is clear from reading the logs that there was some difficulty in distinguishing the upper and lower units during drilling. In an internal company report Turner (1967, p.2) states: "*The Pembroke-Macumber contact is never clear and is always arbitrarily drawn. There are laminated zones in the Pembroke and brecciated zones in the Macumber. I have been picking the contact when laminated carbonate becomes continuous to the top of the Horton.*"

Contouring the upper Macumber thickness revealed an interesting and unexpected feature (Fig. 3-2). The unit is extremely variable in thickness, ranging from 0 feet to 70 feet, and forms two distinct mounds. The first mound is located between sections 1 and 6 on the 690 and 850 levels of the mine. The lateral extent of the mound above the 690 level and to the northwest of section 1 is unknown due to the absence of drilling in these areas. Most of the mound has a thickness of 30-40 feet. The second mound is centred at Section 19 on all mine levels. It has a ridge-like shape that rakes at an angle of 60°S to the mine levels. The ridge has a width of approximately 450 feet and its extent above the 690 level and below the 1200 level are unknown, although it does appear to decrease in thickness in both directions. The second mound has a maximum thickness of 70 feet.

Samples of upper Macumber usually have a mottled appearance in which it is very difficult to recognise primary textures due to the complete replacement of calcite or dolomite by siderite. It is possible to recognise ooids in some samples while others may be laminated or contain angular fragments. The fragments may be laminated or non-laminated and occur in a matrix of unlaminated siderite. The laminations are the same as the first style (caused by stylolites) observed in the lower Macumber. Unlaminated fragments may contain ooids. The fragments range in size from 2mm to greater than 15mm and usually appear to be randomly oriented although in one sample the fragments appear to be rotated in place. Samples of upper Macumber also have more open space than the lower Macumber. The samples are commonly vuggy, with varying degrees of cementation by late ore minerals and calcite.

POST-DEPOSITIONAL EFFECTS

The limestone breccia occurs in narrow lenses either above the Macumber Formation or less commonly between the upper and lower Macumber. In the former case the lenses range in thickness from 1 to 20 feet, although thicknesses of one to five feet are the norm,

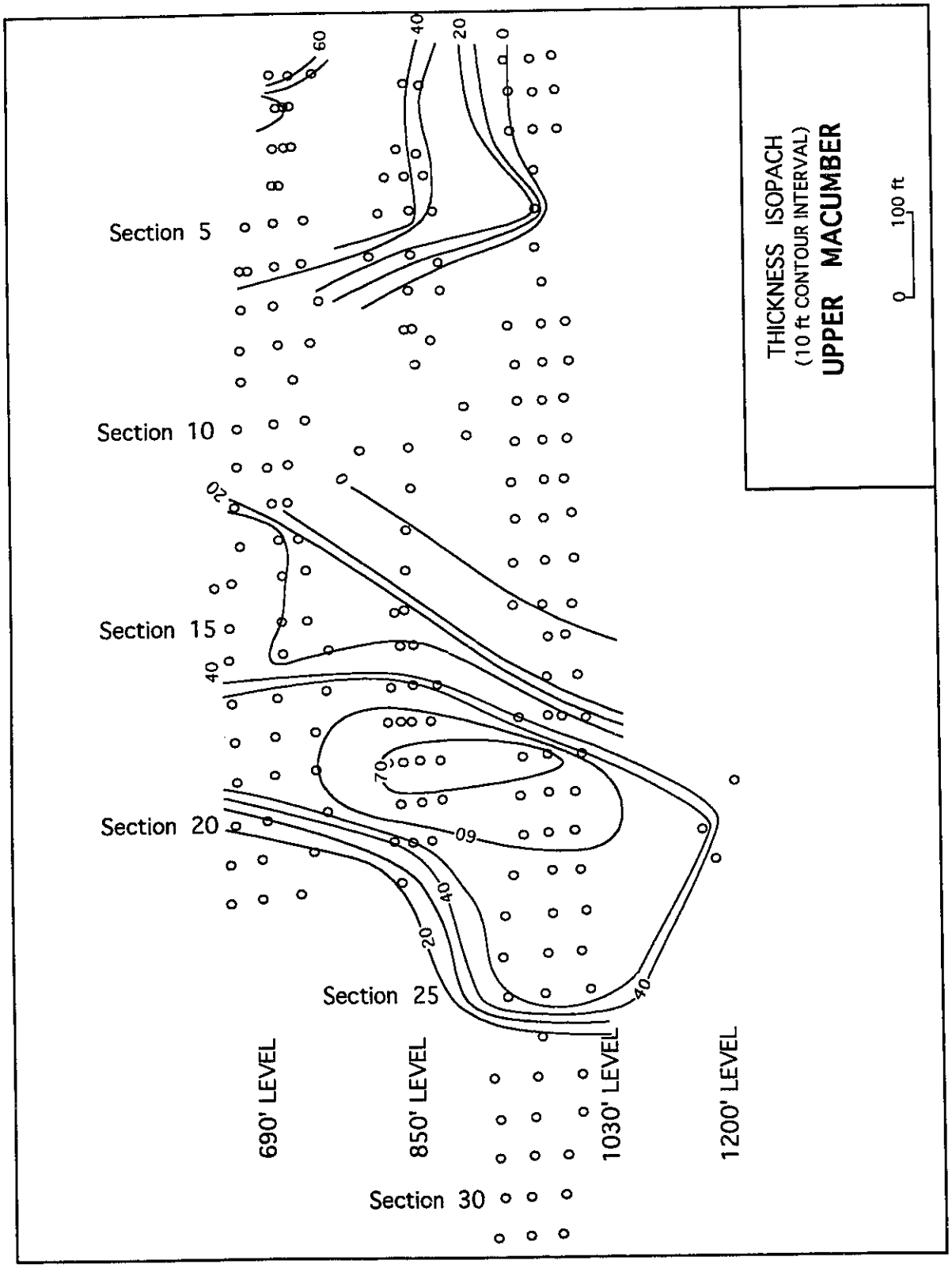

Figure 3-2. Contour map of the upper Macumber thickness. Note that drill hole locations are their approximate intersection with the centre of the upper Macumber. Where the upper Macumber is not present the drill hole intersection with the top of the lower Macumber is shown.

and up to 300 feet in length along a section. In the latter case the limestone is only one or two feet thick and cannot be correlated between drill holes. The limestone breccia is fairly evenly distributed throughout the deposit, occurring at all mine levels and from one end of the B-baseline to the other.

The limestone breccia is always called *Pembroke Formation* in drill logs, however, as has been previously discussed, that term was applied by the mine workers to any non-laminated carbonate in the deposit. This limestone breccia does, however, resemble the breccia seen in outcrop in the Cheverie area which is generally accepted to be the result of solution collapse and karsting (Clifton, 1967; Lavoie, 1994; Lavoie and Sangster, 1995). The limestone has been described as a clastic limestone in the original drill logs, and it bears no resemblance to the carbonate of the upper Macumber. The limestone is crumbly, very porous, petroliferous and contains small angular clasts of siderite. Voids in the limestone may be partially filled with dogtooth calcite.

Also present in the Walton deposit is an unconsolidated red calcareous sand which occurs between the Macumber Formation and the overlying evaporite. In cases where both sand and limestone breccia are present, the sand overlies the limestone breccia. The distribution of the sand is highly irregular, with large variations in its thickness and lateral extent. In many cases the sand appears to cut into the Macumber in place of both host rock and ore. Short intervals of siderite and barite are reported in the sand in some holes, particularly in the upper Macumber.

The relative timing of the limestone breccia and sand deposition and the folding of the deposit host rocks is an interesting problem as it may place constraints on age of mineralisation. The question is whether the breccia and sand were deposited before or after the rocks were folded to their present steeply dipping attitude. There is no evidence from either the drill core or the drill logs that there is any layering within the breccia or the sand which would provide a geopetal indicator. The shape of the sand and limestone infill

does, however, suggest that the folding occurred after the infill deposition. If the breccia and sand filled a funnel shape that was thicker near surface and thinned at depth it would suggest that they were deposited while the host rocks were tilted. This is not the case. The sand and limestone breccia are highly irregular in shape, sometimes thicker at depth than at surface (e.g. sections 18, 19). Of the ten holes in which a contact between Macumber and evaporite was encountered, six were at the 690' level, one was at the 1030' level and three were at the 1200' level. The bottom of the evaporite seems to be folded to the same degree as the Horton/lower Macumber contact and the lower Macumber/upper Macumber contact (e.g. sections 20, 21, 22), again suggesting that folding occurred after sand deposition. Clifton (1967), however, presents evidence that karstic breccia and its attendant cavity fill post date the regional deformation. It is therefore inconclusive whether the limestone breccia and sand formed by a solution collapse karstic process before or after the tilting of the beds to their current attitude.

RECONSTRUCTED SECTIONS

In his report, Patterson (1988b) included 31 vertical cross sections spaced at fifty-foot intervals along the B-baseline. These were prepared from the original drill logs and included the geological contacts and all of the available assay data. In re-examining the drill logs as part of this study, it was immediately apparent that very little was known about the contact between the Macumber and the overlying evaporite. In only a few cases was a hard contact between sideritised Macumber and evaporite encountered. In a majority of cases drilling was stopped when sand or limestone breccia or open space was encountered. Less frequently drilling was continued through the sand/limestone breccia/space into the evaporite. There were also many holes in which the core was lost and the lithology was based on cuttings recovered. Therefore, because of this lack of control, the exact thicknesses of the upper and lower Macumber are not known in many areas.

In this study, an attempt was made to reconstruct each of the sections in order to show the location of both the upper Macumber/lower Macumber contact and the Macumber/evaporite contact prior to deposition of the sand and limestone breccia. This was accomplished through careful examination of the drill logs and the re-plotting of all contacts identified in the logs. For each section geological contacts were re-drawn and were interpolated from the two adjacent sections in areas of less control. Also, the general nature of the geology in areas of good control was applied to areas of less control. Level plans were then constructed for the 690', 850' and 1030' mine levels, based on the reconstructed sections.

In these reconstructions, the position of the lower Macumber/upper Macumber contact was moved in several drill holes relative to their original logged position. Holes 246 and 247 on section 2; 251 and 252 on section 3; and 371 and 372 on section 5 were among the first holes drilled underground on the B-baseline and, based on the descriptions in the logs and the nature of the contact elsewhere, it is believed that the contact was not recognised by the core loggers. The position of the contact on these two sections has been adjusted to reflect a more likely situation.

The reconstruction of new cross-sections contributed greatly to the study, particularily in the identification of the upper Macumber mounds which had been previously unrecognised. The sections also revealed the potentially large volume of mineralisation that may have been lost due to dissolution of the carbonate host rocks; this lost volume is now partially filled with limestone breccia and sand (e.g. Sections 3, 11, and 18 in Appendix I).

CHAPTER 4
ORE PETROGRAPHY

WALLROCK ALTERATION

Horton Group

In some areas the quartz arenites at the top of the Cheverie Formation have been replaced to varying degrees by pyrite and chalcopyrite. This alteration ranges from replacement of clays by very fine euhedral crystals of pyrite to complete replacement of the matrix by pyrite and the filling of fractures in quartz grains by pyrite. Feldspar grains are usually partially altered to clays and quartz grains show signs of dissolution at grain boundaries. Muscovite is more prevalent in the altered sandstones as are marcasite lathes in the matrix. In the most intensely altered areas the matrix is completely replaced by coarse zoned pyrite crystals and colloform pyrite masses. Quartz grains are commonly fractured with the fractures healed by pyrite and chalcopyrite replaces pyrite in both the matrix and fractures. Chalcopyrite veins cross and surround colloform pyrite and contain inclusions of pyrite and marcasite. The most chalcopyrite-rich areas may contain as much as 1.0% Cu over 8 feet.

Windsor Group

All Macumber rocks in diamond drill holes in the Walton deposit consist completely of siderite although, outside the deposit area, the Macumber is normally limestone or dolostone. The nature and position of the transition from limestone to siderite is unknown. Surface samples of Macumber Formation at the mine site are limestone while all samples of Macumber Formation from the uppermost underground drill holes are siderite. Siderite is

also found at the nearby Goshen prospect but again the limestone/siderite contact is not exposed.

In the deposit the lower Macumber is composed entirely of fine grained siderite, including ooids and brachiopod fragments, indicating that the siderite has replaced earlier limestone or dolomite. Although the replacement by siderite has preserved some primary features such as layering in ooids it has generally "blurred" the original textures making it difficult to identify delicate sedimentological features.

MINERAL TEXTURES

Siderite

The most abundant mineral in the Walton deposit is siderite, occurring in the vast majority of samples studied. The siderite has a light brown colour and, in drill core, is usually coated to varying degrees with red-brown iron- and manganese-oxide staining. It occurs in three main forms: i) Type 1, very fine grained (<0.01mm); ii) Type 2, euhedral crystals varying in diameter from 0.05 to 0.2 mm and usually associated with barite; and iii) Type 3, very coarse (>0.5mm) crystals representing the last phase.

Type 1 siderite occurs as masses of very fine (<0.01mm) anhedral crystals that have replaced earlier calcite or dolomite resulting in an interlocking grain texture (Fig. 4-1A). Ooids and shell fragments are also replaced by this type of siderite.

Type 2 siderite, consisting of coarser grains of euhedral crystals ranging in size from 0.05mm to 0.2mm, protrudes into voids in the rock and into crystals of barite. It is interpreted to have formed by recrystallisation of very fine grained siderite possibly during an influx of warm fluid. The common occurrence of barite in the voids suggests the recrystallisation was caused by the same fluids which resulted in the barite mineralisation. There is also a phase which appears to be intermediate between Type 1 and Type 2. It occurs as coarse subhedral grains which occur in veins or irregular masses (Fig. 4-1B). The

A

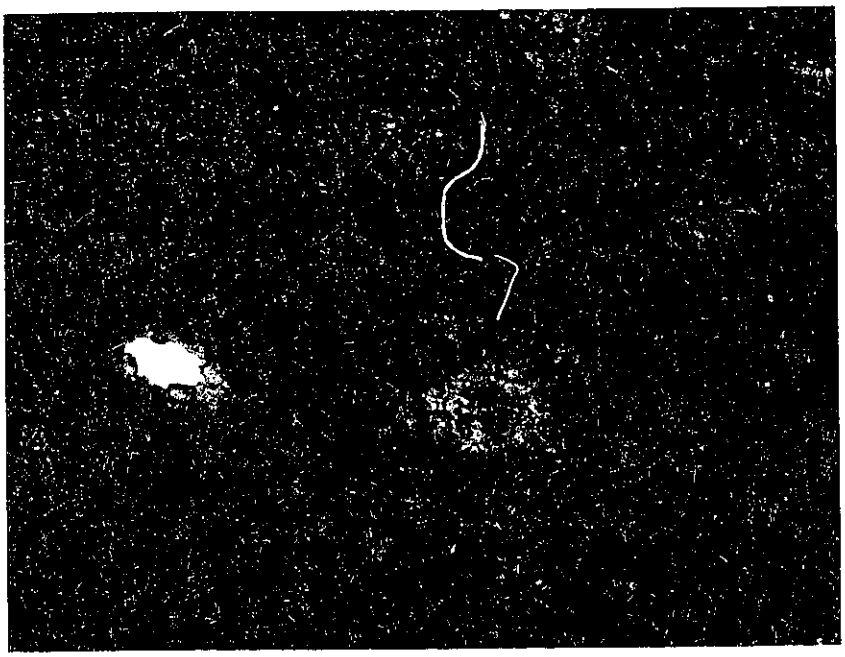

500µm

B

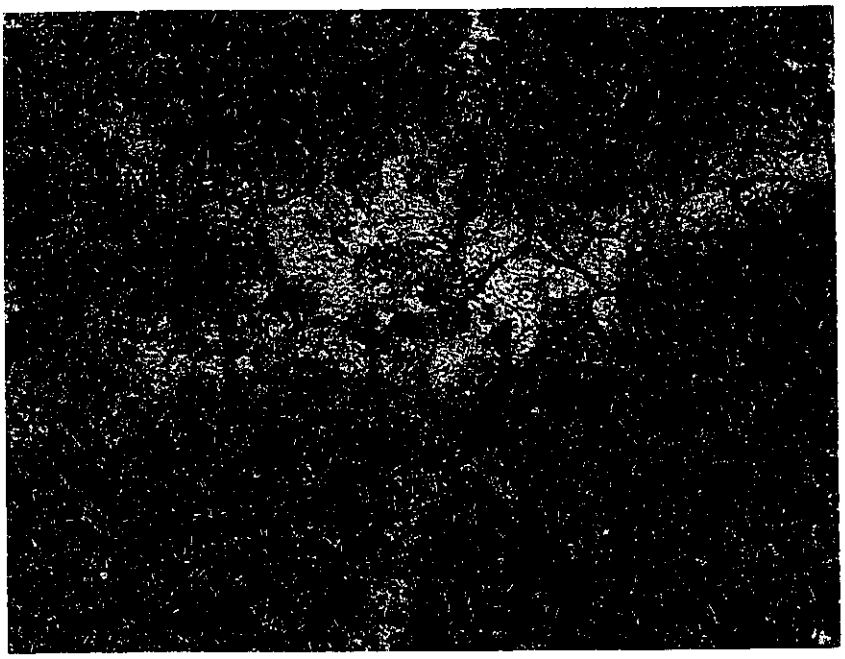

250µm

Figure 4-1. A. Type 1 siderite replacing ooidal lower Macumber. The white mineral in the brachiopod at the left of the photo is barite. Surrounding the barite is a ring of Type 2 siderite. The opaque mineral is framboidal pyrite. B. Type 1 siderite crossed by coarser siderite intermediate between Types 1 and 2. The opaque mineral is framboidal pyrite.

intermediate phase is coarser grained than the Type 1 siderite but lacks the euhedral crystals of the Type 2 siderite.

Type 3 siderite is much less common than Types 1 and 2 and occurs as very coarse grains of siderite ranging in size from 0.5 to 2.0mm. This siderite surrounds Type 2 siderite, coarse blades of barite, and marcasite needles indicating a later origin than those minerals. Type 3 siderite also surrounds coarse euhedral chalcopyrite grains and partially fills voids in the chalcopyrite. The coarse siderite is therefore interpreted to have been one of the last minerals to be deposited.

Barite

Barite occurs in at least trace amounts in most of the samples studied and in at least half of the samples it is a major component. The barite is most commonly a reddish-pink or brownish-white colour in hand samples and has a dense microcrystalline appearance. A number of varieties of barite can be identified in thin section: 1) medium to coarse lathes and needles up to 3mm in length; 2) coarse blobs (up to 2mm diameter) in siderite with very irregular grain boundaries; 3) radiating aggregates up to 2mm long that have a fibrous habit in some cases; 4) interlocking masses of fine to medium grains; and 5) veins.

In any particular sample there may be a combination of barite varieties, but generally, in samples in which the barite is less abundant, the first two types are most common. As the barite content of a sample increases the third and fourth type of barite become the most common forms. Barite veins may occur with any other variety of barite and are late in the paragenetic sequence. Vein barite is usually pink in hand sample while older varieties of barite are brownish-white.

Lathes and needles of barite are usually intimately associated with Type 1 siderite suggesting a contemporaneous formation; however, in some cases it is clear that barite replaces siderite. The lathes contain inclusions of siderite and the siderite-barite grain

contacts are commonly corroded. The needle shape of the siderite/barite intergrowths suggests that they are the result of the replacement of anhydrite crystals. This replacement has been complete as no anhydrite remains. The second variety of barite appears to have formed in voids as the barite is commonly surrounded by euhedral Type 2 siderite crystals. Radiating aggregates, fibrous masses and interlocking crystal masses are the most common forms in the most barite-rich samples. These samples usually contain only minor amounts of siderite. The radiating aggregates may have crenulated grain boundaries. Barite veins cut siderite and earlier barite and may contain chalcopyrite and tennantite between grain boundaries.

Pyrite/Marcasite

Pyrite and/or marcasite can be found in most samples and are the most common sulphide minerals in the Walton deposit. They occur in a number of distinct forms: 1) very fine grained framboids; 2) coarse round crystals; 3) coarse colloform grains; 4) pervasive very fine grained pyrite dust; 5) euhedral crystals; and 6) late rims. Most samples contain several forms of pyrite and/or marcasite. Pyrite and marcasite are closely associated and in many cases it is difficult to establish the paragenetic relationship of the two minerals. It is also difficult to establish the temporal relationship between the various types of pyrite other than the fact that Type 1 pyrite is early and Type 6 is generally late.

Type 1 is framboidal pyrite which is very fine (2 to 5 μm), usually euhedral, crystals of pyrite arranged in a circular pattern. The framboids may contain several rings of pyrite grains and the grains may have intergrown with each other. The clusters tend to occur along linear trends in the samples, commonly in stylolites. Fine lathes of marcasite are also found associated with the pyrite framboids. Type 1 pyrite is found in most samples and is common in samples that contain no barite, other sulphides, or other varieties of

pyrite. The character of the pyrite and its presence in non-mineralised samples suggests a diagenetic origin.

Type 2 pyrite/marcasite forms coarse, round, zoned crystals. The grains may be up to 2mm in diameter and are commonly intergrown, resulting in coarse masses of pyrite and marcasite. Marcasite and pyrite form alternating bands in many of the grains. Grains are commonly fractured, with tennantite or chalcopyrite filling the fractures.

Type 3 is coarse colloform pyrite. The pyrite may be replaced to some degree by tennantite resulting in a very finely banded texture. This variety of pyrite is not associated with marcasite.

Type 4 pyrite forms a fine dusting of very fine pyrite grains. The pyrite is generally in siderite which it is replacing, resulting in a fine net or cobweb texture. The intensity of the replacement varies and in some cases the pyrite has healed together to form coarse pyrite masses.

Type 5 pyrite comprises euhedral crystals which may or may not be zoned. The zoned variety ranges in size from fine to coarse grained. The grains are delicately zoned with alternating bands of "normal" pyrite and a slightly grayer pyrite. There are also bands of marcasite in the crystals. The pyrite may be fractured, cutting the banding in the pyrite and the fractures may be filled with tennantite or chalcopyrite. There are also barite crystals between pyrite grains which also cut the banding. Type 5 pyrite is commonly rimmed by later pyrite or marcasite (Type 6). The non-zoned Type 5 pyrite commonly contains inclusions of siderite, galena and barite.

Type 6 is a late rim of pyrite or marcasite that surrounds earlier pyrite generations.

Galena

Galena occurs as a (major)-minor phase in association with sphalerite or as a minor-trace phase when not in association with sphalerite. In the first case it replaces sphalerite leaving only remnant blebs of sphalerite in the galena. The sphalerite/galena banding is cut by galena without sphalerite inclusions. Coarse masses of galena commonly have a euhedral siderite grain at the centre of the mass. Galena also replaces barite associated with pyrite and occurs as fine to medium grains in siderite.

Sphalerite

Sphalerite occurs as a minor phase in several of the samples studied, commonly in association with galena. It usually forms coarse colloform masses or orbicles up to 5mm in diameter. The orbicles commonly have a siderite grain or pyrite sphere as a core. Sphalerite is always replaced to some degree by galena resulting in bands of fine, rounded sphalerite remnants in a matrix of galena. The degree of replacement varies from zones completely replaced by galena through zones of half sphalerite and half galena to zones of just sphalerite. Trace amounts of sphalerite occur as fine disseminated grains in siderite and barite.

Much less sphalerite was encountered in the samples studied than was anticipated. Boyle (1972) reported that sphalerite was the third most common sulphide in the deposit after pyrite and galena. In this study, sphalerite is also less abundant than tennantite and chalcopyrite. Boyle (1972), however, studied the main barite pipe and its underlying sulphide zone while this study is focused on the B-baseline sulphide zone.

Chalcopyrite

Chalcopyrite occurs in at least trace amounts in almost every sample studied. It occurs late in the paragenesis and replaces most earlier minerals. Its principle association

is with tennantite in which it occurs as fine inclusions. Chalcopyrite commonly replaces pyrite and marcasite and fills fractures in those minerals. Chalcopyrite also occurs with tennantite in late barite veins. Where the veins crosscut siderite or barite, chalcopyrite occurs with tennantite as fine crystals along barite grain boundaries but where the veins crosscut pyrite, chalcopyrite is prevalent with only minor barite. Chalcopyrite also occurs as medium grained euhedral crystals in Type 3 siderite.

Tennantite

Tennantite, a major phase in several samples, occurs most commonly as a coarse mass of crystals, filling space between and replacing pyrite, siderite and barite grains. Individual grain boundaries are indistinguishable in reflected light but in transmitted infrared light the centres of tennantite grains exhibit a texture similar to that of fine grained siderite suggesting either a replacement of siderite by tennantite or a recrystallisation event (D. Kontak, pers. comm.). Tennantite is commonly associated with pyrite, filling voids between colloform pyrite grains and preferentially replacing bands in the colloform pyrite. The replacement texture is very delicate, resulting in very fine alternating bands of pyrite and tennantite. These fine bands in turn may be cut by coarse tennantite. In some cases tennantite rims euhedral pyrite/marcasite grains with tennantite in turn rimmed by later pyrite or tennantite rims late pyrite which in turn rims an earlier euhedral pyrite grain. Tennantite fills fractures in pyrite grains and surrounds both barite and siderite grains, replacing siderite. Fine grains of chalcopyrite commonly occur in tennantite, in an early stage of tennantite replacement by chalcopyrite.

Trace amounts of tennantite occur in association with sphalerite and galena. The tennantite is usually very fine grained and has inclusions of sphalerite and sometimes chalcopyrite. The grains are slightly rounded and irregular in shape and occur in sphalerite and galena.

Other Minerals

Calcite occurs in several samples of upper Macumber as schalenohedral crystals and in veins. In either case it fills vugs and open spaces in the rock and is a paragenetically late mineral.

(Para)rammelsbergite ($NiAS_2$) occurs in veins with tennantite and chalcopyrite. It formed before tennantite and chalcopyrite in the veins. It also occurs in several other samples surrounding tennantite grains. This mineral was identified by electron microprobe and its presence in the Walton deposit was previously unreported.

Boyle and Jambor (1966) and Boyle (1972) report the presence of the silver-bearing minerals acanthite, gersdorffite, stromeyerite, proustite and pearceite in samples from the Walton deposit. None of these minerals is present in B-baseline samples examined in this study.

PARAGENESIS

Based on the mineral textures reported above, a paragenetic sequence of mineral deposition has been derived (Fig. 4-2). It must be noted that in many cases the paragenesis is complex and cannot be exactly determined because of the continued, sometimes rhythmic, replacement of one mineral by another.

The first stage in the mineralising history was the replacement of the original host rock carbonate (calcite/dolomite) by siderite and the deposition of siderite in voids. Replacement left no remnants of the original carbonate minerals although diagenetic pyrite and marcasite framboids were unaffected. Barite mineralisation began prior to the end of siderite deposition resulting in some contemporaneity, however, the bulk of the barite mineralisation followed deposition of siderite. The barite replaced and filled voids in the siderite.

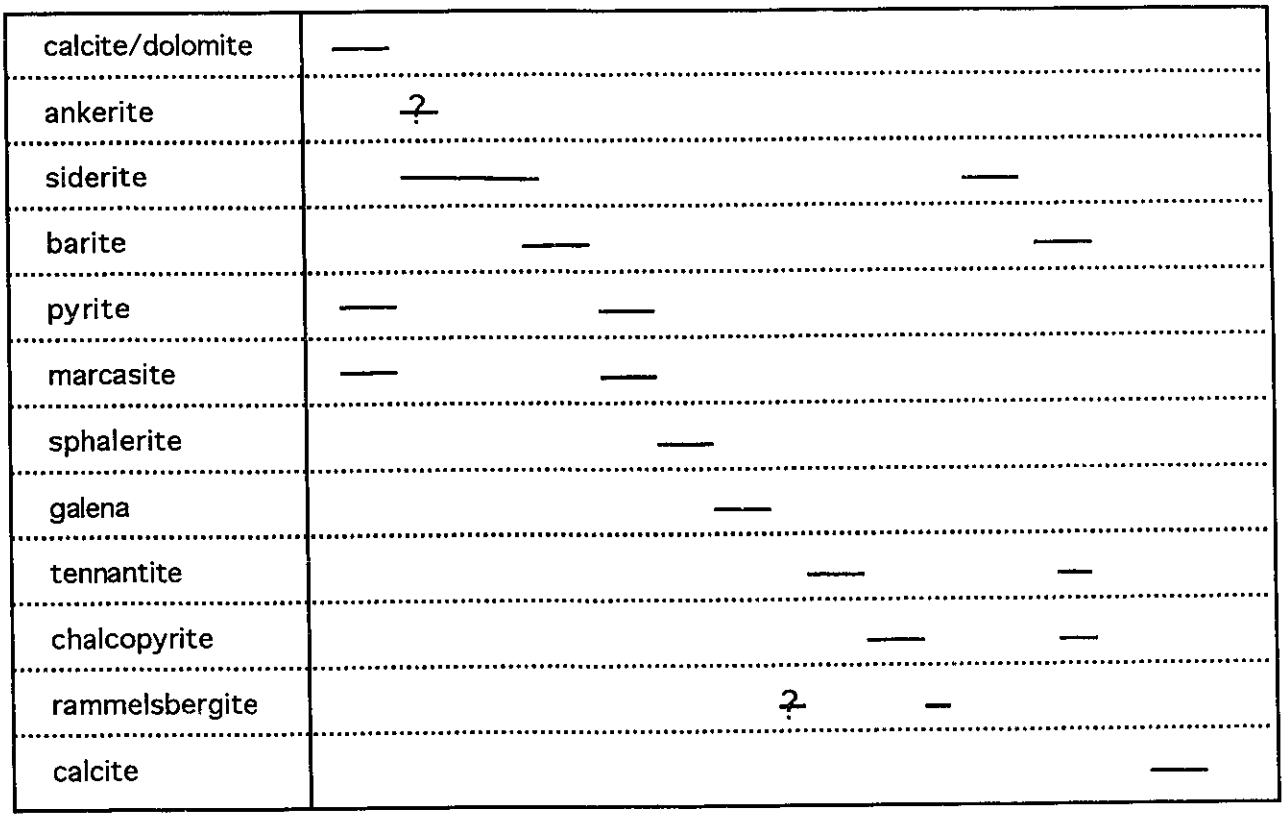

Figure 4-2. Paragenesis of the principal minerals in the B-baseline deposit at Walton.

Pyrite and marcasite were the next minerals to be deposited, replacing and filling voids in the siderite. In some places there was alternating deposition of pyrite and marcasite resulting in banded grains.

Sphalerite was the first of the ore sulphides to be deposited and it was subsequently replaced by galena. There is some evidence for the deposition of minor amounts of sphalerite after galena; however this relationship is difficult to corroborate due to the scarcity of sphalerite. A second generation of galena cuts sphalerite which has been partially replaced by galena. Tennantite occurs after pyrite, filling fractures and delicately replacing colloform bands in that mineral. The temporal relationship between tennantite and galena or sphalerite is much more difficult to establish as they seldom occur together. Chalcopyrite replaces all earlier phases. A small amount of rammelsbergite then formed.

The final stage of mineralisation consisted of the deposition of a small amount of late siderite followed by vein barite accompanied by tennantite and chalcopyrite. Finally dogtooth and vein calcite formed.

CHAPTER 5
MINERAL CHEMISTRY

INTRODUCTION

The composition of the host rocks and of the ore minerals was determined by electron microprobe. This study did not undertake a comprehensive examination of the geochemistry of the Walton deposit but, rather, was restricted to a preliminary look at the composition of the major mineral phases.

HOST ROCK CHEMISTRY

Samples of both upper and lower Macumber from the Walton deposit were analysed, as were samples of Macumber limestone and dolostone from locations outside the deposit. The samples were analysed for CaO, MgO, MnO, FeO, BaO, SrO, ZnO, and SO_3 using the electron microprobe at the Geological Survey of Canada, Ottawa. Two methods were used to make the analyses. The usual method was to analyse individual mineral grains which had been selected during the petrographic examinations and, in most cases, three analyses were made for each grain. The three analyses were randomly located within each grain on points which appeared to be representative of the grain and free of inclusions and impurities.

In some Macumber samples, particularly those from outside the Walton deposit, a scan was made in which the starting and end points of a traverse across a slide were defined and thirty point analyses made at equal intervals along the traverse. Due to the nature of the scan, some analysed points may not have been carbonate material (i.e. sulphides, carbonaceous material, other minerals in stylolites). Therefore, some analyses do not sum to 100 weight percent (wt.%) due to non-carbonate minerals which contain elements which were not analysed.

From the resulting wt.% oxide data, $CaCO_3$, $MnCO_3$, $FeCO_3$, and $MgCO_3$ weight percent and mole percent end members were calculated. The sum of the weight percent end members was also calculated to determine the quality of the analysis. Analyses with a total weight percent of between 95 and 105 were accepted; those with a total of less than 95 or greater than 105 were rejected. The breakdown of data acceptance is summarised in Table 5-1.

Regional Macumber

Several samples of Macumber Formation from outside the Walton deposit were analysed in order to determine the normal composition of the carbonate. The samples were collected from an outcrop near Brook Village on Cape Breton Island; from an outcrop known as Black Rock near the mouth of the Shubenacadie River; from drill core from hole GC-80-9 in the Cheverie area; and from drill core from hole GT-80-2 near the Tennycape mine (Figure 5-1). Samples of lower Macumber from outside the Walton deposit plot in two distinct fields on a mol% $CaCO_3$ - $MgCO_3$ - ($FeCO_3$+$MnCO_3$) ternary diagram (Fig. 5-2). The first is a relatively pure $CaCO_3$ limestone field and the second is a dolomite - ferroan dolomite - ankerite field. The limestone samples are from the Brook Village and Black Rock outcrops and the average mol% compositions for these samples are shown in Table 5-2.

The dolostone samples are from drillcore at Cheverie and Tennycape. With the exception of five analyses, all samples have an $FeCO_3$ content of less than 8.0 mol%, a $MnCO_3$ content of less than 2.5 mol% and a $MgCO_3$ content of 39.0 to 48.0 mol%. This places the composition in the ferroan dolomite field of Deer et al. (1962). The data are summarised in Table 5-3. The other five analyses have a much higher iron and manganese content and a lower magnesium content. Four of those analyses are of carbonate in a late vein in the Cheverie sample and average 50.4 mol% $CaCO_3$, 32.8 mol% $MgCO_3$, 13.6 mol% $FeCO_3$, and 3.1 mol% $MnCO_3$, typical of ankerite. The one additional analysis is from a scan

	Accepted	Rejected
Walton deposit		
Type 1 siderite	40	9
Type 1 ankerite	6	0
Type 2 siderite	9	0
Type 3 siderite	6	0
late calcite	9	0
Kennetcook Basin - Macumber Formation		
Tennycape	24	6
Cheverie	15	19
Shubenacadie Basin - Macumber Formation		
Black Rock	27	4
Cape Breton Island - Macumber Formation		
Brook Village	44	22

Table 5-1. Summary of microprobe data acceptance for Macumber Formation samples.

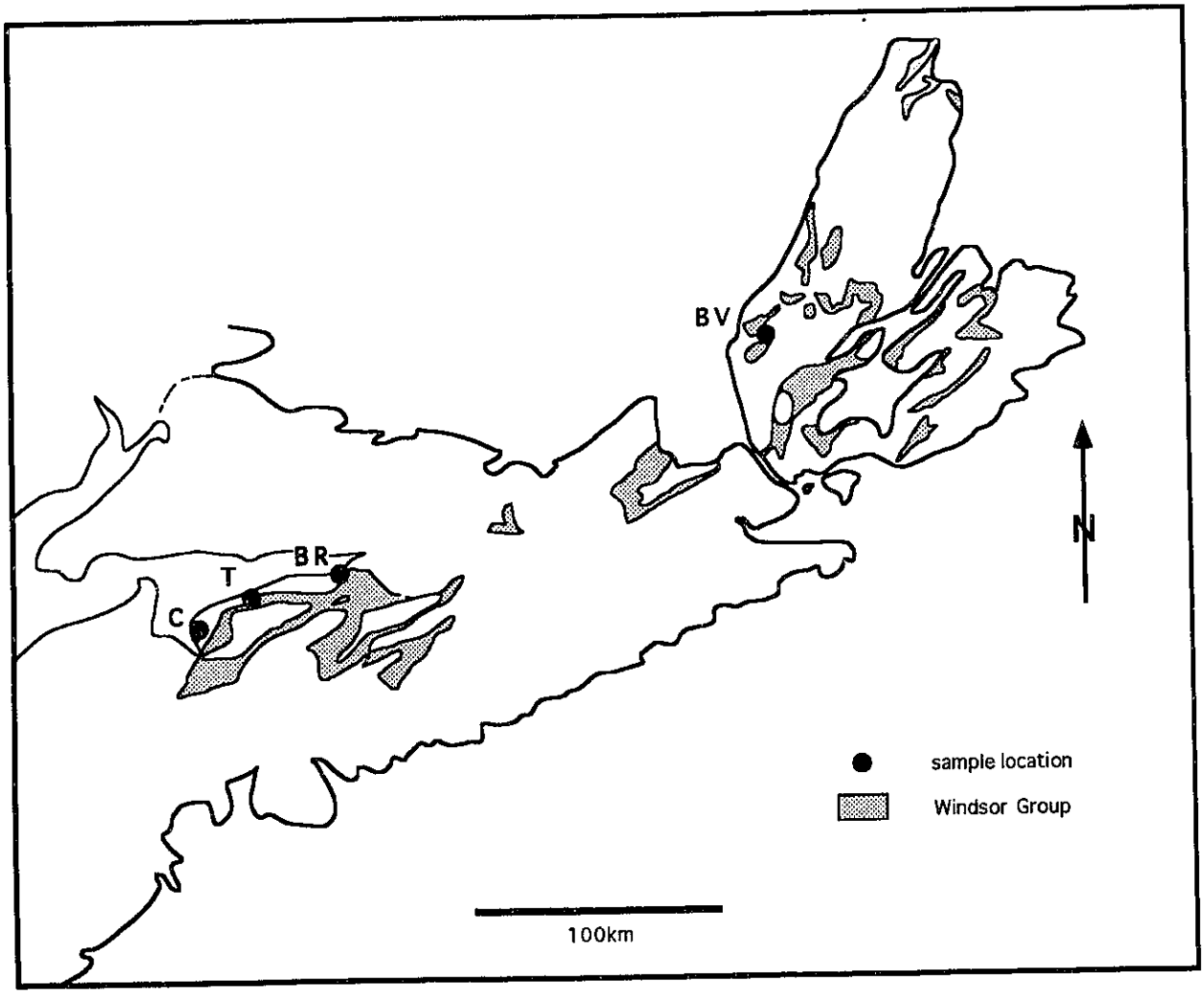

Figure 5-1. Sample location map for Macumber limestone and dolostone from outside the Walton mine area. BV-Brook Village, BR-Black Rock, T-Tennycape and C-Cheverie.

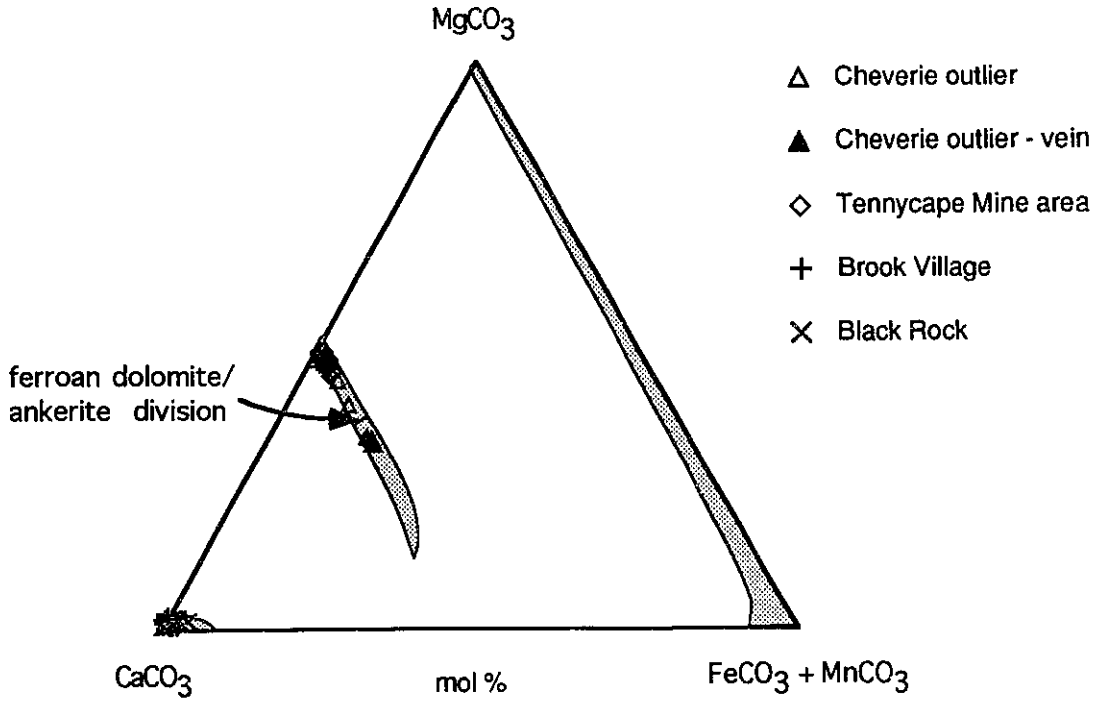

Figure 5-2. $MgCO_3$-($FeCO_3$+$MnCO_3$)-$CaCO_3$ ternary plot of unmineralised Macumber limestone and dolostone compositions from outside the Walton area. Also shown are five ankerite vein samples from Cheverie. Siderite, calcite and dolomite-ankerite compositional fields modified from Klein and Hurlbut (1993). Division between ferroan dolomite and ankerite from Deer et al. (1962).

		$CaCO_3$ mol%	$MgCO_3$ mol%	$FeCO_3$ mol%	$MnCO_3$ mol%
Black Rock Macumber (n=27)	avg	98.31	1.21	0.12	0.09
	max	98.95	1.99	1.45	0.22
	min	97.41	0.62	0.00	0.00
Brook Village Macumber (n=44)	avg	97.76	0.95	0.33	0.54
	max	99.18	1.74	1.34	2.28
	min	94.93	0.16	0.00	0.00

Table 5-2. Average, maximum, and minimum compositions of limestones from Black Rock and Brook Village.

		$CaCO_3$ mol%	$MgCO_3$ mol%	$FeCO_3$ mol%	$MnCO_3$ mol%
Cheverie Macumber (n=15)	avg	50.68	45.68	2.56	0.94
	max	51.41	47.23	7.49	2.22
	min	49.9	39.22	0.92	0.53
Tennycape Macumber (n=24)	avg	50.29	47.87	1.31	0.39
	max	51.17	49.04	3.82	0.87
	min	49.75	44.25	0.66	0.11

Table 5-3. Average, maximum, and minimum compositions of dolostones from Cheverie and Tennycape.

of the Cheverie sample and has a composition between that of the normal Cheverie dolomite and the vein ankerite.

Based on these results the composition of "normal" lower Macumber is either a limestone of 97-98 mol% $CaCO_3$ and 2-3 mol% ($FeCO_3$+$MgCO_3$) or a ferroan dolomite of 50 mol% $CaCO_3$, 47 mol% $MgCO_3$, and 3 mol% ($FeCO_3$ + $MnCO_3$).

Walton Macumber

In contrast to "normal" Macumber, most Walton Macumber samples are siderite or ankerite (Fig. 5-3). The ankerite has an average composition of 49.5 mol% $CaCO_3$, 31.0 mol% $MgCO_3$, 14.7 mol% $FeCO_3$, and 4.7 mol% $MnCO_3$ which is similar to that of the vein ankerite in the Cheverie sample. As shown in Figure 5-3 there is a wide range in siderite composition, primarily due to differences in the $MgCO_3$: ($FeCO_3$+$MnCO_3$) ratio. With the exception of coarse siderite crystals in sample SP-5190, this change correlates well with the stratigraphic position of the sample (Fig. 5-4). Samples of lower Macumber generally have a lower magnesium content, a slightly lower manganese content, a higher iron content, and a slightly higher calcium content than samples of upper Macumber (Table 5-4).

These variations appear to be unrelated to the type of siderite, in fact within each sample all types of siderite have approximately the same composition.

Coarse siderite, intermediate between Type 1 and 2, from sample SP-5190 does not follow this trend. During selection of analysis points on the microprobe, two different siderite compositions were recognised. Although the differences could be seen as different shades on the probe monitor, they were not visible using reflected microscopy nor was it possible to recognise any petrographic relationships between the siderites. The compositions of this siderite range from the highest $MgCO_3$ encountered in upper Macumber samples to the most $FeCO_3$ rich encountered in the lower Macumber and cover the spread from one extreme to the other. The $MnCO_3$ content of these samples is at the high end of the scale for

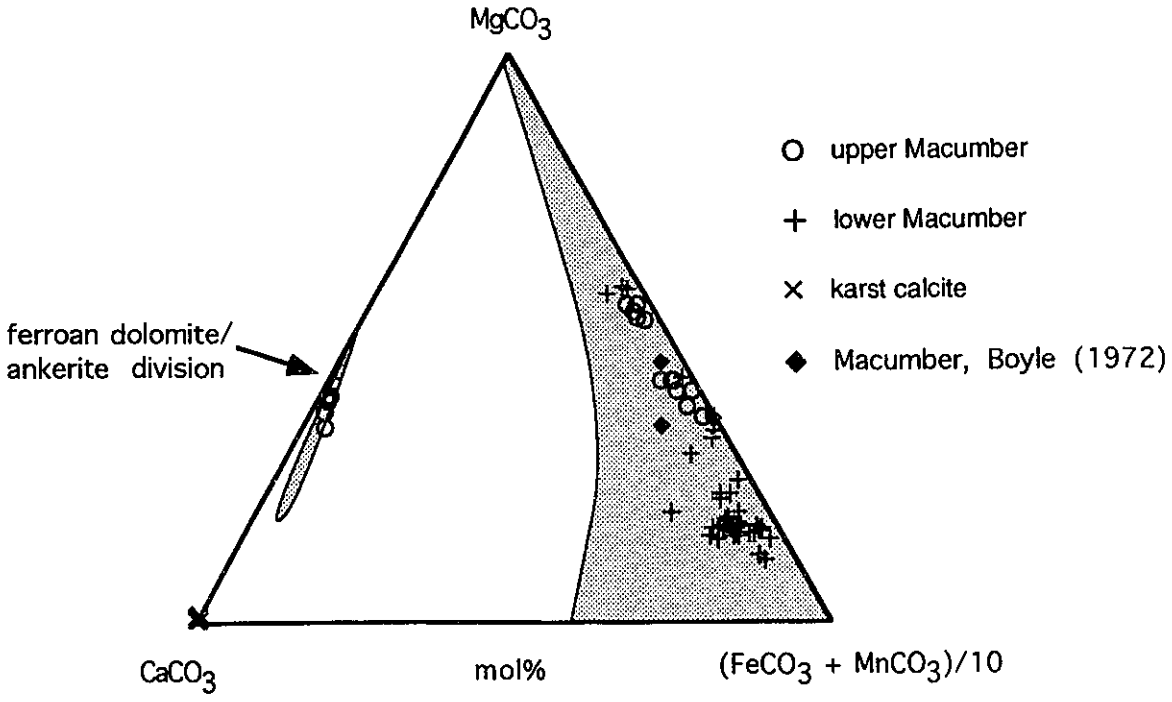

Figure 5-3. $MgCO_3$-($FeCO_3$+$MnCO_3$)/10-$CaCO_3$ ternary plot of siderite and ankerite compositions from Walton. Also shown are three siderite analyses from Boyle (1972). Siderite and dolomite-ankerite compositional fields modified from Klein and Hurlbut (1993).

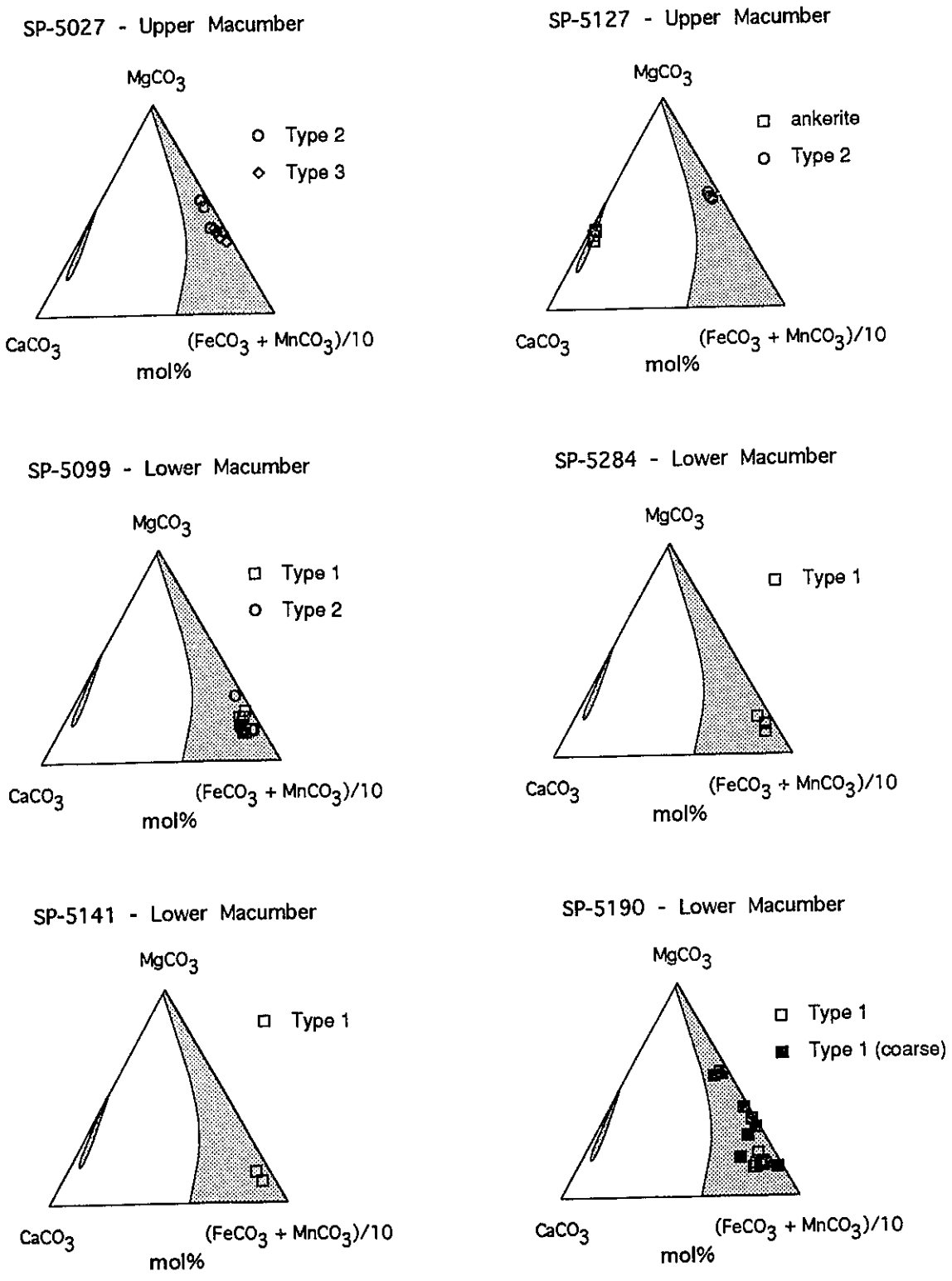

Figure 5-4. $MgCO_3$-($FeCO_3$+$MnCO_3$)/10-$CaCO_3$ ternary plots of siderite and ankerite compositions for individual samples. Labels Type 1-3 refer to different textures (see text for details). Siderite and dolomite-ankerite compositional fields modified from Klein and Hurlbut (1993).

		$CaCO_3$ mol%	$MgCO_3$ mol%	$FeCO_3$ mol%	$MnCO_3$ mol%
lower Macumber siderite (n=43)	avg	0.76	3.47	85.27	10.31
	max	2.17	13.16	89.24	12.53
	min	0.11	1.24	79.32	8.34
upper Macumber siderite (n=12)	avg	0.55	8.43	78.31	12.51
	max	0.90	11.92	83.79	14.42
	min	0.19	5.34	73.49	10.16

Table 5-4. Average, maximum, and minimum compositions of Walton siderite samples from the upper and lower Macumber.

the lower Macumber, but is fairly constant. The change in composition is therefore due to large variations in the $FeCO_3$:$MgCO_3$ ratio.

Nine analyses were made of late vein and scalenohedral calcite from the Walton deposit. The calcite has an average composition of 95.82 mol% $CaCO_3$, 0.47 mol% $MgCO_3$, 1.97 mol% $FeCO_3$ and 1.59 mol% $MnCO_3$.

ORE MINERAL CHEMISTRY

All sulphide minerals were analysed by electron microprobe for Cu, Hg, Ag, Au, Fe, Zn, Sb, As, Se, In, Cd, Ge, Pb, Bi, Te, V, Mn, and S. Barite was analysed for BaO, CaO, SrO, PbO, SO_3, and SeO_3. The analyses were made in the same manner as the carbonate samples with the exception that no scans were performed. Two sulphide analyses, both of pyrite, were rejected due to total weight percent of less than 95 wt.%.

Barite

The barite is very pure with only minor amounts of strontium and calcium. The average end-member composition for 21 analyses is 98.69 mol% $BaSO_4$, 0.23 mol% $CaSO_4$, and 1.08 mol% $SrSO_4$. The range of $SrSO_4$ content is shown in Figure 5-5. There were no relationships identified between Sr content, barite type or stratigraphic position of the sample.

Sphalerite

A total of nineteen analyses were made of Walton sphalerite. All sphalerite probed has a relatively pure ZnS composition with only a minor iron component. Contents of other metals are as follows: Fe avg.= 2280ppm; Mn avg.= 140ppm; and Cd avg.= 1480ppm (Fig. 5-6).

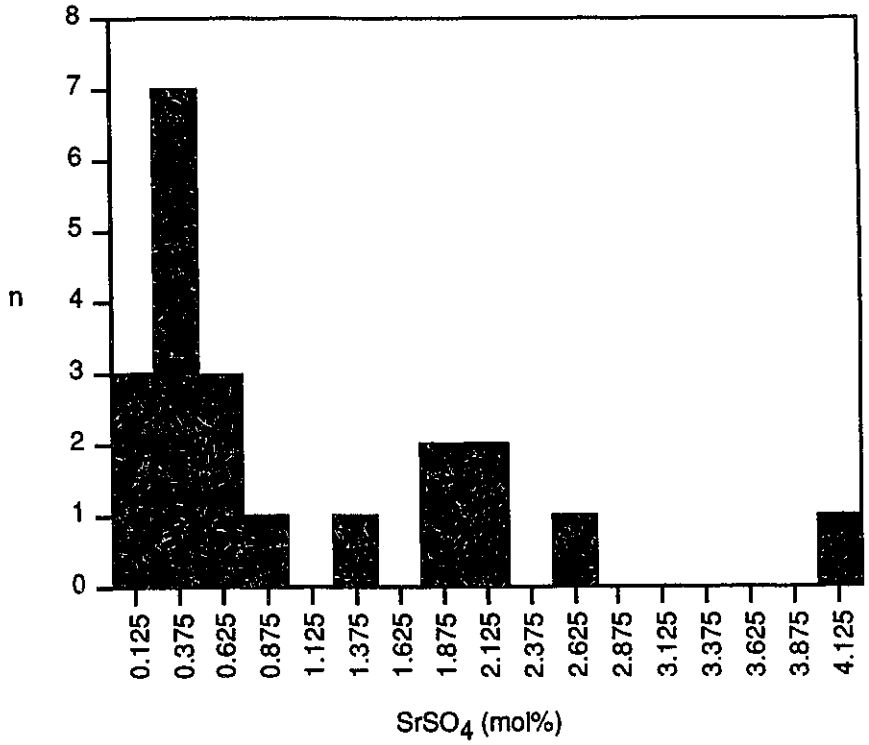

Figure 5-5. Frequency histogram of $SrSO_4$ content of 21 barite samples from Walton. n, number of data values.

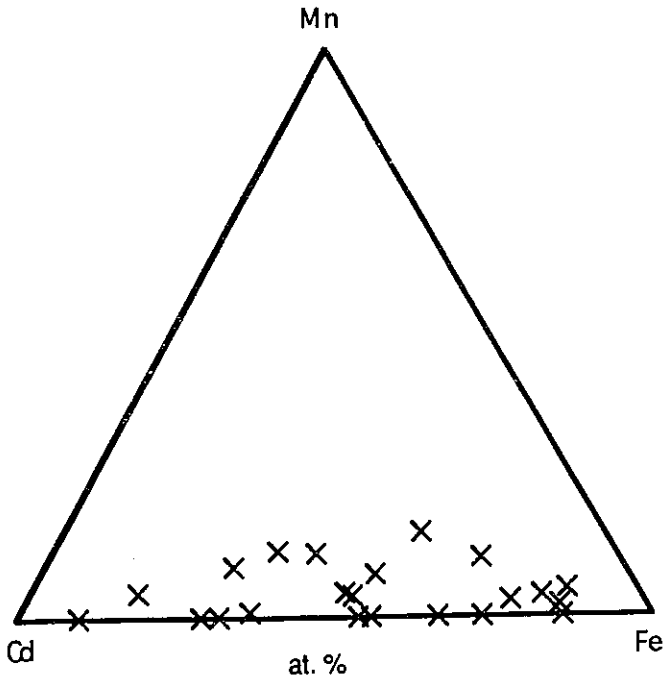

Figure 5-6. Mn-Fe-Cd ternary plot of sphalerite samples.

Tennantite

Tennantite is the As-rich end-member of the tennantite-tetrahedrite series which has the general formula $(Cu,Ag)_6Cu_4(Fe,Zn,Cu,Hg,Cd)_2(Sb,As,Bi,Te)_4(S,Se)_{13}$ (Johnson et al., 1986). The composition of the tennantite plots in two fields (Fig. 5-7). The first field, of coarse tennantite and tennantite bands in pyrite, has the approximate composition $Cu_{10}Fe_{1.3}Zn_{0.6}As_4S_{13}$. The second field is defined by one analysis of fine grained tennantite associated with sphalerite and galena; this sample has the composition $Cu_8Ag_{0.8}Fe_1Zn_{1.8}As_{3.8}S_{13}$.

Pyrite/ Marcasite

The most significant variation in the composition of pyrite and marcasite is in the arsenic content. Fifty-three analyses were made of pyrite and marcasite, 14 of pre-ore framboidal pyrite and 39 of ore-stage pyrite and marcasite. The framboidal pyrite has a low arsenic content averaging 0.85 atomic percent (at.%) As. The majority of the ore stage pyrite also has a low arsenic content, the same or even slightly lower than the framboidal pyrite, and an average of 0.18 at.% As. There are, however, a number of exceptions. Four pyrites with high arsenic content are very closely associated with tennantite, which has replaced bands in the pyrite. The arsenic and iron contents of these samples plot very close to a line drawn between the usual pyrite composition and tennantite composition (Fig. 5-8). The fact that these four samples also have very high Cu and slightly elevated Zn contents clearly suggests the presence of sub-microscopic inclusions of tennantite in the pyrite. Five other ore-stage pyrites have slightly higher than normal As. They are either late pyrite rims which are, in turn, rimmed by tennantite or they are late pyrite replacing siderite.

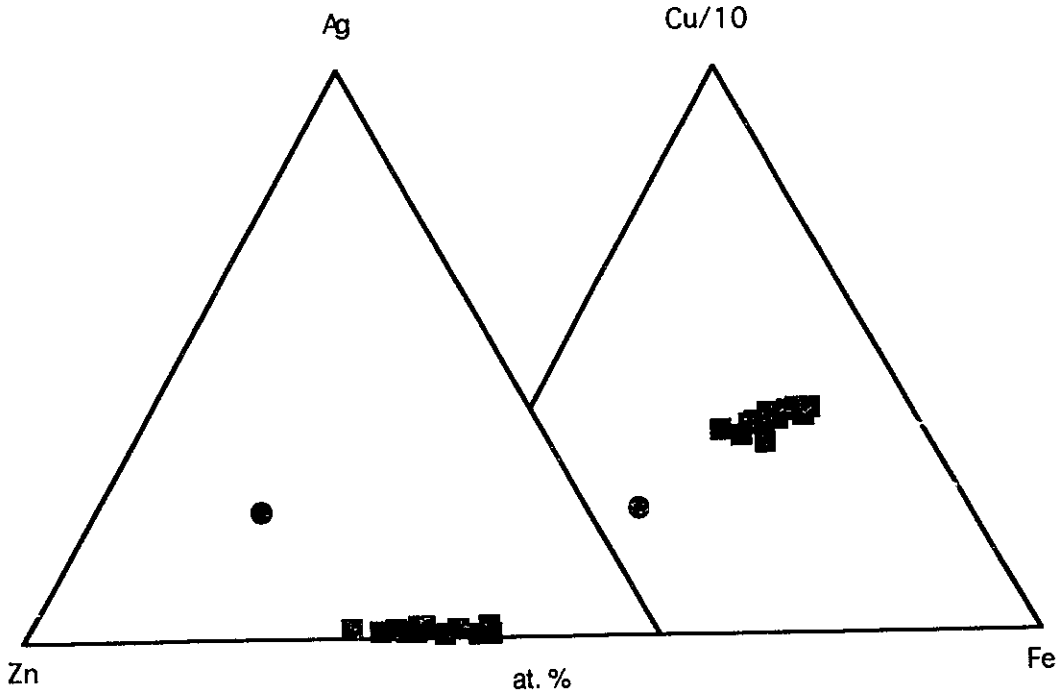

■ coarse grain
avg.$Cu_{10}Fe_{1.3}Zn_{0.6}As_4S_{13}$

● fine grain
avg.$Cu_8Ag_{0.8}Fe_1Zn_{1.8}As_{3.8}S_{13}$

Figure 5-7. Ag-Fe-Zn and Cu/10-Fe-Zn ternary plots of tennantite compositions.

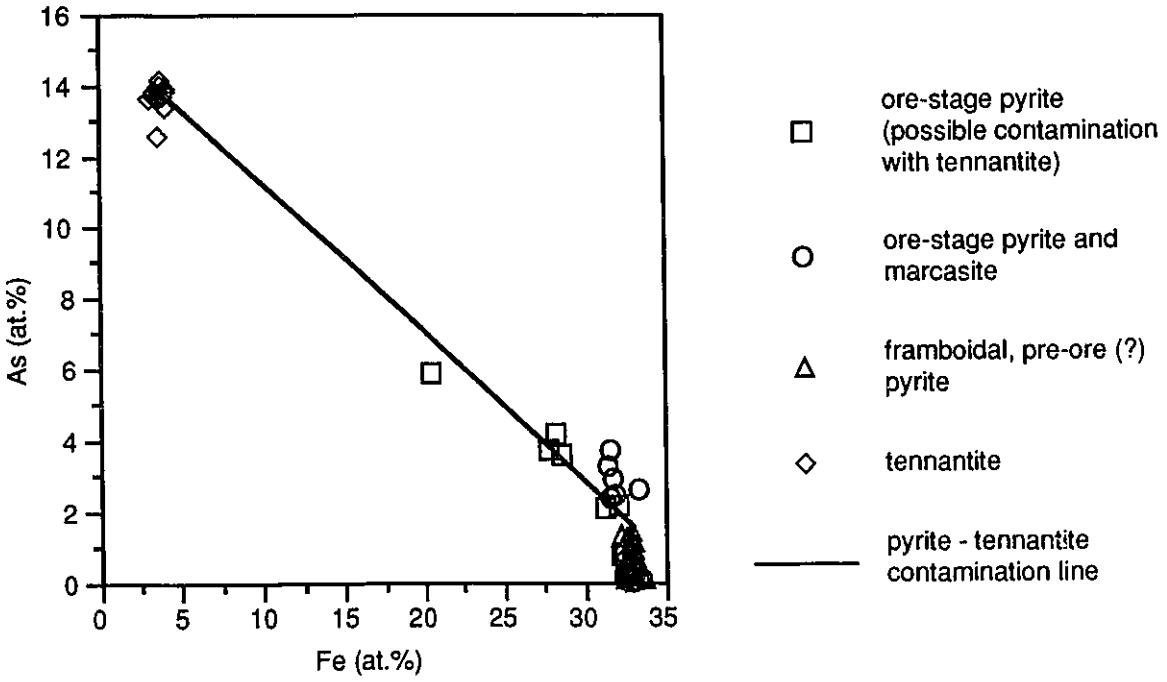

Figure 5-8. As vs Fe plot of pyrite compositions. Also shown are tennantite compositions and a proposed contamination line between pyrite and tennantite.

Chalcopyrite

Three analyses were made of chalcopyrite which is $CuFeS_2$. There was no significant substitution by other elements.

Rammelsbergite

An unidentified mineral which occurs in veins with tennantite and chalcopyrite, was probed for the elements Fe, Co, As, Ni, Sb, Se, and S. Six analyses have the average composition 1.20 at.% Fe, 8.94 at.% S, 2.00 at.% Co, 58.04 at.% As, and 29.02 at.% Ni. The simple mineral formula is $NiAs_2$, (para)rammelsbergite. This mineral was previously unreported in the Walton deposit.

CHAPTER 6
ORE TYPE CLASSIFICATION

INTRODUCTION

The Magnet Cove Barium Corporation analysed most mineralised intersections encountered in drilling along the B-baseline. As a result it is possible to study changes in metal content along each hole in detail and to relate these changes from one hole to the next. Samples from 843 intersections ranging in length from 6" to 26' were analysed. The frequency distribution of sample intervals is relatively constant, with 84% between 1.01' and 8.0' in length (Fig. 6-1). In addition, correlation coefficients between grade and sample interval range between -0.18 and 0.06 for the metals analysed indicating there is no systematic link between the two. For these reasons the analytical results were not normalised to a common sample interval. All samples were analysed for $BaSO_4$, Cu, Pb, Zn, Ag, and some were also analysed for Au, Cd, SiO_2, CaO, MgO, and Fe_2O_3 or FeO as well.

The average Cu, Pb, Zn, and Ag contents of the samples were calculated for the Horton, lower Macumber and upper Macumber (Table 6-1). These have also been plotted on ternary plots with the production grades for the entire deposit (Fig. 6-2).

DEFINITION OF ORE TYPES

Based on the analyses, a number of ore types were defined according to barite and metal ratios and contents. (It must be noted that although the term ore type is used, there is no economic implication to the term ore as it is used here.) The main ore type division is based on the ratio $BaSO_4/(BaSO_4+Pb+Cu)$ (Fig. 6-3). This ratio divides samples into those containing barite, hereafter called Type I, and those not containing barite, hereafter called Type II.

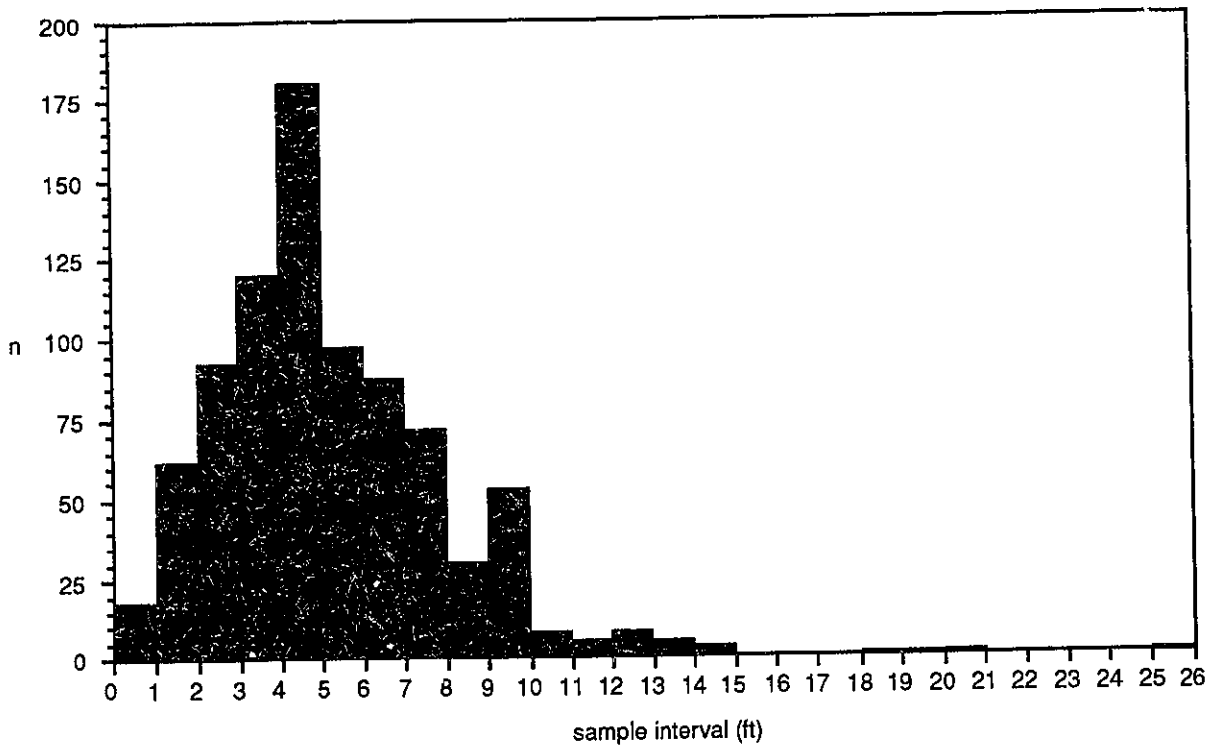

Figure 6-1. Frequency histogram of drill core sample intervals. n, number of data values.

	n	Cu (%)	Pb (%)	Zn (%)	Ag (g/t)	$BaSO_4$ (%)
upper and lower Macumber	827	0.33	1.94	0.15	109	22.00
upper Macumber	319	0.2	1.8	0.04	72	21.94
lower Macumber	508	0.41	2.03	0.22	132	22.03
Horton	15	0.26	0.2	0	56	0
production	-	0.52	4.28	1.3	350	-

Table 6-1. Average of drill core analyses for each stratigraphic unit and production grade (percentages are wt.%). n, number of samples analysed.

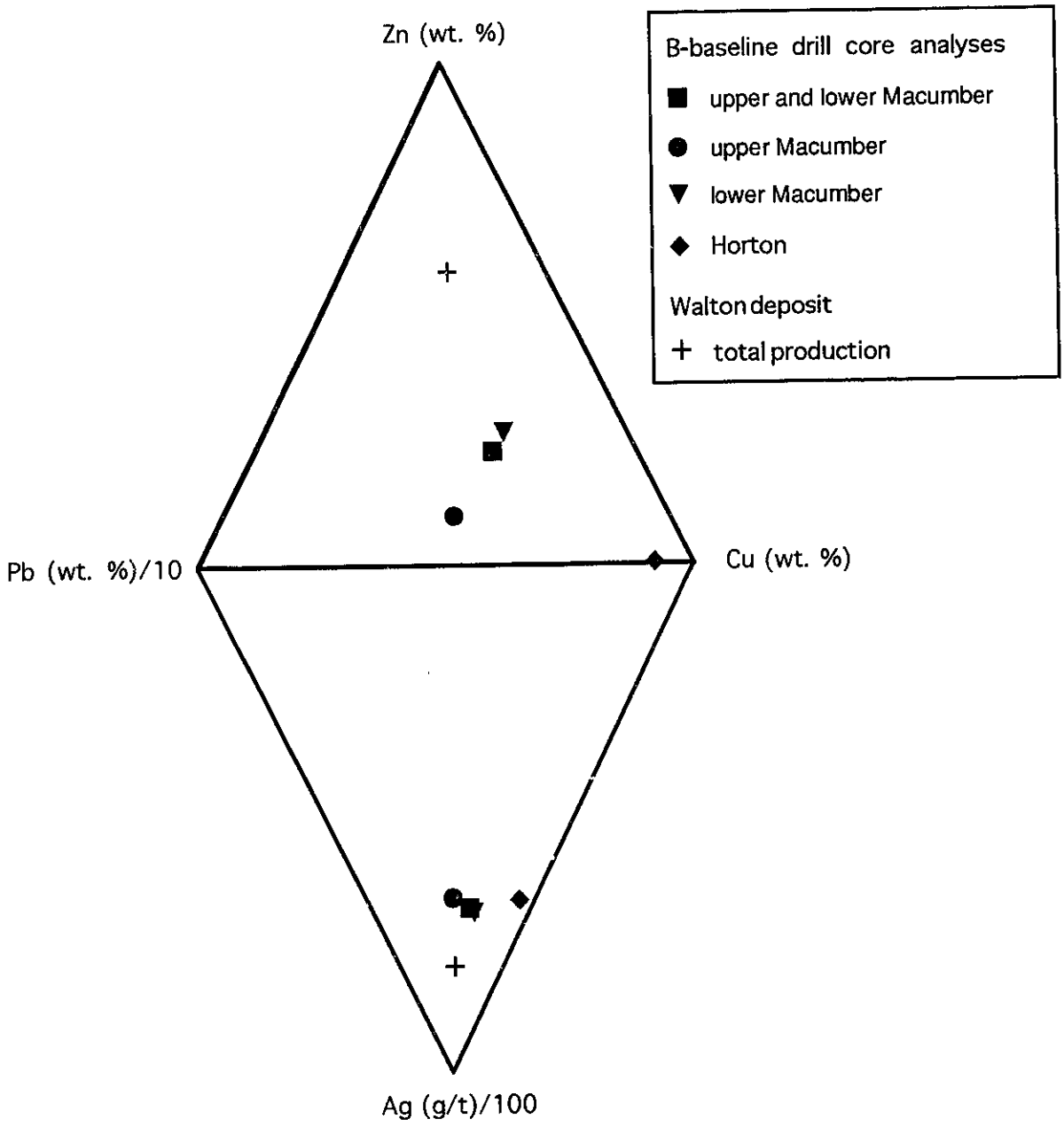

Figure 6-2. Cu-Zn-Pb and Cu-Pb-Ag ternary plots of average drill core analyses for upper and lower Macumber Formation and Horton Group samples. The production grades from the deposit are also plotted.

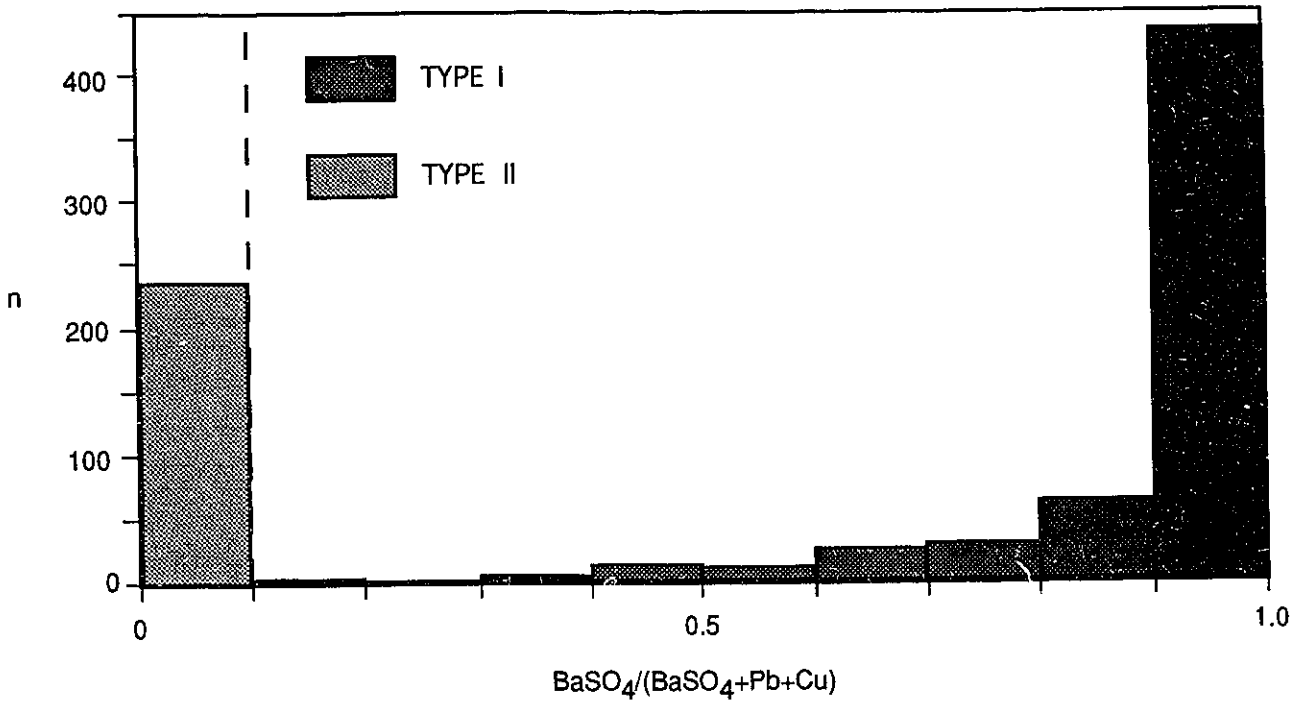

Figure 6-3. Frequency histogram of $BaSO_4/(BaSO_4+Pb+Cu)$ showing Type I and Type II ore. n, number of data values.

It appears that the majority of samples analysed contain either no barite or no Pb+Cu. This is more apparent than real as barite concentrations are generally an order of magnitude greater than either copper or lead contents. The average barite content is 31.15% whereas the average metal content is 0.27% Cu and 2.59% Pb for Type I ore. This results in most of the Type I samples plotting in the 90-100% $BaSO_4/(BaSO_4+Pb+Cu)$ range in Figure 6-3.

Within each ore type there is also a variation in the metal content as shown in histograms of Pb/(Pb+Cu) (Fig. 6-4). A majority of samples contain copper but no lead. Samples that do contain lead usually have small amounts of copper present as well. Depending on the amount of copper or lead present, each sample can also be classed as lead- or copper-rich. In some cases the sample may be lead- and copper-rich. The threshold between "normal" and "rich" has been taken at the 80th percentile. For lead this equates to >0% Pb for both Type I and Type II ore (Fig. 6-5). For copper this equates to >0.3% Cu for Type I ore and >0.6% Cu for Type II ore (Fig. 6-6). The definition of ore types is summarised in Figure 6-7.

SPATIAL DISTRIBUTION OF ORE TYPES

When the ore type definitions are applied to each of the analysed samples some interesting spatial patterns become apparent. When plotted on cross-sections of the deposit, the distribution of the ore types can be clearly seen and, when interpolated between sections, a three dimensional representation of the ore can be constructed. Initially the distribution of Type I and Type II ore will be explored, followed by examination of the lead-rich and copper-rich zones. The cross sections showing the geology and the ore zones are contained in Appendix I. It must be noted that during reconstruction of the cross-sections no attempt was made to interpolate the ore zones through the sand and limestone.

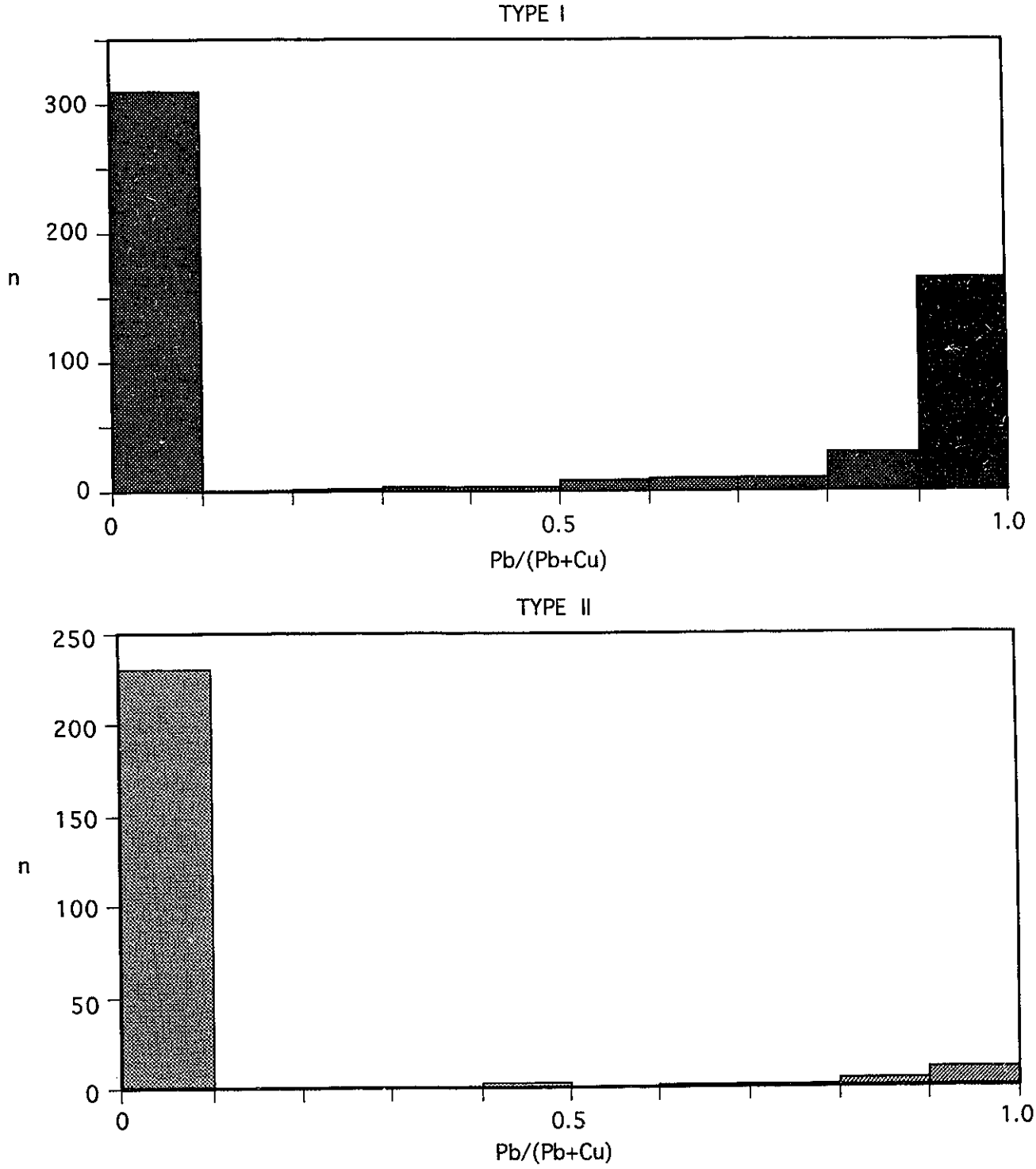

Figure 6-4. Frequency histogram of Pb/(Pb+Cu) for Type I and Type II ore. n, number of data values.

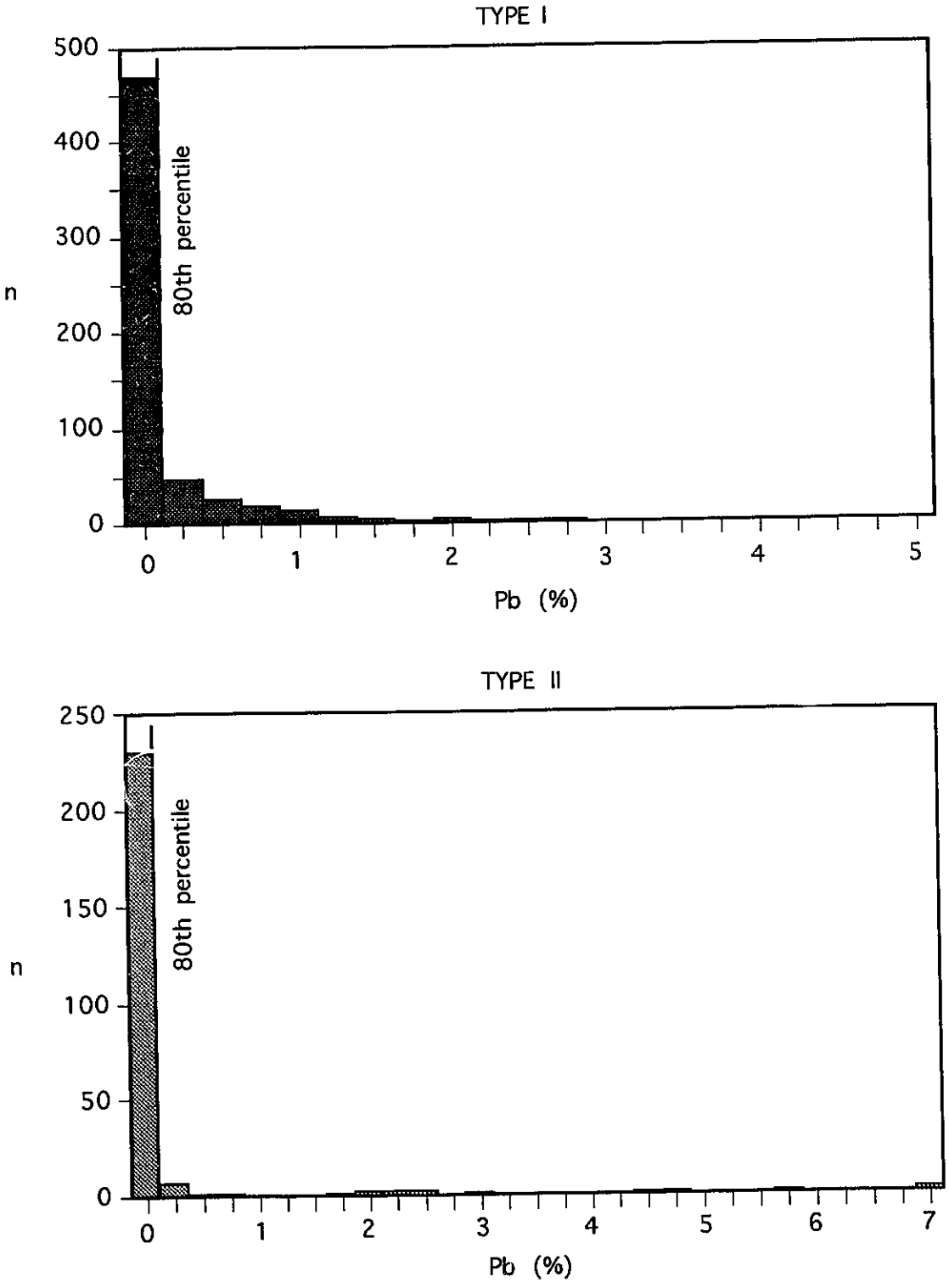

Figure 6-5. Frequency histogram of lead concentration for Type I and Type II ore, showing the 80th percentile division between Pb-rich and Pb-poor samples. n, number of data values.

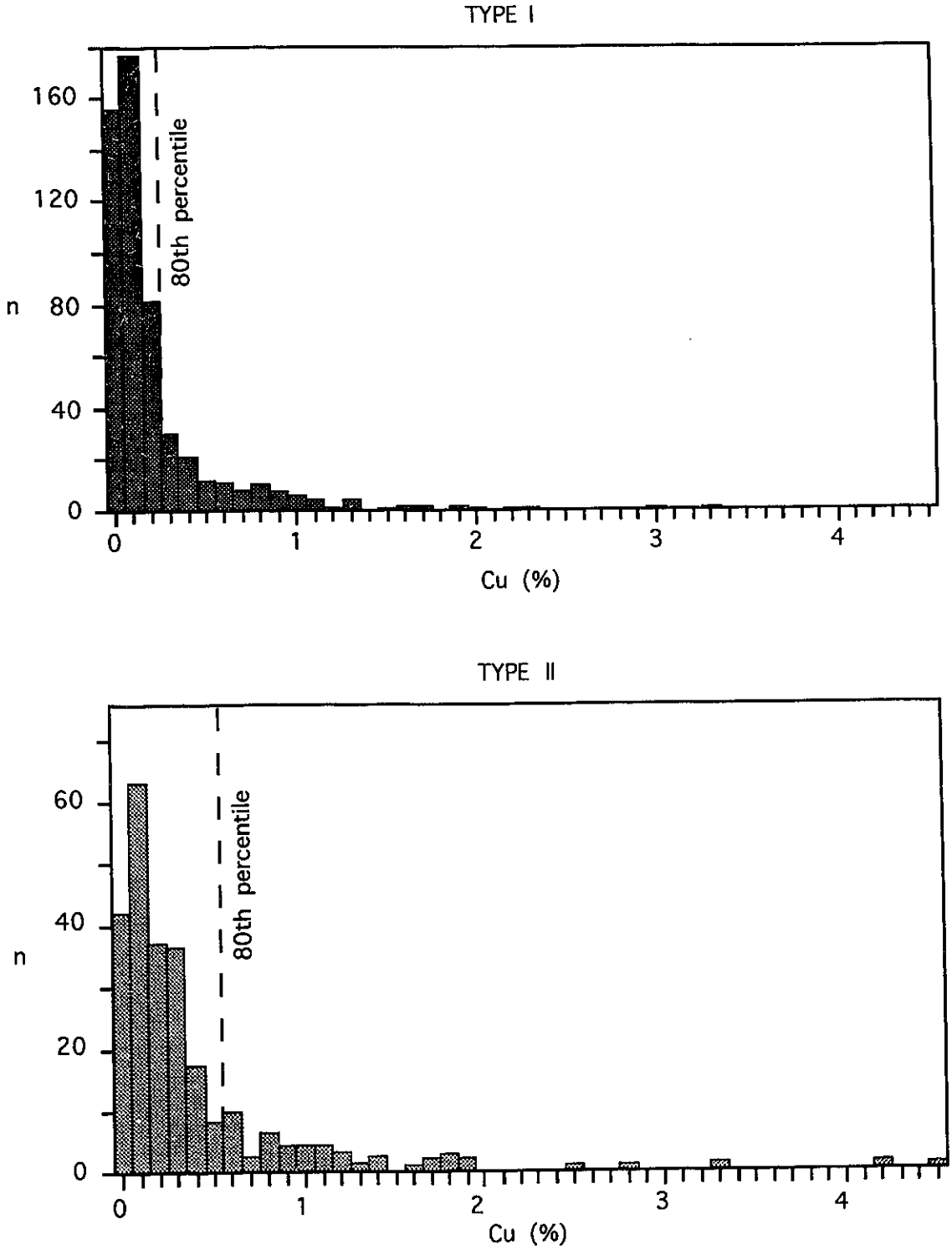

Figure 6-6. Frequency histogram of copper concentration for Type I and Type II ore, showing the 80th percentile division between Cu-rich and Cu-poor samples. n, number of data values.

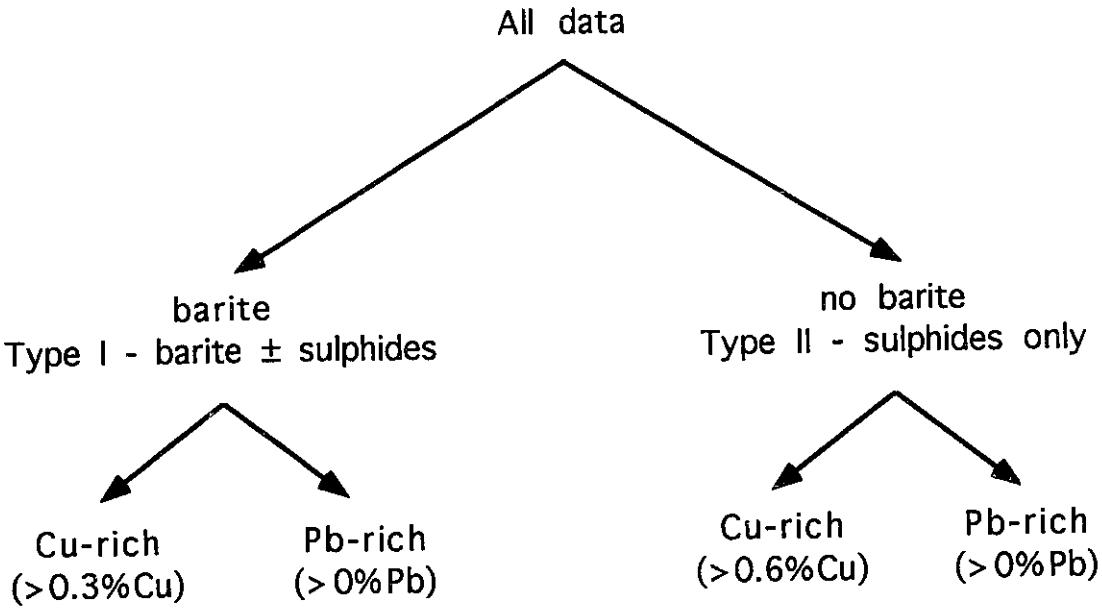

Figure 6-7. Summary of ore type classification.

Distribution of Type I Ore

In most sections the Type I (barite) ore occurs on all three mine levels on which drilling occurred, and an orebody can be interpolated by joining Type I ore in adjacent drill holes. In most cases the orebody is continuous between the drill holes on each mine level and can commonly be interpolated between mine levels. Within a section, the Type I orebody forms a generally uniform band immediately above and/or below the lower Macumber/upper Macumber contact (Fig. 6-8). The band ranges in thickness from approximately five to sixty-five feet throughout the deposit. Where Type I ore occurs in areas of thick upper Macumber, the orebody tends to thicken upwards into the upper Macumber. Barite ore never extends to the base of the lower Macumber, although, in many cases, it reaches the top of the Macumber present in a section whether it be upper or lower Macumber.

The band of Type I ore can also be interpolated between adjacent sections to form an almost continuous tabular body, along the B-baseline at all levels (Fig. 6-9). The only area where the barite orebody does not occur is the centre of the upper Macumber mound. Between sections 15 and 22 and mainly on the 850' level the barite orebody appears to be truncated by Type II ore.

Distribution of Type II Ore

Type II ore is much more restricted in its distribution than Type I ore and is much less continuous. It occurs mainly in an area between sections 15 and 24 and on the 850' and 1030' mine levels (Fig. 6-10). This area is coincident with the area of thick upper Macumber, although the Type II ore is most commonly found in the lower Macumber and the Horton. In many cases it is not possible to interpolate Type II ore from one drill hole to another, let alone from one level to another or from one section to another. The exception to this is at the centre of the upper Macumber mound, where Type II ore forms a more massive

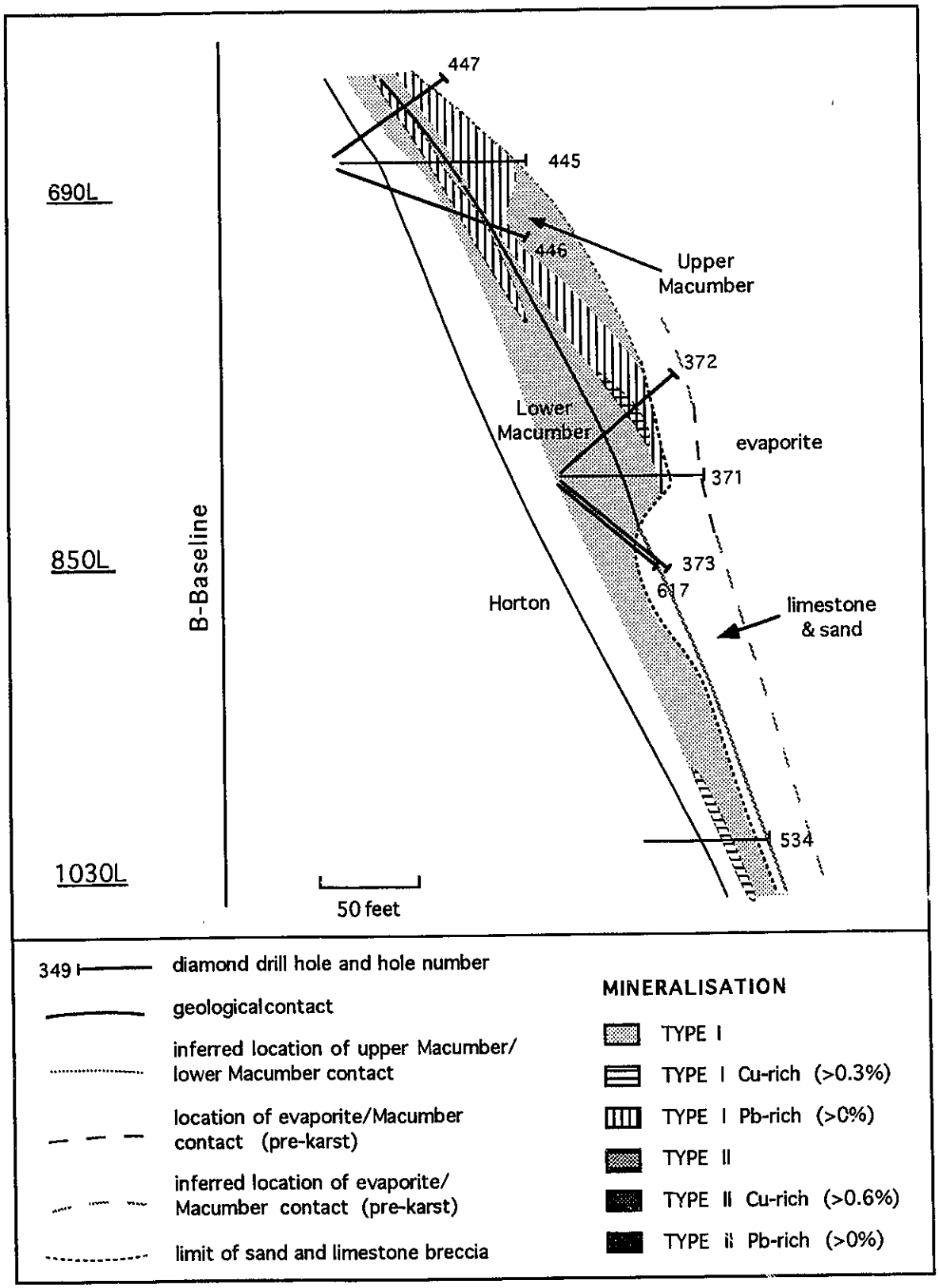

Figure 6-8. Cross-section #5, B-baseline, showing the continuous nature of Type I ore. Pb-rich zones occur as lenses within the Type I ore. Location of section #5 shown in Fig. 2-3.

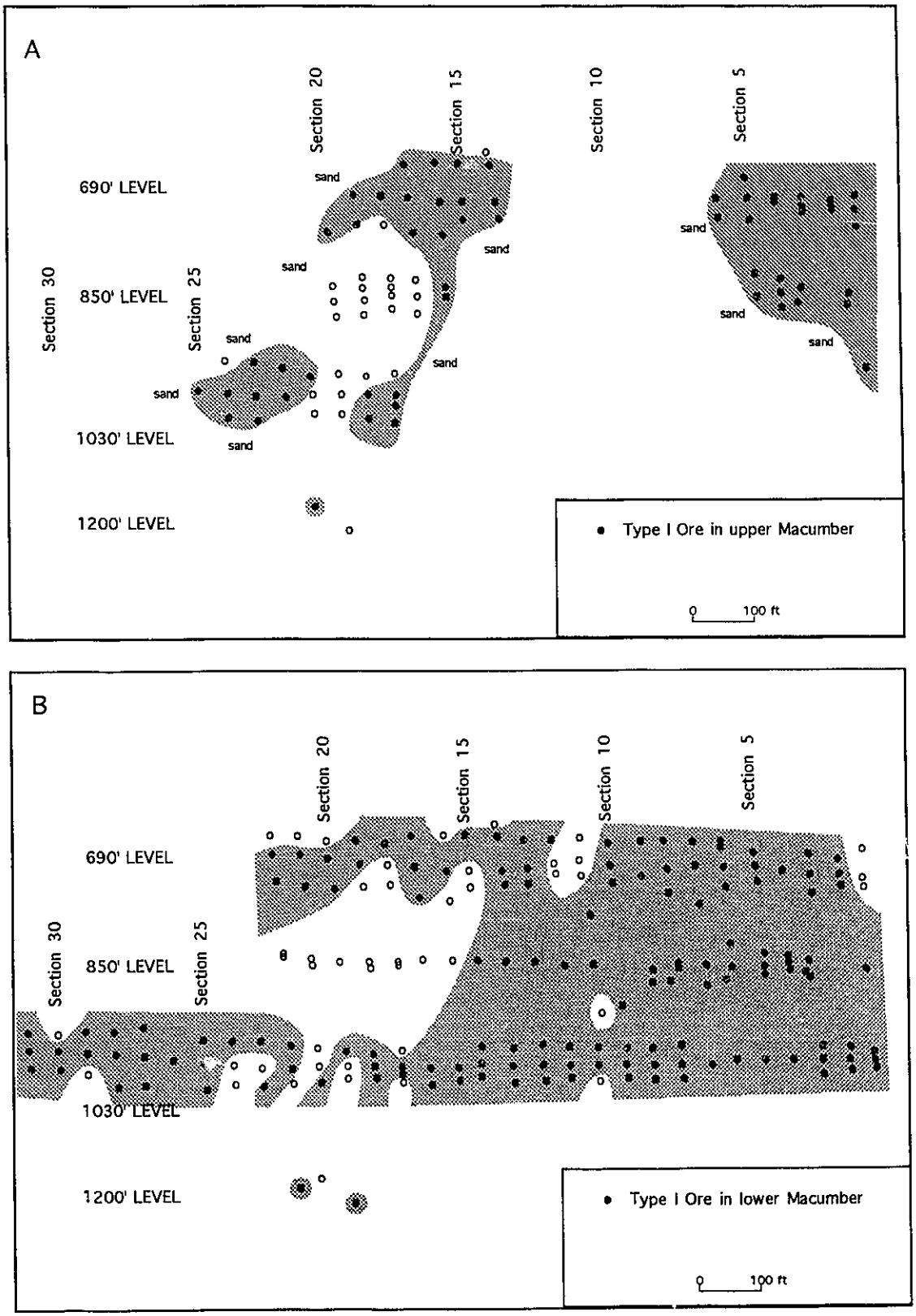

Figure 6-9. Plan maps of Type I ore distribution within the upper (A) and lower (B) Macumber. Type I ore within the upper Macumber is often cut by sand or limestone. Note that drill hole locations are their approximate intersection with the centre of the upper (A) or lower (B) Macumber.

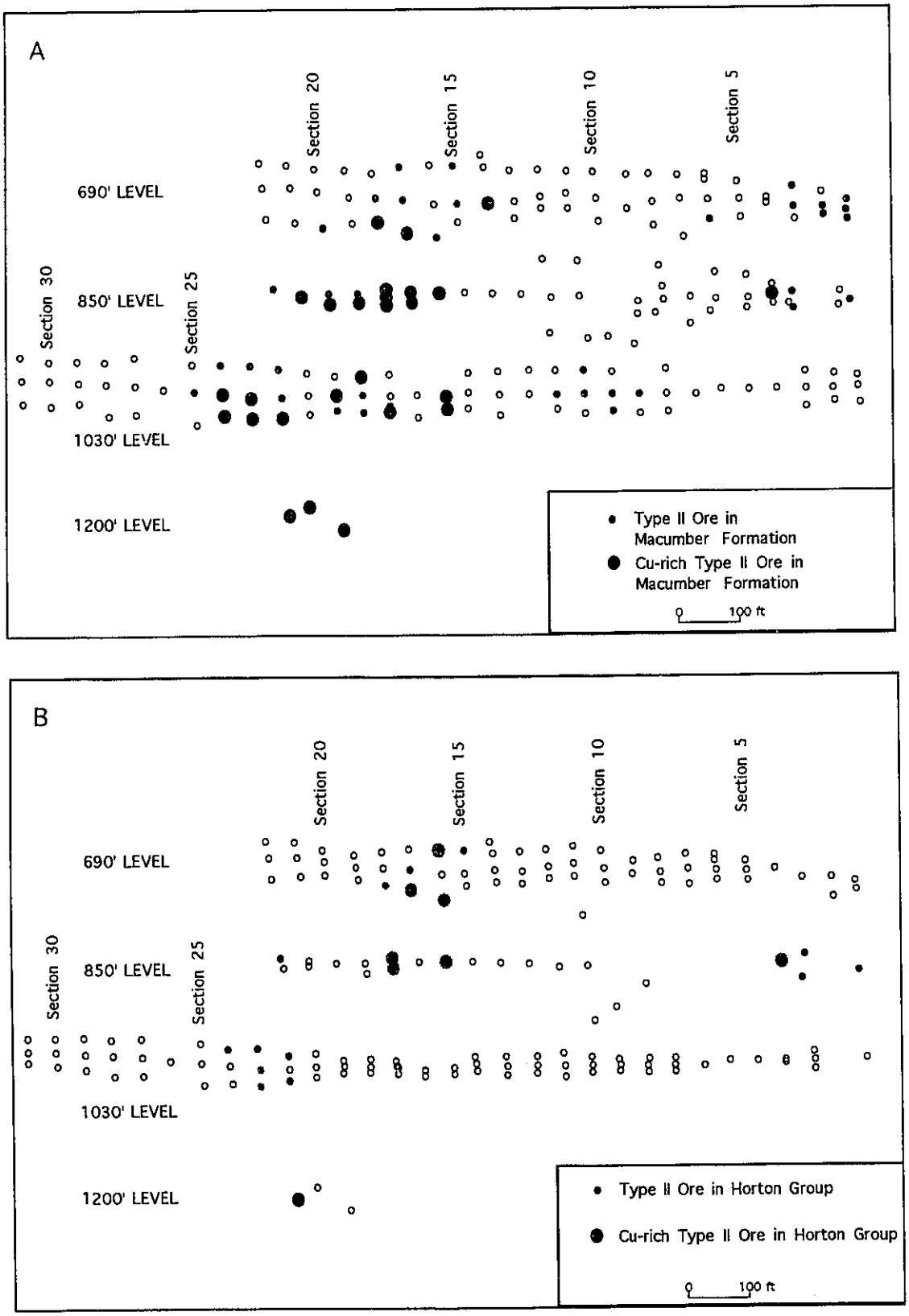

Figure 6-10. A. Plan map of Type II ore distribution within the Macumber, showing both Cu-rich and Cu-poor ore types. B. Plan map of Type II ore distribution within the Horton sandstone. Note that drill hole locations are their approximate intersection with the lower Macumber/upper Macumber contact (A) or the Horton/lower Macumber contact (B).

zone from the Horton sandstone to the top of the upper Macumber (Fig. 6-11). This zone occurs on the 850 level of sections 18, 19 and 20. There are much more limited Type II ore zones between sections 1 and 3 on the 690 level and between sections 8 and 12 on the 1030 level.

Unlike Type I ore, Type II ore may occur in the footwall Horton sandstone, usually immediately below the Horton/Macumber contact. Type II ore in sandstone is also coincident with the presence of thick upper Macumber (Fig. 6-10).

Distribution of Lead-Rich Ore

In some areas of the deposit it is possible to interpolate a lead-rich zone in much the same way it is to define a Type I ore zone. The Pb-rich orebody is more restricted in its distribution than the barite orebody and is less continuous. The lead-rich ore most commonly occurs within the Type I barite orebody, forming tabular to lenticular zones. The lead-rich zones may occur at any stratigraphic level within the barite: at the base of the barite orebody; immediately above and/or below the upper Macumber/lower Macumber contact; and within and at the top of the upper Macumber (Fig. 6-8). In some cases there is a lead-poor band at the upper Macumber/lower Macumber contact with lead-rich zones stratigraphically above and below the lead-poor zone. As with the barite ore, the lead-rich zones tend to be stratigraphically higher where the upper Macumber is thickest.

Lead-rich ore also occurs in several sections outside the barite ore. The best example of this is in section 20, where the lead-rich ore zone extends out of the Type I orebody and into the Type II orebody. While based on only two drill holes, the lead-rich zone appears to be continuous and independent of the Type I ore to Type II ore transition.

The lead-rich ore zone is most continuous over all three mine levels between sections 1 and 14 (Fig. 6-12). From sections 14 to 20 it occurs predominantiy within

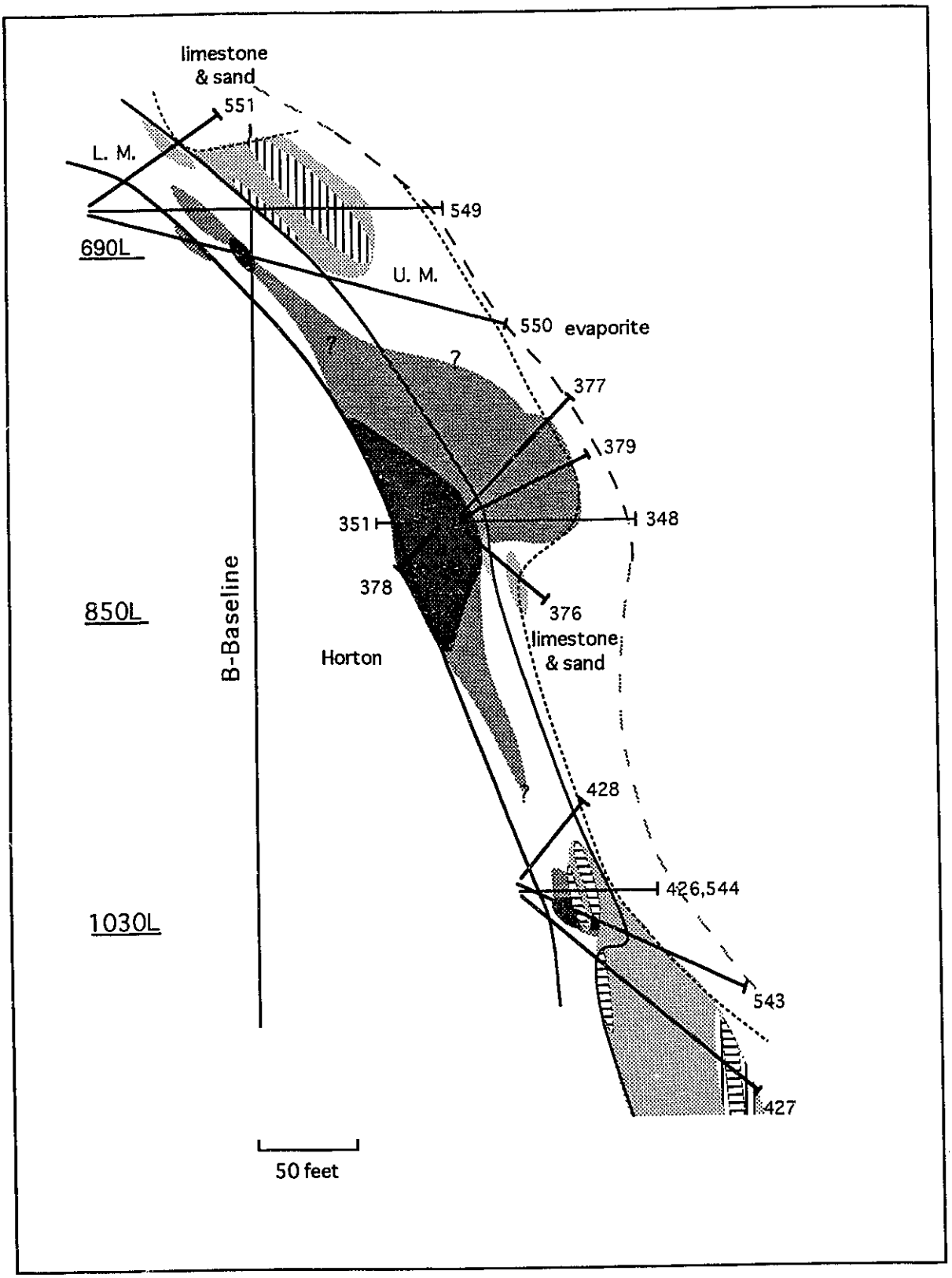

Figure 6-11. Cross-section #18, B-baseline, showing a Type II ore zone within the lower and upper Macumber. Cu-rich Type II ore extends into the top of the Horton sandstone. Type I ore is truncated by the Type II ore zone. Location of section #18 is shown in Fig. 2-3. See Figure 6-8 for legend.

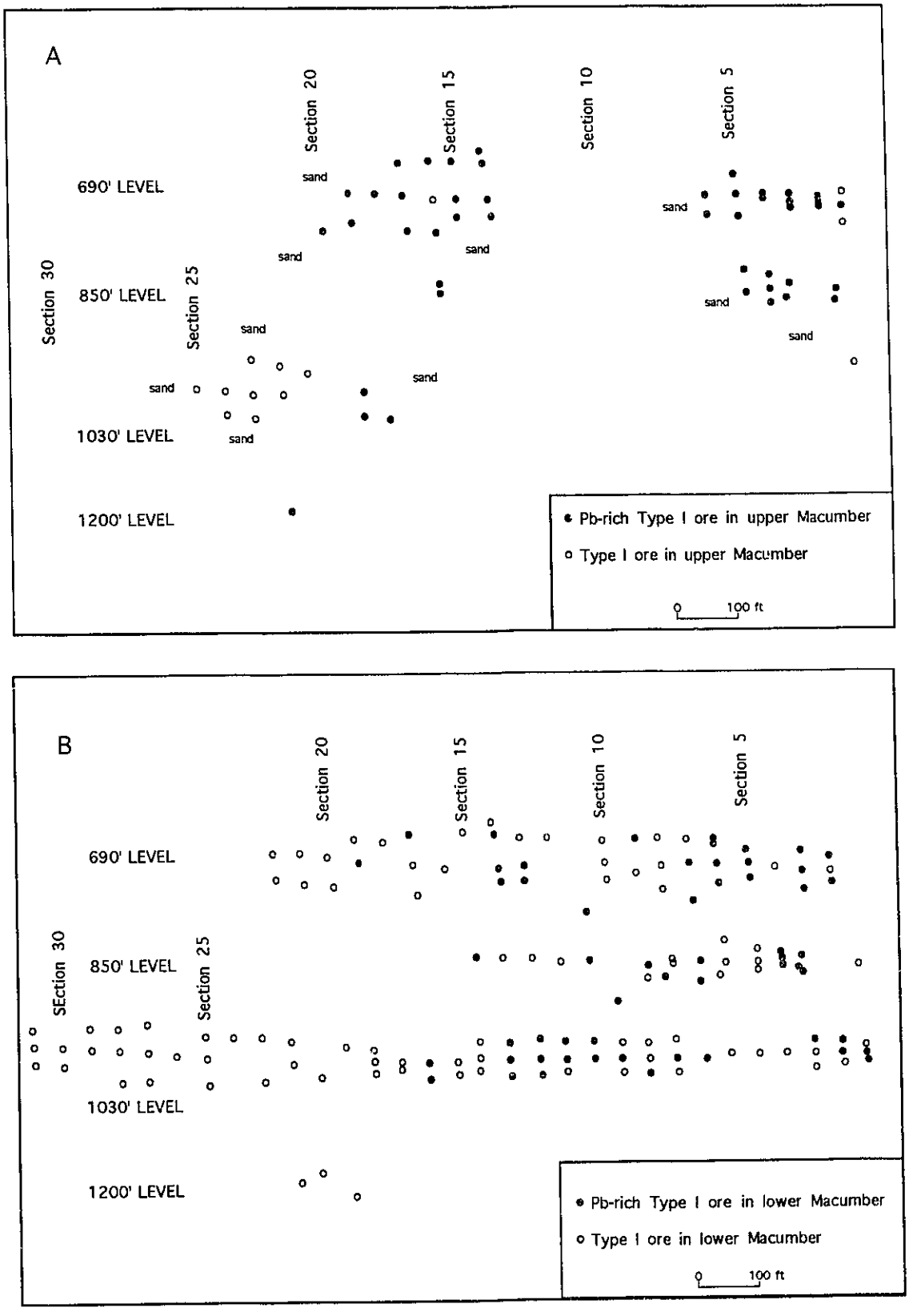

Figure 6-12. Plan map of Pb-rich Type I ore distribution within the (A) upper and (B) lower Macumber. Note that drill hole locations are their approximate intersection with the centre of the upper (A) or lower (B) Macumber.

theupper Macumber, forming a ring around the area of thickest Macumber. Lead-rich ore is absent from the 1030 level between sections 20 and 31.

Distribution of Copper-Rich Ore

Copper-rich ore may be of either Type I or Type II. Cu-rich Type I ore is very discontinuous and cannot be traced from one drill hole to another. There are however a few distinct regions in which the ore type occurs. It is most common on the 1030 level where it forms a discontinuous ribbon at or near the base of the Type I barite ore. It is also found in a zone between Sections 1 and 6 on the 850 level. On the 690 level it is only found in scattered individual drill holes. In the area of the upper Macumber mound on the 1030 level the Cu-rich Type I ore forms a continuous ribbon with Type II ore.

Copper-rich Type II ore is localised in the area of the thickest upper Macumber mound where it occurs at the base and in the core of the normal Type II ore. It occurs mainly in the lower Macumber but also in the Horton sandstone.

METAL ZONING

The average barite and metal contents for Type I and Type II ore are 0.3% Cu, 2.5% Pb, 0.2% Zn, 133g/t Ag, and 31.2% $BaSO_4$ and 0.5% Cu, 0.5% Pb, 0.1% Zn, 51 g/t Cu, and 0% $BaSO_4$ respectively (Table 6-2). As was shown in Table 6-1, the average metal contents for the lower Macumber are higher than those for the upper Macumber, a trend that is also true within each ore type (Table 6-2). A general trend in metal zoning can be summarised as increasing lead, zinc and silver and decreasing copper away from the upper Macumber mounds and a decrease in all metals upward through the Macumber.

The distribution of silver remains problematic. No systematic pattern of silver distribution (other than the general trend noted above) was recognised in this study.

	n	Cu (%)	Pb (%)	Zn (%)	Ag (g/t)	$BaSO_4$ (%)
Type I	583	0.27	2.53	0.18	133	31.2
upper Macumber	227	0.19	2.41	0.05	80	30.83
lower Macumber	356	0.32	2.61	0.27	167	31.43
Type II	259	0.45	0.51	0.08	51	0
upper Macumber	92	0.23	0.29	0.03	50	0
lower Macumber	152	0.61	0.67	0.11	50	0
Horton	15	0.26	0.2	0	56	0

Table 6-2. Average of drill core analyses (percentages are wt.%) for each ore type and stratigraphic unit. n, number of samples analysed.

Patterson (1987; 1988a,b; 1989) also failed to identify a clear relationship between silver distribution and the other metals.

CHAPTER 7

DISCUSSION, GENESIS, AND EXPLORATION GUIDELINES

DISCUSSION

The presence of an exceptional thickness of upper Macumber was very important in the formation of the Walton deposit because the larger rock volume enhanced the potential site of mineralisation. There also appears to be a relationship between the upper Macumber breccia mounds, mineralisation in the Horton Group rocks, and Type II ore zones. The most likely cause of these phenomena could be synsedimentary faulting although no direct evidence of faulting is evident in the available cross-sections. Lavoie and Sangster (1995) attribute the mound to synsedimentary slumping and suggest that the presence of interbedded evaporite may have been important in inducing synsedimentary movement along depositional slopes. The upper Macumber is unrecognised elsewhere in the Kennetcook basin and it is perhaps significant that other base metal occurrences in the basin are very small and are hosted solely by lower Macumber carbonate.

The absence of any banding within the stratiform Type I ore suggests that the Walton deposit did not form as the product of an exhalative event. Had the ore fluids exhaled onto the open sea floor, in the form of either a heavy brine or a buoyant plume, it would be expected that some layering or banding of the barite and sulphide minerals, typical of exhalative deposits, would have occurred. The absence of such layering, coupled with the abundant replacement and open space filling textures of the minerals, indicates that ore deposition was epigenetic. Since the first stage of the mineralising process was the replacement of limestone or dolostone by siderite, the age of this initial event may place constraints on the timing of mineralisation. Unfortunately the only evidence with respect to age of

sideritisation is that it occurred after synsedimentary slumping of the upper Macumber (Lavoie and Sangster, 1995) and prior to karsting.

Replacement of the original Macumber carbonate by siderite was the first stage of the mineralising process. A few minor pods of ankerite are considered to be an intermediate stage of the replacement process and occur in the uppermost part of the upper Macumber mound. Sideritisation is widespread; calculations show that more than 10 million tonnes of siderite are present in the B-baseline area alone, prior to replacement by barite and sulphides and post-ore karsting. Since the actual extent of the sideritisation is unknown, this figure is based on a known strike length of 1750' (length of B-baseline is 1500'), a width of 750' (from 450' below surface to 1200' below surface), an average thickness of the Macumber of 70' and a specific gravity of 3.85. The actual mass of siderite, including the area of the main pipe, could easily double that figure. By comparison, the Helen siderite deposit near Wawa, Ontario produced approximately 60 million tonnes of siderite (Morton and Nebel, 1984).

The fact that siderite is contained entirely within the Macumber Formation and occurs neither within the alteration zones in the footwall Horton sandstones nor in the evaporite suggests that there was no CO_2 in the iron-rich fluids which formed the siderite. Formation of siderite was by substitution of Fe^{2+} for Ca^{2+} and Mg^{2+} in the carbonate, with no CO_3^{2-} provided by the mineralising fluid. Alteration of the Horton sandstone by the iron-rich fluids resulted in the precipitation of pyrite rather than siderite.

The composition of the siderite appears to be related more to stratigraphic position than to textural type (and therefore relative age) of siderite. Siderite compositions from upper Macumber samples have a lower $FeCO_3/(FeCO_3+MgCO_3)$ value than samples from the lower Macumber (Fig. 5-5). As has been previously mentioned, some samples from the upper Macumber have the composition of ankerite, a much less iron-rich phase. It is therefore suggested that the uppermost Macumber was less affected by the iron-rich fluids

than the lower parts of the Macumber. The lack of variation in siderite composition among siderite types within a single sample (Fig. 5-6) suggests that the different siderite types are the result of recrystallisation rather than the influx of a fluid of a new composition. The recrystallisation probably resulted from the injection of a hot fluid responsible for a later mineral stage, usually barite.

The paragenetic sequence of minerals in the B-baseline portion of the deposit is, for the most part, very similar to that determined by Boyle (1972) for the main barite pipe and its underlying sulphide zone (Fig. 7-1). There are, however, a few differences, the most significant of which is the absence of discrete silver minerals in the B-baseline portion of the deposit. Boyle (1972) recognised a series of sulphosalt minerals including proustite (Ag_3AsS_3), pearcite ($(Ag,Cu)_{32}As_4S_{22}$), acanthite (Ag_2S), stromeyerite (CuAgS), and gersdorffite (NiAsS), which formed late in the paragenesis, after barite veins. Since these minerals were not encountered in samples from the B-baseline, it must be concluded that conditions effecting metal deposition in the sulphide zone below the main pipe were different from those on the B-baseline, or the fluid which mineralised the two areas had different compositions. It has been previously noted that the sulphide zone below the main pipe is more zinc-rich than the B-baseline, another reflection of differing conditions between the two areas.

Perhaps the most significant finding of this study is the recognition of two main ore types with distinct compositions and distributions within the deposit. Barite-rich Type I ore has a continuous tabular shape within the carbonate host rocks except where it is interrupted by the more discordant Type II sulphide ore.

Type I ore has a widespread distribution throughout the deposit, occurring as a semi-conformable sheet replacing siderite. It is difficult to assign an exact thickness to the barite body because, in many locations, dissolution has removed the upper part of the Macumber with subsequent infilling with limestone breccia and sand. In areas where the top

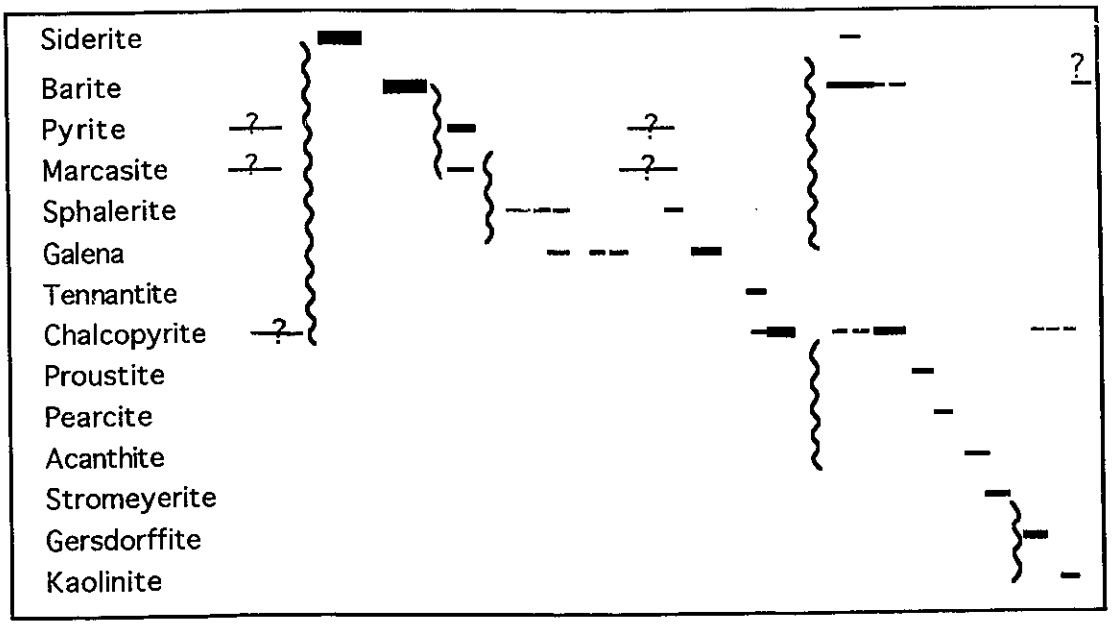

Figure 7-1. Paragenesis of the principal hypogene minerals in the Walton deposit. From Boyle (1972).

of the barite ore is intact, Type I ore thickness ranges from 8' to 67' averaging 28'. As may be expected, Type I ore is generally thickest where the Macumber is thickest, although it is not present in the area of thickest upper Macumber where it is cut by Type II ore. Type I ore is not continuous across the upper Macumber mound between sections 17 and 21 and it appears that Type II ore has replaced the Type I ore. On section 20 (Appendix I) the lead-rich zones are continuous between the Type I ore and the Type II ore. The truncated nature of the barite zones, the continuation of lead-rich zones across the Type I - Type II boundary, the presence of a few intersections of barite within the Type II ore, and the late paragenetic position of chalcopyrite compared to barite all suggest that Type I ore was once continuous across the mound but that the barite was replaced by the Type II mineralisation. This is similar to patterns observed in some sedimentary-exhalative (Hamilton et al., 1983) and volcanogenic massive sulphide deposits (Lydon, 1984).

Type I ore usually straddles the lower Macumber/upper Macumber contact and never extends down to the lower Macumber/Horton contact. One possible explanation for this pattern is that the fluids moved laterally through the porous upper Macumber breccia and entered the lower Macumber from above, thereby preferentially replacing the upper portion of the lower Macumber. A second possibility is that there was a lithological control on mineralisation. There are two lithosomes within the Macumber Formation, an upper finely laminated unit, and a lower ooid bearing unit. The upper unit contains carbonaceous material in stylolites which may have aided the reduction of sulphate and therefore localised the site of mineral precipitation.

Type II ore shows a close association with the upper Macumber mounds and is most commonly found within the mounds or in the lower Macumber below the mounds (Fig. 6-10). The upper Macumber mounds are also coincident with several local copper occurrences in the footwall Horton sandstone. Copper at the Horton-Macumber contact is widespread in Nova Scotia and Kirkham (1974) states that these regional occurrences are remarkably

similar throughout Nova Scotia, consisting of red conglomerate overlain by a thin layer of green conglomerate, in turn overlain by a sandy limestone. Mineralisation is in the form of disseminated pyrite, chalcopyrite, and, at some localities, bornite and chalcocite, within the upper part of the green conglomerate and the lower part of the limestone. This is clearly different from the mineralisation in the Horton sandstone at Walton, which occurs in sandstones rather than conglomerate and is more massive than disseminated. In all, 167 drill holes on the B-baseline intersected the Horton Group and of these only 21 intersected copper mineralisation. All 21 intersections were located only below the mounds rather than being dispersed over the entire length of the B-baseline. It is therefore concluded that the mineralisation in the Horton sandstone formed as part of the large scale and localised process at Walton rather than as a separate event related to regionally occurring copper mineralisation such as that described by Kirkham (1974).

There are a number of similarities between the B-baseline barite-sulphide zone and the barite and sulphide zones of the main pipe. Figure 7-2 shows a plan map of the 690' level combining results of this study and those of Boyle (1972). The main pipe has been re-drawn to show the massive barite of Boyle as Type I ore and all sulphide mineralisation of Boyle as Type II ore. Boyle's (1972) cross-sections through the main deposit resemble those through the ore zones of the B-baseline (Fig. 7-3). Section A-B (Fig. 7-3A) shows a massive barite zone above a variable thickness of Macumber. This pattern is the same as Type I ore within the upper portion of the lower Macumber on the B-baseline (Fig. 6-8). Section C-D shows a sulphide-rich zone at the base of the Macumber. The sulphides are overlain by barite and underlain by pyritic Horton sandstone. If all Boyle's "sulphide ore" is re-interpreted to be equivalent to Type II ore (Fig. 7-3B) the pattern on section C-D is analogous to Type II ore zones on the B-baseline (Fig. 6-11). The major difference between the two areas is the volume of the alteration and mineralisation. The barite ore shown on section A-B has a thickness of between 40' and 100', whereas the Type I ore on the B-

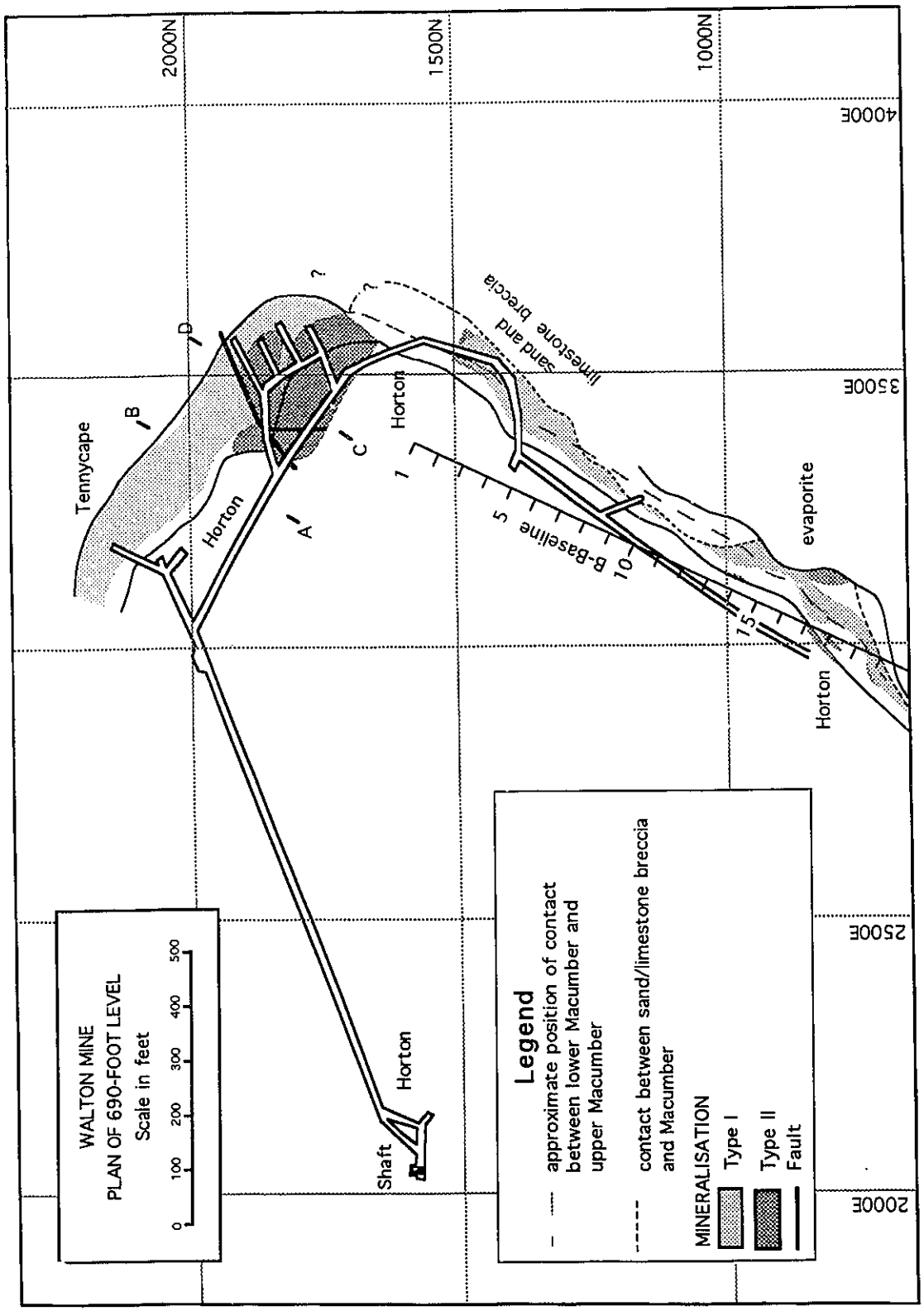

Figure 7-2. Plan map of 690' level; composite plan from Boyle (1972; Fig. 6) and this study. Sections A-B and C-D are shown in Figure 7-3.

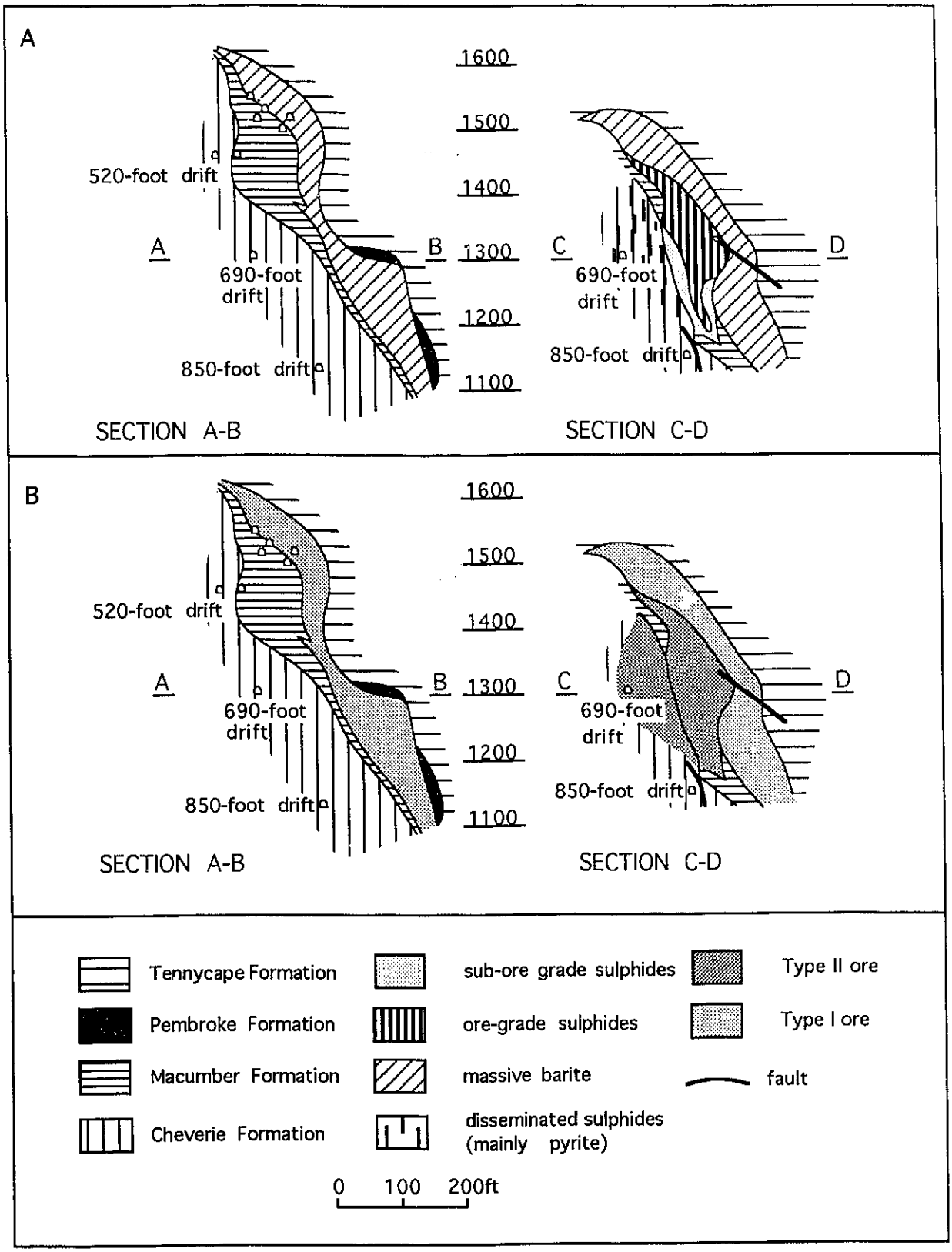

Figure 7-3. A. Cross-sections A-B and C-D through the main deposit (see Fig. 7-2) as shown in Boyle (1972; Fig. 6). B. Cross-sections A-B and C-D modified to show the massive barite as Type I ore and sulphide zones as Type II ore.

baseline ranges between 8' and 67', with an average thickness of 28'. This discrepancy may be largely due to the removal of portions of the top of the Type I ore by karst processes, with the original thickness of the barite ore being controlled by the thickness of the Macumber. On section C-D the sulphide zone in the Macumber Formation ranges from 40' to 100' in thickness, which is comparable to Type II ore on the B-baseline. The volume of alteration in the footwall sandstone is much greater under the main pipe than under any part of B-baseline. In section C-D the pyritisation is shown to extend more than 75' into the footwall in an area of 200' radius. This scale of footwall alteration has not been recognised on the B-baseline, where alteration does not appear to extend deeper than about 10' into the sandstone and is much more limited in lateral extent. It should be noted that a 690' level drift passes through the pyrite alteration zone below the sulphide zone on section C-D, whereas on the B-baseline there was only limited drilling into the Horton below the Type II ore zone (i.e. 850' level between sections 17 and 21). Drill holes in that area only extend 10 to 15 feet into the Horton, and it is possible that, had drilling continued deeper into the Horton, a much larger pyrite zone may have been defined.

Post-ore karsting has had the effect of removing a large portion of the mineralisation at Walton. In many cases an unknown volume of the upper portions of Type I ore has been removed; calcareous sands and limestone breccias now occur in its place. The sand and limestone breccia may represent the products of karsting and infill and may be equivalent to the solution collapse products recognised by Clifton (1967) and to the *Pembroke Breccia* of Lavoie and Sangster (1995) and others. An attempt was made in this study to interpret the original position of the Macumber/evaporite contact, in order to give some idea of the actual thickness of both the upper and lower Macumber prior to karsting. The thickness of the sand and limestone infill ranges from 0' to 90', with an average thickness of about 25'. Assuming a strike length of 1750' (length of B-baseline 1500') and that the karst extends from surface to a depth of 1100' (deepest occurrence of sand), the

volume of sand and limestone breccia infill on the B-baseline is in the order of 1.4 million m^3.

GENESIS

Factors to be Considered

Fluids

Source

Mineralisation at Walton shows no obvious relationship to any igneous body, the only igneous rocks in the area being two small diabase sills (Triassic) in Johnson Cove 10km west of Walton and Triassic North Mountain basalts 16km west of Walton (Boyle, 1972). This lack of igneous association coupled with the style and stratigraphic position of the mineralisation clearly indicates a sedimentary origin for the ore-forming fluids.

A source for the ore-forming fluids to the north of the Kennetcook basin is suggested by several factors. The most obvious indication is that all significant mineral occurrences are located along the north rim of the Kennetcook basin. The same is true for the nearby Shubenacadie - Musquodoboit basin, where most occurrences are located in the northernmost Shubenacadie basin. At the Gays River deposit, which is located on a palaeotopographic high between the Shubenacadie and Musquodoboit basins, high grade mineralisation only occurs on the north side of the carbonate mound, also suggesting that ore fluids originated to the north (Sangster and Savard, 1994).

Ravenhurst et al. (1989) suggested the fluids which formed lead-zinc and barite deposits in and around the Kennetcook, Shubenacadie and Musquodoboit basins originated deep within the Magdalen Basin to the north, but they would prefer an unknown deep basin south of the Cobequid-Chedabucto fault as a more attractive source for the fluids. They also acknowledge the possibility that the fluids may have originated deep within the granite-metasedimentary basement.

Driving mechanism

There are a number of possible mechanisms by which an ore fluid can be transported from deep within a sedimentary basin to the site of ore deposition including basin water expulsion by sediment compaction (Jackson and Beales, 1967), episodic dewatering due to overpressuring (Cathles and Smith, 1983), and gravity driven fluid flow (Garven, 1985). Cathles and Smith (1983) found that normal rates of basin subsidence and compaction result in flow rates that are too low to transport the 100+°C fluids necessary for ore formation to the near surface. They concluded that the expulsion of geopressured brines must occur episodically in order to preserve the temperatures necessary to be important in ore formation. Other studies have shown that some basins may never have been geopressured enough to be significant in the fluid flow history (Garven, 1985). Alternatively, it has been demonstrated that fluid flow can be rapidly driven by the hydraulic gradient created by a sloping water table. Fluid flow will be across formations in the elevated recharge area of the basin and will be strongly focused along permeable aquifers within and at the margins of the basin (Garven and Freeze, 1984a,b). Continuous recharge at the area of uplift within the basin allows enormous quantities of fluids to pass through the basin. With stable tectonic conditions, these flow systems may persist for geologically significant periods of time. In the Walton area gravity driven fluid flow is seen as the most likely model for fluid migration.

Initiation of flow requires uplift in the basin and many MVT deposits and districts have ages which coincide with orogenic events (Bethke and Marshak, 1990; Symons and Sangster, 1994). The late Carboniferous was a particularly tectonically active time in central Nova Scotia. The Hercynian/Alleghenian orogeny began in Namurian to Westphalian B time and the Cobequid highlands 30 km to the north of the Kennetcook basin were uplifted due to movement on the Cobequid-Chedabucto fault (Fig. 7-4). The presence of coarse conglomerates both north and south of the Cobequid uplift provide evidence for dip-slip

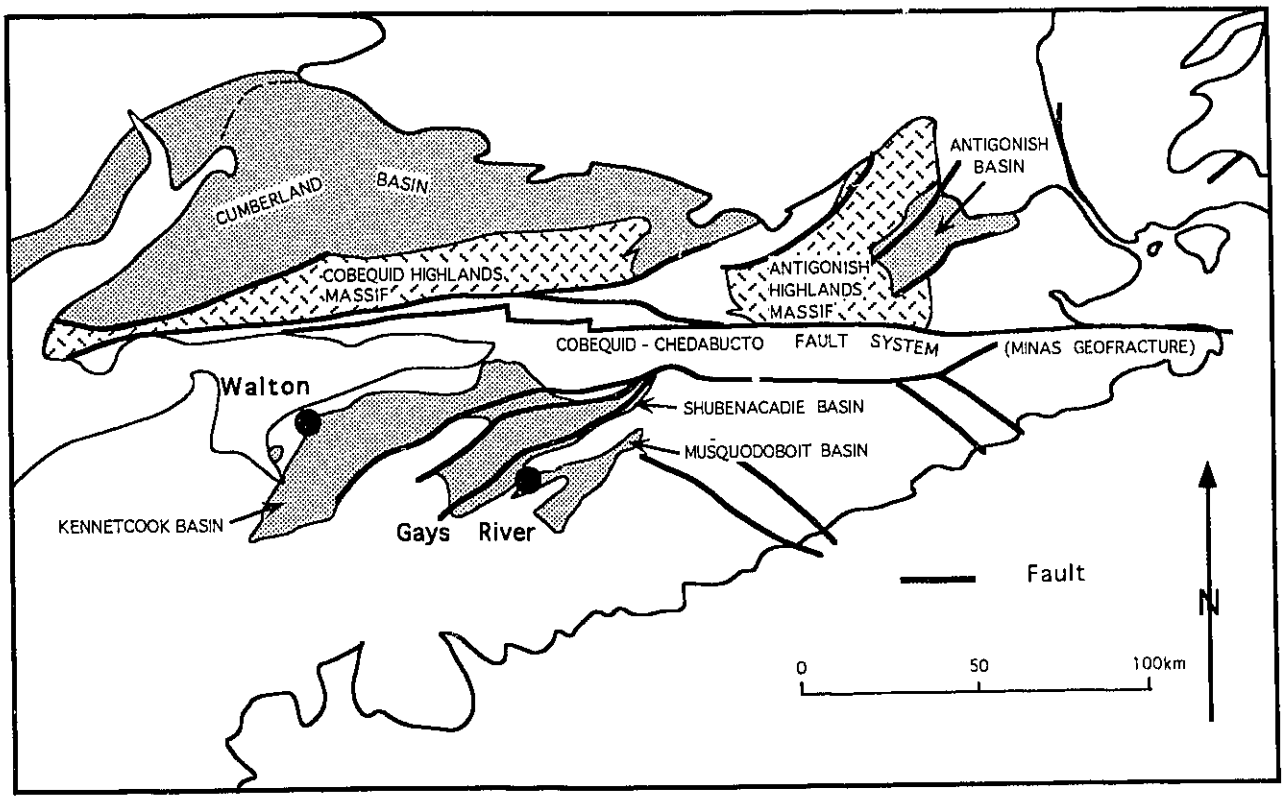

Figure 7-4. Map of central Nova Scotia showing Carboniferous basins, major faults and the Antigonish and Cobequid Highlands. From Ryan and Boehner (1994).

movement and indicate the age of uplift. Three episodes of uplift are recorded: the first in the late Devonian; the second in the late Namurian to Westphalian A; and the third in Westphalian B to Stephanian time (Donohoe and Wallace, 1985; Ryan et al, 1987; Ryan and Boehner, 1994). Gravity driven fluid flow also requires continuous recharge by meteoric waters in the uplifted area to produce the large volumes of brine required to form deposits. The arid climate of the Viséan, which existed during the deposition of the Windsor Group, gave way to a more moderate pluvial to seasonal climatic regime in the Namurian to Westphalian (Ryan and Boehner, 1994). Rocks of the late Carboniferous to early Permian record the evolution to a drier climate (Ryan and Boehner, 1994). Uplift of the Cobequid Highlands in the Namurian to Westphalian, a time of abundant rainfall, may therefore have provided the topographic relief necessary to initiate gravity driven fluid flow.

The Cobequid highlands are presently located immediately north of the Cobequid-Chedabucto fault and the Kennetcook basin. Due to strike-slip movement along the fault, however, it is uncertain as to the location of Walton relative to the uplift at the time of mineralisation. If the uplift of the Cobequid Highlands was responsible for the initiation of fluid flow which formed the deposit, then the Walton area must have been adjacent to the uplift at the time mineralisation began. The degree and time of strike-slip movement along the fault is poorly constrained. Keppie (1982) estimates that 165km of dextral movement related to the Hercynian orogeny occurred between the early Westphalian and the Permian and 75km of sinistral movement occurred in the Mesozoic. Donohoe and Wallace (1985) estimated that between 20 and 85km of dextral strike-slip movement has occurred on the fault but do not suggest when this movement occurred. As a result of this movement it is possible that Walton was located up to 90km east of its present location during Namurian time. This would place Walton at the extreme eastern end of the Cobequid highlands allowing the possibility that their uplift was responsible for the initiation of fluid flow.

Timing

The timing of mineralisation at Walton is not particularly well constrained. Sideritisation occurred after deposition of the lower Macumber and after the slumping that formed the upper Macumber, but there is little indication of how long after deposition the mineralisation took place. Timing would be constrained by both the karsting event and the folding event, however the age relationships of these events are not always evident. Karsting clearly post dates the mineralisation, as is illustrated by the cross cutting relationship of the sand and limestone breccia to the ore zones and the presence of siderite fragments in the limestone breccia. The age of the subaerial exposure that resulted in the collapse karsting is poorly constrained but is likely Westphalian or younger (Lavoie and Sangster, 1995). Clifton (1967) constrained the age of cavity fill and breccia found in the Walton area to post-Triassic, pre-Pleistocene. Karst sediments occupying a similar stratigraphic position at Gays River are believed to be of Cretaceous age (Kontak, 1992).

The relationship between folding and mineralisation is less clear, as is the relationship between folding and karsting. The age of deformation of the Walton host rocks is constrained to the period between Viséan and Westphalian C by the presence of the Scotch Village Formation unconformably overlying deformed Windsor Group strata (Boehner, 1991). The extent of the deformation during this time is unknown, however, as the overlying Scotch Village Formation has itself been gently folded. It is difficult to determine if mineralisation occurred prior to, during, or after the folding of the host rocks. On one hand the stratiform nature of the Type I ore suggests that mineralisation formed while the beds were flat lying, while on the other it is possible that the primary control on mineralisation was lithological and that mineralisation occurred during or after the folding of the host rocks.

While the age of mineralisation at Walton is unknown, the age of mineralisation at the Gays River Zn-Pb deposit in the nearby Shubenacadie-Musquodoboit basin has been

determined by a number of methods. It is not unreasonable to assume that mineralisation at Walton formed at the same time as mineralisation at Gays River, if the two deposits formed by the same regional fluid flow system. Deposits occurring over much larger areas have been interpreted to have similar ages, as has been reported for deposits in Ireland (Hitzman, 1995) and in the Mississippi Valley (Symons and Sangster, 1994). It is therefore not unreasonable to apply the Gays River age to the Walton deposit as this does not contradict any known geological relationships.

The epigenetic Gays River deposit is hosted by lower Windsor Group rocks of Viséan (352-333 Ma) age, so the maximum age is 333 Ma. Ravenhurst et al. (1989) suggest an age of mineralisation of 300-330 Ma based on limited Rb-Sr isotope data which give an age of about 300 Ma; fission track dates on zircons from footwall Meguma metasedimentary rocks of about 320 Ma; and K-Ar dates on clays from altered clastic material of 320 Ma. Fission track dating of apatites from basement rocks immediately underlying the deposit constrains mineralisation to a minimum age of 240 Ma (Arne et al., 1990). Measurements of palaeomagnetic pole positions indicate an age of 300-320 Ma (Pan et al., 1993). Whole rock ^{40}Ar-^{39}Ar data for basal breccia fragments suggest an age of mineralisation of 297±27 Ma (Kontak et al., 1994). The age of mineralisation at Gays River is therefore taken to be 320 to 300 Ma (Westphalian).

The Gays River ages and those of some other relevant events are summarised in Figure 7-5. Two periods of uplift are suggested by the presence of conglomerates north and south of the Cobequid Highlands, the first beginning in the late Namurian and the second beginning in the middle-late Westphalian. The Gays River age range corresponds with the age of uplift of the Cobequid highlands, either in the late Namurian at approximately 320 Ma or in the mid-Westphalian at approximately 310 Ma. If mineralisation at Walton formed as a result of the uplift, it would have an age which may correspond to that of Gays River. Two scenarios for the time of Walton mineralisation are presented in Figure 7-5, the first in

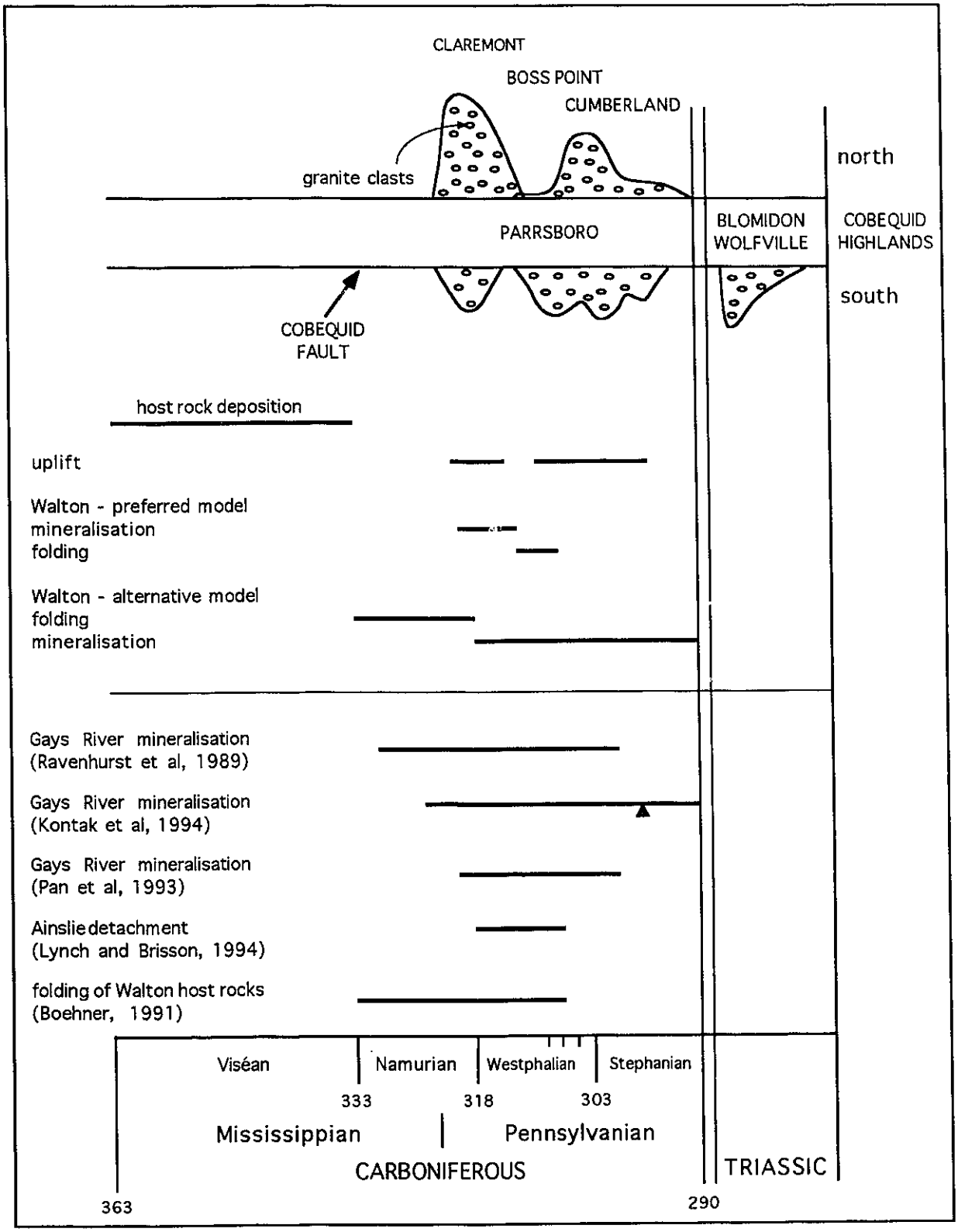

Figure 7-5. Age of uplift of the Cobequid Highlands, as recorded by the presence of conglomerate units on the north and south side of the Cobequid Highlands Massif, related to the maximum range of Walton host rock deformation, Gays River mineralisation and the Ainslie detachment fault. Modified from Ryan and Boehner (1994).

which mineralisation formed as a result of uplift in the late Namurian and was followed by folding of the Walton host rocks in the mid-Westphalian; and the second in which folding occurred prior to the initiation of mineralisation as a result of uplift in either the late Namurian or the mid-Westphalian. In the former alternative, folding of the host rocks may have been related to the tectonic activity which caused the mid-Westphalian uplift, while in the latter the folding may have been related to tectonic activity which caused the late Namurian uplift.

Path

The ore-forming fluids were driven, as a result of a topographic gradient caused by uplift of the Cobequid highlands, through a basal aquifer to the southern margin of the basin. The aquifer was likely within the Horton Group, a thick (~1.4km), relatively unmetamorphosed sequence of conglomerates, sandstones, siltstones and mudstones. Within the Horton Group, the Horton Bluff Formation probably contained the aquifer as it is the basal unit in the Horton Group and it is enriched in minor and trace elements (see below).

It is interesting to correlate the absence of Horton Group sediments within the Musquodoboit basin with the absence of mineralisation within that basin. Windsor Group rocks in the Musquodoboit basin rest directly on basement rocks of the Meguma Group which, due to their highly metamorphosed and folded nature, are an unlikely aquifer. Alternatively the absence of mineralisation may have been due to fluids from the north failing to reach this more southerly basin.

Ore-forming fluids were likely released from the basal aquifer into the Macumber carbonate along faults or fractures. The main barite pipe is localised at the intersection of two faults which were interpreted by Boyle (1972) to have existed at the time of mineralisation, although he presents no evidence for this conclusion. Based on indirect evidence two possible locations of fractures have been recognised on the B-baseline, each in the area of one of the upper Macumber mounds. It must be noted that no offset in the geology

has been recognised and that the existence of the fractures is based on the presence of the mounds, the presence of cross-cutting Type II mineralisation in the Macumber, and the presence of Cu mineralisation in the upper portion of the Horton Group sandstones.

Stable isotopes

The H and O isotope data presented by Ravenhurst et al. (1989) for several Carboniferous deposits in central Nova Scotia suggest a basinal brine source for the ore-forming fluids, although mixing with metamorphic and igneous fluids cannot be ruled out. The data also suggest that Carboniferous seawater was not directly involved in the mineralising process. In the Walton deposit there is a clear distinction in C and O isotope values between siderite and limestone/dolostone (Sangster et al., 1994). The difference is mainly in $\delta^{13}C$ values possibly reflecting a higher content of biogenic carbon in siderite. Siderite is slightly depleted in ^{18}O relative to limestone/dolostone.

Source of Metals

There is substantial evidence that the source of the metal in the Walton deposit was the aquifer through which the basinal brines passed. The process of aquifer leaching by basinal fluids has been described by Sverjensky (1989) as a method of generating ore-forming fluids. Pb-isotope values for galena from Carboniferous Pb-Zn deposits in central Nova Scotia are uniform suggesting either the source of lead from which the ore-forming fluids were derived was homogeneous or fluids containing lead from different sources were homogenised prior to deposition (Ravenhurst et al., 1989). The data also suggest that the source of lead was clastic material derived from the Meguma basement and deposited as part of the Horton Group in adjacent sedimentary basins (Ravenhurst et al., 1989). The lead isotope data therefore suggests that the ore-forming fluids leached their lead from sediments of the Horton Group.

Within the Horton Group, the Horton Bluff Formation is slightly enriched in zinc, copper, lead, silver, arsenic, antimony, tin, molybdenum, nickel and cobalt and the minor and trace element content of the Cheverie Formation is less than that of the Horton Bluff Formation except for arsenic, nickel and barium, for which the two formations of the Horton Group have similar concentrations (Boyle, 1972; Boyle et al., 1976). The trace element content of Macumber Formation is relatively low compared to the Horton Group, indicating it was not an important source of metal (Boyle, 1972; Boyle et al., 1976). The Horton Bluff Formation is therefore suggested to have been both the aquifer and the source of metals.

Source of sulphur

The source of sulphur in the Walton deposit was the focus of a sulphur isotope study by Boyle et al. (1976). They determined that the isotopic composition of barite in the massive pipe is the same as that in the overlying gypsum and anhydrite, indicating that the evaporites were the source of sulphur and suggesting that the barite formed by replacement of Ca^{2+} by Ba^{2+}. Barite in pods and veins and all of the sulphides are much more depleted in ^{34}S and have isotopic compositions that suggest formation by reduction of sulphate from deeply circulating brines (Boyle et al., 1976). Since this study is focused on the B-baseline, which contains pods and veins of barite, the results of Boyle et al. (1976) suggest that the source of sulphur for all of the minerals in the B-baseline was sulphate carried in deeply circulating brines.

Temperature

Fluid inclusion studies have been carried out on barite samples from Walton in order to provide an indication of the temperature of the ore-forming fluids (Kontak and Sangster, 1994). Two types of barite have been identified: Type 1 - early replacement barite; and type 2 - late veinlets or barite cement. Thermometric measurements indicate temperatures

of homogenisation ranging from 120-320°C for both Type 1 and Type 2 barite. Measurements also indicate salinities of 20-25 wt.% equiv. NaCl for Type 1 barite and two populations of low salinities for Type 2 barite, either <0.5 wt.% equiv. NaCl (meteoric component?) or 10-15 wt.% equiv. NaCl (Kontak and Sangster, 1994). Homogenisation temperatures of 155-233°C are reported for two barite samples by Ravenhurst et al. (1989), however, details of the type of inclusions studied, their origin or their paragenetic position are not discussed.

Genetic Model

Previous models

A number of genetic models have been considered for the Walton deposit and other deposits at the same stratigraphic interval throughout Nova Scotia. Boyle (1972) favoured formation of Walton by replacement and fracture filling of limestone conglomerate (the upper Macumber of this study), fissile limestone and anhydrite. The origin of the mineralisation has been interpreted by Boyle (1972, p. 137) as follows: *"In late Carboniferous time, during and following the period of severe faulting, brines, their salt probably partly of connate origin but largely derived from the Windsor evaporites, pervaded the Horton and Cheverie rocks and leached out various elements, the most important being Ba, Sr, Ca, Mn, S, As, Cu, Pb, Zn, Ag, and CO_3. This process probably went on for a long time, well into the Triassic when the heat wave associated with underlying volcanic action may have had a particularly stimulating effect on the dissolution processes. Concomitant with dissolution, large-scale diffusion of the various metals, carbonate, sulphur, and arsenic took place through the brine, followed by deposition in chemically replaceable rocks, in plant-bearing zones, and in dilatant zones along faults. In the hypogene zone of reduction the deposition processes led to the formation of barite, manganiferous siderite, and sulphides. As the remaining diffusing constituents rose into the hypogene zone*

of oxidation where free oxygen was available from downward diffusion or from oxygenated meteoric waters, they were precipitated as various manganese oxides with traces of the metals, calcite, and minor barite."

Boyle's model is somewhat dated in that it does not incorporate some of the more current concepts in carbonate-hosted ore deposit formation. The model presented in this study updates the model of Boyle, combining modern concepts of ore genesis with a better understanding of Nova Scotia geology.

Ravenhurst et al. (1989) proposed compaction-driven expulsion of over-pressured basinal fluids under an evaporite cap as a model for many Carboniferous Pb-Zn and barite occurrences in central Nova Scotia. They envisaged rapid transfer and focusing of mineralising fluids in a series of pulses from >5km deep in the Magdalen Basin resulting in the high thermal anomalies that are recorded in some mineral deposits. Where the metal-bearing solutions encountered areas of low pressure, ore deposit formation occurred. They also suggest that the rapid fluid expulsion may have resulted in hydrofracturing of carbonate, forming the *Pembroke Breccia.*

This model relies heavily on the episodic dewatering model of Cathles and Smith (1983) which requires rapid rates of sedimentation (>1km/Ma; Bethke and Marshak, 1990) to produce the over-pressuring neccessary to drive the fluids. These sedimentation rates were not acheived in the Magdalen basin where total sediment accumulation was only 12km in the entire Carboniferous period. The work of Lavoie (1994) and Lavoie and Sangster (1995) on the origin of the *Pembroke Breccia* suggests that hydrofracturing did not play a role in the formation of the breccia as was suggested by Ravenhurst et al. (1989).

Lynch and Brisson (1994) inferred a genetic link between the Ainslie Detachment, a low angle fault at the top of the Macumber Formation on Cape Breton Island, and Pb-Zn mineralisation in the Lower Windsor based on the temporal and spatial overlap of the two. They suggest that detachment faulting breached the evaporite cap proposed by Ravenhurst et

al. (1989), allowing surface waters to mix with deep basinal fluids. Faulting would also have increased permeability and assisted fluid migration due to hydraulic pumping.

While the Ainslie Detachment may have played a role in mineralisation on Cape Breton Island, there is no evidence to suggest that the detachment occurred in the Kennetcook basin. It is therefore unlikely that the Ainslie Detachment had a role in the formation of the Walton deposit.

Preferred model

The preferred model for the genesis of the Walton deposit draws upon the factors discussed in the previous sections. Basinal brines were gravity driven from the north, as a result of uplift of the Cobequid Highlands in the late Namurian, through a basal aquifer within the Horton Bluff Formation. As discussed earlier, humid conditions in the Namurian and Westphalian allowed recharge of the aquifer by large volumes of meteoric water. Leaching of the aquifer by fluid of up to 320°C increased the salinity and trace element contents of the basinal brine. Metals, barite and sulphur were transported in a reduced form (model 3 of Sverjensky, 1986). When the hot, saline fluids reached the Walton area they were released from the aquifer, along fractures, into the flat, overlying Macumber carbonate, replacing the original calcite or dolomite with manganiferous siderite (Fig. 7-6). Replacement was complete, except in the top portions of the upper Macumber where some ankerite formed as a result of incomplete alteration. Following sideritisation the fluids flowed either through the more porous upper Macumber or, where the upper Macumber is not present, along the lower Macumber/evaporite contact. As the fluids flowed through the bottom portion of the upper Macumber and percolated downward into the top portions of the lower Macumber barite, pyrite, galena, sphalerite, tennantite and chalcopyrite formed, each replacing earlier phases. This resulted in the formation of a continuous sheet of barite, containing lenses of lead-rich ore and scattered pods of copper-rich ore, straddling the

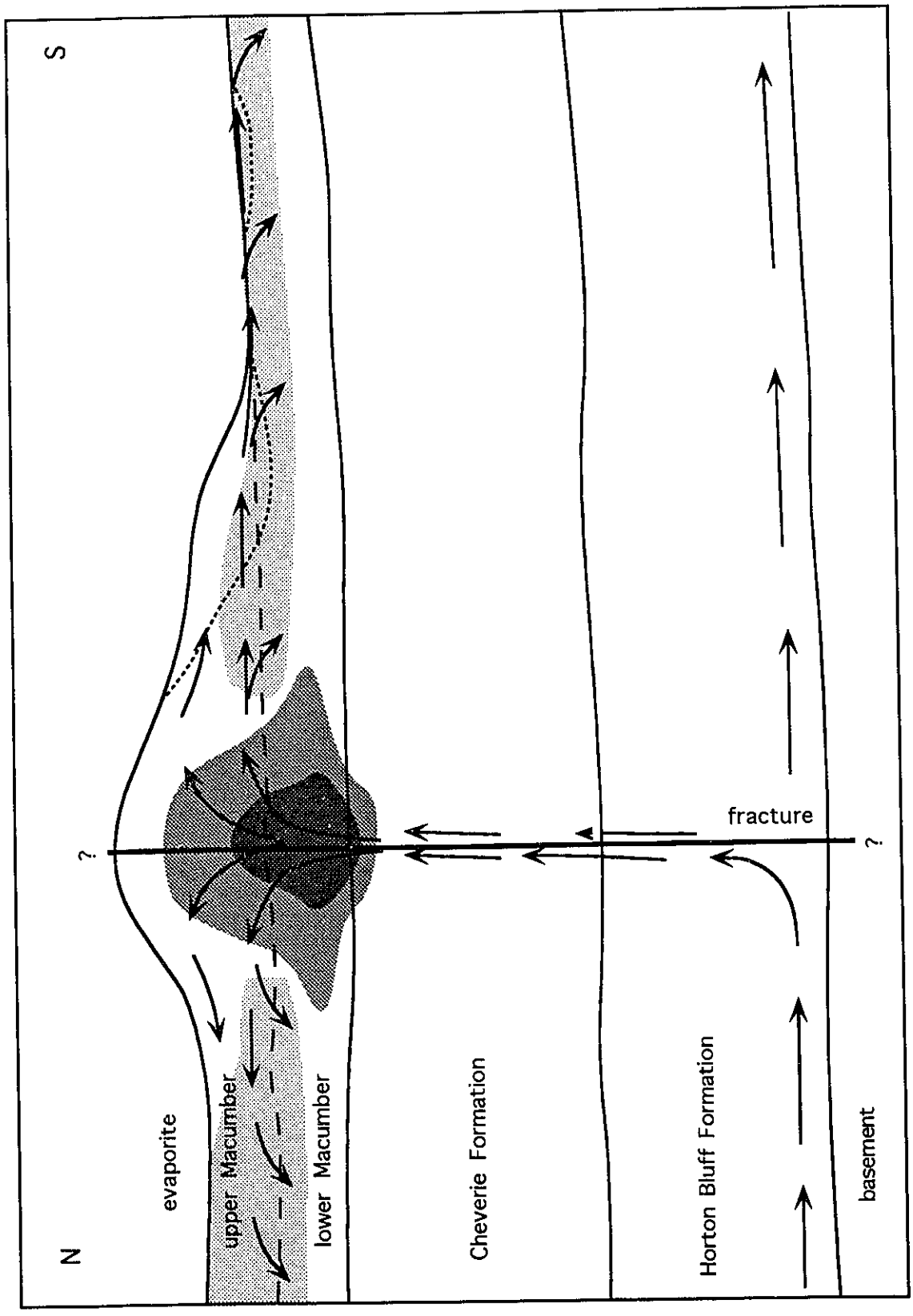

Figure 7-6. Schematic section showing preferred genetic model for the B-baseline. Arrows show the path of fluid flow. See Figure 6-8 for ore type legend

upper Macumber/lower Macumber contact. In the areas close to the faults, barite was deposited and then subsequently dissolved and replaced by copper mineralisation, forming a copper-rich pod which cuts the tabular barite zone. Pyrite and chalcopyrite also formed at the top of the Horton sandstone, in the vicinity of the faults. Deposition of metals was primarily due to a reduction in the pH of the fluid as a result of reaction with carbonate. Folding in the mid-Westphalian, possibly related to the tectonic activity which caused further uplift of the Cobequid Highlands, and in post-Carboniferous times tilted the deposit to its present steeply dipping attitude. Dissolution and solution collapse removed some of the upper part of the mineralisation and filled the resulting cavity with sand and limestone breccia.

Alternate Model

While a model in which folding post-dated mineralisation is preferred, it is also possible that mineralisation formed after the folding of the host rocks. In general the model is the same as above, although, a few points need further discussion. The aquifer is still envisaged to have been in the Horton Bluff Formation. Folding of the Horton Group is not believed to have prevented fluid flow, as the Horton Group is locally tightly folded but regionally is only gently flexed (Boyle et al., 1976). The depth of penetration of ore-forming fluids into the lower Macumber was probably controlled by the nature of the carbonate host rock. Replacement of the host rock carbonates by siderite may have reduced the porosity of the unit by cementation of pore space. The top portion of the lower Macumber, however, is well laminated and the laminations may have allowed the flow of fluid, whereas the basal portion of the lower Macumber is poorly laminated, restricting the flow of fluid. While this difference in lithology may also have been a factor in the preferred model, it is required in this model to explain the consistent extent of Type I mineralisation into the steeply dipping beds. In this model there is little to explain the relationship between the upper Macumber breccia and Type II mineralisation other than to suggest that the

fractures which localised the mineralisation are somehow related to faulting which caused formation of the breccia. In this model, folding took place in the Namurian and mineralisation formed as a result of uplift in the late Namurian or in the mid-Westphalian.

EXPLORATION GUIDELINES

Exploration Criteria

The potential for further Walton-style mineralisation exists in the Walton mine area, in the Kennetcook basin, and in other Carboniferous basins of Nova Scotia. A number of exploration criteria have been identified as follows:

1. Basal Windsor carbonates. Because basal Windsor carbonates host the mineralisation their presence, either as Macumber or Gays River Formations or their lateral equivalents, is required.

2. Thicker than normal carbonate sequence. Since mineralisation is carbonate-hosted, the presence of a thick carbonate sequence increases the size of the potential deposit. The increased thickness may be due to a syn-sedimentary breccia as in Walton or a carbonate build-up as in the Gays River deposit.

3. Horton Group sediments. The presence of Horton Group sediments is also important as they were the most likely aquifer for the ore-forming fluids. It is suggested here that the absence of mineralisation in the Musquodoboit basin is probably in part due to the lack of a Horton aquifer. While Horton Group sediments are not found within the Gays River deposit, they pinch out nearby as they onlap the Meguma basement high.

4. Evaporite cap. An evaporite cap above the carbonate is also interpreted to be an important feature in the formation this deposit type. Walton, Gays River and Jubilee are all situated below a thick sequence of evaporites which probably aided in localising fluid flow through the carbonate, and in the case of Walton, was the source of sulphate for the main barite pipe (Boyle et al., 1976).

5. Siderite. The alteration of the Macumber Formation appears to be basin specific, occurring as: siderite at Walton and other Kennetcook basin occurrences such as Goshen, Tennycape and Lower Burlington; dolomite at Gays River in the Shubenacadie-Musquodoboit basin (Kontak, 1992) and calcite at Jubilee in the River Denys basin (Fallara et al., 1994). The presence of siderite is therefore considered to be an exploration criteria in the Kennetcook basin.

6. Mineralisation. Within an area in which several of the previous criteria exist, the presence of pyrite or chalcopyrite within the upper part of the Horton Group suggests proximity to a site of discordant Cu-rich mineralisation and possibly an upper Macumber mound. Barite and/or sulphides immediately above or below the lower Macumber/upper Macumber contact are also features of mineralisation.

Specific Sites for Exploration

A number of specific sites which potentially host undiscovered mineralisation in the Kennetcook basin have also been identified.

Very little is known about the geology between the main barite pipe and a small limestone-hosted manganese prospect, known as the Stephens prospect, approximately 1.5km to the north. Little mention is made of the geology of that area in the assessment reports filed with the Nova Scotia Dept. of Natural Resources. No record of diamond drilling north of the open pit was found in the assessment reports and there is little or no outcrop in that area. The existence of mineralisation along the fold limb immediately south of the main deposit suggests the possibility exists for similar mineralisation on the fold limb to the north of the deposit. The Windsor - Horton horizon between the Walton deposit and the Stephens manganese prospect is therefore considered to be worthy of further exploration. North of the Stephens prospect the location of the Horton Group/Windsor Group contact is

poorly constrained and exploration along the contact between the Stephens prospect and the Tennycape Mn occurrence, 25km NE of the Walton deposit, may be warranted.

Within the B-baseline area itself there is the potential for further mineralisation both updip and downdip of the existing mine workings. As noted by Patterson (1989), the extent of mineralisation above the 690' level and below the 1030' level is unknown. Based on comparison with the main barite pipe, where mineralisation is primarily barite at shallower depths giving way to barite-sulphide mineralisation at deeper levels, there is the potential for mineralisation on the B-baseline at least as deep as 1700' (Patterson, 1989). All three drill holes on the 1200' level of the B-baseline intersected mineralisation. Below 1700' the attitude of the folded host stratigraphy at depth is unknown. Deep drilling by Gunnar Gold Inc. did not intersect the Macumber Formation at the projected location, leading Boehner (1991) to suggest that the stratigraphy may be overturned at depth (Fig. 2-4). Thus, exploration for mineralisation below depths of 1700' must take into consideration the possibility that the host stratigraphy is overturned.

Patterson (1988, 1989) also identified sulphide ore shoots plunging to the south-west (Fig. 7-7), a trend that was confirmed in the present study. The majority of the Cu-rich and Pb-rich ore intersections identified in this study fall within these ore shoots as would be expected (Figs. 6-10, 6-12). This study has also shown that Type II copper mineralisation is strongly related to the presence of mounds of upper Macumber. It is therefore evident that the southern-most ore shoot of Patterson (1988, 1989), which is the most Cu-rich of the shoots he identifies, reflects the presence of the upper Macumber mound. The ore shoots at the north end of the B-baseline are more lead-rich and are coincident with most Pb-rich Type I ore and Type II ore intersections (Fig. 6-12). Patterson (1988, 1989) recommended the updip and downdip extensions of his ore shoots as exploration targets, a recommendation which is supported by this study, bearing in mind that the Cu-rich ore shoot is actually due to the presence of an upper Macumber mound.

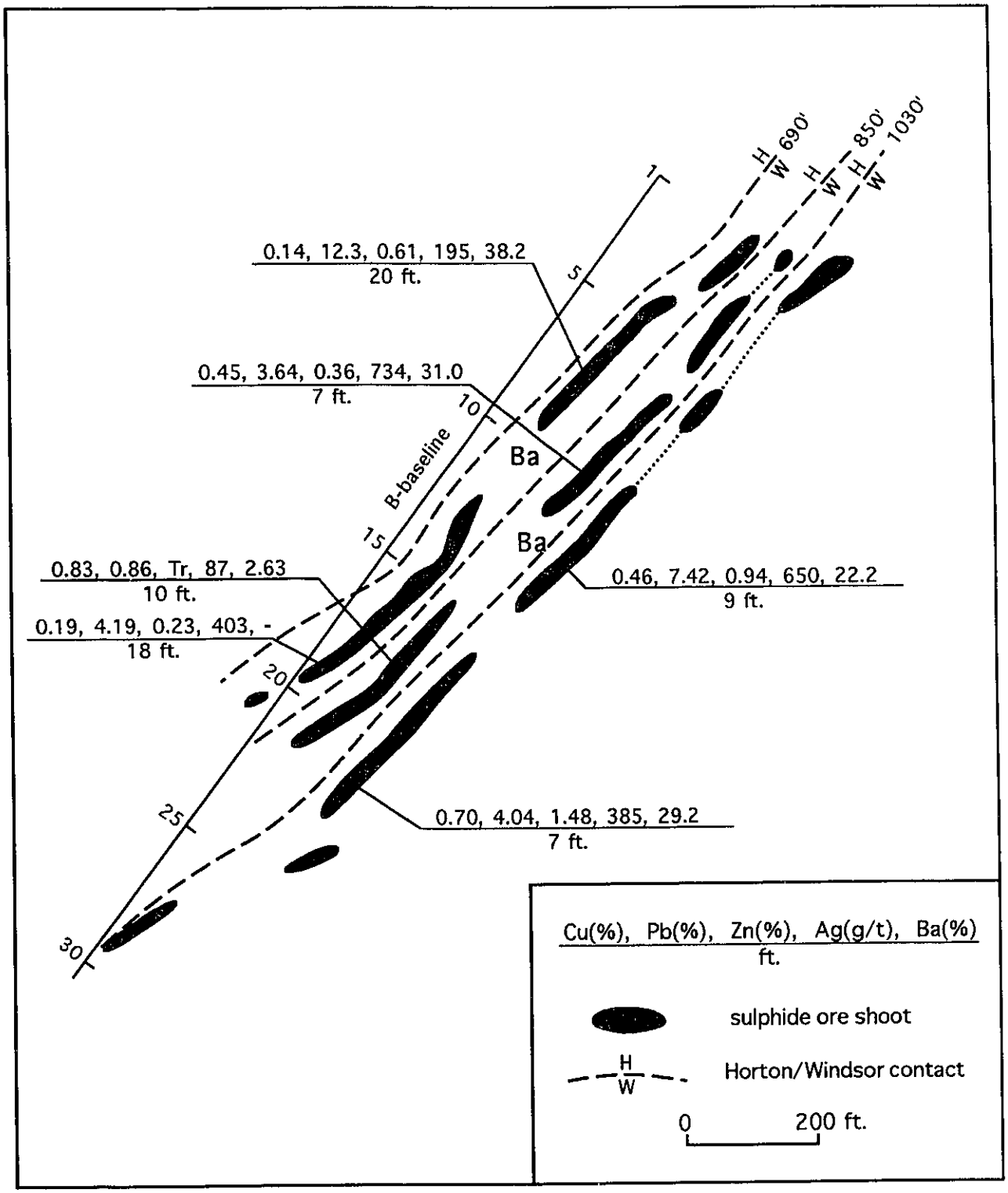

Figure 7-7. Location of ore shoots relative to the B-baseline and the Horton - Windsor contact at various mine levels. Modified from Patterson (1986).

CHAPTER 8

SUMMARY AND CONCLUSIONS

- Host rocks - The Walton deposit is hosted by carbonate rocks of the Macumber Formation. Outside the immediate mine area the carbonate is either a limestone with a composition of 97-98 mol% $CaCO_3$ and 2-3 mol% ($FeCO_3$+$MgCO_3$) or a dolostone with a composition of 50 mol% $CaCO_3$, 47 mol% $MgCO_3$, and 3 mol% ($FeCO_3$+$MnCO_3$). The Macumber Formation in the deposit has been divided into two units, the lower Macumber and the upper Macumber. The lower Macumber is an ooidiferous or laminated carbonate with a relatively uniform thickness of 30-40' throughout the deposit. The upper Macumber is a synsedimentary slump breccia which ranges in thickness from 0-70' and forms two mounds.
- B-baseline - The B-baseline is located along the southern limb of the fold which localises the Walton deposit and has slightly different mineralisation than that of the main barite pipe and its underlying sulphide zone. The B-baseline has less zinc than the main sulphide zone and none of the silver sulphosalt minerals which occur in the main zone.
- Wallrock alteration - The Macumber Formation in the Walton deposit has been altered by ore-forming fluids to manganiferous siderite. The composition of the siderite ranges from about 1 mol% $CaCO_3$, 12 mol% $MgCO_3$, 73 mol% $FeCO_3$ and 14 mol% $MnCO_3$ to about 1 mol% $CaCO_3$, 1 mol% $MgCO_3$, 89 mol% $FeCO_3$ and 9 mol% $MnCO_3$. In general the upper Macumber has lower $FeCO_3$:$MgCO_3$ ratios than the lower Macumber. Manganese content is relatively constant, averaging 10 mol% $MnCO_3$ in the lower Macumber and 12 mol% in the upper Macumber. Within an individual sample there is little variation in composition between textural generations of siderite. A few samples of upper Macumber have an ankerite composition of 49 mol% $CaCO_3$, 31 mol% $MgCO_3$, 15 mol% $FeCO_3$ and 5 mol% $MnCO_3$ and are interpreted to be the result of incomplete alteration by the ore-forming fluids.

- Ore mineralogy - Barite is 99 mol% pure with approximately 1 mol% $SrSO_4$; sphalerite is end-member ZnS. Tennantite is the As end-member of the tennantite-tetrahedrite series, containing less than 0.4 at.% Sb, and having the approximate composition $Cu_{10}Fe_{1.3}Zn_{0.6}As_4S_{13}$. Pyrite generally contains less than 2 at.% As, but late pyrite rims have arsenic contents as high as 4 at.% As.

The paragenetic sequence of mineralisation is siderite, barite, pyrite/marcasite, sphalerite, galena, tennantite, chalcopyrite and (para)rammelsbergite followed by further siderite, barite, tennantite and chalcopyrite. Each mineral replaces earlier minerals to varying degrees. Calcite related to karsting was the last mineral to form.

- Ore types - Based on barite and metal content two main ore types can be defined for the B-baseline. Type I ore contains barite and variable sulphide contents, whereas Type II ore contains only sulphides. Within Type I ore, further subdivision can be made into Cu-rich ore, containing >0.3% Cu and Pb-rich ore, containing >0% Pb. Type II ore is defined as Cu-rich if it contains >0.6% Cu. Type I ore has a bulk composition of 0.3% Cu, 2.5% Pb, 0.2% Zn, 133g/t Ag and 31.2% $BaSO_4$ and Type II ore has a composition of 0.5% Cu, 0.5% Pb, 0.1% Zn, 51 g/t Cu and 0% $BaSO_4$.

The two ore types have distinct distributions within the B-baseline deposit. Type I ore forms a stratiform sheet which straddles the upper Macumber/lower Macumber contact and contains lenses of Pb-rich and Cu-rich ore. Type II ore is most commonly associated with the upper Macumber mound in which it forms a large pod which cuts the Type I ore zone. Type II ore also occurs within the footwall Horton sandstones, directly below the upper Macumber mound.

There is also a stratigraphic zonation in metal content, with the lower Macumber containing a higher metal content than the upper Macumber for all metals and for each ore type. No pattern could be established for the distribution of silver.

- Post-ore effects - The B-baseline deposit has been subject to folding and karsting. The host stratigraphy is presently steeply dipping and the folding is considered to have post-dated the mineralising event. Karsting post-dates the mineralisation and probably the folding and had the effect of removing the stratigraphically upper part of the orebody. The cavity is now partially filled by sand and limestone breccia.
- Genetic model - Uplift of the Cobequid Highlands in the late Namurian initiated gravity driven flow of basinal fluids through a basal aquifer within the Horton Bluff Formation. The hot fluids leached salts and metals from the Meguma-derived sediments as they flowed south toward the basin margin. In the Walton area they were released along faults into the overlying Macumber carbonate and synsedimentary carbonate breccia, which they replaced with manganiferous siderite. Fluid flow was primarily laterally through the porous upper Macumber and from there downward into the lower Macumber. Barite replaced the siderite and was in turn replaced by pyrite, sphalerite, galena, tennantite and chalcopyrite, each of which replaced earlier phases. Around the faults, the barite sheet at the lower Macumber/upper Macumber contact was removed and a discordant pod of copper-rich ore formed. After mineralisation the host rocks were folded and karsting had the effect of removing the top of the orebody.

REFERENCES

ARNE, D. C., DUDDY, I. R. AND SANGSTER, D. F. 1990: Thermochronological constraints on ore formation at the Gays River deposit, Nova Scotia, Canada, from apatite fission track analysis; Canadian Journal of Earth Sciences, v. 27, p. 1013-1022.

BELL, W. A. 1929: Horton-Windsor District, Nova Scotia; Geological Survey of Canada, Memoir 155, 268p.

BELT, E. S. 1968: Post-Acadian rifts and related facies, eastern Canada; *in* Studies in Appalachian Geology, eds. E. Zen, W. S. White, J. B. Hadley and J. B. Thompson, Wiley Intersci., New York, p. 95-116.

BETHKE, C. M., AND MARSHAK, S. 1990: Brine migrations across North America - the plate tectonics of groundwater; Annual Reviews in Earth and Planetary Sciences, v. 18, p. 287-315.

BOEHNER, R. C. 1991: Seismic interpretation, potential overthrust geology and mineral deposits in the Kennetcook Basin; *in* Mines and Minerals Branch, Report on Activities 1990; Nova Scotia Dept. of Mines and Energy, Report 91-1, p. 37-47.

BOYLE, R. W. AND JAMBOR, J. L. 1966: Mineralogy, geochemistry, and origin of the Magnet Cove barite-sulfide deposit, Walton, N.S.; Trans. Can. Inst. Mining, vol. LXIX, p. 394-413.

BOYLE, R. W. 1972: The geology, geochemistry, and origin of the barite, manganese, and lead-zinc-copper-silver deposits of the Walton-Cheverie area, Nova Scotia; Geological Survey of Canada Bulletin, v.166, 181p.

BOYLE, R. W., WANLESS, R. K. AND STEVENS, R. D. 1976: Sulfur isotope investigation of the barite, manganese, and lead-zinc-copper-silver deposits of the Walton-Cheverie area, Nova Scotia, Canada; Economic Geology, v. 71, p. 749-762.

CATHLES, L. M. AND SMITH, A. T. 1983: Thermal constraints on the formation of Mississippi Valley-type lead-zinc deposits and their implications for episodic basin dewatering and deposit genesis; Economic Geology, v. 78, p. 983-1002.

CLIFTON, H. E. 1967: Solution collapse and cavity filling in the Windsor Group, Nova Scotia, Canada; Geological Society of America Bulletin, v. 78, p. 819-832.

CRANSTONE, D. A. 1982; An analysis of ore discovery cost and rates of ore discovery in Canada over the period 1946 to 1977; unpublished Ph.D. thesis, Harvard University.

CROSBY, D. G. 1962: Wolfville map area, Nova Scotia; Geological Survey of Canada, Memoir 325, 67p.

DEER, W. A. , HOWIE, R. A. AND ZUSSMAN, J. 1962: Rock forming minerals, Volume 5. Non-silicates; Longmans, Green and Co. Ltd., London, 371p.

DONOHOE, H. V. AND WALLACE, P. I. 1985: Repeated orogeny, faulting and stratigraphy in the Cobequid Highlands, Avalon terrain of northern Nova Scotia; Geological Association of

Canada - Mineralogical Association of Canada Joint Annual Meeting, Field Trip Excursion 3, p. 1-75.

FALLARA, F., SAVARD, M. M., LYNCH, G. AND PARADIS, S. 1994: Preliminary geological and geochemical results characterizing the mineralization processes in the Jubilee Pb-Zn deposit, Cape Breton Island, Nova Scotia; *in* Current Research 1994-D, Geological Survey of Canada, p. 63-71.

FLETCHER, H. 1894: Summary of work in the eastern parts of Hants County, Nova Scotia; Geological Survey of Canada, Summary Report 1893, p.60-66.

GARVEN, G. 1985: The role of regional fluid flow in the genesis of the Pine Point Deposit, Western Canada sedimentary basin; Economic Geology, v. 80, p. 307-324.

GARVEN, G. AND FREEZE, R. A. 1984a: Theoretical analysis of the role of groundwater flow in the genesis of stratabound ore deposits: 1. Mathematical and numerical model; American Journal of Science, v. 284, p.1085-1124.

GARVEN, G. AND FREEZE, R. A. 1984b: Theoretical analysis of the role of groundwater flow in the genesis of stratabound ore deposits: 2. Quantitative results; American Journal of Science, v. 284, p.1125-1174.

GELDSETZER, H. H. J. 1977: The Windsor Group of Cape Breton Island, Nova Scotia; *in* Geological Survey of Canada, Report of Activities, Part A; Geological Survey of Canada, Paper 77-1A, p. 425-428.

GELDSETZER, H. H. J. 1978: The Windsor Group in Atlantic Canada - an update; *in* Geological Survey of Canada, Report of Activities, Part C; Geological Survey of Canada, Paper 78-1C, p. 43-48.

GILES, P. S. 1981: Major transgressive-regressive cycles in the Middle to Late Viséan rocks of Nova Scotia; Nova Scotia Dept. of Mines and Energy, Paper 81-2, 27p.

HAMILTON, J. M., DELANEY, G. D., HAUSER, R. L. AND RANSOM, P. W. 1983: Geology of the Sullivan deposit, Kimberley, B.C., Canada; *in* Short course in sediment-hosted stratiform lead-zinc deposits, ed. D.F. Sangster; Mineralogical Association of Canada, p. 31-83.

HARLAND, W. B., ARMSTRONG, R. L., COX, A. V., CRAIG, L. E., SMITH, A. G. AND SMITH D. G. 1990: A geologic time scale, 1989; Cambridge Univ. Press, Cambridge, 263 p.

HITZMAN, M. W. 1995: Mineralization in the Irish Zn-Pb-(Ba-Ag) orefield; *in* Irish carbonate-hosted Zn-Pb deposits, eds. K. Anderson, J. Ashton, G. Earls, M. Hitzman, and S. Tear; Society of Economic Geology Guidebook Series, Volume X, p. 25-61.

HOWIE, R. D. AND BARSS, M. S. 1975: Upper Paleozoic rocks of the Atlantic provinces, Gulf of St. Lawrence and adjacent continental shelf; *in* Offshore Geology of Eastern Canada; Geological Society of Canada, Paper 74-30, p. 35-50.

JACKSON, S. A. AND BEALES, F. W. 1967: An aspect of sedimentary basin evolution, the concentration of Mississippi Valley type ores during the late stage of diagenesis; Bulletin of Canadian Petroleum Geology, v. 15, p. 393-433.

JOHNSON, N. E., CRAIG, J. R. AND RIMSTIDT, J. D. 1986: Compositional trends in tetrahedrite; Canadian Mineralogist, v. 24, p. 385-397.

KEPPIE, J. D. 1982: The Minas Geofracture; *in* Major Structural Zones and Faults of the Northern Appalachians. eds. P. St. Julien and J. Beland; Geological Association of Canada, Special Paper 24, p. 263-280.

KIRKHAM, R. V. 1974: A synopsis of Canadian stratiform copper deposits in sedimentary sequences; *in* Gisements stratiformes et provinces cuprifères, ed. P. Bartholomé; Société Géologique de Belgique, Liège, p. 367-382.

KIRKHAM, R. V. 1978: Base metal and uranium distribution along the Windsor-Horton contact, central Cape Breton Island, Nova Scotia; *in* Geological Survey of Canada, Report of Activities, Part B; Geological Survey of Canada, Paper 78-1B, p. 121-135.

KLEIN, C. AND HURLBUT, C. S. JR. 1993: Manual of Mineralogy (after J. D. Dana), 21st edition; John Wiley and Sons, Inc., New York, 681p.

KONTAK, D. J. 1992: A preliminary report on geological, geochemical, fluid inclusion and isotopic studies of the Gays River Zn-Pb deposit, Nova Scotia; Nova Scotia Dept. of Natural Resources, Open File Report 92-014, 223p.

KONTAK, D. J., FARRAR, E. AND MCBRIDE, S. L.,1994: $^{40}Ar/^{39}Ar$ dating of fluid migration in a Mississippi Valley type deposit: The Gays River Zn-Pb deposit, Nova Scotia, Canada; Economic Geology, v. 89, p. 1501-1517.

KONTAK, D. J. AND SANGSTER, D. F. 1994: Fluid migration and mineralization in the Lower Windsor Group, Nova Scotia: 7. Preliminary results of fluid inclusion studies at the Walton Ba-base metal and related Ba-Mn deposits, Kennetcook sub-basin; *in* Program and Summaries, Eighteenth Annual Review of Activities, ed. D. R. MacDonald; Nova Scotia Dept. of Natural Resources, Mines and Energy Branches, Report 94-2, p. 52.

LAVOIE, D. 1994: Lithology and preliminary paleoenvironmental interpretations of the Macumber and Pembroke formations (Windsor Group, Early Carboniferous), Nova Scotia; *in* Current Research 1994-D, Geological Survey of Canada, p. 79-88.

LAVIOE, D. AND SANGSTER, D. F. 1995: Basal Windsor carbonate breccias: origins and timing; *in* Current Research 1995-D, Geological Survey of Canada, p. 1-10.

LAVOIE, D., SAVARD, M. M. AND SANGSTER, D. F. 1994: Fluid migration and mineralization in the Lower Windsor Group, Nova Scotia: 2. The Pb-Zn-rich, lower Carboniferous (Viséan) basal Windsor carbonate; *in* Program and Summaries, Eighteenth Annual Review of Activities, ed. D. R. MacDonald; Nova Scotia Dept. of Natural Resources, Mines and Energy Branches, Report 94-2, p. 47.

LYNCH, G. AND BRISSON, H. 1994: Ainslie Detachment in the Carboniferous River Denys basin of Cape Breton Island, Nova Scotia, with implications for Pb-Zn mineralization; *in* Current Research 1994-D, Geological Survey of Canada, p. 57-62.

LYDON, J. W. 1984: Ore deposit models - 8. Volcanogenic massive sulphide deposits Part I: A descriptive model; Geoscience Canada, v. 11, p. 195-202.

MOORE, R. G. 1994: Geology of the Walton-Rainy Cove Brook map area, Hants County, Nova Scotia; Nova Scotia Dept. of Natural Resources, Mines and Energy Branch, Open File Report 94-022, 36p.

MOORE, R. G. AND RYAN, R. J. 1976: Guide to the invertebrate fauna of the Windsor Group in Atlantic Canada; Nova Scotia Dept. of Mines and Energy, Paper 76-5, 79p.

MORTON, R. L. AND NEBEL, M. L. 1984: Hydrothermal alteration of felsic volcanic rocks at the Helen Siderite deposit, Wawa, Ontario; Economic Geology, v. 79, p.1319-1333.

PAN, H., SYMONS, D. T. A. AND SANGSTER D. F., 1993: Paleomagnetism of the Gays River zinc-lead deposit, Nova Scotia; Pennsylvannian ore genesis, Geophysical Research Letters, v. 20, p. 1159-1162.

PATTERSON, J. M. 1986: Base metal project; *in* Program and Summaries, Tenth Annual Review of Activities, eds. J. L. Bates and D. R. MacDonald; Nova Scotia Dept. of Mines and Energy, Report 86-1, p. 107-117.

PATTERSON, J. M. 1987: Investigation of the argentiferous base metal potential at the Walton deposit, Hants County; *in* Report of Activities, 1987, Part A, eds. J. L. Bates and D. R. MacDonald; Nova Scotia Dept. of Mines and Energy, Report 87-5, p. 79-81.

PATTERSON, J. M. 1988a: Exploration potential for argentiferous base metals at the Walton deposit, Hants County, Nova Scotia. *in* Report of Activities 1987, Part B, eds. D. R. MacDonald and Y. Brown; Nova Scotia Dept. of Mines and Energy, Report 88-1, p. 129-134.

PATTERSON, J. M. 1988b: Walton Project: Final Report; Nova Scotia Dept. of Mines and Energy, Open File Report 88-045.

PATTERSON, J. M. 1989: Exploration potential for argentiferous base metals at the Walton deposit, Hants County, Nova Scotia; Nova Scotia Dept. of Mines and Energy, Open File Report 89-022.

POUCHU, J. L. AND PICHOIR, F. 1985: "PAP" O(pz) procedure for improved quantitative microanalysis; Microbeam Analysis, v. 20, p. 104-106.

RAVENHURST, C. E., REYNOLDS, P. H., ZENTILLI, M., KRUEGER, H. W. AND BLENKINSOP, J. 1989: Formation of Carboniferous Pb-Zn and barite mineralization from basin-derived fluids, Nova Scotia, Canada; Economic Geology, v. 84, p. 1471-1488.

RYAN, R. J., BOEHNER, R. C. AND CALDER, J. H. 1991: Lithostratigraphic revision of the Upper Carboniferous to Lower Permian strata in the Cumberland Basin, Nova Scotia, and the regional implications for the Maritimes Basin in Atlantic Canada; Bulletin of the Canadian Society of Petroleum Geologists, v. 39, p. 289-314.

RYAN R. J., CALDER, J. H., DONOHOE, H. V., JR. AND NAYLOR, R. 1987: Sedimentation and basin evolution adjacent to the Cobequid Highlands Massif, Eastern Canada; *in* Basins and

Basin-forming Mechanisms, eds. C. Beaumont and A. Tankard; Canadian Society of Petroleum Geologists, Memoir 12, p. 311-317.

RYAN, R. J. AND BOEHNER, R. C. 1994: Geology of the Cumberland Basin, Cumberland, Colchester and Pictou Counties, Nova Scotia; Nova Scotia Dept. of Natural Resources, Mines and Energy Branches, Memoir 10, 222p.

SANGSTER, D. F. 1994: Fluid migration and mineralization in the Lower Windsor Group, Nova Scotia: 1. Background; *in* Program and Summaries, Eighteenth Annual Review of Activities, ed. D. R. MacDonald; Nova Scotia Dept. of Natural Resources, Mines and Energy Branches, Report 94-2, p. 46.

SANGSTER, D. F. AND SAVARD, M. M. 1994: Fluid migration and mineralization in the Lower Windsor Group, Nova Scotia: 12. Summary and Conclusions; *in* Program and Summaries, Eighteenth Annual Review of Activities, ed. D. R. MacDonald; Nova Scotia Dept. of Natural Resources, Mines and Energy Branches, Report 94-2, p. 57.

SANGSTER, D. F., SAVARD, M. M. AND BURTT, M. D. 1994: Fluid migration and mineralization in the Lower Windsor Group, Nova Scotia: 4. Isotope geochemistry of the Macumber Formation and altered equivalents, Walton Deposit area, Kennetcook sub-basin; *in* Program and Summaries, Eighteenth Annual Review of Activities, ed. D. R. MacDonald; Nova Scotia Dept. of Natural Resources, Mines and Energy Branches, Report 94-2, p. 49.

SCHENK, P. E. 1967: The Macumber Formation of the Maritime Provinces, Canada - A Mississippian analogue to recent strand-line carbonates of the Persian Gulf; Journal of Sedimentary Petrology, v. 37, p. 365-376.

SCHENK, P. E. 1969: Carbonate-sulfate-red bed facies and cyclic sedimentation of the Windsorian Stage (Middle Carboniferous), Maritime Provinces; Canadian Journal of Earth Sciences, v. 6, p. 1037-1066.

SMITH, L. AND COLLINS, J. A. 1979: Unconformities, sedimentary copper mineralization, and thrust faulting in the Horton and Windsor Groups, Cape Breton Island and central Nova Scotia; Ninth International Geological Congress of Carboniferous Stratigraphy and Geology, v. 3, p. 105-116.

STEVENSON, I. M. 1959: Shubenacadie and Kennetcook map areas, Colchester, Hants and Halifax Counties, Nova Scotia; Geological Survey of Canada, Memoir 302,

SVERJENSKY, D. A., 1986: Genesis of Mississippi Valley-type lead-zinc deposits; Annual Review of Earth and Planetary Sciences, v. 14, p. 177-199.

SVERJENSKY, D. A., 1989: Chemical evolution of basinal brines that formed sediment-hosted Cu-Pb-Zn deposits; *in* Sediment-hosted Stratiform Copper Deposits, eds. R. W. Boyle, C. W. Jefferson, E. C. Jowett, and R. V. Kirkham; Geological Association of Canada, Special Paper 36, p. 127-134.

SYMONS, D. T. A. AND SANGSTER, D. F. 1994: Palaeomagnetic methods for dating the genesis of Mississippi Valley-type lead-zinc deposits; *in* Sediment-hosted Zn-Pb ores, eds. L. Fontboté and M. Boni; Society of Geology Applied to Mineral Deposits, Special Publication No. 10, p. 42-58.

TURNER, R. 1967: Internal company letter; *in* Nova Scotia Dept. of Mines and Energy Assessment Report 21H/01 06-I-51(09).

TENNY, R. E. 1951: The Walton barite deposit; Nova Scotia Dept. of Mines, Annual Report 1951, pt. 2., p. 127-143.

WEEKS, L. J. 1948: Londonderry and Bass River map areas, Colchester and Hants Counties, Nova Scotia; Geological Survey of Canada, Memoir 245, 86p.

VON BITTER, P. H., SCOTT, S. D. AND SCHENK, P. E. 1990: Early Carboniferous low-temperature hydrothermal vent communities from Newfoundland; Nature, v. 344, p. 145-147.

APPENDIX I

RECONSTRUCTED SECTIONS AND PLANS

The thirty-one vertical cross-sections drawn by Patterson (1988b) have been re-drawn to reflect the probable location of the upper Macumber/lower Macumber contact and the probable location of the Macumber/evaporite contact prior to karsting. Type I and Type II ore distribution is also included on the sections. The location of the sections, spaced at 50' intervals along the B-baseline, is shown in Figure 2-3. From the sections three plan maps, of the 690', 850' and 1030' levels, were drawn, also showing the distribution of the ore types. The legend and scale (1"=66.7') for all sections is shown on page A2. The legend also applies to the plan maps, although the scale is different from that of the sections.

LEGEND

349 ——— diamond drill hole and hole number

——— geological contact

- - - - - - inferred location of upper Macumber/ lower Macumber contact

— — — location of evaporite/Macumber contact (pre-karst)

- - - - - inferred location of evaporite/ Macumber contact (pre-karst)

..... limit of sand and limestone breccia

MINERALISATION

- TYPE I
- TYPE I Cu-rich (>0.3%)
- TYPE I Pb-rich (>0%)
- TYPE II
- TYPE II Cu-rich (>0.6%)
- TYPE II Pb-rich (>0%)

50 feet

Section #1

A3

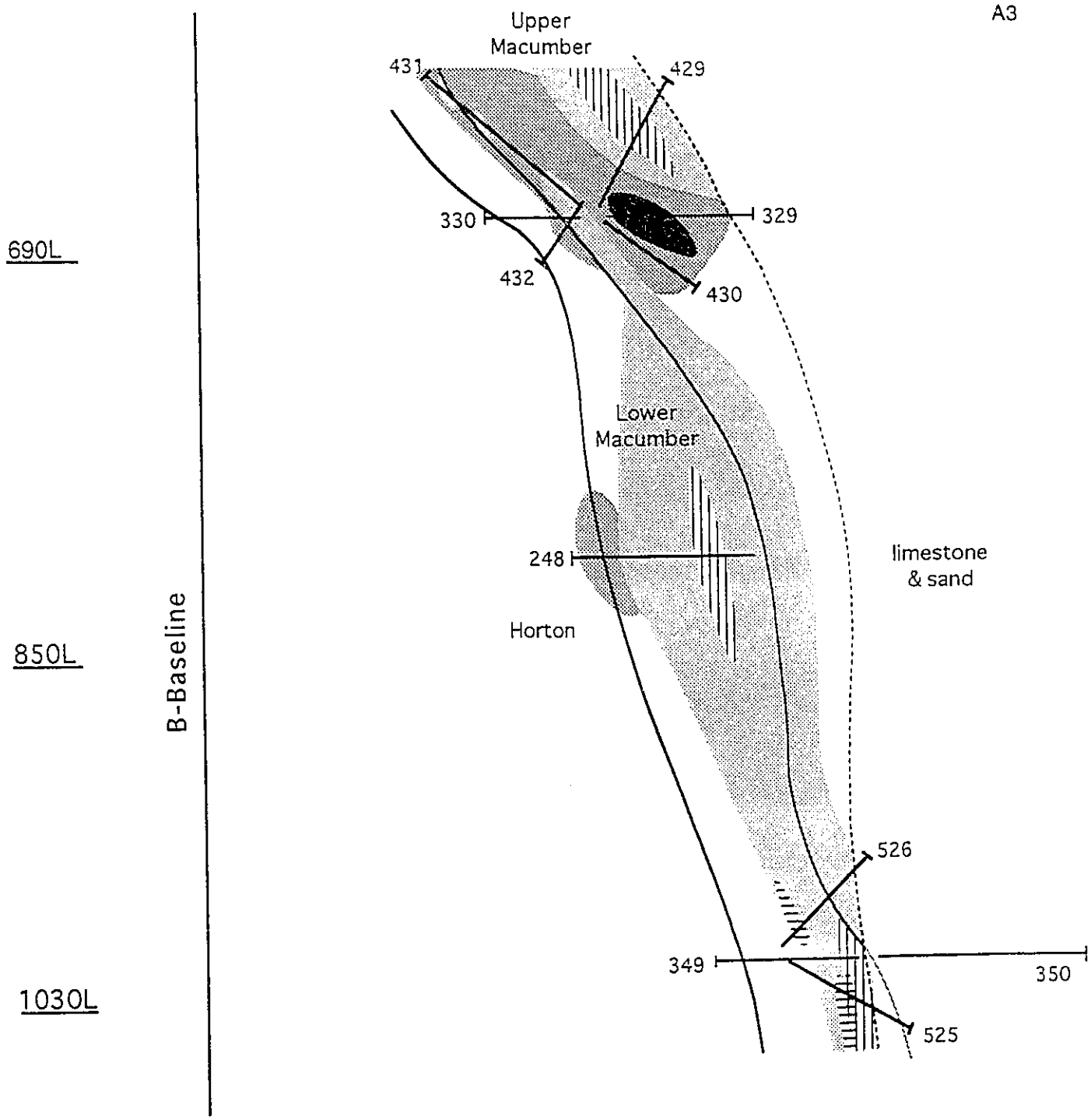
690L
850L
1030L
B-Baseline
Upper
Macumber
431
429
330
329
432
430
Lower
Macumber
248
limestone
& sand
Horton
526
349
350
525

Section #2

A4

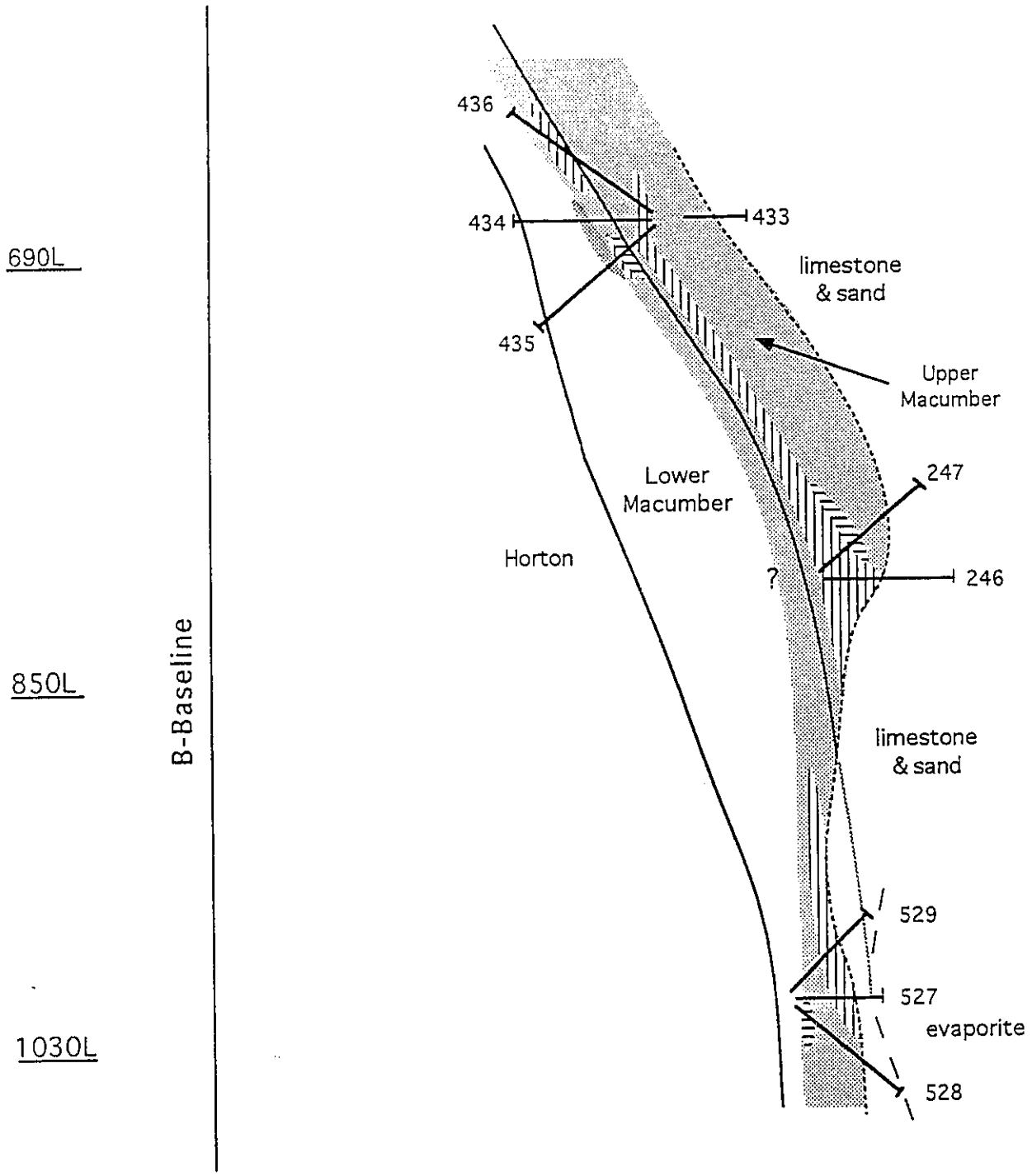
690L
850L
1030L
B-Baseline
436
434
435
433
limestone
& sand
Upper
Macumber
Lower
Macumber
Horton
?
247
246
limestone
& sand
529
527
evaporite
528

Section #3

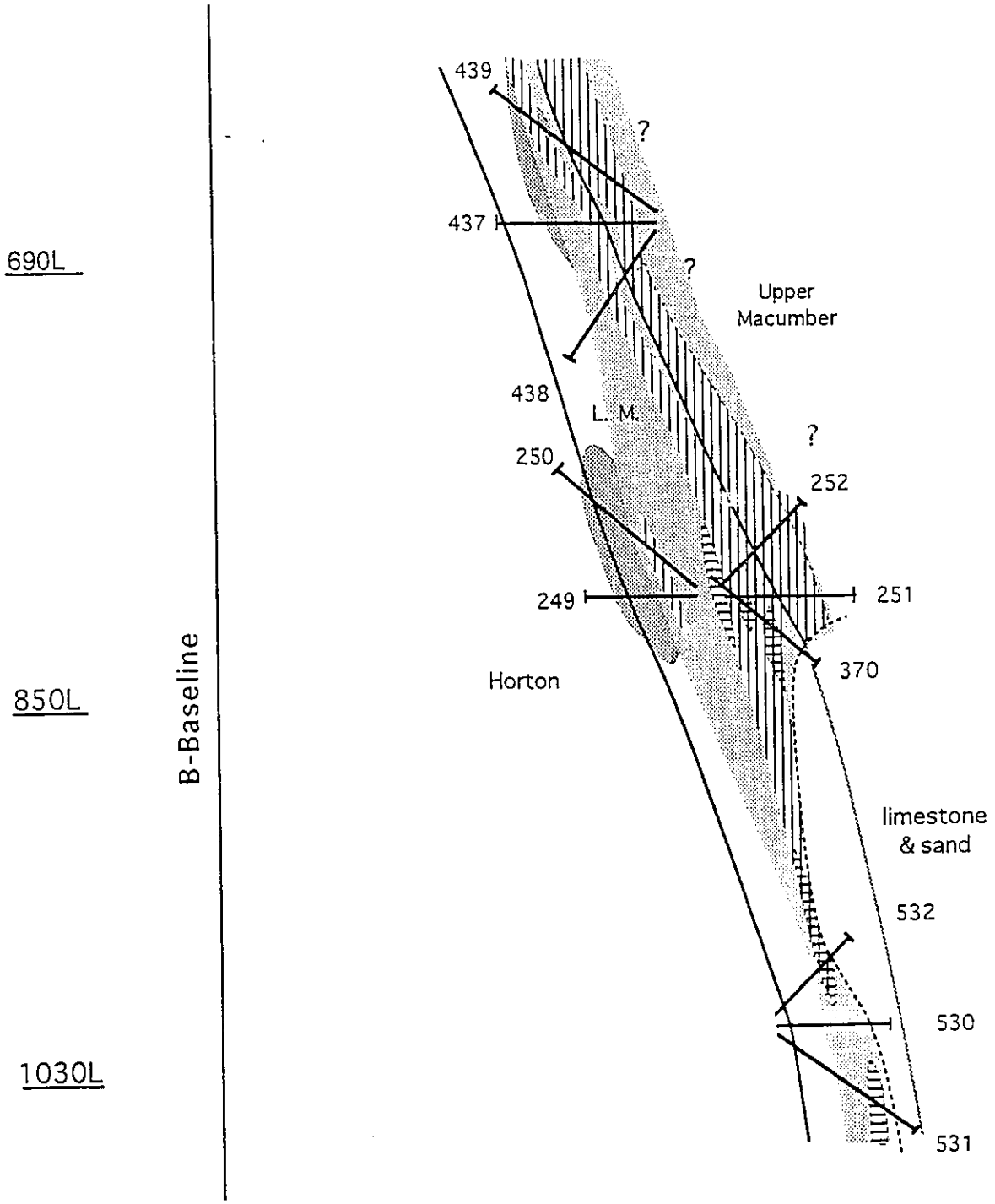
690L
850L
1030L
B-Baseline
439
437
438
250
249
252
251
370
532
530
531
?
?
?
Upper
Macumber
L. M.
Horton
limestone
& sand

Section #4

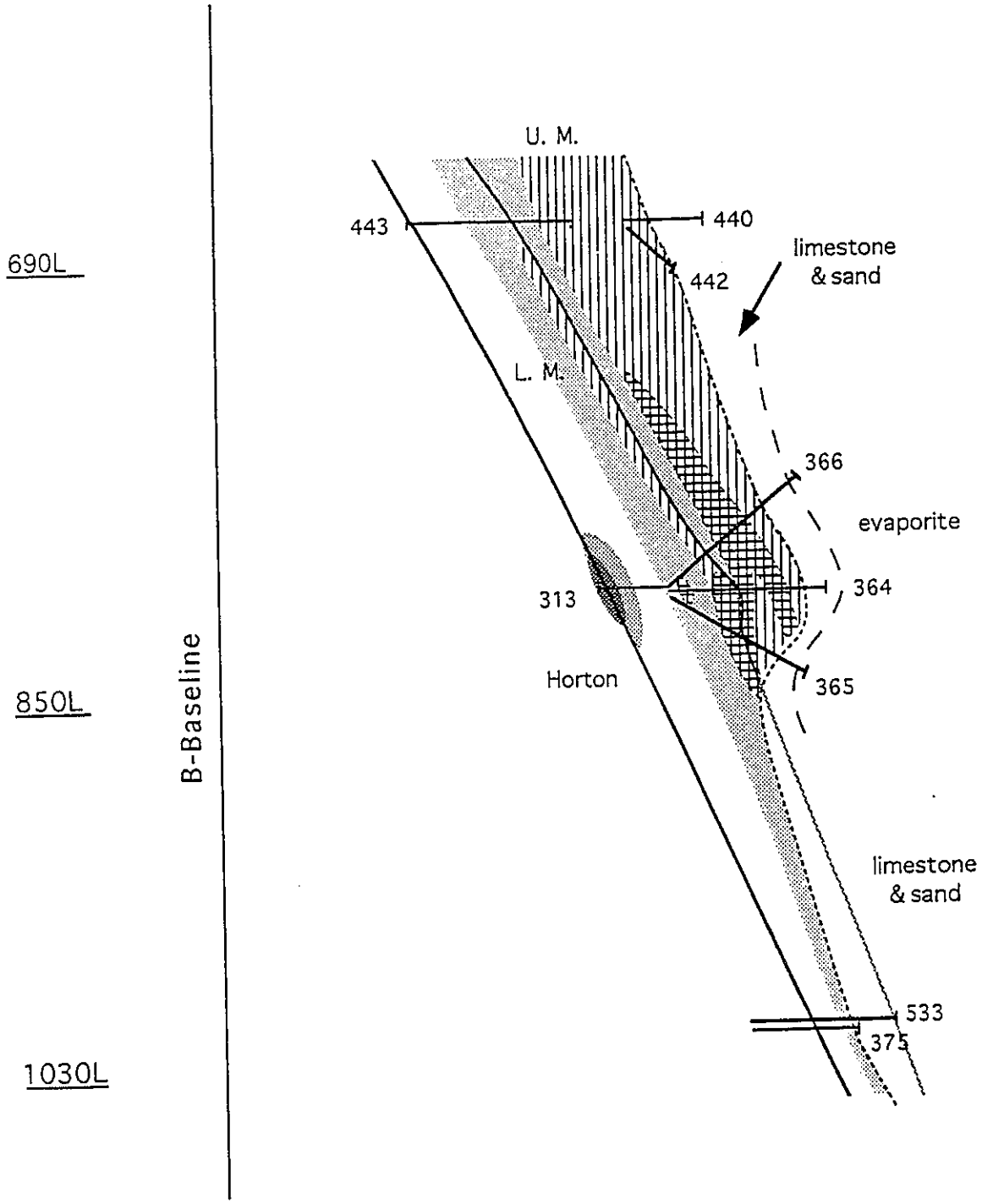
690L
850L
1030L
B-Baseline
U. M.
443
440
442
limestone
& sand
L. M.
366
evaporite
313
364
Horton
365
limestone
& sand
533
375

Section #5

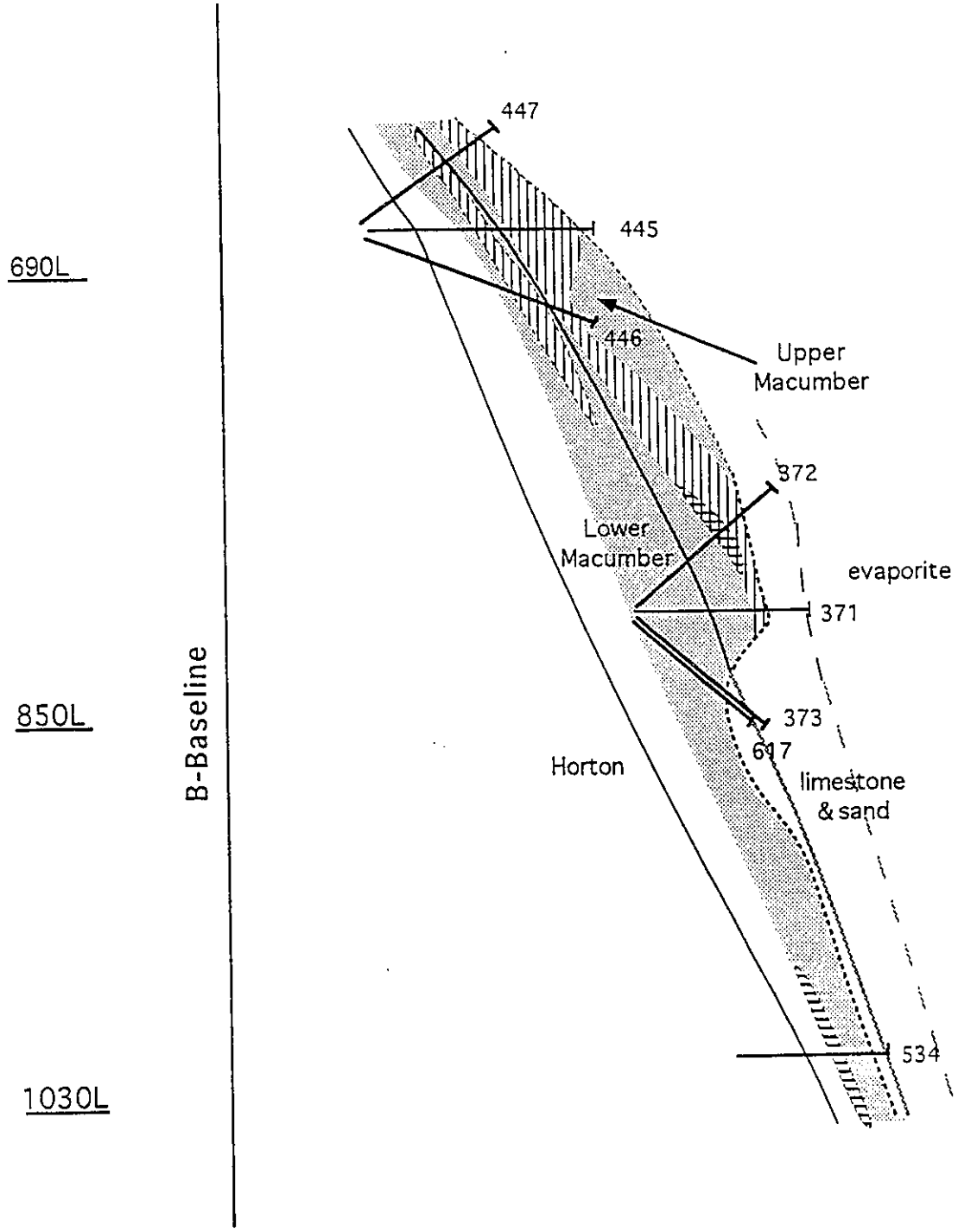
690L
850L
1030L
B-Baseline
447
445
446
Upper
Macumber
372
Lower
Macumber
evaporite
371
373
617
Horton
limestone
& sand
534

Section #6

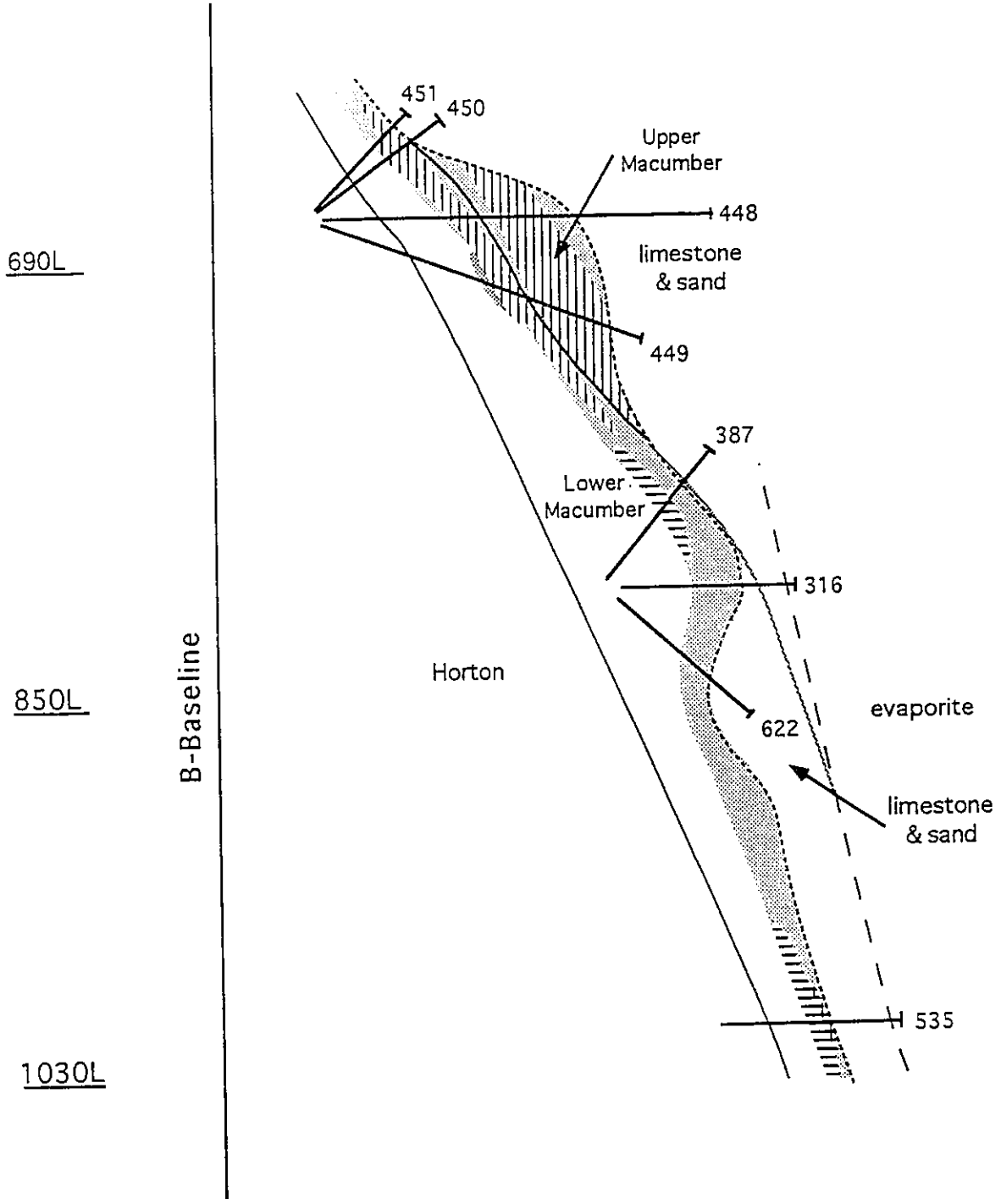
690L
850L
1030L
B-Baseline
451
450
Upper
Macumber
448
limestone
& sand
449
387
Lower
Macumber
316
Horton
evaporite
622
limestone
& sand
535

Section #7

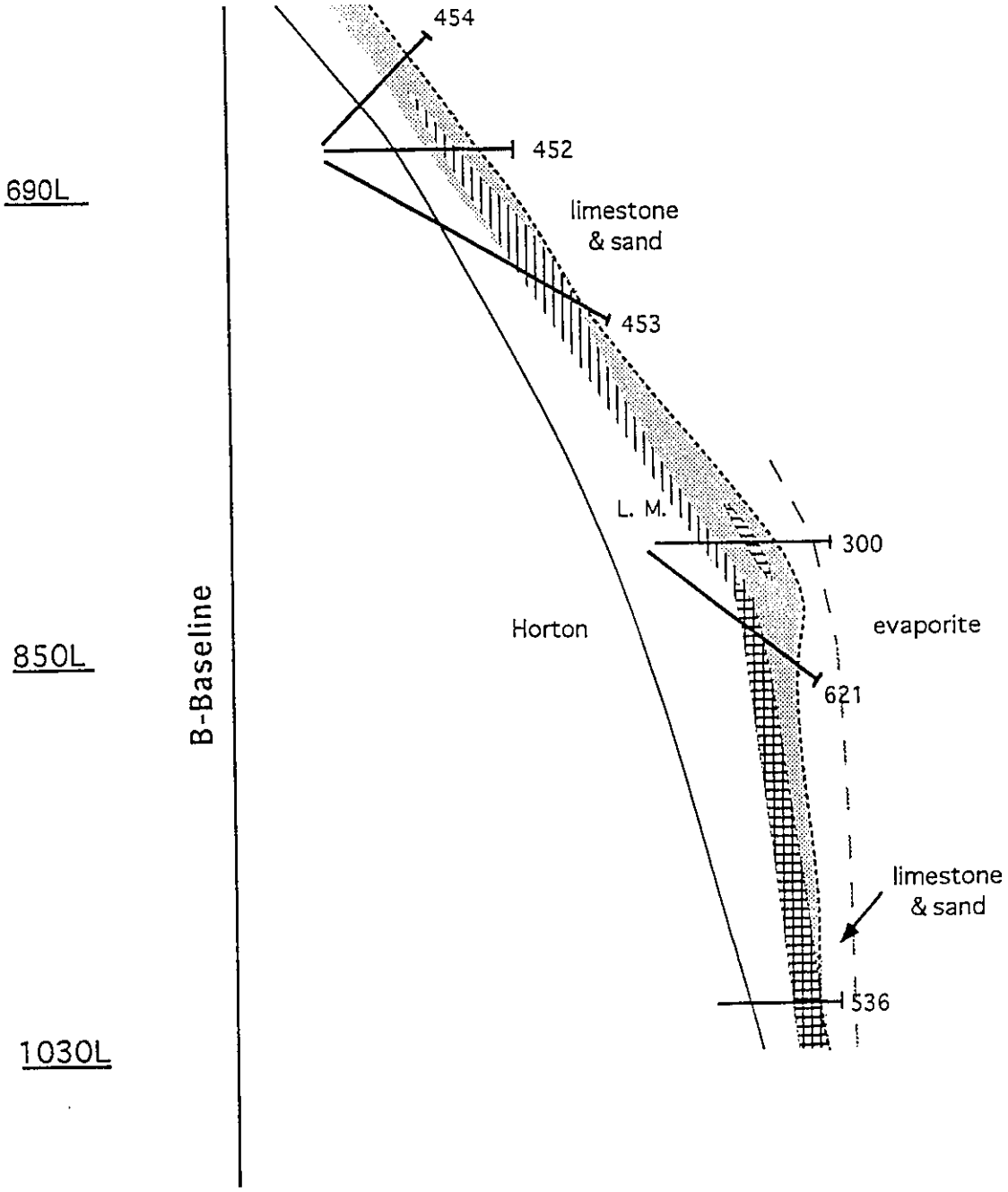
690L
850L
1030L
B-Baseline
454
452
limestone
& sand
453
L. M.
300
Horton
evaporite
621
limestone
& sand
536

Section #8

A10

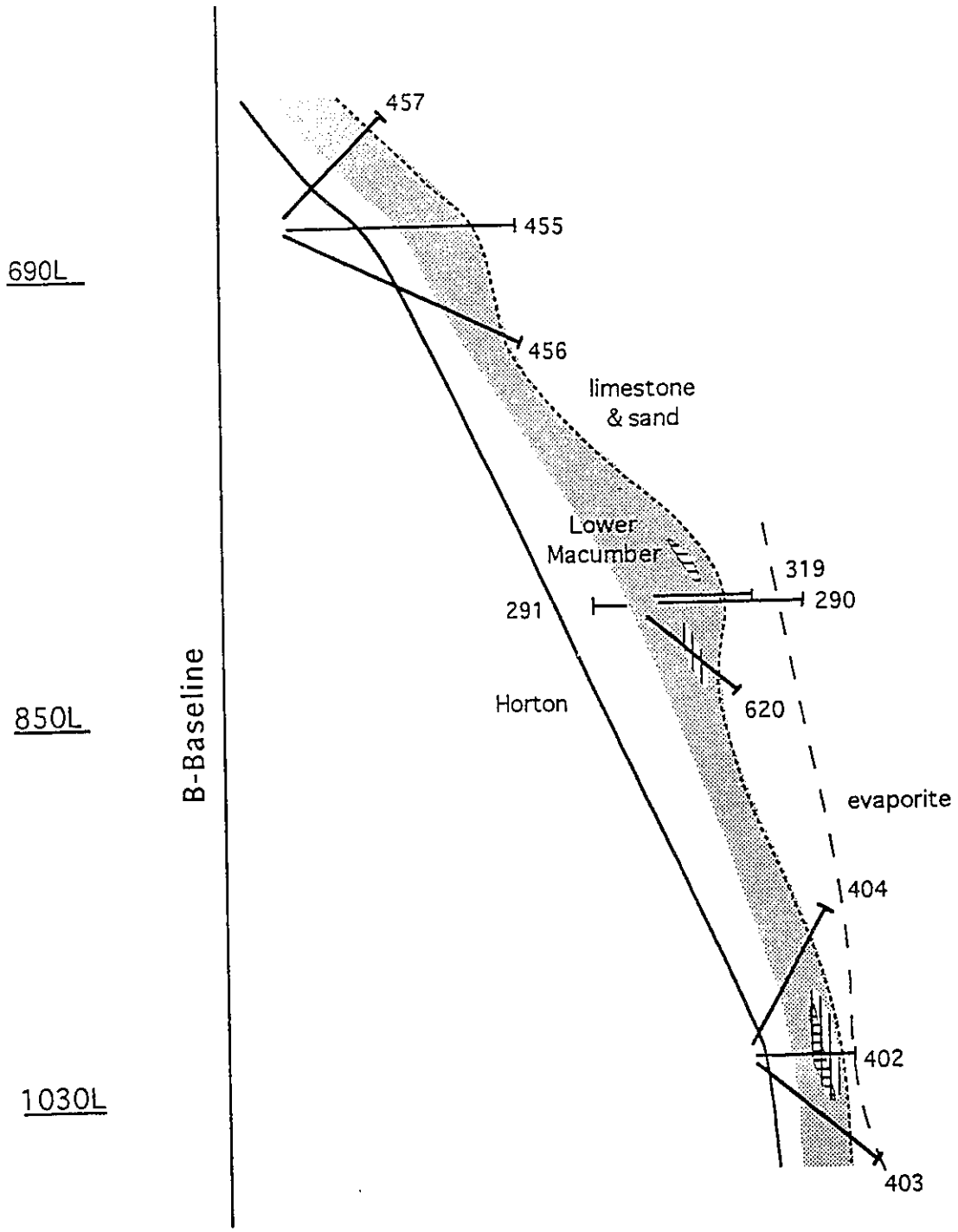

Section #9

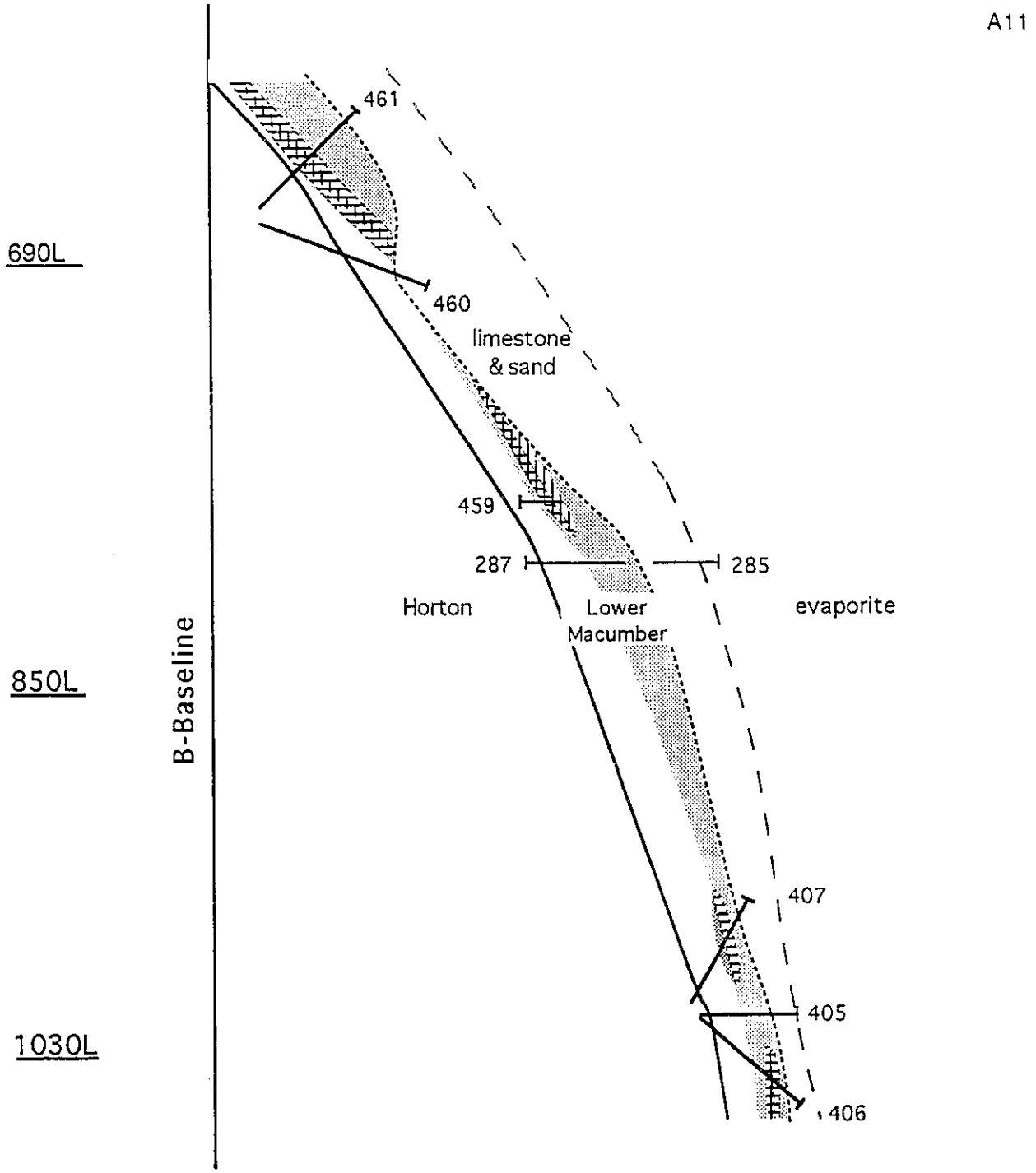
690L
850L
1030L
B-Baseline
461
460
limestone
& sand
459
287
285
Horton
Lower
Macumber
evaporite
407
405
406

Section #10

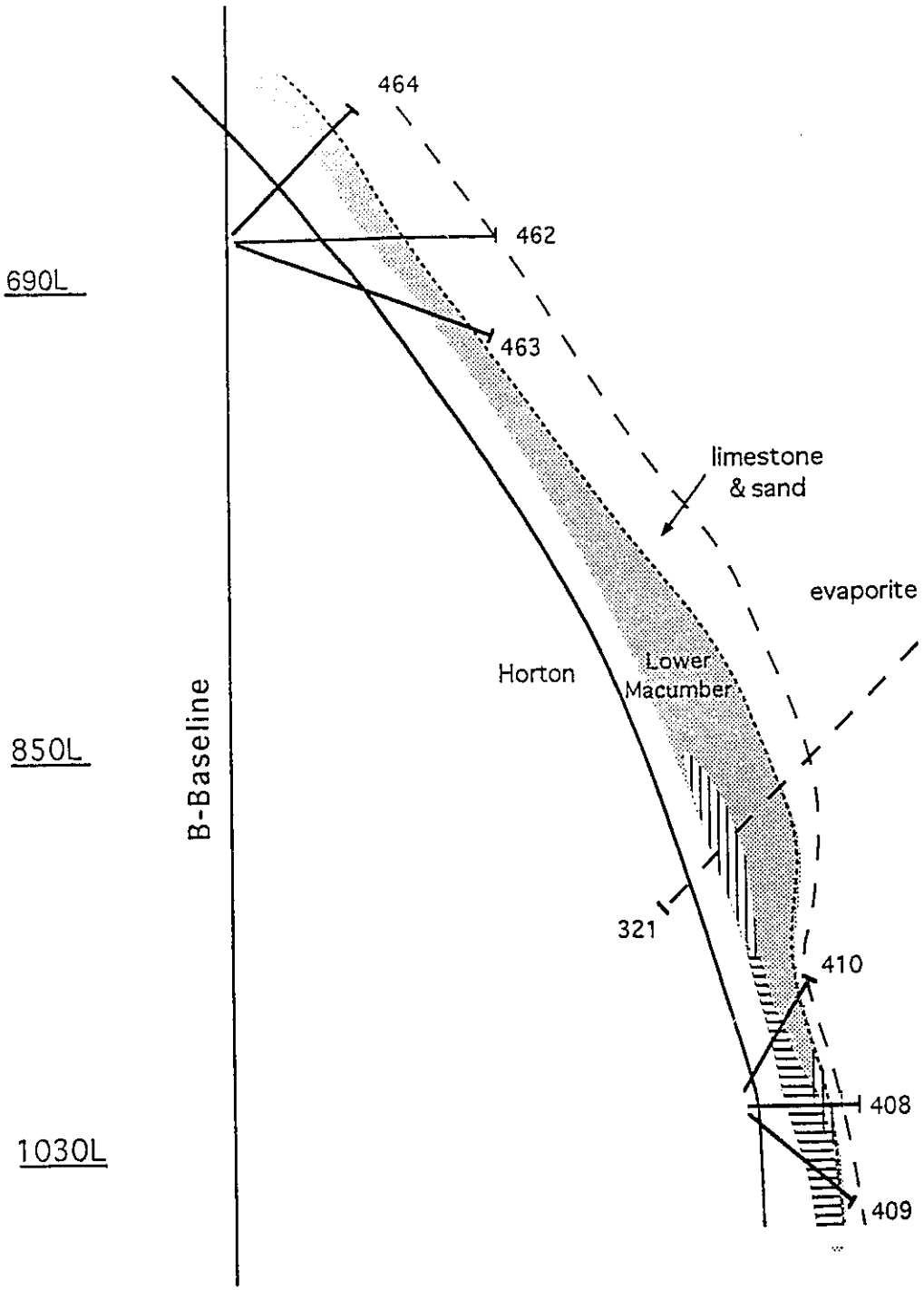
464
462
463
690L
limestone
& sand
evaporite
Horton
Lower
Macumber
B-Baseline
850L
321
410
408
1030L
409

Section #11

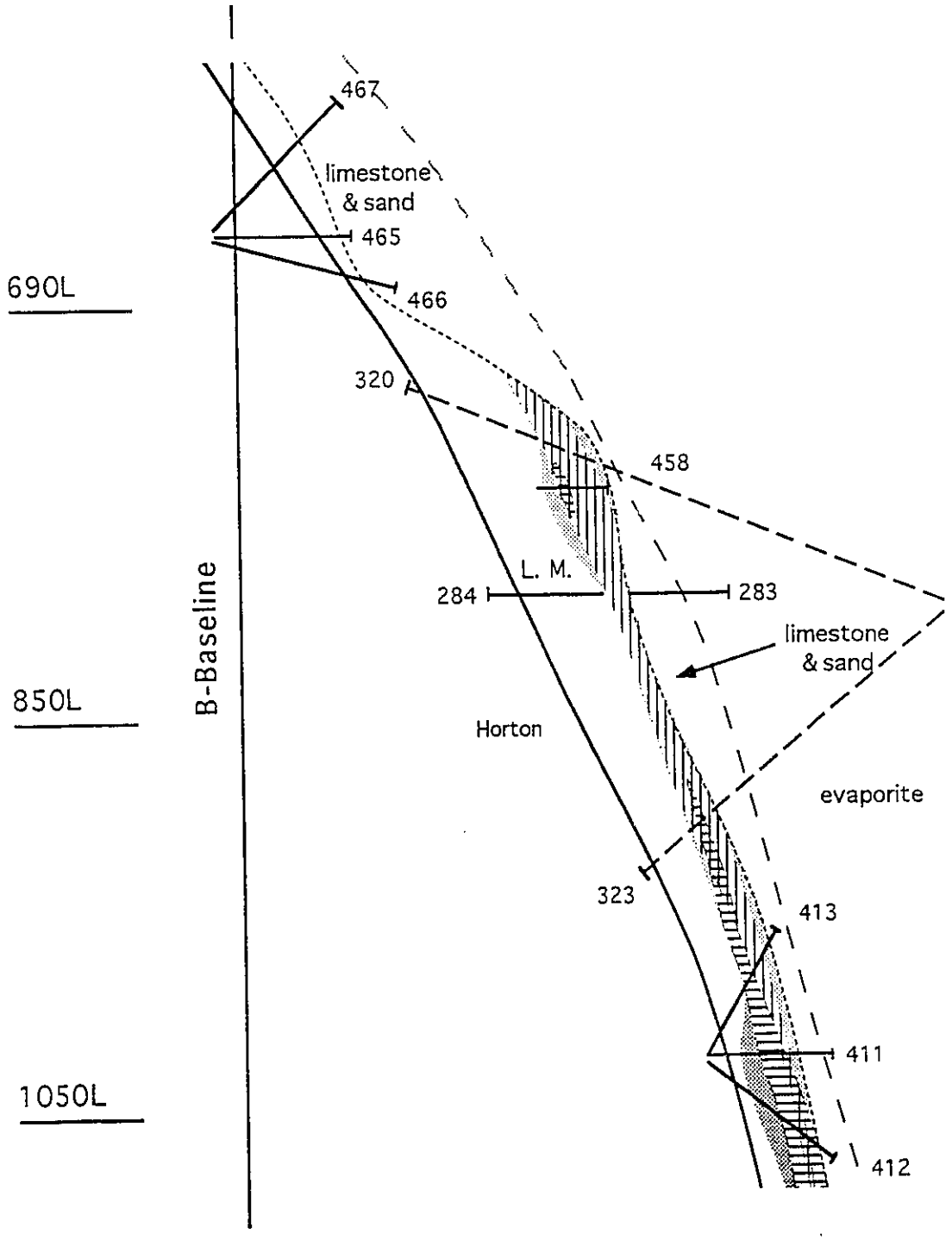
467
limestone
& sand
465
466
690L
320
458
L. M.
284
283
limestone
& sand
B-Baseline
850L
Horton
evaporite
323
413
411
412
1050L

Section #12

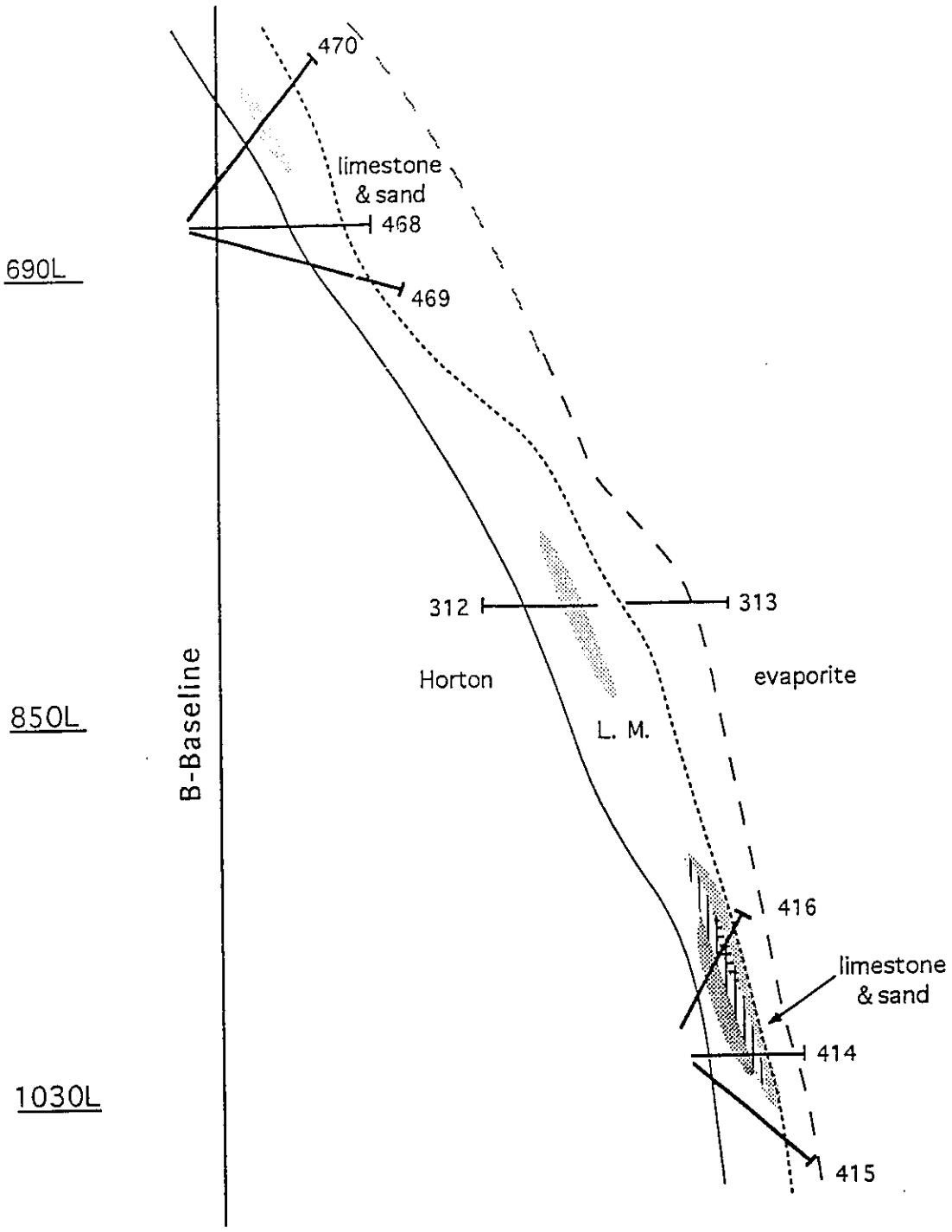
470
limestone
& sand
468
690L
469
312
313
Horton
evaporite
850L
B-Baseline
L. M.
416
limestone
& sand
414
1030L
415

Section #13

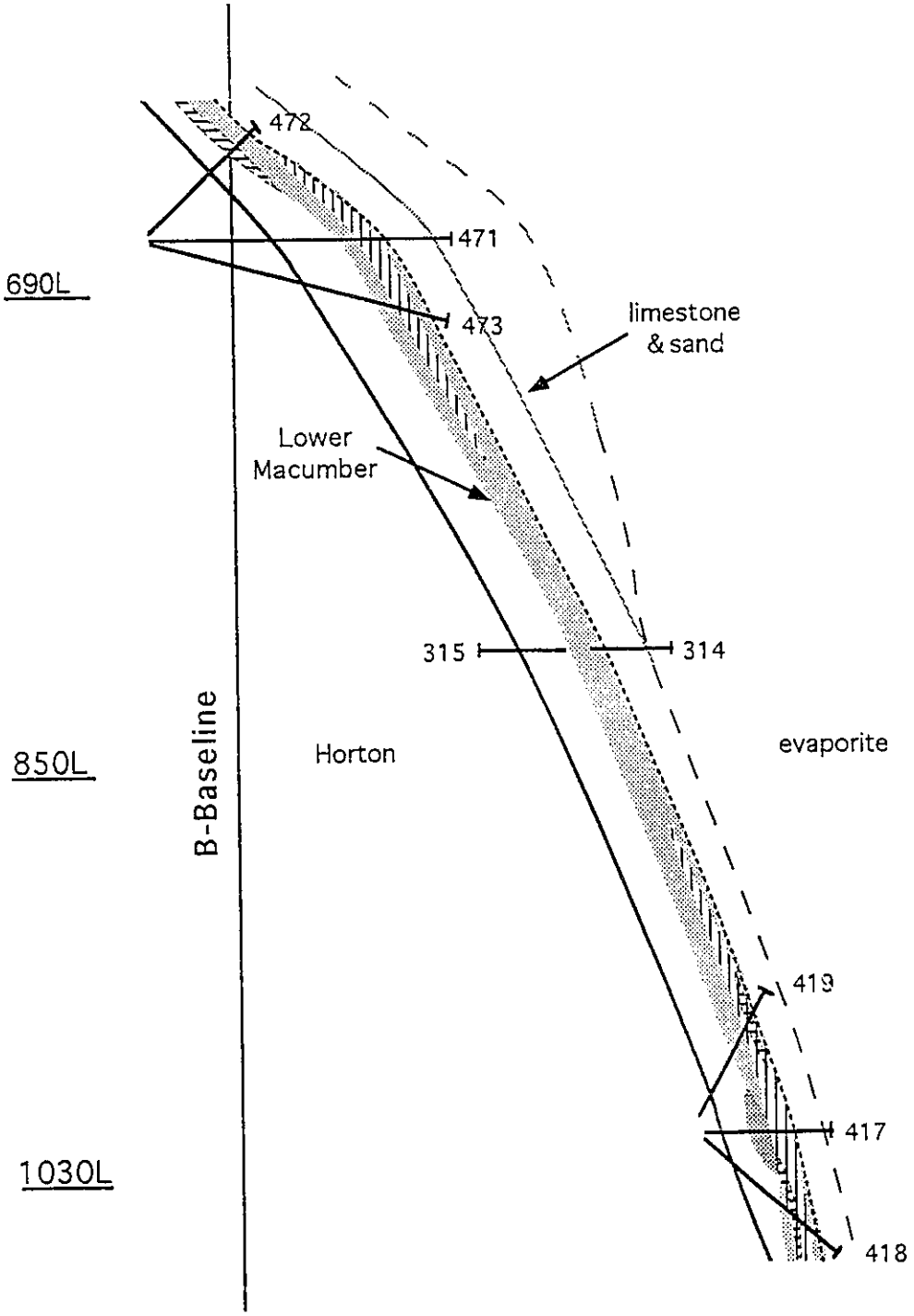
472
471
473
690L
limestone
& sand
Lower
Macumber
315
314
B-Baseline
850L
Horton
evaporite
419
417
1030L
418

Section #14

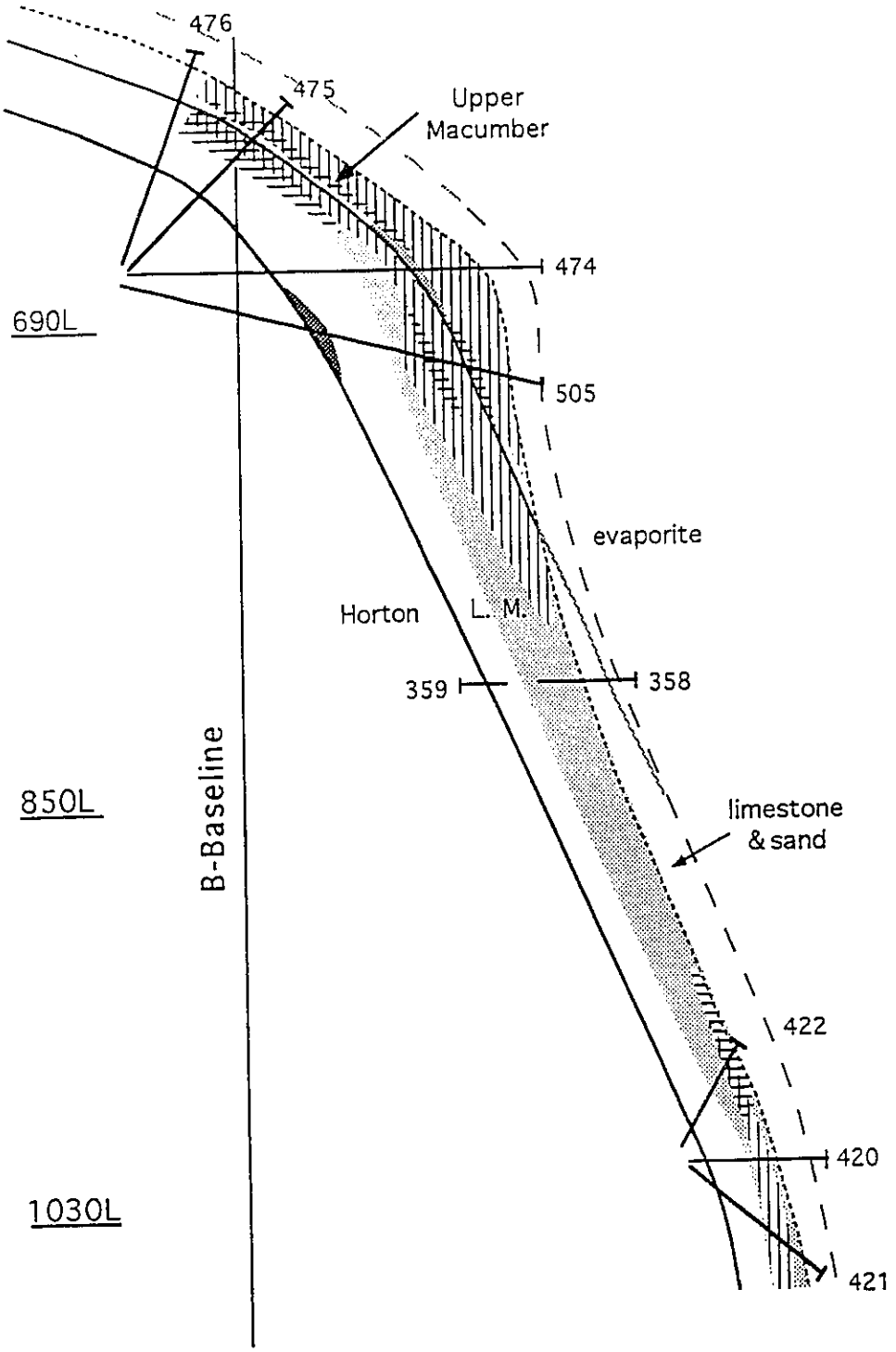
476
475
Upper
Macumber
474
690L
505
evaporite
Horton
L. M.
359
358
B-Baseline
850L
limestone
& sand
422
420
1030L
421

Section #15

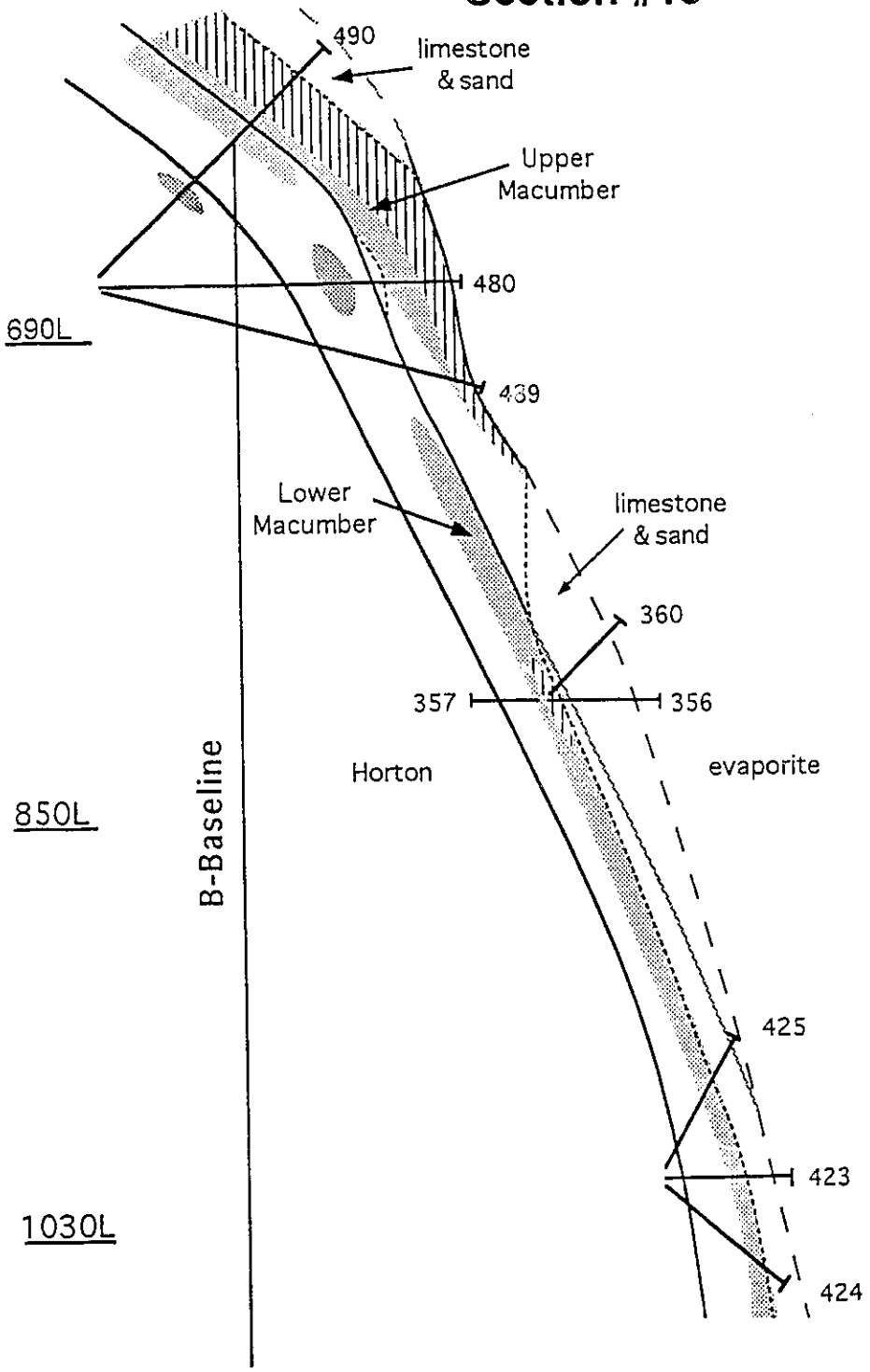
490
limestone
& sand
Upper
Macumber
480
690L
439
Lower
Macumber
limestone
& sand
360
357
356
B-Baseline
Horton
evaporite
850L
425
423
1030L
424

Section #16

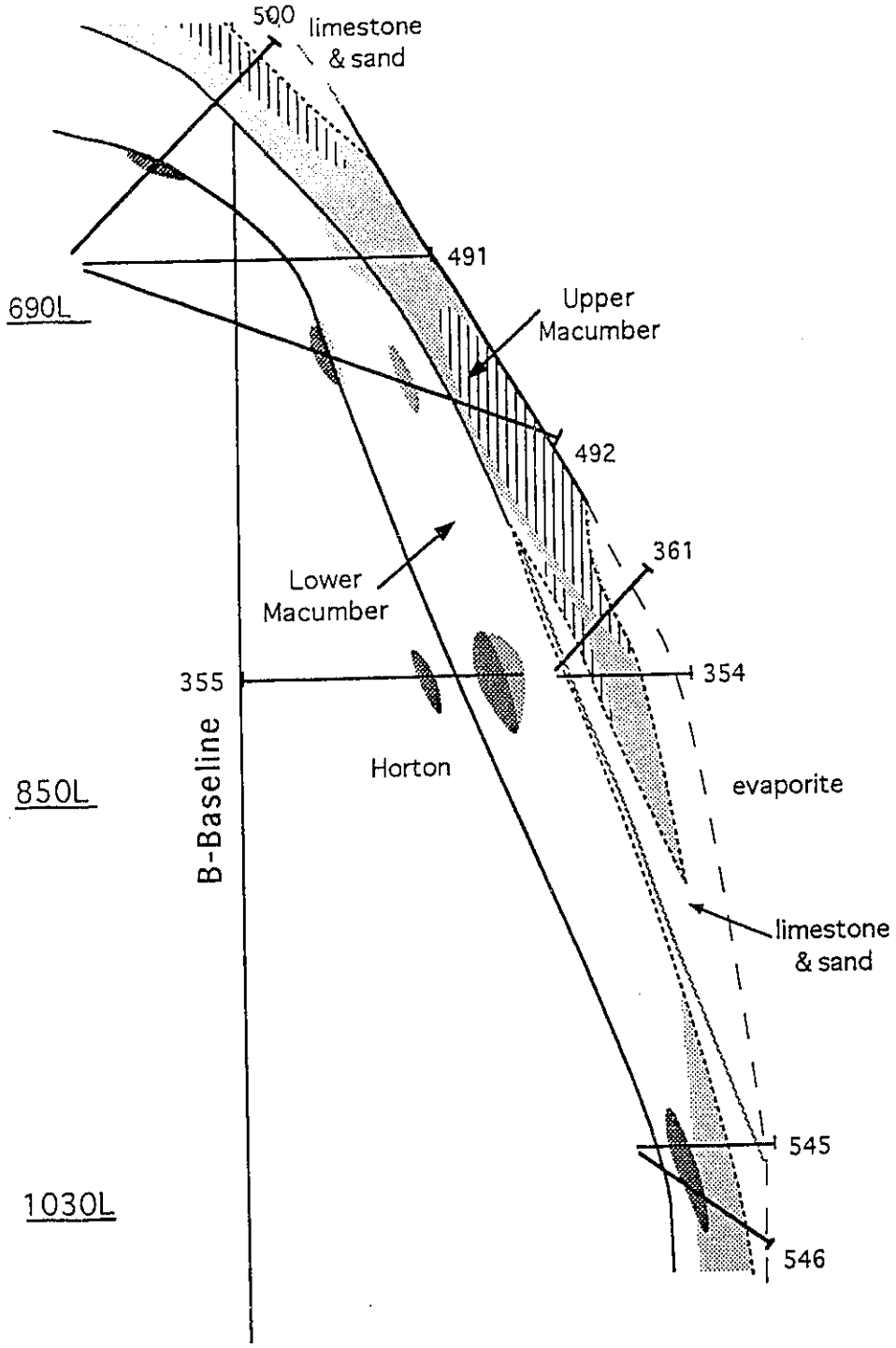
500
limestone
& sand
491
690L
Upper
Macumber
492
361
Lower
Macumber
355
354
B-Baseline
Horton
850L
evaporite
limestone
& sand
545
1030L
546

Section #17

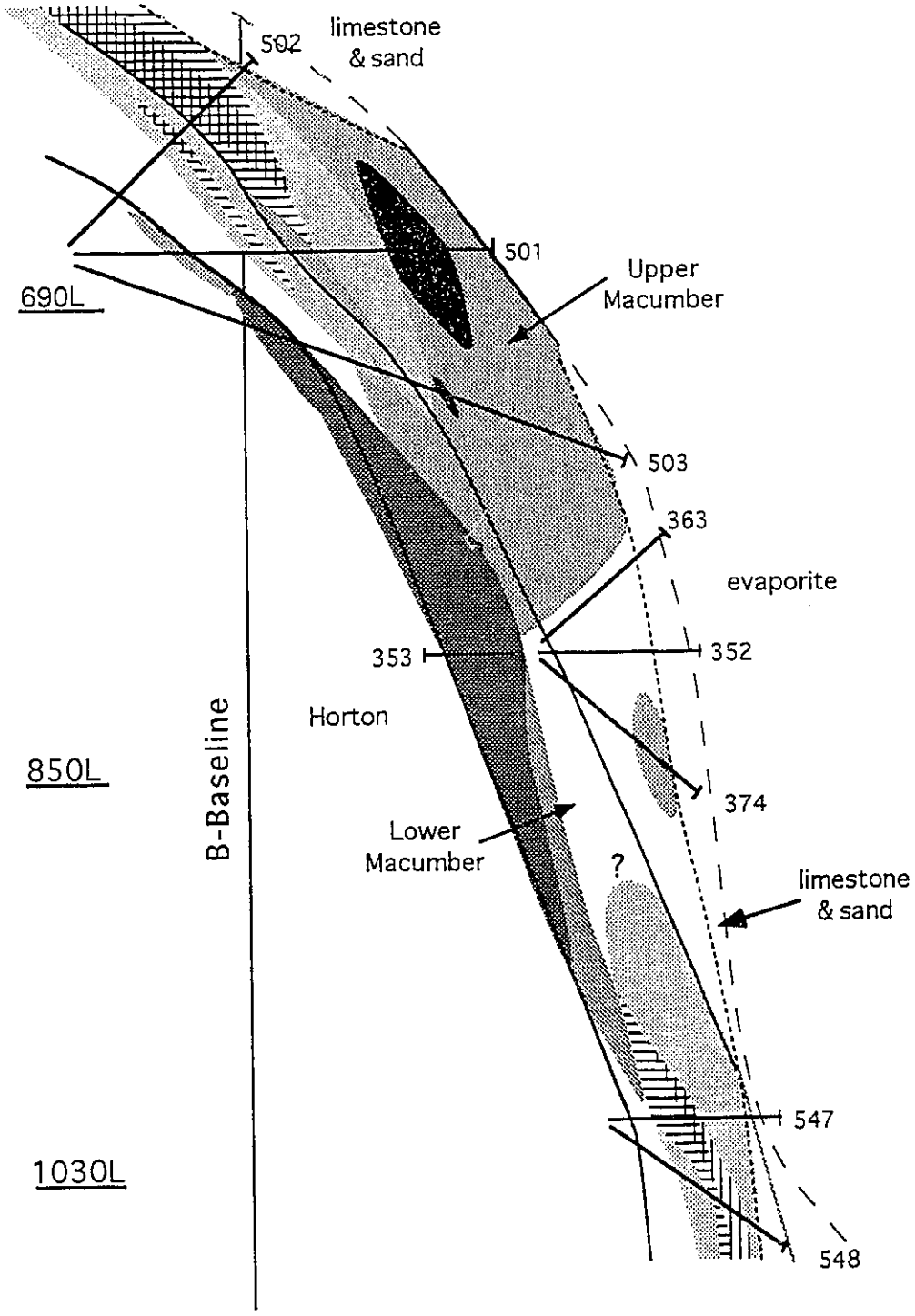
502
limestone
& sand
501
690L
Upper
Macumber
503
363
evaporite
353
352
Horton
850L
B-Baseline
374
Lower
Macumber
?
limestone
& sand
547
1030L
548

Section #18

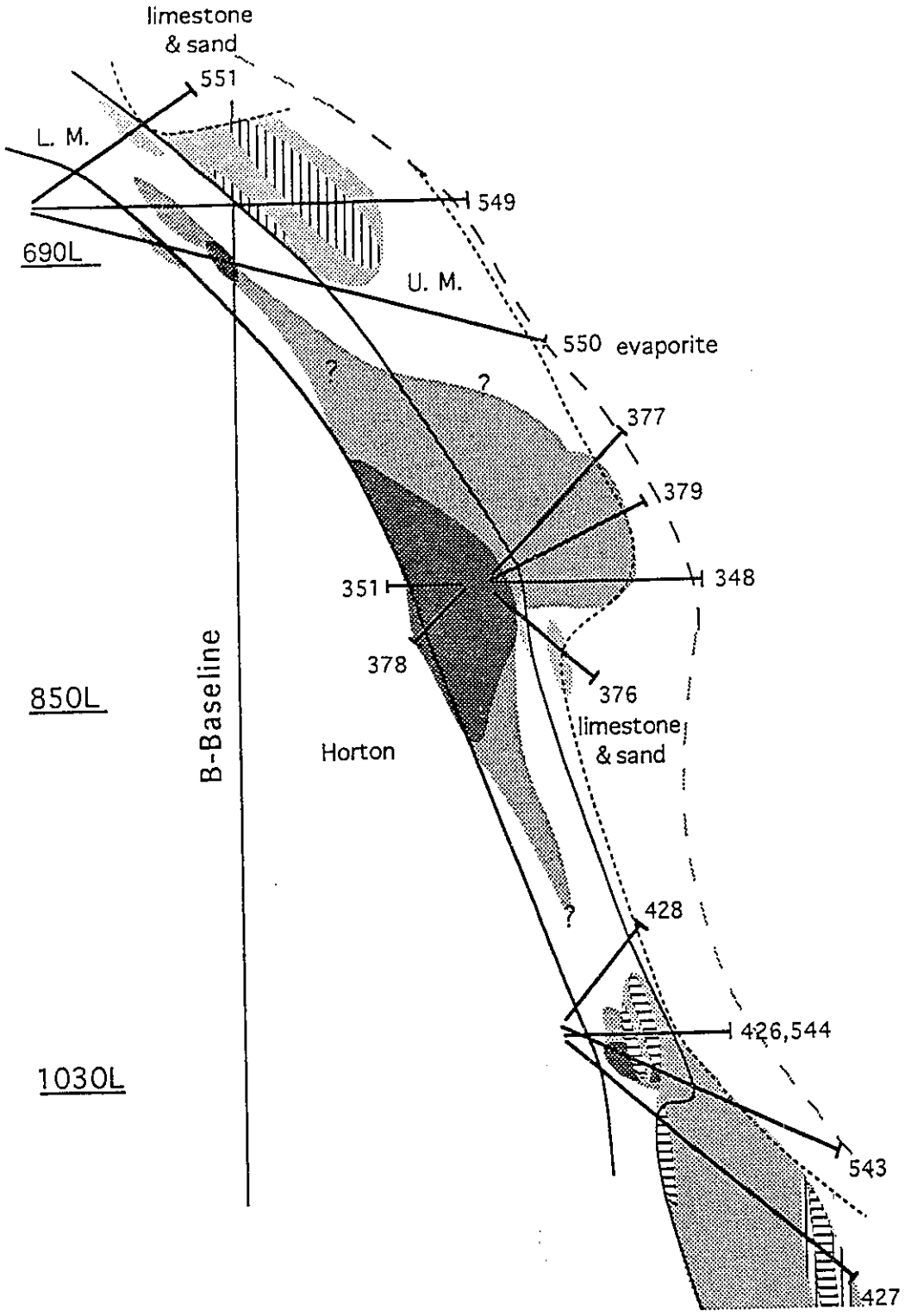
limestone
& sand
551
L. M.
549
690L
U. M.
550 evaporite
?
?
377
379
348
351
378
376
850L
B-Baseline
Horton
limestone
& sand
?
428
426,544
1030L
543
427

Section #19

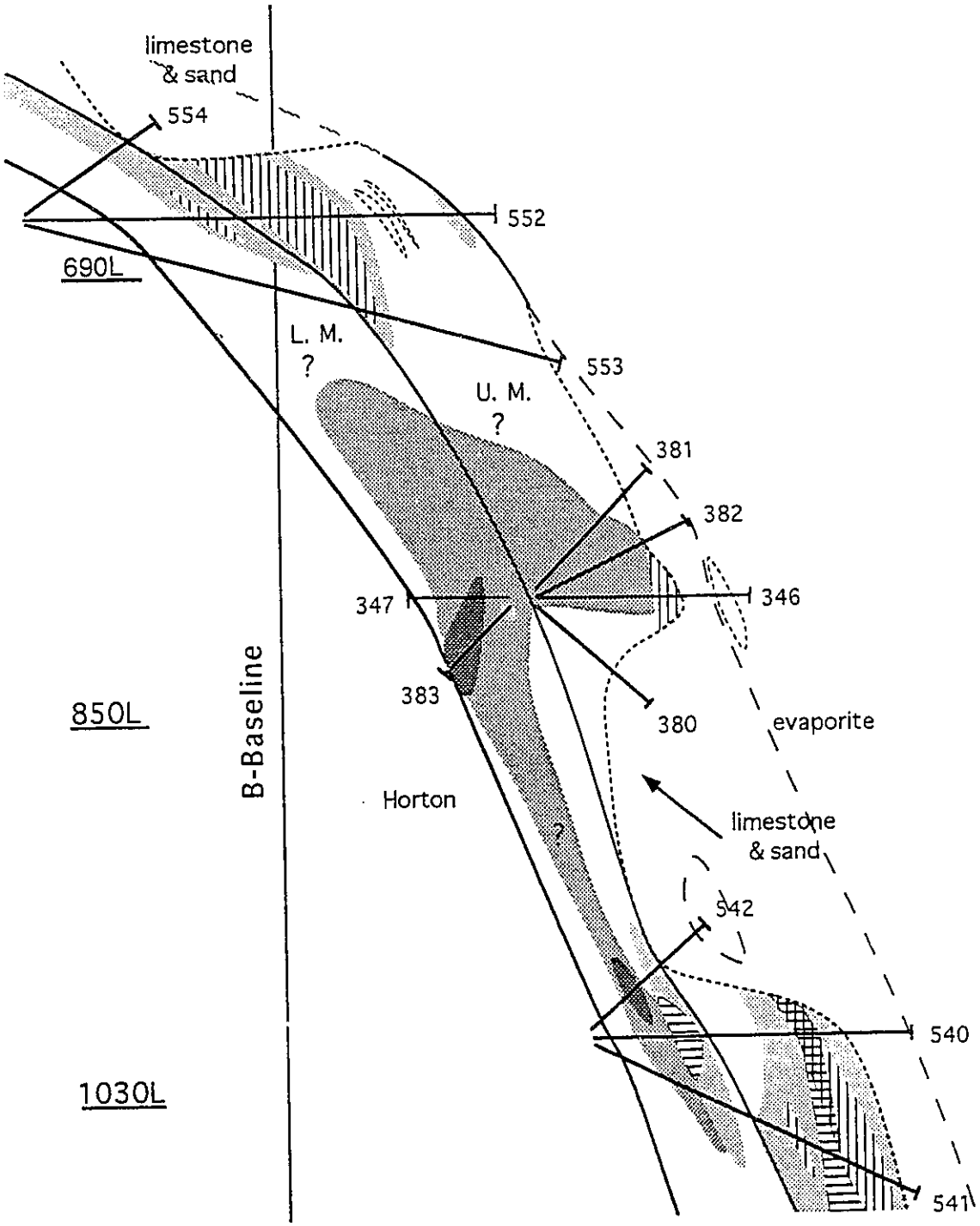
limestone
& sand
554
552
690L
L. M.
?
553
U. M.
?
381
382
347
346
383
380
evaporite
850L
B-Baseline
Horton
limestone
& sand
542
540
1030L
541

Section #20

A22

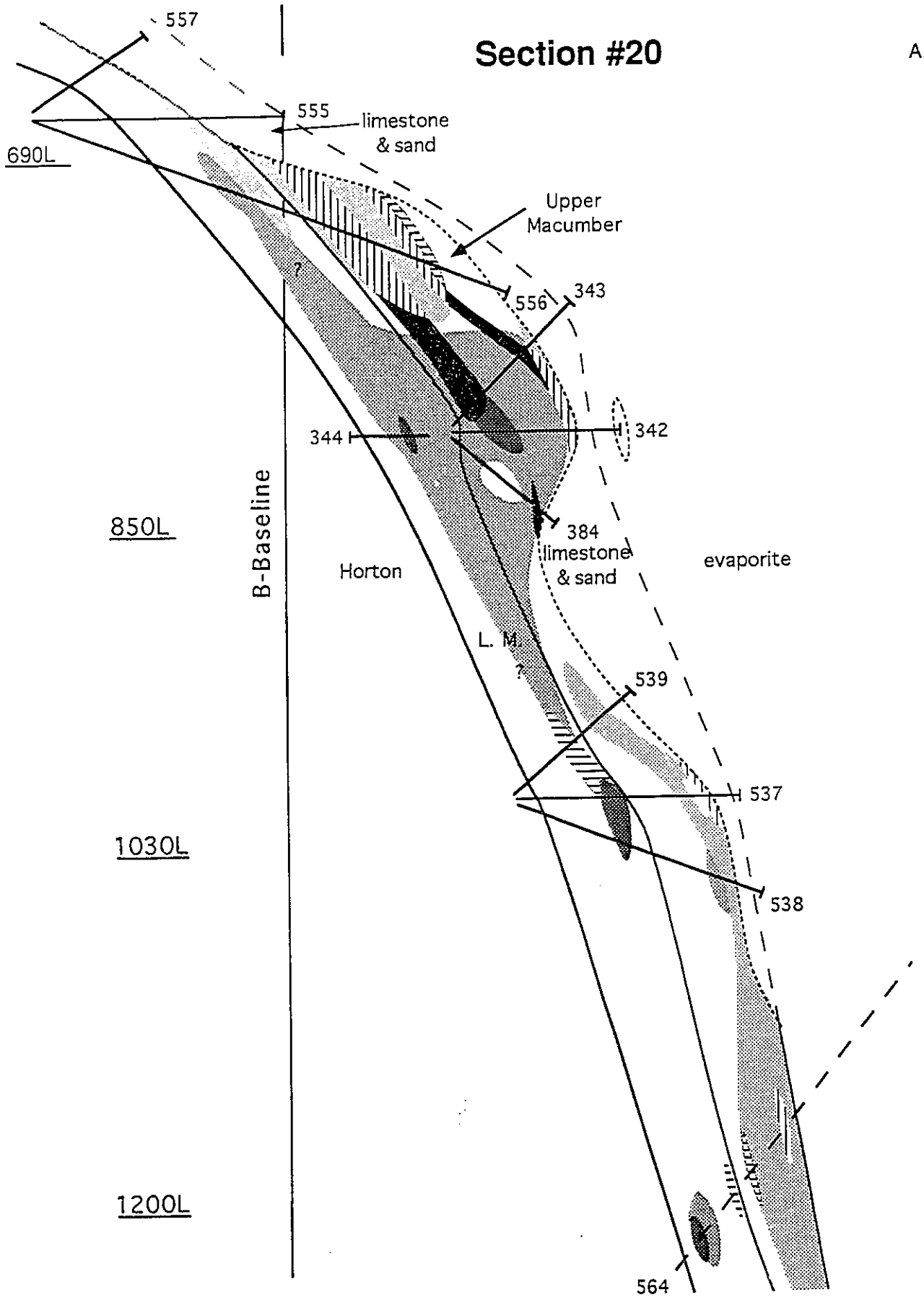

Section #21

A23

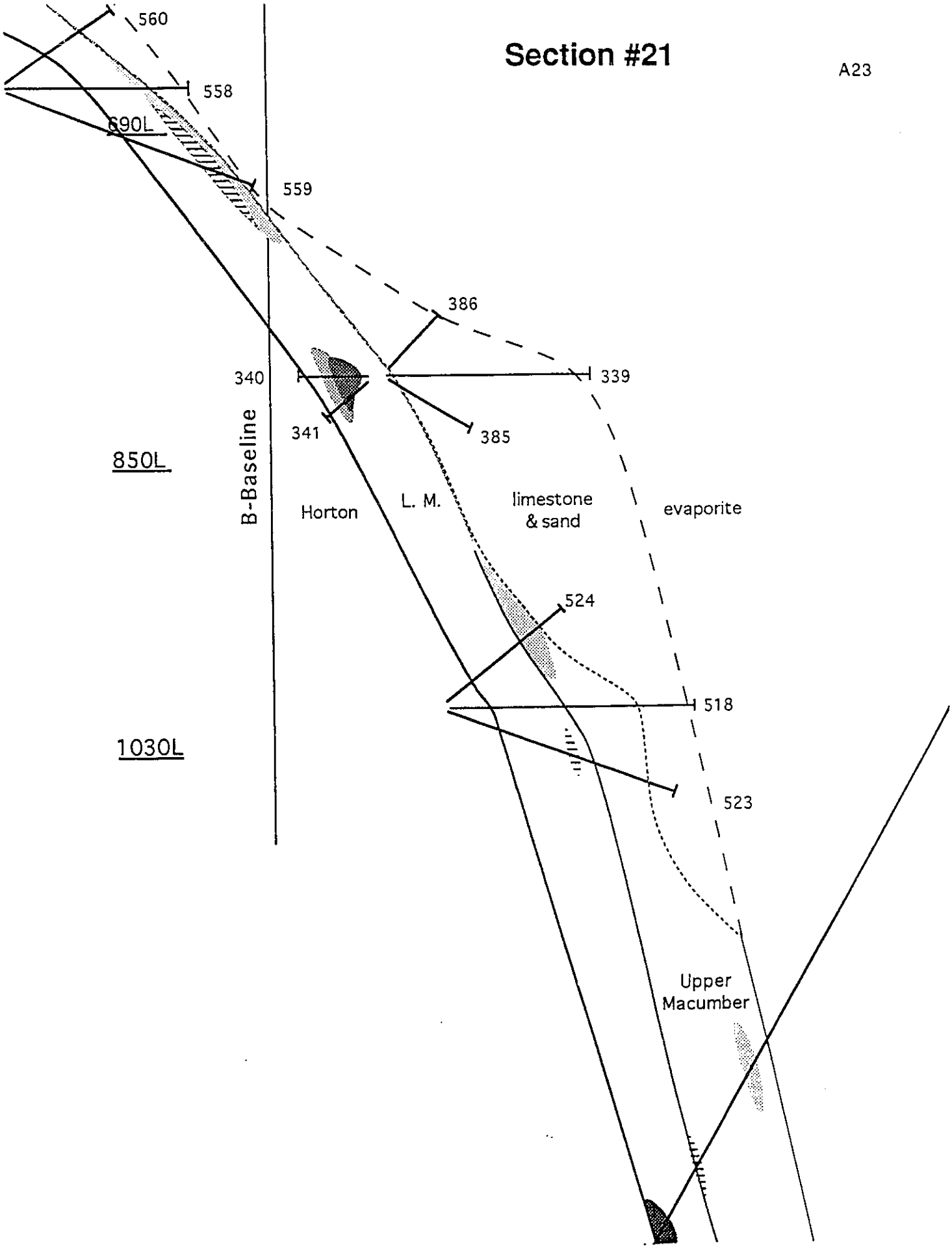

Section #22

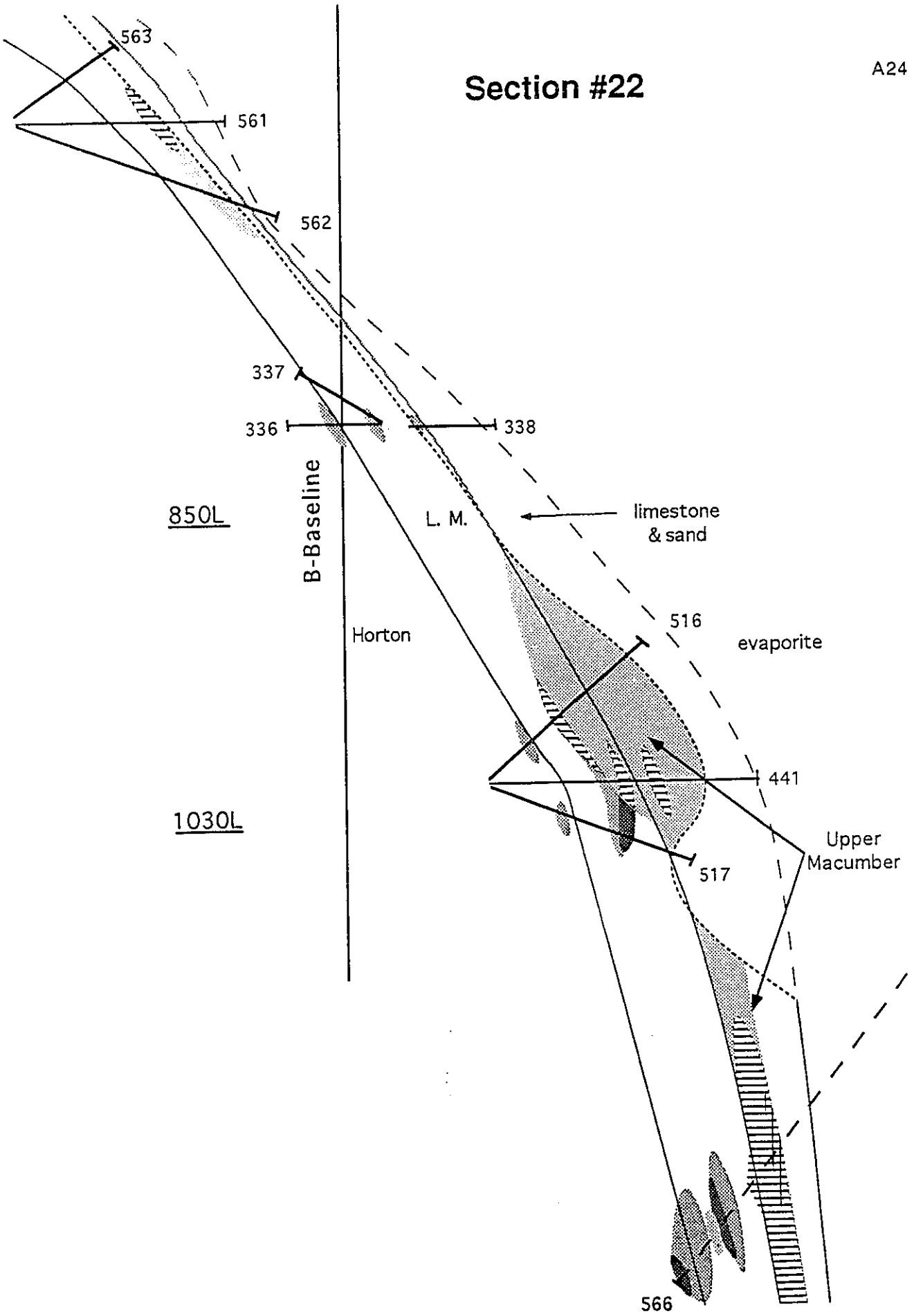
563
561
562
337
336
338
B-Baseline
850L
L. M.
limestone
& sand
Horton
516
evaporite
441
1030L
517
Upper
Macumber
566

Section #23

690L

850L

1030L

B-Baseline

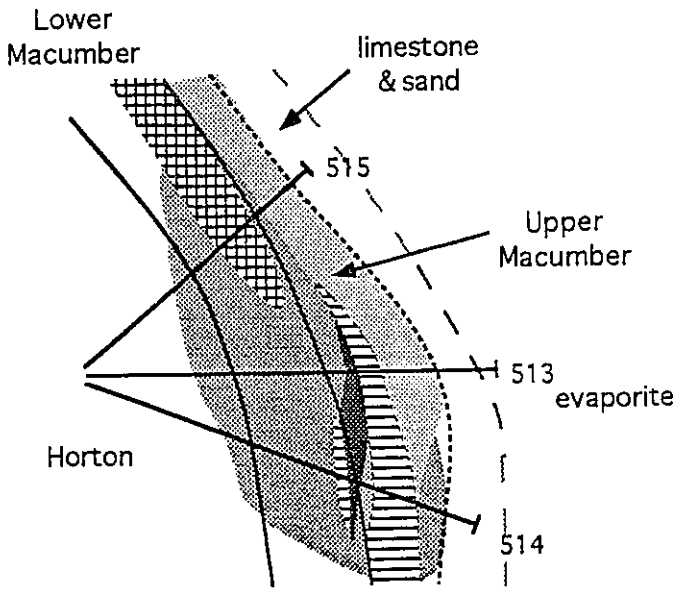

Section #24

690L

850L

1030L

B-Baseline

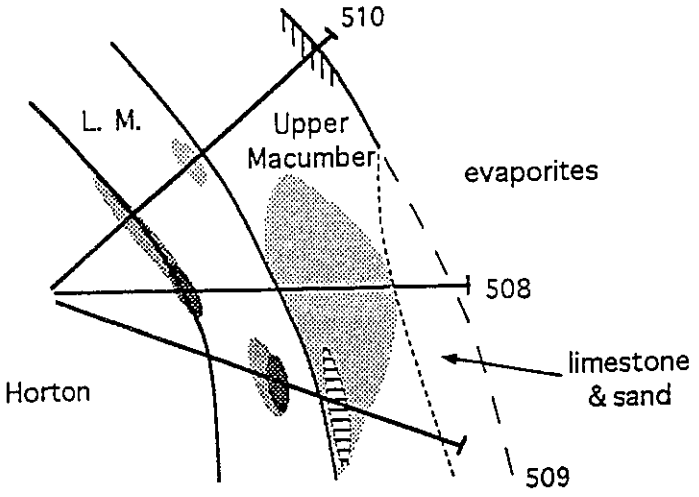

Section #25

690L

850L

1030L

B-Baseline

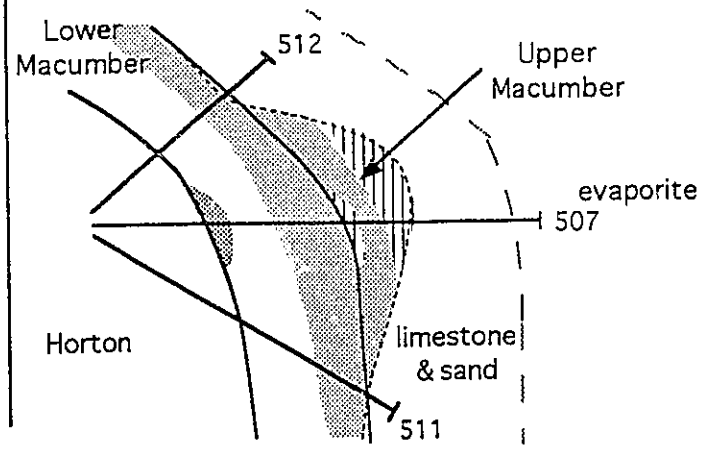

Section #26

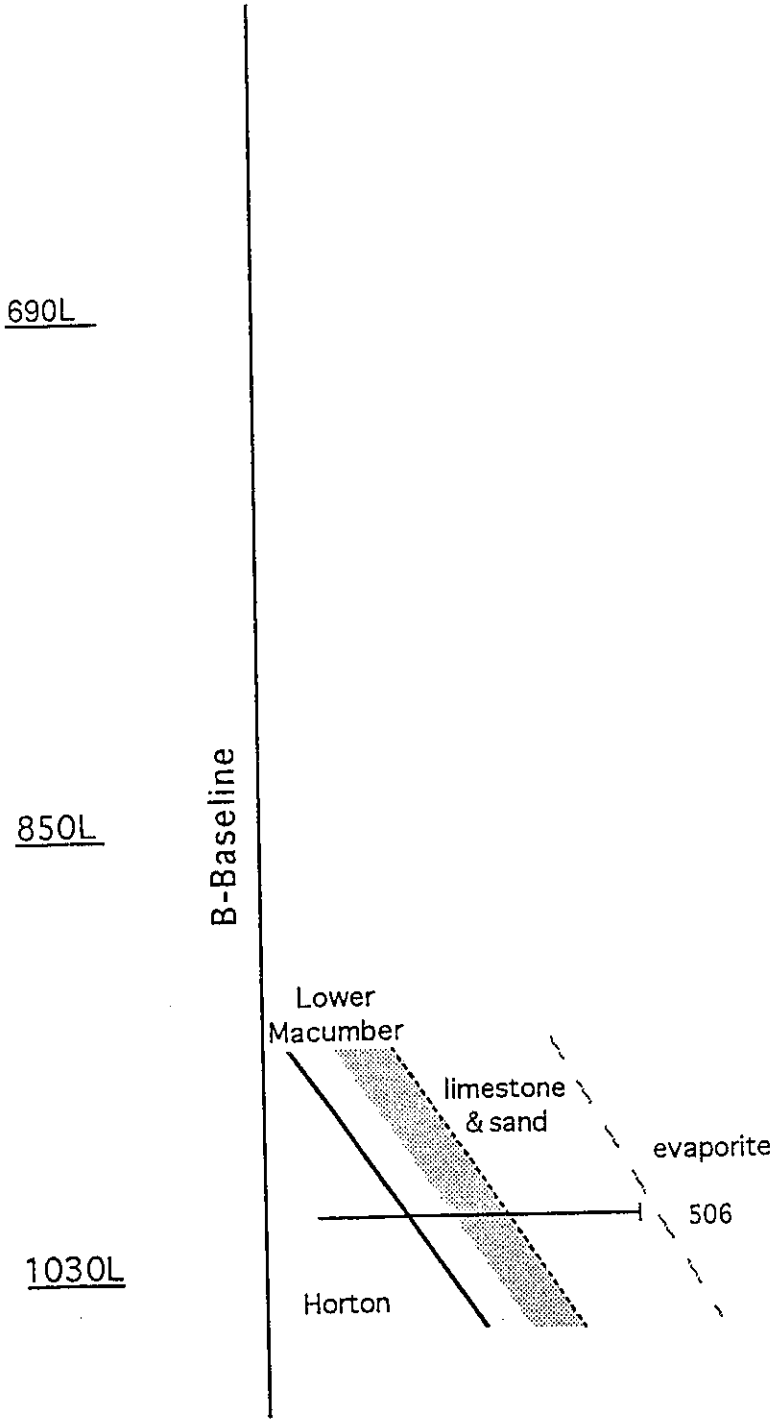
690L
850L
1030L
B-Baseline
Lower
Macumber
limestone
& sand
evaporite
506
Horton

Section #27

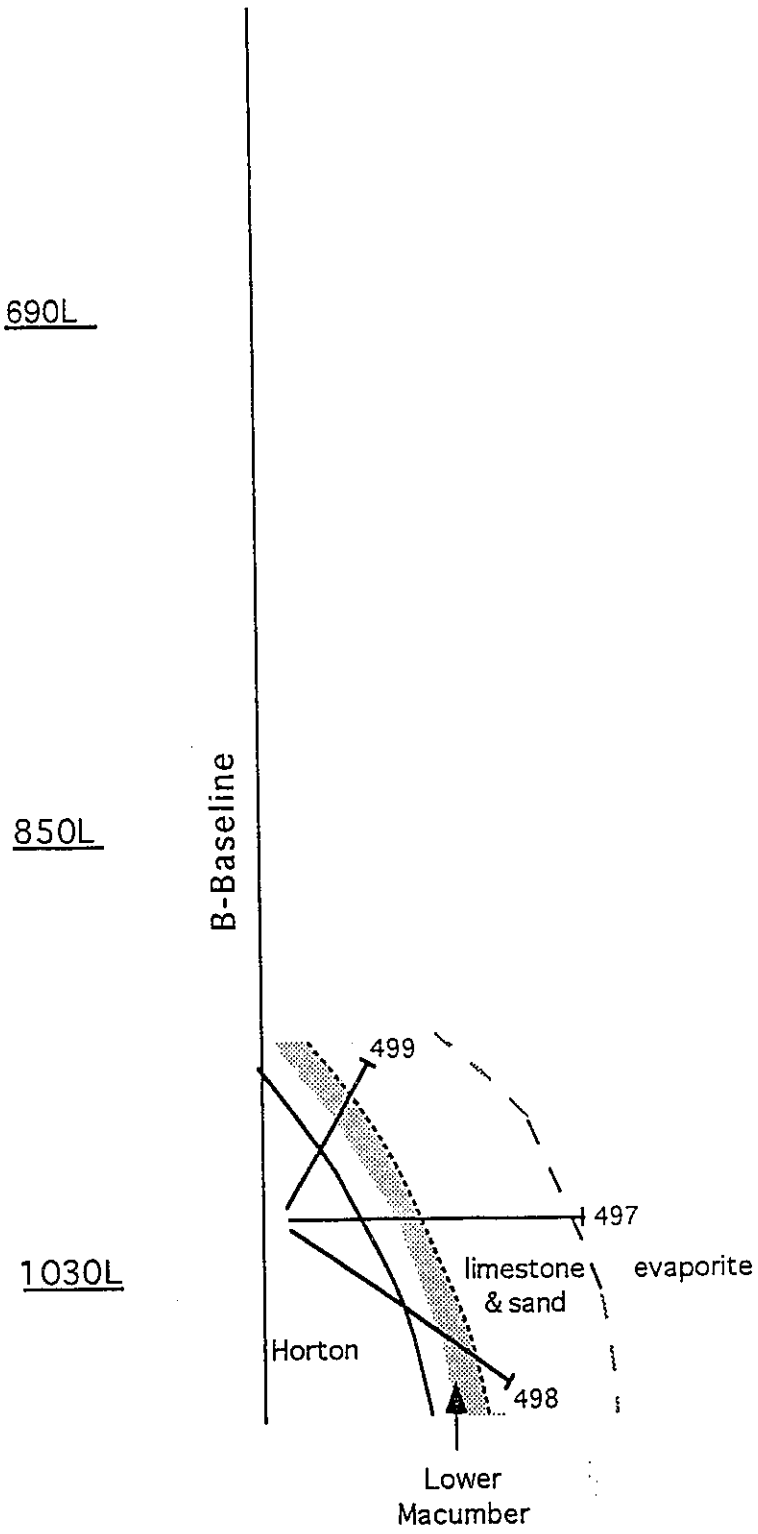
690L
850L
1030L
B-Baseline
499
497
498
limestone
& sand
evaporite
Horton
Lower
Macumber

Section #28

A30

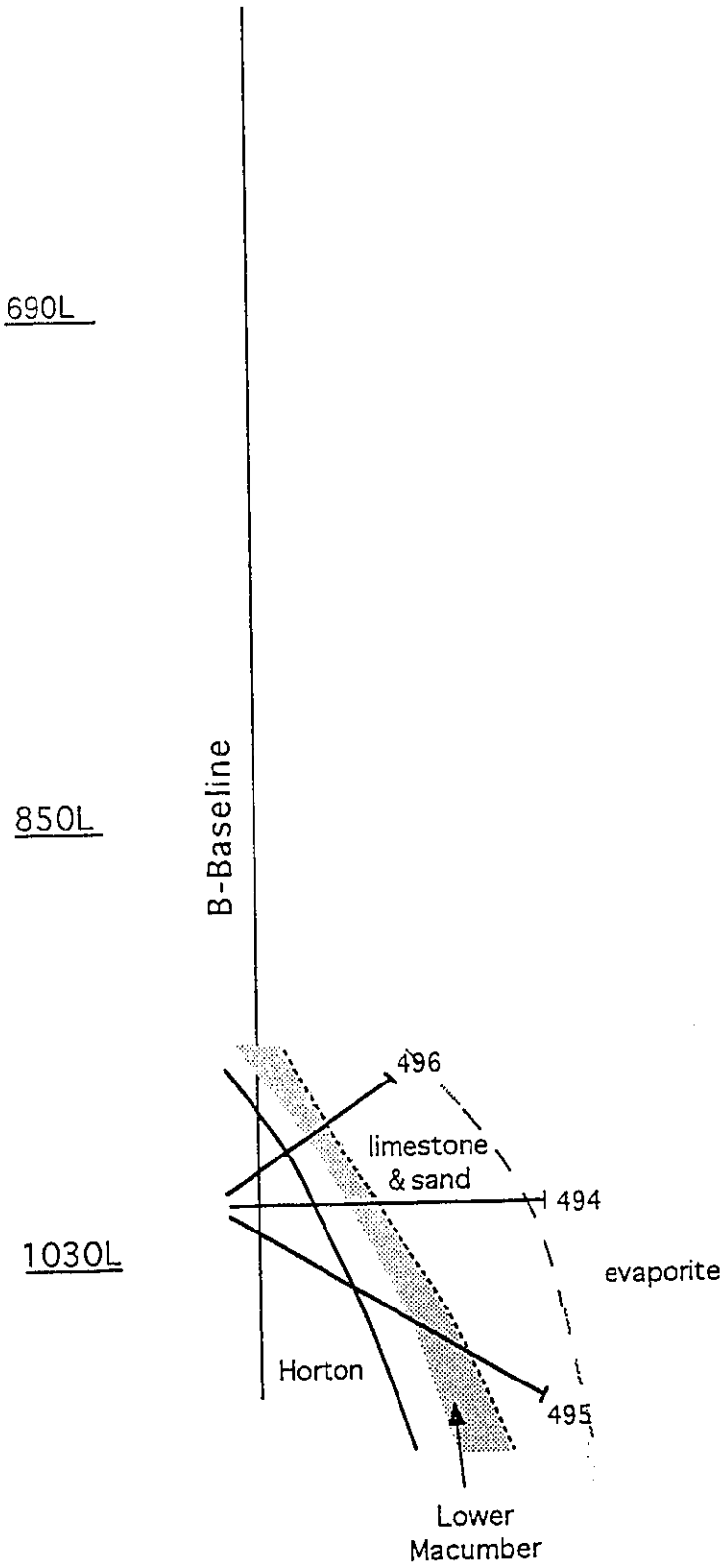

Section #29

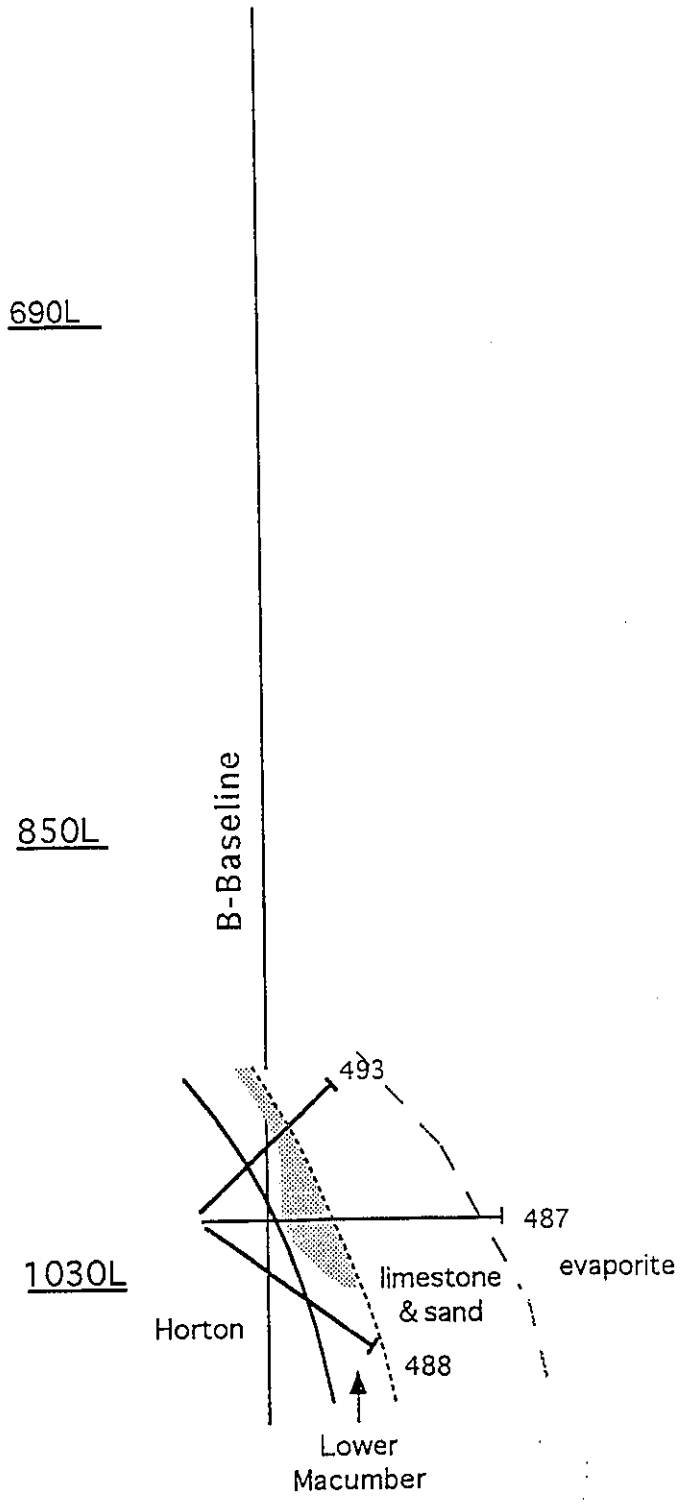
690L
850L
1030L
B-Baseline
493
487
limestone
& sand
evaporite
Horton
488
Lower
Macumber

Section #30

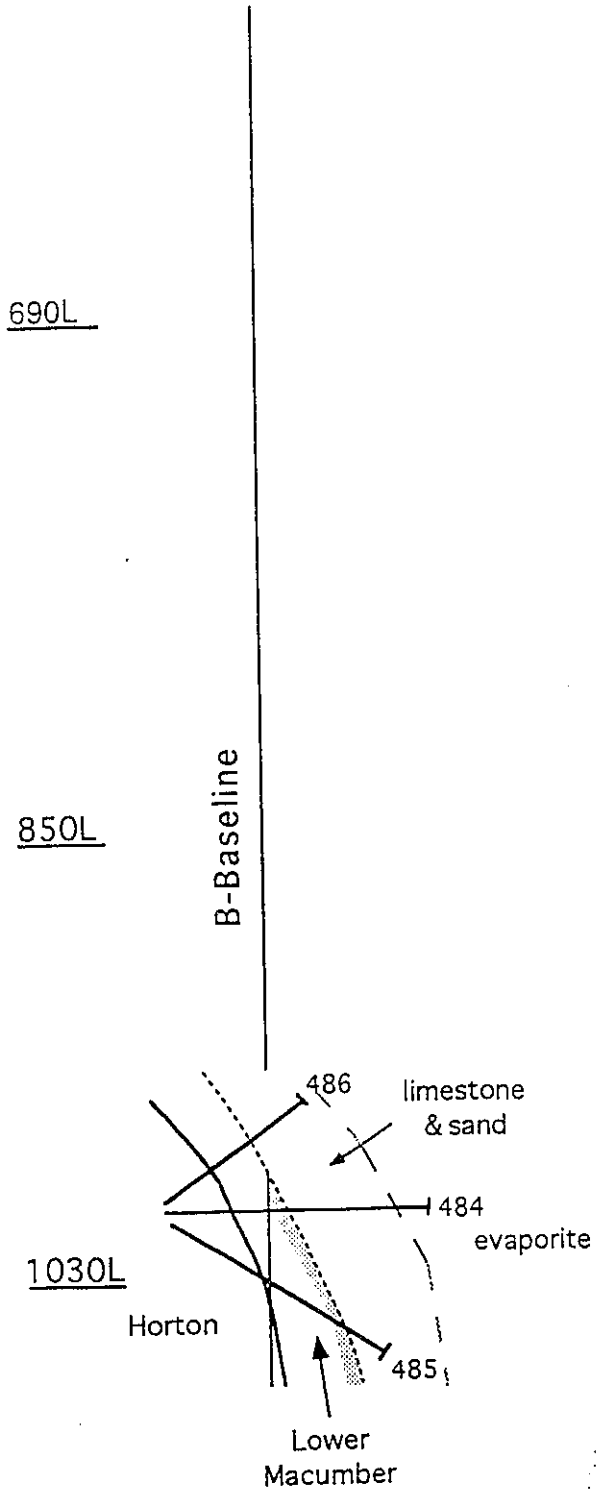
690L
850L
1030L
B-Baseline
486
limestone
& sand
484
evaporite
Horton
485
Lower
Macumber

Section #31

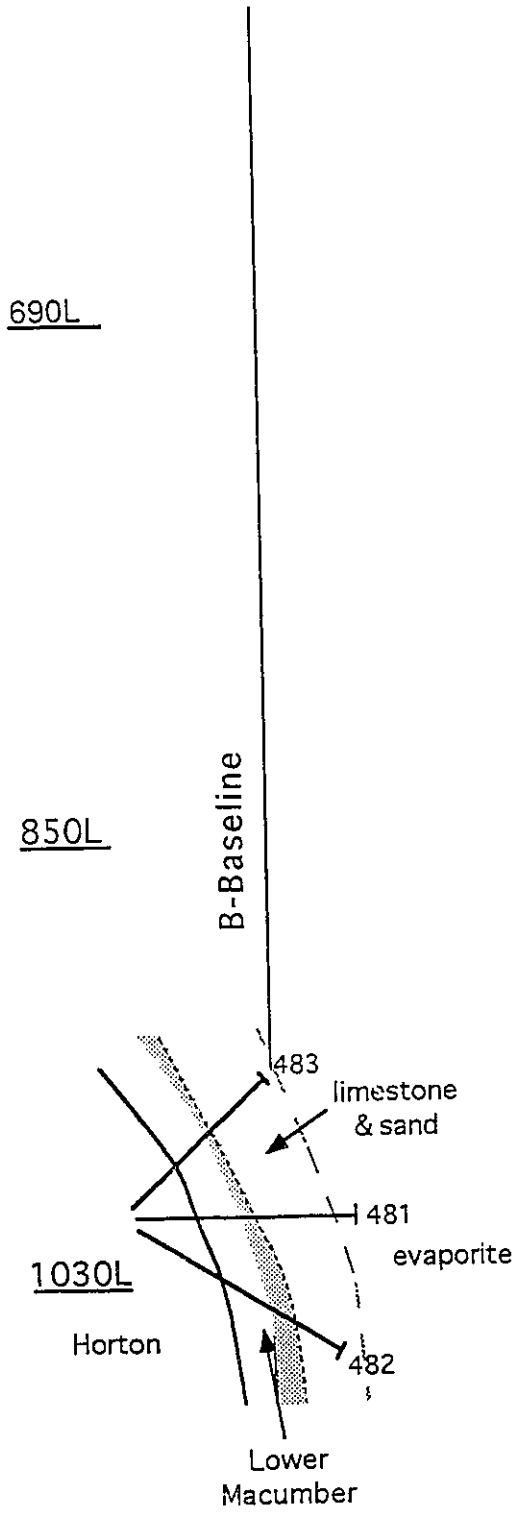
690L
850L
1030L
B-Baseline
483
limestone
& sand
481
evaporite
Horton
482
Lower
Macumber

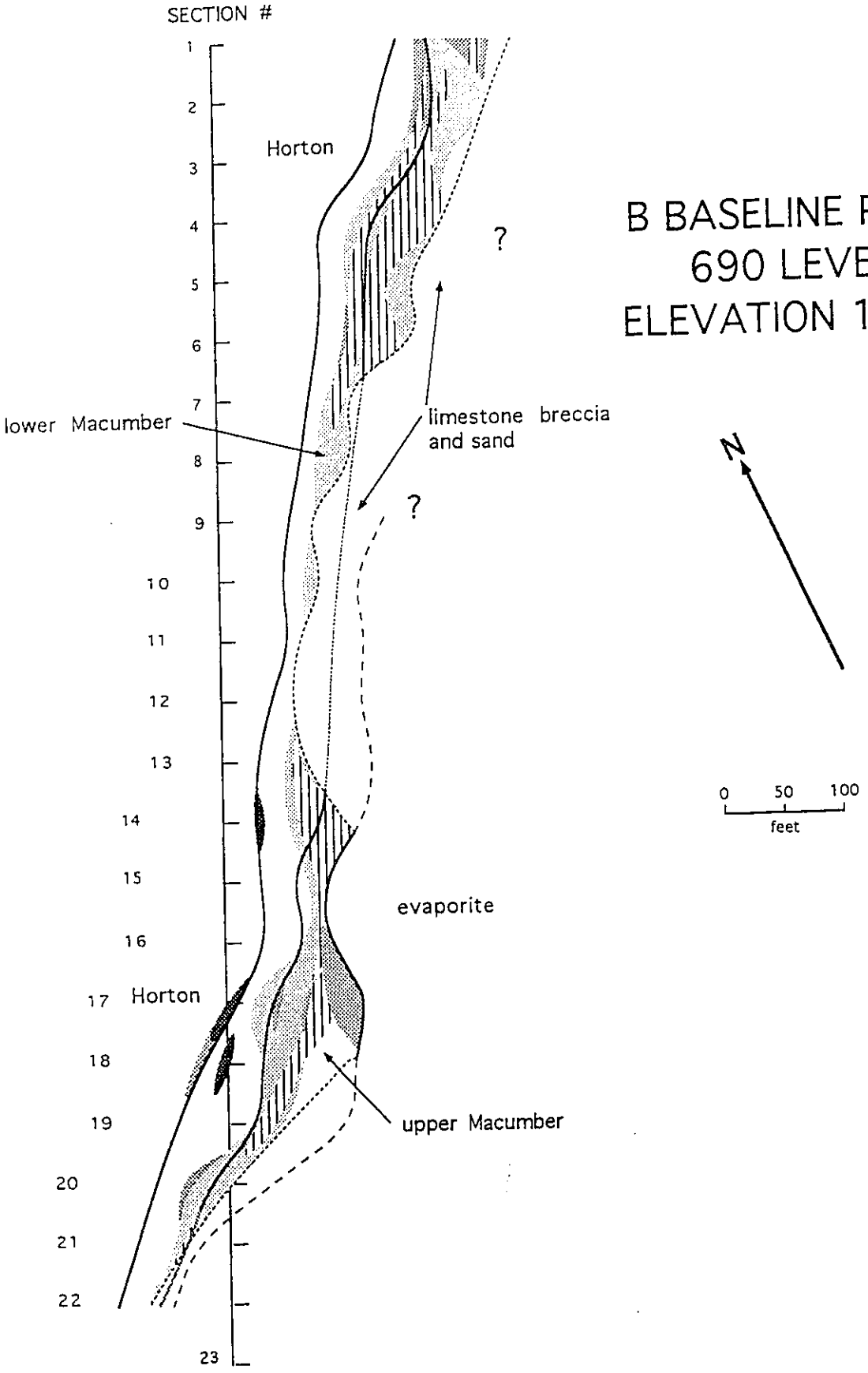

B BASELINE PLAN
690 LEVEL
ELEVATION 1300'

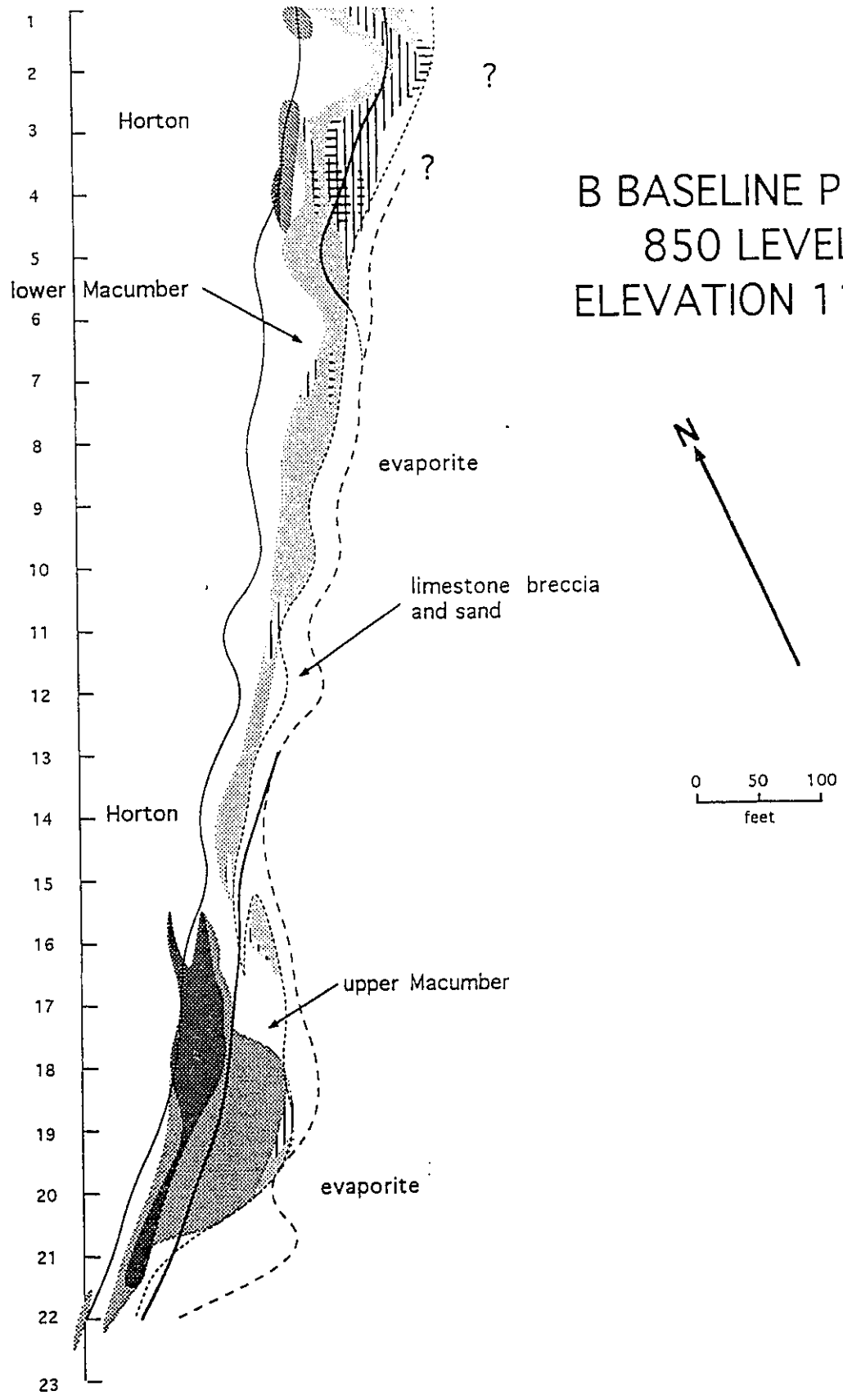
SECTION #
1
2
3
4
5
6
7
8
9
10
11
12
13
14
15
16
17
18
19
20
21
22
23
Horton
?
?
lower Macumber
evaporite
limestone breccia
and sand
Horton
upper Macumber
evaporite
B BASELINE PLAN
850 LEVEL
ELEVATION 1125'
N
0
50
100
feet

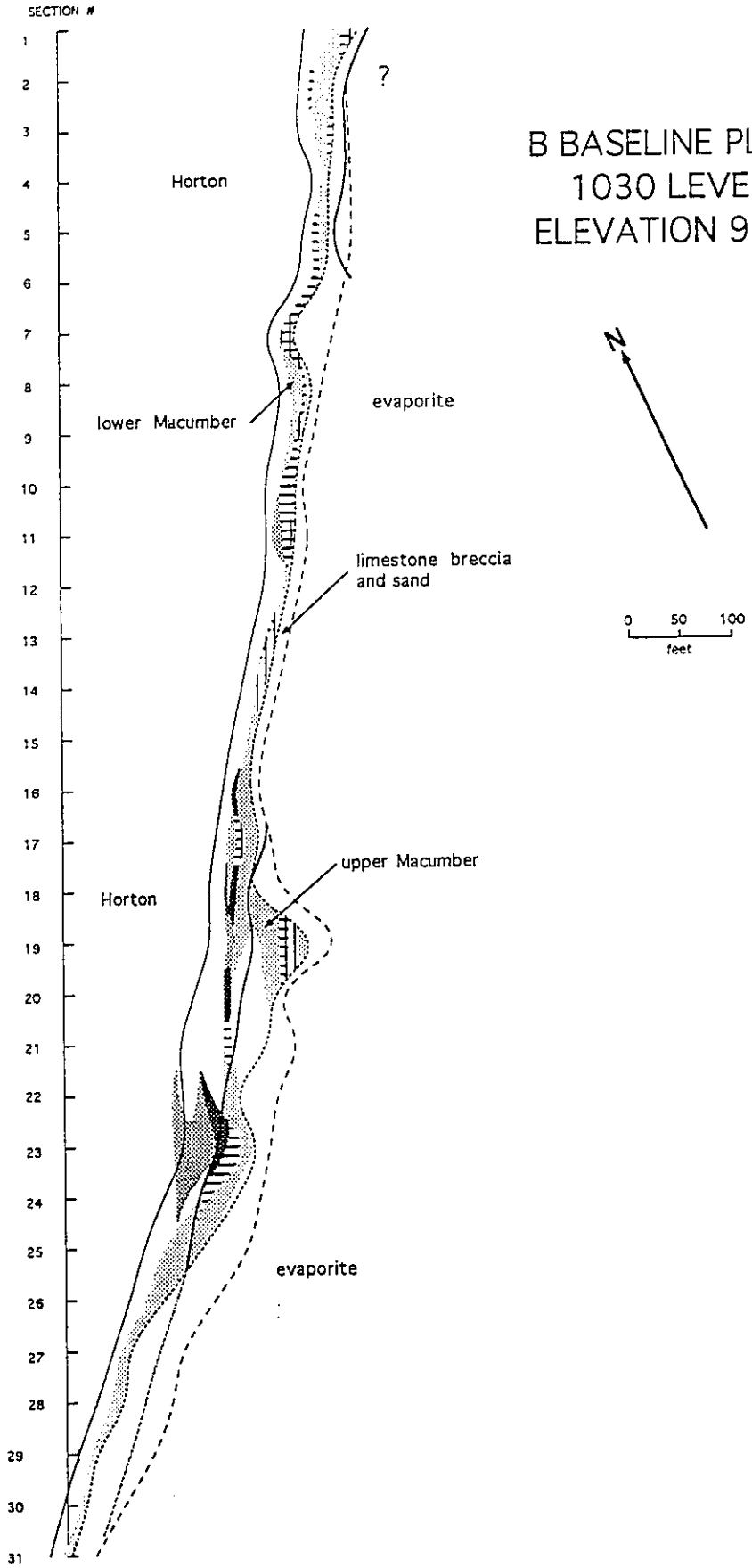
SECTION #
1
2
3
4
5
6
7
8
9
10
11
12
13
14
15
16
17
18
19
20
21
22
23
24
25
26
27
28
29
30
31
?
Horton
lower Macumber
evaporite
limestone breccia
and sand
upper Macumber
Horton
evaporite
B BASELINE PLAN
1030 LEVEL
ELEVATION 950'
N
0
50
100
feet

APPENDIX II

MICROPROBE ANALYSES

The microprobe analyses were performed with the assistance of J. Stirling on the Cameca SX50 electron microprobe at the Geological Survey of Canada. The microprobe has has four wavelength dispersive spectrometers and was operated at 15kV with a beam current of 10 or 30 nA depending on the element, and sample stability and size. The raw counts were corrected to elemental concentartions using the Cameca PAP program (Pouchou and Pichoir, 1985).

Weight percent oxides were converted to mol% end-members for carbonates and barite, and atomic proportions for sulphides. Both are presented in the following tables. The sample number listed is coded as follows: the first two letters correspond to the mineral being probed (note that some minerals were misidentified when coded prior to probing); the first three numbers correspond to the last three numbers of the thin section number; and the last two numbers are the analysis number for that sample. The sample locations are given on page A38.

Microprobe Sample Locations

Probe Sample #	Thin section Sample #	DDH	footage	Section #	Page#
099	SP- 5099	503	21	17	A19
114	SP- 5114	503	161	17	A19
127	SP- 5127	503	211	17	A19
137	SP- 5137	447	50.5	5	A7
141	SP- 5141	448	58	6	A8
146	SP- 5146	448	80.5	6	A8
147	SP- 5147	448	84	6	A8
160, 5160	SP- 5160	529	24	2	A4
178	SP- 5178	378	2.5	18	A20
190, 5190	SP- 5190	378	17.5	18	A20
193	SP- 5193	378	22	18	A20
207	SP- 5207	379	35	18	A20
284	SP- 5284	543	39	18	A20
296	SP- 5296	431	2.5	1	A3
350	SP- 5350	429	40.5	1	A3
352	SP- 5352	429	60.5	1	A3
355	SP- 5355	505	126	14	A16
360	SP- 5360	505	134	14	A16
535	SP- 5535	GC-80-9	Cheverie		
537	SP- 5537	GT-80-2	Tennycape		
574	SP- 5574	outcrop	Brook Village		
575	SP- 5575	outcrop	Brook Village		
577	SP- 5577	outcrop	Black Rock		

SD-siderite
BA-barite
MC-marcasite
PY-pyrite
SP-sphalerite
CP-chalcopyrite
TN-tennantite
CA-calcite

	CaO wt%	MgO wt%	FeO wt%	MnO wt%	SrO wt%	BaO wt%	ZnO wt%	SO4 wt%	Total wt%	CaCO3	MgCO3	FeCO3	MnCO3	SrCO3	BaCO3	ZnCO3	Total	CaCO3	MgCO3	FeCO3	MnCO3	SrCO3	BaCO3	ZnCO3
										wt% end member								mol% end member						
SD141-01	0.300	0.630	53.770	6.200	0.050	0.290	0.080	0.000	61.320	0.535	1.318	86.707	10.047	0.071	0.373	0.123	99.175	0.622	1.817	87.009	10.161	0.056	0.220	0.114
SD141-04	0.267	0.423	54.301	5.295	0.018	0.156	0.000	0.007	60.468	0.477	0.885	87.563	8.580	0.026	0.201	0.000	97.731	0.562	1.239	89.244	8.814	0.021	0.120	0.000
SD099-01	0.234	0.633	54.683	5.711	0.013	0.032	0.111	0.067	61.485	0.418	1.324	88.179	9.254	0.019	0.041	0.171	99.406	0.483	1.819	88.174	9.327	0.015	0.024	0.158
SD099-02	0.430	0.799	54.683	5.931	0.000	0.174	0.166	0.000	62.182	0.767	1.671	88.179	9.611	0.000	0.224	0.256	100.709	0.876	2.265	86.946	9.551	0.000	0.130	0.233
SD099-03	0.403	0.696	54.546	6.181	0.000	0.000	0.166	0.182	62.174	0.719	1.456	87.958	10.016	0.000	0.000	0.256	100.405	0.823	1.978	86.982	9.983	0.000	0.000	0.234
SD099-04	0.147	0.685	55.900	5.402	0.086	0.022	0.000	0.000	62.243	0.262	1.433	90.142	8.753	0.123	0.028	0.000	100.741	0.300	1.943	88.941	8.705	0.095	0.016	0.000
SD099-05	0.118	1.123	54.446	6.084	0.059	0.105	0.034	0.032	62.001	0.211	2.349	87.797	9.859	0.084	0.135	0.052	100.487	0.240	3.184	86.586	9.799	0.065	0.078	0.048
SD099-06	0.400	0.640	55.510	5.970	0.060	0.000	0.000	0.000	62.580	0.720	1.340	89.510	9.680	0.000	0.090	0.000	101.340	0.820	1.800	87.750	9.570	0.000	0.070	0.000
SD099-07	0.270	1.016	55.519	5.384	0.025	0.032	0.000	0.032	62.280	0.482	2.125	89.527	8.724	0.036	0.041	0.000	100.936	0.548	2.867	87.900	8.633	0.027	0.024	0.000
SD099-08	0.382	1.050	54.894	6.071	0.157	0.000	0.000	0.000	62.554	0.682	2.197	88.520	9.837	0.224	0.000	0.000	101.459	0.771	2.947	86.430	9.681	0.171	0.000	0.000
SD099-09	0.456	0.647	55.257	5.923	0.098	0.092	0.376	0.729	63.577	0.814	1.353	89.105	9.598	0.140	0.118	0.579	101.707	0.921	1.818	87.106	9.457	0.107	0.068	0.523
SD099-10	0.376	0.655	54.183	5.991	0.015	0.065	0.000	0.032	61.318	0.671	1.370	87.373	9.708	0.021	0.084	0.000	99.227	0.778	1.885	87.475	9.796	0.017	0.049	0.000
SD099-11	0.481	0.774	55.514	5.184	0.013	0.458	0.011	0.032	62.469	0.858	1.619	89.519	8.400	0.019	0.589	0.017	101.022	0.978	2.190	88.126	8.335	0.014	0.341	0.015
SD099-12	0.150	1.607	53.283	6.426	0.000	0.482	0.000	0.067	62.016	0.268	3.362	85.922	10.413	0.000	0.620	0.000	100.584	0.305	4.542	84.477	10.319	0.000	0.358	0.000
SD099-13	0.174	0.701	55.896	5.452	0.058	0.215	0.088	0.000	62.585	0.311	1.466	90.135	8.834	0.083	0.277	0.136	101.242	0.353	1.980	88.571	8.750	0.064	0.160	0.123
SD127-01	0.327	3.958	46.730	9.053	0.099	0.306	0.000	0.000	60.474	0.584	8.280	75.355	14.670	0.141	0.394	0.000	99.423	0.659	11.096	73.492	14.420	0.108	0.225	0.000
SD127-02	0.407	4.344	48.153	8.423	0.000	0.051	0.000	0.000	61.379	0.726	9.087	77.649	13.649	0.000	0.066	0.000	101.177	0.803	11.918	74.112	13.130	0.000	0.037	0.000
SD127-03	0.304	3.905	48.929	8.229	0.096	0.227	0.000	0.000	61.689	0.543	8.169	78.901	13.334	0.137	0.292	0.000	101.375	0.601	10.745	75.523	12.864	0.103	0.164	0.000
SD127-04	25.667	9.984	16.778	3.810	0.035	0.000	0.081	0.000	56.356	45.810	20.886	27.055	6.174	0.050	0.000	0.125	100.100	46.047	24.922	23.494	5.403	0.034	0.000	0.100
SD127-05	29.296	13.683	9.193	2.904	0.045	0.186	0.093	0.107	55.509	52.287	28.624	14.824	4.706	0.064	0.239	0.143	100.887	50.543	32.846	12.380	3.961	0.042	0.117	0.111
SD127-06	28.271	12.207	10.831	3.612	0.038	0.037	0.000	0.067	55.063	50.457	25.536	17.466	5.853	0.054	0.048	0.000	99.414	49.949	30.009	14.937	5.045	0.036	0.024	0.000
SD127-07	28.913	13.701	8.824	3.396	0.048	0.080	0.000	0.032	54.996	51.603	28.662	14.229	5.503	0.068	0.103	0.000	100.168	50.193	33.094	11.957	4.661	0.045	0.051	0.000
SD127-08	28.547	13.217	9.629	3.295	0.045	0.000	0.024	0.025	54.782	50.950	27.649	15.527	5.339	0.064	0.000	0.037	99.567	49.996	32.208	13.163	4.562	0.043	0.000	0.029
SD127-09	28.803	13.668	8.852	3.392	0.048	0.080	0.000	0.000	54.844	51.407	28.593	14.274	5.496	0.068	0.103	0.000	99.942	50.121	33.093	12.023	4.666	0.045	0.051	0.000
SD284-04	0.292	0.469	55.827	5.631	0.044	0.018	0.000	0.075	62.356	0.521	0.981	90.024	9.124	0.063	0.023	0.000	100.737	0.596	1.332	88.926	9.084	0.049	0.013	0.000
SD284-05	0.299	0.841	54.311	6.250	0.067	0.224	0.000	0.000	61.993	0.534	1.759	87.579	10.128	0.095	0.288	0.000	100.384	0.611	2.392	86.655	10.100	0.074	0.167	0.000
SD284-06	0.193	0.637	54.395	5.747	0.033	0.000	0.000	0.000	61.005	0.344	1.333	87.715	9.312	0.047	0.000	0.000	98.751	0.401	1.843	88.273	9.446	0.037	0.000	0.000
SD207-01	0.094	2.272	52.029	7.445	0.052	0.041	0.088	0.142	62.164	0.168	4.753	83.900	12.064	0.074	0.053	0.136	101.147	0.189	6.341	81.457	11.805	0.056	0.030	0.122
SD207-02	0.294	2.406	51.152	8.470	0.000	0.143	0.000	0.142	62.607	0.525	5.033	82.485	13.725	0.000	0.184	0.000	101.952	0.584	6.653	79.351	13.308	0.000	0.104	0.000
SD207-03	0.122	1.864	52.122	6.239	0.050	0.000	0.288	0.007	60.691	0.218	3.899	84.050	10.110	0.071	0.000	0.444	98.791	0.251	5.341	83.785	10.158	0.056	0.000	0.409
SD207-04	0.266	2.084	51.165	7.887	0.031	0.092	0.000	0.057	61.581	0.475	4.360	82.506	12.780	0.044	0.118	0.000	100.283	0.539	5.871	80.863	12.625	0.034	0.068	0.000
SD207-05	0.277	2.544	51.736	7.794	0.077	0.046	0.088	0.000	62.561	0.494	5.322	83.427	12.629	0.110	0.059	0.136	102.177	0.549	7.012	79.997	12.206	0.083	0.033	0.120
SD207-06	0.297	2.532	50.563	7.693	0.004	0.019	0.000	0.125	61.232	0.530	5.297	81.536	12.466	0.006	0.024	0.000	99.858	0.601	7.135	79.929	12.317	0.004	0.014	0.000
SD207-10	0.200	3.747	49.169	8.062	0.044	0.065	0.000	0.100	61.388	0.357	7.838	79.288	13.064	0.063	0.084	0.000	100.693	0.398	10.383	76.431	12.693	0.047	0.047	0.000
SD207-11	0.430	2.482	47.943	7.813	0.000	0.632	0.067	1.481	60.848	0.767	5.192	77.311	12.660	0.000	0.813	0.103	96.847	0.900	7.231	78.355	12.933	0.000	0.484	0.097
SD207-12	0.252	4.189	49.890	7.496	0.021	0.000	0.000	0.000	61.847	0.450	8.763	80.450	12.147	0.030	0.000	0.000	101.840	0.495	11.438	76.417	11.629	0.022	0.000	0.000
SD190-01	0.111	0.592	56.479	5.817	0.053	0.201	0.000	0.000	63.253	0.198	1.238	91.075	9.426	0.076	0.259	0.000	102.272	0.223	1.657	88.665	9.249	0.058	0.148	0.000
SD190-02	0.101	2.487	51.481	7.135	0.033	0.004	0.000	0.000	61.242	0.180	5.203	83.016	11.562	0.047	0.005	0.000	100.013	0.204	7.004	81.335	11.417	0.036	0.003	0.000
SD190-03	0.695	4.812	48.444	6.952	0.061	0.000	0.212	0.017	61.194	1.240	10.066	78.119	11.265	0.087	0.000	0.327	101.104	1.366	13.160	74.320	10.802	0.065	0.000	0.287
SD190-04	0.330	4.761	48.722	7.378	0.009	0.093	0.078	0.092	61.463	0.589	9.960	78.567	11.955	0.013	0.120	0.120	101.324	0.648	13.012	74.701	11.457	0.010	0.067	0.106
SD190-05	0.088	1.695	52.542	6.988	0.040	0.000	0.244	0.025	61.623	0.157	3.546	84.727	11.323	0.057	0.000	0.376	100.186	0.179	4.796	83.404	11.235	0.044	0.000	0.342
SD190-06	1.042	0.943	50.592	7.601	0.025	0.240	0.000	0.150	60.594	1.860	1.973	81.582	12.317	0.036	0.309	0.000	98.076	2.173	2.736	82.349	12.531	0.028	0.183	0.000
SD190-07	0.481	1.509	51.810	7.297	0.009	0.166	0.000	0.000	61.273	0.858	3.157	83.546	11.824	0.013	0.214	0.000	99.612	0.985	4.298	82.776	11.808	0.010	0.124	0.000
SD190-08	0.238	4.603	48.709	7.100	0.034	0.116	0.067	0.042	60.910	0.425	9.629	78.546	11.505	0.048	0.149	0.103	100.406	0.472	12.712	75.463	11.141	0.037	0.084	0.092
SD190-09	0.057	1.995	53.026	7.209	0.000	0.037	0.022	0.000	62.347	0.102	4.173	85.507	11.681	0.000	0.048	0.034	101.545	0.114	5.557	82.862	11.410	0.000	0.027	0.030
SD190-10	0.253	4.630	48.623	7.175	0.098	0.013	0.000	0.042	60.835	0.452	9.686	78.407	11.626	0.140	0.017	0.000	100.327	0.502	12.788	75.336	11.259	0.105	0.009	0.000
190 Scan	0.547	0.604	46.747	6.104	0.067	0.103	0.000	0.000	54.171	0.976	1.264	75.382	9.891	0.095	0.133	0.000	87.741	1.279	1.965	85.303	11.281	0.085	0.088	0.000
190 Scan	0.451	0.582	46.704	5.648	0.134	0.085	0.011	0.150	53.764	0.805	1.218	75.313	9.152	0.191	0.109	0.017	86.804	1.066	1.915	86.198	10.558	0.171	0.074	0.018
190 Scan	0.523	0.725	49.878	6.273	0.086	0.019	0.067	3.324	60.895	0.933	1.517	80.431	10.165	0.123	0.024	0.103	93.296	1.149	2.216	85.523	10.894	0.102	0.015	0.101
190 Scan	0.702	0.663	51.962	7.200	0.075	0.162	0.111	0.000	60.875	1.253	1.387	83.792	11.667	0.107	0.208	0.171	98.585	1.461	1.920	84.407	11.846	0.084	0.123	0.159
190 Scan	0.509	0.711	52.624	6.738	0.065	0.041	0.000	0.032	60.721	0.908	1.487	84.859	10.918	0.093	0.053	0.000	98.319	1.062	2.063	85.662	11.109	0.073	0.031	0.000
190 Scan	0.445	0.764	54.263	6.918	0.007	0.000	0.177	0.165	62.739	0.794	1.598	87.502	11.210	0.010	0.000	0.273	101.387	0.900	2.149	85.639	11.058	0.008	0.000	0.247
190 Scan	0.481	0.808	54.955	6.411	0.037	0.069	0.000	0.150	62.910	0.858	1.690	88.618	10.388	0.053	0.089	0.000	101.697	0.969	2.266	86.458	10.215	0.040	0.051	0.000
190 Scan	0.432	0.701	52.792	6.643	0.015	0.000	0.011	0.042	60.638	0.771	1.466	85.130	10.764	0.021	0.000	0.017	98.170	0.902	2.037	86.060	10.968	0.017	0.000	0.016
190 Scan	0.411	0.642	53.349	6.528	0.075	0.152	0.000	0.092	61.249	0.734	1.343	86.028	10.578	0.107	0.196	0.000	98.985	0.853	1.853	86.388	10.706	0.084	0.115	0.000
190 Scan	0.383	0.877	45.604	5.987	0.027	0.202	0.203	2.567	55.852	0.684	1.835	73.539	9.701	0.038	0.260	0.313	86.370	0.908	2.894	84.429	11.226	0.035	0.175	0.332
190 Scan	0.632	0.620	51.984	6.714	0.111	0.000	0.000	0.365	60.427	1.128	1.297	83.827	10.879	0.158	0.000	0.000	97.290	1.332	1.818	85.534	11.189	0.127	0.000	0.000

	CaO	MgO	FeO	MnO	SrO	BaO	ZnO	SO4	Total
	wt%	wt%	wt%	wt%	wt%	wt%	wt%	wt%	wt%
190 Scan	0.267	0.439	23.347	2.821	0.017	0.046	0.118	7.951	35.007
190 Scan	0.347	0.746	53.986	5.714	0.114	0.009	0.000	0.050	61.966
190 Scan	0.529	0.713	54.323	6.620	0.046	0.092	0.066	0.075	62.464
190 Scan	0.484	0.779	54.203	6.620	0.056	0.000	0.000	0.000	62.142
190 Scan	0.501	0.788	46.226	5.716	0.143	0.056	0.000	0.092	53.522
190 Scan	0.234	0.303	22.336	3.144	0.038	0.208	0.000	8.038	34.301
190 Scan	0.382	0.638	51.982	6.067	0.046	0.157	0.000	0.549	59.822
190 Scan	0.095	0.323	17.858	1.756	0.065	0.000	0.083	9.307	29.488
190 Scan	0.215	0.483	27.535	3.145	0.090	0.194	0.187	4.138	35.987
190 Scan	0.344	0.516	38.515	4.620	0.078	0.025	0.000	3.436	47.533
190 Scan	0.164	0.151	11.612	1.682	0.069	0.041	0.061	6.003	19.783
190 Scan	0.249	0.380	40.591	2.799	0.000	0.000	0.213	34.376	78.608
190 Scan	0.508	0.745	53.713	6.448	0.108	0.078	0.000	0.042	61.642
190 Scan	0.539	0.816	48.826	6.220	0.111	0.070	0.000	0.042	56.624
190 Scan	0.378	0.841	48.459	5.773	0.098	0.070	0.056	0.050	55.725
190 Scan	0.403	0.711	37.320	5.024	0.156	0.058	0.092	0.177	43.942
190 Scan	0.635	0.738	53.269	6.846	0.009	0.217	0.000	0.117	61.832
190 Scan	0.416	0.970	52.765	6.366	0.083	0.162	0.000	0.092	60.853
190 Scan	0.337	0.711	50.437	5.665	0.109	0.037	0.034	0.107	57.436
190 Scan	0.315	0.731	54.825	6.109	0.002	0.128	0.000	0.100	62.210
CA574-01	57.156	0.315	0.544	0.618	0.044	0.028	0.151	0.135	58.991
CA574-02	55.074	0.501	0.336	0.081	0.137	0.000	0.127	0.200	56.456
CA574-03	55.185	0.172	0.028	0.079	0.616	0.000	0.035	0.095	56.210
574 Scan	54.724	0.184	0.014	0.000	0.661	0.000	0.000	0.000	55.583
574 Scan	54.181	0.285	0.279	0.160	0.619	0.259	0.000	0.087	55.871
574 Scan	14.262	0.342	0.404	0.158	0.167	0.011	0.061	0.150	15.554
574 Scan	0.050	0.008	0.000	0.000	0.026	0.000	0.000	0.050	0.135
574 Scan	51.909	0.657	0.455	0.324	0.455	0.000	0.000	0.165	53.985
574 Scan	55.029	0.260	0.084	0.061	0.699	0.000	0.000	0.007	56.140
574 Scan	38.491	2.144	4.597	0.099	0.149	0.104	0.258	0.300	46.141
574 Scan	54.979	0.211	0.118	0.065	0.750	0.088	0.000	0.040	56.250
574 Scan	54.089	0.267	0.057	0.108	0.684	0.006	0.000	0.200	55.410
574 Scan	54.075	0.179	0.057	0.054	0.634	0.060	0.011	0.025	55.095
574 Scan	54.128	0.464	0.252	0.089	0.130	0.000	0.070	0.280	55.413
574 Scan	0.000	0.000	0.000	0.025	0.043	0.000	0.112	0.042	0.222
574 Scan	32.939	1.106	1.512	0.217	0.364	0.104	0.000	0.564	36.806
574 Scan	47.409	0.849	0.823	0.093	0.083	0.199	0.000	0.217	49.673
574 Scan	52.874	0.539	0.630	0.000	0.060	0.017	0.059	0.055	54.234
574 Scan	54.705	0.226	0.441	0.252	0.252	0.039	0.035	0.142	56.091
574 Scan	54.986	0.181	0.000	0.065	0.422	0.000	0.185	0.112	55.951
574 Scan	30.701	0.466	0.912	0.118	0.309	0.000	0.000	0.000	32.506
574 Scan	54.618	0.265	0.006	0.102	0.601	0.071	0.000	0.025	55.689
574 Scan	54.965	0.244	0.118	0.116	0.662	0.000	0.000	0.087	56.193
574 Scan	55.499	0.156	0.063	0.004	0.440	0.083	0.081	0.095	56.420
574 Scan	54.625	0.406	0.084	0.081	0.479	0.000	0.128	0.120	55.923
574 Scan	36.306	0.839	1.191	0.192	0.233	0.044	0.060	0.122	38.988
574 Scan	0.053	0.013	0.160	0.010	0.026	0.077	0.000	9.295	9.634
574 Scan	54.812	0.201	0.098	0.112	0.850	0.077	0.000	0.167	56.318
574 Scan	54.763	0.121	0.028	0.174	0.663	0.022	0.220	0.127	56.120
574 Scan	54.707	0.282	0.084	0.004	0.624	0.199	0.163	0.240	56.303
574 Scan	53.500	0.323	0.427	0.303	0.273	0.105	0.000	0.215	55.147
574 Scan	55.358	0.063	0.000	0.000	0.449	0.060	0.151	0.095	56.176
574 Scan	55.277	0.186	0.035	0.137	0.674	0.127	0.024	0.055	56.514
CA577-01	54.209	0.454	0.322	0.108	0.148	0.171	0.000	0.055	55.467
CA577-02	54.768	0.365	0.126	0.143	0.102	0.000	0.000	0.000	55.503
CA577-03	54.885	0.570	0.210	0.048	0.095	0.017	0.000	0.047	55.872
577 Scan	56.274	0.501	0.021	0.021	0.287	0.155	0.035	0.469	57.763
577 Scan	48.173	0.922	0.296	0.075	0.138	0.083	0.176	0.087	49.950

	CaCO3	MgCO3	FeCO3	MnCO3	SrCO3	BaCO3	ZnCO3	Total
	wt% end member							
190 Scan	0.477	0.918	37.648	4.571	0.024	0.059	0.182	43.880
190 Scan	0.619	1.561	87.055	10.879	0.162	0.012	0.000	100.289
190 Scan	0.944	1.492	87.599	10.727	0.066	0.118	0.102	101.047
190 Scan	0.864	1.630	87.405	10.727	0.080	0.000	0.000	100.706
190 Scan	0.894	1.648	74.542	9.262	0.204	0.072	0.000	86.623
190 Scan	0.418	0.634	36.018	5.095	0.054	0.268	0.000	42.486
190 Scan	0.682	1.335	83.824	9.831	0.066	0.202	0.000	95.939
190 Scan	0.170	0.676	28.797	2.845	0.093	0.000	0.128	32.708
190 Scan	0.384	1.010	44.402	5.096	0.128	0.250	0.288	51.558
190 Scan	0.614	1.079	62.108	7.486	0.111	0.032	0.000	71.430
190 Scan	0.293	0.316	18.725	2.726	0.098	0.053	0.094	22.304
190 Scan	0.444	0.795	65.455	4.536	0.000	0.000	0.328	71.558
190 Scan	0.907	1.558	86.615	10.448	0.154	0.100	0.000	99.783
190 Scan	0.962	1.707	78.735	10.079	0.158	0.090	0.000	91.731
190 Scan	0.675	1.759	79.143	9.355	0.140	0.090	0.086	90.247
190 Scan	0.719	1.487	60.181	8.141	0.222	0.075	0.142	70.967
190 Scan	1.133	1.544	85.899	11.093	0.013	0.279	0.000	99.962
190 Scan	0.742	2.029	85.086	10.315	0.118	0.208	0.000	98.500
190 Scan	0.601	1.487	81.332	9.180	0.155	0.048	0.052	92.856
190 Scan	0.562	1.529	88.408	9.899	0.003	0.165	0.000	100.566
CA574-01	102.011	0.659	0.877	1.001	0.063	0.036	0.233	104.880
CA574-02	98.295	1.048	0.542	0.131	0.195	0.000	0.196	100.407
CA574-03	98.493	0.360	0.045	0.128	0.878	0.000	0.054	99.957
574 Scan	97.670	0.385	0.023	0.000	0.942	0.000	0.000	99.019
574 Scan	96.701	0.596	0.450	0.259	0.882	0.333	0.000	99.222
574 Scan	25.454	0.715	0.651	0.256	0.238	0.014	0.094	27.423
574 Scan	0.089	0.017	0.000	0.000	0.037	0.000	0.000	0.143
574 Scan	92.646	1.374	0.734	0.525	0.648	0.000	0.000	95.927
574 Scan	98.214	0.544	0.135	0.099	0.996	0.000	0.000	99.989
574 Scan	68.698	4.485	7.413	0.160	0.212	0.134	0.398	81.500
574 Scan	98.125	0.441	0.190	0.105	1.069	0.113	0.000	100.044
574 Scan	96.537	0.559	0.092	0.175	0.975	0.008	0.000	98.344
574 Scan	96.512	0.374	0.092	0.088	0.903	0.077	0.017	98.063
574 Scan	96.606	0.971	0.406	0.144	0.185	0.000	0.108	98.421
574 Scan	0.000	0.000	0.000	0.041	0.061	0.000	0.173	0.274
574 Scan	58.789	2.314	2.438	0.352	0.519	0.134	0.000	64.545
574 Scan	84.614	1.776	1.327	0.151	0.118	0.256	0.000	88.243
574 Scan	94.368	1.138	1.016	0.000	0.085	0.022	0.091	96.710
574 Scan	97.636	0.473	0.711	0.408	0.359	0.050	0.054	99.692
574 Scan	98.138	0.379	0.000	0.105	0.601	0.000	0.295	99.508
574 Scan	54.794	0.975	1.471	0.191	0.440	0.000	0.000	57.871
574 Scan	97.481	0.554	0.010	0.165	0.856	0.091	0.000	99.158
574 Scan	98.100	0.510	0.190	0.188	0.943	0.000	0.000	99.932
574 Scan	99.053	0.326	0.102	0.006	0.627	0.107	0.125	100.346
574 Scan	97.493	0.849	0.135	0.131	0.682	0.000	0.197	99.489
574 Scan	64.798	1.755	1.921	0.311	0.332	0.057	0.092	69.266
574 Scan	0.095	0.027	0.258	0.016	0.037	0.099	0.000	0.532
574 Scan	97.627	0.420	0.158	0.181	1.211	0.099	0.000	99.897
574 Scan	97.740	0.253	0.045	0.282	0.945	0.028	0.339	99.632
574 Scan	97.640	0.590	0.135	0.006	0.869	0.256	0.251	99.768
574 Scan	95.486	0.676	0.689	0.491	0.389	0.135	0.000	97.865
574 Scan	98.802	0.132	0.000	0.000	0.640	0.077	0.233	99.883
574 Scan	98.657	0.389	0.056	0.222	0.960	0.163	0.037	100.485
574 Scan	96.751	0.950	0.519	0.175	0.211	0.220	0.000	98.826
CA577-01	97.749	0.764	0.203	0.232	0.145	0.000	0.000	99.092
CA577-02	97.957	1.192	0.339	0.078	0.135	0.022	0.000	99.724
CA577-03	100.437	1.048	0.034	0.034	0.409	0.199	0.054	102.215
577 Scan	85.978	1.929	0.477	0.122	0.197	0.107	0.271	89.080

	CaCO3	MgCO3	FeCO3	MnCO3	SrCO3	BaCO3	ZnCO3
	mol% end member						
190 Scan	1.245	2.849	85.002	10.402	0.043	0.076	0.379
190 Scan	0.710	2.123	86.179	10.855	0.126	0.007	0.000
190 Scan	1.074	2.014	86.077	10.624	0.051	0.068	0.092
190 Scan	0.985	2.206	86.097	10.650	0.062	0.000	0.000
190 Scan	1.185	2.592	85.308	10.684	0.183	0.048	0.000
190 Scan	1.132	2.039	84.338	12.023	0.099	0.368	0.000
190 Scan	0.818	1.900	86.841	10.265	0.053	0.123	0.000
190 Scan	0.595	2.815	87.315	8.696	0.220	0.000	0.358
190 Scan	0.856	2.676	85.578	9.900	0.194	0.283	0.513
190 Scan	0.988	2.061	86.317	10.487	0.121	0.026	0.000
190 Scan	1.510	1.934	83.445	12.242	0.344	0.138	0.387
190 Scan	0.715	1.518	90.990	6.355	0.000	0.000	0.422
190 Scan	1.044	2.131	86.170	10.477	0.120	0.059	0.000
190 Scan	1.203	2.535	85.091	10.979	0.134	0.057	0.000
190 Scan	0.858	2.656	85.860	10.360	0.120	0.058	0.088
190 Scan	1.163	2.854	84.038	11.458	0.244	0.061	0.183
190 Scan	1.303	2.107	85.313	11.105	0.010	0.163	0.000
190 Scan	0.865	2.807	85.646	10.465	0.093	0.123	0 000
190 Scan	0.744	2.185	86.965	9.693	0.130	0.030	0.052
190 Scan	0.643	2.076	87.328	9.855	0.002	0.096	0.000
CA574-01	97.460	0.747	0.724	0.833	0.041	0.017	0.177
CA574-02	97.894	1.239	0.466	0.114	0.132	0.000	0.156
CA574-03	98.781	0.428	0.039	0.112	0.597	0.000	0.043
574 Scan	98.871	0.463	0.020	0.000	0.646	0.000	0.000
574 Scan	97.885	0.716	0.393	0.229	0.605	0.171	0.000
574 Scan	93.127	3.107	2.059	0.816	0.590	0.026	0.274
574 Scan	66.487	14.802	0.000	0.000	18.711	0.000	0.000
574 Scan	96.700	1.703	0.662	0.477	0.459	0.000	0.000
574 Scan	98.472	0.647	0.117	0.086	0.677	0.000	0.000
574 Scan	84.713	6.565	7.897	0.172	0.177	0.084	0.391
574 Scan	98.433	0.526	0.165	0.092	0.727	0.058	0.000
574 Scan	98.410	0.676	0.081	0.155	0.674	0.004	0.000
574 Scan	98.706	0.455	0.081	0.078	0.626	0.040	0.014
574 Scan	98.130	1.170	0.357	0.128	0.128	0.000	0.087
574 Scan	0.000	0.000	0.000	16.440	19.358	0.000	64.201
574 Scan	91.333	4.267	3.272	0.476	0.546	0.105	0.000
574 Scan	95.923	2.390	1.300	0.149	0.091	0.147	0.000
574 Scan	97.562	1.384	0.907	0.000	0.060	0.011	0.075
574 Scan	98.147	0.564	0.618	0.357	0.245	0.026	0.043
574 Scan	98.816	0.453	0.000	0.092	0.410	0.000	0.229
574 Scan	94.986	2.006	2.202	0.289	0.517	0.000	0.000
574 Scan	98.547	0.665	0.008	0.145	0.587	0.047	0.000
574 Scan	98.421	0.608	0.165	0.164	0.642	0.000	0.000
574 Scan	98.942	0.387	0.088	0.006	0.425	0.054	0.100
574 Scan	98.128	1.015	0.118	0.115	0.466	0.000	0.158
574 Scan	93.721	3.014	2.400	0.392	0.326	0.042	0.107
574 Scan	21.535	7.349	50.744	3.212	5.717	11.443	0.000
574 Scan	98.326	0.502	0.137	0.159	0.825	0.051	0.000
574 Scan	98.478	0.303	0.039	0.247	0.645	0.014	0.273
574 Scan	98.233	0.705	0.118	0.006	0.606	0.131	0.202
574 Scan	97.791	0.821	0.600	0.438	0.270	0.070	0.000
574 Scan	99.182	0.157	0.000	0.000	0.435	0.039	0.186
574 Scan	98.534	0.461	0.049	0.193	0.650	0.083	0.029
574 Scan	97.992	1.142	0.454	0.154	0.145	0.113	0.000
CA577-01	98.606	0.914	0.177	0.204	0.099	0.000	0.000
CA577-02	98.118	1.418	0.293	0.068	0.092	0.011	0.000
CA577-03	98.312	1.218	0.029	0.029	0.271	0.099	0.042
577 Scan	96.399	2.567	0.462	0.119	0.149	0.061	0.243

	CaO	MgO	FeO	MnO	SrO	BaO	ZnO	SO4	Total	CaCO3	MgCO3	FeCO3	MnCO3	SrCO3	BaCO3	ZnCO3	Total	CaCO3	MgCO3	FeCO3	MnCO3	SrCO3	BaCO3	ZnCO3
	wt%	wt%	wt%	wt%	wt%	wt%	wt%	wt%	wt%	wt% end member								mol% end member						
577 Scan	55.159	0.323	0.057	0.052	0.101	0.033	0.081	0.055	55.861	98.446	0.676	0.092	0.084	0.144	0.042	0.125	99.610	98.822	0.805	0.080	0.074	0.098	0.022	0.100
577 Scan	54.345	0.705	0.049	0.133	0.164	0.000	0.000	0.160	55.556	96.994	1.475	0.079	0.216	0.234	0.000	0.000	98.997	97.817	1.766	0.069	0.189	0.160	0.000	0.000
577 Scan	49.197	1.240	1.194	0.048	0.077	0.160	0.011	0.000	51.927	87.806	2.594	1.925	0.078	0.110	0.206	0.017	92.735	94.610	3.318	1.792	0.073	0.080	0.113	0.015
577 Scan	54.906	0.804	0.000	0.110	0.319	0.033	0.000	0.215	56.388	97.995	1.682	0.000	0.178	0.454	0.042	0.000	100.352	97.530	1.987	0.000	0.154	0.307	0.021	0.000
577 Scan	18.513	0.574	0.296	0.115	0.227	0.088	0.049	0.132	19.994	33.042	1.201	0.477	0.186	0.323	0.113	0.075	35.418	93.394	4.029	1.166	0.459	0.620	0.162	0.170
577 Scan	54.323	0.406	0.211	0.054	0.116	0.105	0.000	0.032	55.247	96.954	0.849	0.340	0.088	0.165	0.135	0.000	98.532	98.418	1.023	0.298	0.077	0.114	0.070	0.000
577 Scan	54.945	0.595	0.189	0.041	0.057	0.077	0.035	0.215	56.154	98.065	1.245	0.305	0.066	0.081	0.099	0.054	99.915	98.053	1.477	0.263	0.058	0.055	0.050	0.043
577 Scan	55.428	0.551	0.126	0.052	0.033	0.067	0.000	0.255	56.511	98.927	1.153	0.203	0.084	0.047	0.086	0.000	100.500	98.318	1.360	0.174	0.073	0.032	0.043	0.000
577 Scan	54.296	0.736	0.035	0.000	0.427	0.077	0.000	0.430	56.000	96.906	1.540	0.056	0.000	0.608	0.099	0.000	99.210	97.643	1.842	0.049	0.000	0.416	0.051	0.000
577 Scan	1.311	0.229	0.153	0.046	0.274	0.006	0.012	0.110	2.142	2.340	0.479	0.247	0.075	0.390	0.008	0.018	3.557	67.432	16.389	6.143	1.870	7.627	0.113	0.425
577 Scan	54.637	0.615	0.071	0.075	0.162	0.056	0.045	0.182	55.844	97.515	1.287	0.114	0.122	0.231	0.072	0.071	99.411	98.008	1.535	0.099	0.106	0.157	0.037	0.057
577 Scan	54.895	0.318	0.035	0.031	0.187	0.116	0.000	0.135	55.717	97.975	0.665	0.056	0.050	0.266	0.149	0.000	99.163	98.851	0.797	0.049	0.044	0.182	0.076	0.000
577 Scan	55.806	0.396	0.006	0.160	0.127	0.193	0.000	0.120	56.808	99.601	0.828	0.010	0.259	0.181	0.248	0.000	101.128	98.549	0.973	0.008	0.223	0.121	0.125	0.000
577 Scan	54.966	0.481	0.120	0.058	0.161	0.050	0.000	0.262	56.098	98.102	1.006	0.194	0.094	0.229	0.064	0.000	99.689	98.364	1.198	0.168	0.082	0.156	0.033	0.000
577 Scan	55.769	0.333	0.175	0.017	0.060	0.000	0.081	0.040	56.476	99.535	0.697	0.282	0.028	0.085	0.000	0.125	100.752	98.757	0.820	0.242	0.024	0.058	0.000	0.099
577 Scan	55.015	0.290	0.000	0.127	0.183	0.011	0.000	0.055	55.681	98.189	0.607	0.000	0.206	0.261	0.014	0.000	99.277	98.909	0.725	0.000	0.181	0.178	0.007	0.000
577 Scan	55.261	0.471	0.120	0.034	0.384	0.000	0.000	0.335	56.605	98.629	0.985	0.194	0.055	0.547	0.000	0.000	100.410	98.251	1.165	0.167	0.048	0.369	0.000	0.000
577 Scan	54.745	0.456	0.000	0.096	0.467	0.017	0.000	0.255	56.035	97.708	0.954	0.000	0.156	0.665	0.022	0.000	99.504	98.260	1.139	0.000	0.136	0.454	0.011	0.000
577 Scan	41.847	0.552	0.142	0.000	0.253	0.000	0.000	0.137	42.931	74.688	1.155	0.229	0.000	0.360	0.000	0.000	76.432	97.630	1.792	0.259	0.000	0.319	0.000	0.000
577 Scan	54.877	0.247	0.134	0.096	0.173	0.000	0.152	0.040	55.718	97.943	0.517	0.216	0.156	0.246	0.000	0.234	99.312	98.700	0.618	0.188	0.136	0.168	0.000	0.188
577 Scan	55.442	0.453	0.147	0.054	0.267	0.000	0.046	0.327	56.736	98.952	0.948	0.237	0.088	0.380	0.000	0.071	100.675	98.291	1.117	0.203	0.076	0.256	0.000	0.056
577 Scan	54.765	0.773	0.000	0.096	0.324	0.033	0.174	0.454	56.619	97.743	1.617	0.000	0.156	0.462	0.042	0.268	100.288	97.405	1.513	0.000	0.135	0.312	0.021	0.213
577 Scan	55.708	0.582	0.042	0.112	0.173	0.071	0.000	0.400	57.088	99.426	1.218	0.068	0.181	0.246	0.091	0.000	101.231	98.149	1.427	0.058	0.156	0.165	0.046	0.000
577 Scan	3.887	1.549	33.211	0.019	0.158	0.000	0.174	0.085	39.083	6.937	3.240	53.555	0.031	0.225	0.000	0.268	64.256	12.077	6.696	80.542	0.047	0.266	0.000	0.373
577 Scan	54.351	0.499	0.042	0.000	0.200	0.138	0.011	0.047	55.289	97.004	1.044	0.068	0.000	0.285	0.178	0.017	98.595	98.383	1.257	0.059	0.000	0.196	0.091	0.014
577 Scan	54.678	0.504	0.140	0.000	0.061	0.000	0.233	0.135	55.751	97.588	1.054	0.226	0.000	0.087	0.000	0.359	99.314	98.197	1.259	0.196	0.000	0.059	0.000	0.286
577 Scan	55.183	0.358	0.000	0.021	0.136	0.000	0.000	0.255	55.953	98.489	0.749	0.000	0.034	0.194	0.000	0.000	99.466	98.945	0.893	0.000	0.030	0.132	0.000	0.000
577 Scan	55.913	0.383	0.000	0.054	0.122	0.050	0.000	0.310	56.832	99.792	0.801	0.000	0.088	0.174	0.064	0.000	100.919	98.834	0.942	0.000	0.075	0.117	0.032	0.000
537 Scan	30.207	20.657	0.502	0.216	0.067	0.032	0.047	0.050	51.779	53.913	43.213	0.810	0.350	0.095	0.041	0.072	98.494	50.690	48.231	0.658	0.287	0.061	0.020	0.054
537 Scan	29.446	20.062	0.987	0.298	0.060	0.098	0.189	0.202	51.343	52.555	41.968	1.592	0.483	0.085	0.126	0.291	97.100	50.279	47.664	1.315	0.402	0.055	0.061	0.222
537 Scan	29.324	20.502	0.798	0.230	0.095	0.044	0.000	0.110	51.102	52.337	42.889	1.287	0.373	0.135	0.057	0.000	97.077	49.936	48.578	1.061	0.310	0.088	0.027	0.000
537 Scan	29.639	20.576	0.536	0.247	0.072	0.076	0.000	0.160	51.306	52.899	43.044	0.864	0.400	0.103	0.098	0.000	97.408	50.279	48.567	0.710	0.331	0.066	0.047	0.000
537 Scan	21.791	11.524	5.069	1.435	0.117	0.238	0.000	0.694	40.868	38.892	24.107	8.174	2.325	0.167	0.306	0.000	73.972	50.598	37.232	9.187	2.634	0.147	0.202	0.000
537 Scan	25.807	18.870	2.253	0.367	0.129	0.000	0.166	0.042	47.633	46.060	39.475	3.633	0.595	0.184	0.000	0.256	90.202	47.531	48.357	3.239	0.534	0.129	0.000	0.211
537 Scan	28.601	19.681	0.989	0.356	0.060	0.159	0.036	0.025	49.907	51.046	41.171	1.595	0.577	0.085	0.205	0.055	94.735	50.042	47.913	1.351	0.492	0.057	0.102	0.043
537 Scan	29.260	20.021	1.185	0.369	0.066	0.093	0.000	0.227	51.221	52.223	41.883	1.911	0.598	0.094	0.120	0.000	96.828	50.100	47.698	1.584	0.499	0.061	0.058	0.000
537 Scan	29.561	19.530	0.840	0.257	0.060	0.017	0.202	0.100	50.566	52.760	40.855	1.355	0.416	0.085	0.022	0.311	95.805	51.169	47.037	1.135	0.352	0.056	0.011	0.241
537 Scan	30.384	18.953	2.916	0.611	0.090	0.060	0.011	0.125	53.150	54.229	39.648	4.702	0.990	0.128	0.077	0.017	99.792	50.986	44.252	3.819	0.811	0.082	0.037	0.013
537 Scan	29.937	20.958	0.530	0.182	0.021	0.032	0.036	0.192	51.889	53.431	43.843	0.855	0.295	0.030	0.041	0.055	98.550	50.143	48.843	0.693	0.241	0.019	0.020	0.042
537 Scan	29.499	20.802	0.508	0.168	0.083	0.000	0.000	0.185	51.245	52.649	43.516	0.819	0.272	0.118	0.000	0.000	97.375	49.984	49.043	0.672	0.225	0.076	0.000	0.000
537 Scan	30.010	20.805	0.587	0.083	0.063	0.000	0.236	0.117	51.901	53.561	43.523	0.947	0.134	0.090	0.000	0.364	98.618	50.286	48.507	0.768	0.110	0.057	0.000	0.273
537 Scan	29.863	20.453	0.980	0.360	0.104	0.000	0.000	0.125	51.886	53.299	42.786	1.580	0.583	0.148	0.000	0.000	98.397	50.252	47.888	1.287	0.479	0.095	0.000	0.000
537 Scan	30.386	20.777	0.720	0.164	0.066	0.000	0.024	0.135	52.272	54.232	43.464	1.161	0.266	0.094	0.000	0.037	99.254	50.610	48.150	0.936	0.216	0.059	0.000	0.028
537 Scan	29.257	20.183	0.692	0.124	0.136	0.000	0.000	0.142	50.535	52.217	42.222	1.116	0.201	0.194	0.000	0.000	95.949	50.399	48.375	0.930	0.169	0.127	0.000	0.000
537 Scan	29.165	19.895	0.856	0.155	0.076	0.055	0.000	0.202	50.403	52.053	41.619	1.380	0.251	0.108	0.071	0.000	95.483	50.547	47.976	1.158	0.212	0.071	0.035	0.000
537 Scan	29.207	20.241	1.320	0.172	0.057	0.093	0.024	0.100	51.213	52.128	42.343	2.129	0.279	0.081	0.120	0.037	97.116	49.826	48.045	1.758	0.232	0.053	0.058	0.028
537 Scan	26.761	18.988	1.027	0.429	0.086	0.000	0.000	0.060	47.350	47.762	39.722	1.656	0.695	0.123	0.000	0.000	89.958	49.222	48.594	1.474	0.624	0.086	0.000	0.000
537 Scan	28.405	19.346	1.553	0.411	0.040	0.098	0.200	0.032	50.086	50.697	40.471	2.504	0.666	0.057	0.126	0.308	94.829	49.785	47.179	2.125	0.569	0.038	0.063	0.242
537 Scan	29.355	20.243	0.735	0.234	0.047	0.159	0.000	0.032	50.805	52.392	42.347	1.185	0.379	0.067	0.205	0.000	96.575	50.297	48.260	0.983	0.317	0.044	0.100	0.000
537 Scan	29.103	19.832	1.559	0.640	0.032	0.060	0.000	0.142	51.369	51.942	41.487	2.514	1.037	0.046	0.077	0.000	97.103	49.783	47.202	2.082	0.865	0.030	0.038	0.000
537 Scan	30.116	21.115	0.678	0.209	0.047	0.000	0.011	0.050	52.227	53.750	44.171	1.093	0.339	0.067	0.000	0.017	99.437	50.008	48.784	0.879	0.274	0.042	0.000	0.013
537 Scan	28.037	19.342	1.292	0.340	0.060	0.164	0.000	0.000	49.235	50.040	40.462	2.083	0.551	0.085	0.211	0.000	93.433	49.782	47.786	1.791	0.477	0.058	0.107	0.000
537 Scan	29.537	20.140	1.002	0.371	0.006	0.093	0.035	0.075	51.258	52.717	42.132	1.616	0.601	0.009	0.120	0.054	97.248	50.322	47.742	1.332	0.500	0.006	0.058	0.041
537 Scan	30.552	21.069	0.791	0.232	0.034	0.000	0.059	0.017	52.754	54.528	44.075	1.276	0.376	0.048	0.000	0.091	100.394	50.310	48.274	1.017	0.302	0.030	0.000	0.067
537 Scan	30.343	20.571	0.516	0.271	0.132	0.082	0.000	0.117	52.033	54.155	43.033	0.832	0.439	0.188	0.106	0.000	98.753	50.840	47.957	0.675	0.359	0.120	0.050	0.000
537 Scan	29.865	20.873	0.904	0.311	0.063	0.006	0.189	0.060	52.271	53.302	43.665	1.458	0.504	0.090	0.008	0.291	99.318	49.754	48.384	1.176	0.410	0.057	0.004	0.217
537 Scan	29.214	19.750	1.482	0.356	0.108	0.011	0.319	0.050	51.290	52.140	41.316	2.390	0.577	0.154	0.014	0.492	97.082	50.011	47.043	1.980	0.482	0.100	0.007	0.376
537 Scan	29.092	19.323	2.031	0.630	0.066	0.000	0.000	0.110	51.252	51.923	40.422	3.275	1.021	0.094	0.000	0.000	96.735	50.075	46.278	2.729	0.657	0.061	0.000	0.000

	CaO	MgO	FeO	MnO	SrO	BaO	ZnO	SO4	Total
	wt%	wt%	wt%	wt%	wt%	wt%	wt%	wt%	wt%
CA575-01	54.695	0.153	0.000	0.761	0.086	0.116	0.000	0.087	55.898
575 Scan	54.026	0.534	0.323	0.639	0.163	0.000	0.105	0.200	55.989
575 Scan	52.428	0.423	0.310	0.661	0.037	0.056	0.082	0.160	54.157
575 Scan	51.561	0.665	0.611	0.591	0.128	0.155	0.163	0.257	54.131
575 Scan	0.288	0.272	0.322	0.000	0.403	0.033	0.112	0.000	1.431
575 Scan	54.372	0.126	0.071	0.890	0.035	0.111	0.082	0.145	55.831
575 Scan	53.116	0.458	0.217	0.702	0.061	0.111	0.047	0.370	55.083
575 Scan	47.871	0.637	0.077	0.403	0.128	0.078	0.000	0.162	49.356
575 Scan	50.650	0.542	0.127	0.285	0.195	0.000	0.093	0.225	52.118
575 Scan	50.813	0.555	0.337	0.692	0.096	0.282	0.280	0.232	53.289
575 Scan	54.346	0.507	0.189	0.749	0.114	0.033	0.093	0.120	56.152
575 Scan	53.307	0.638	0.253	0.678	0.170	0.000	0.000	0.217	55.264
575 Scan	52.921	0.551	0.162	0.504	0.232	0.000	0.070	0.569	55.008
575 Scan	52.560	0.514	0.197	0.538	0.060	0.056	0.000	0.225	54.150
575 Scan	46.123	0.745	0.311	0.598	0.119	0.166	0.153	0.007	48.223
575 Scan	38.798	0.551	0.405	0.511	0.246	0.077	0.118	0.097	40.804
575 Scan	52.325	0.584	0.316	0.559	0.220	0.033	0.141	0.272	54.450
575 Scan	50.469	0.594	0.466	0.515	0.070	0.189	0.035	0.112	52.449
575 Scan	51.721	0.499	0.935	1.568	0.167	0.028	0.000	0.000	54.918
575 Scan	53.275	0.685	0.211	0.518	0.164	0.000	0.000	0.330	55.182
575 Scan	16.863	2.162	4.352	0.274	0.202	0.125	0.640	0.075	24.693
575 Scan	52.667	0.595	0.282	0.377	0.117	0.239	0.000	0.145	54.422
575 Scan	52.862	0.473	0.373	0.736	0.103	0.116	0.000	0.097	54.760
575 Scan	51.030	0.575	0.296	0.408	0.067	0.022	0.117	0.282	52.799
575 Scan	52.595	0.441	0.324	0.792	0.086	0.045	0.000	0.257	54.540
575 Scan	53.331	0.560	0.140	0.377	0.061	0.000	0.035	0.272	54.777
575 Scan	29.424	0.605	0.568	0.407	0.114	0.127	0.024	0.272	31.560
575 Scan	52.690	0.501	0.801	0.613	0.179	0.028	0.000	0.280	55.091
575 Scan	53.188	0.483	0.225	0.582	0.032	0.000	0.000	0.257	54.767
575 Scan	50.921	0.141	0.205	0.484	0.088	0.116	0.398	0.315	52.667
575 Scan	54.051	0.423	0.169	0.723	0.060	0.000	0.000	0.240	55.666
CA352-01	52.318	0.118	1.222	0.975	0.092	0.122	0.117	0.072	55.036
CA352-02	52.183	0.153	1.299	1.070	0.078	0.060	0.000	0.080	54.924
CA352-03	53.035	0.216	1.313	0.859	0.043	0.022	0.128	0.522	56.138
CA352-04	51.257	0.224	1.496	1.050	0.092	0.039	0.011	0.482	54.651
CA352-05	51.591	0.227	1.362	0.940	0.053	0.000	0.152	0.432	54.758
CA352-06	51.573	0.383	1.917	1.463	0.130	0.000	0.000	0.410	55.876
CA352-07	53.921	0.060	0.830	0.705	0.057	0.000	0.000	0.105	55.677
CA352-08	52.978	0.121	1.208	1.274	0.025	0.000	0.000	0.120	55.726
CA352-09	51.875	0.167	1.717	1.516	0.035	0.204	0.000	0.072	55.588
CA535-01	29.182	13.877	9.521	2.014	0.058	0.065	0.000	0.042	54.760
CA535-02	28.674	13.549	9.721	2.291	0.052	0.027	0.000	0.050	54.363
CA535-03	28.860	13.224	10.541	2.266	0.000	0.027	0.268	0.000	55.186
CA535-04	28.458	13.144	10.121	2.287	0.066	0.032	0.000	0.067	54.176
535 Scan	28.661	18.530	2.515	0.634	0.040	0.000	0.000	0.572	50.952
535 Scan	29.596	19.351	1.859	0.634	0.034	0.000	0.000	0.050	51.524
535 Scan	30.091	19.739	0.687	0.482	0.102	0.011	0.000	0.075	51.186
535 Scan	27.370	18.372	1.001	0.469	0.108	0.000	0.000	0.035	47.354
535 Scan	26.343	17.558	1.645	0.695	0.045	0.093	0.000	0.195	46.574
535 Scan	23.484	15.767	1.333	0.380	0.127	0.000	0.000	0.295	41.385
535 Scan	20.444	12.343	1.651	0.952	0.073	0.044	0.000	0.127	35.634
535 Scan	28.642	19.034	1.253	0.635	0.095	0.071	0.000	0.152	49.882
535 Scan	29.166	16.180	5.509	1.615	0.041	0.059	0.153	0.042	52.767
535 Scan	22.629	14.580	1.204	0.495	0.025	0.017	0.000	2.300	41.250
535 Scan	25.068	16.223	2.496	0.873	0.030	0.032	0.000	0.699	45.421
535 Scan	23.125	15.267	3.503	0.604	0.051	0.000	0.024	2.240	44.813
535 Scan	28.414	19.006	1.515	0.550	0.047	0.077	0.000	0.227	49.837
535 Scan	28.686	17.771	3.315	1.050	0.089	0.060	0.000	0.092	51.063

	CaCO3	MgCO3	FeCO3	MnCO3	SrCO3	BaCO3	ZnCO3	Total
	wt% end member							
	97.618	0.320	0.000	1.233	0.123	0.149	0.000	99.443
	96.424	1.117	0.521	1.035	0.232	0.000	0.162	99.492
	93.572	0.885	0.500	1.071	0.053	0.072	0.126	96.279
	92.025	1.391	0.985	0.958	0.182	0.199	0.251	95.992
	0.514	0.569	0.519	0.000	0.574	0.042	0.173	2.391
	97.042	0.264	0.114	1.442	0.050	0.143	0.126	99.181
	94.800	0.958	0.350	1.138	0.087	0.143	0.072	97.548
	85.439	1.333	0.124	0.653	0.182	0.100	0.000	87.832
	90.399	1.134	0.205	0.462	0.278	0.000	0.143	92.620
	90.690	1.161	0.543	1.121	0.137	0.363	0.431	94.447
	96.995	1.061	0.305	1.214	0.162	0.042	0.143	99.923
	95.141	1.335	0.408	1.099	0.242	0.000	0.000	98.225
	94.452	1.153	0.261	0.817	0.331	0.000	0.108	97.121
	93.808	1.075	0.318	0.872	0.085	0.072	0.000	96.230
	82.319	1.558	0.502	0.969	0.170	0.214	0.236	85.967
	69.246	1.153	0.653	0.828	0.350	0.090	0.182	72.511
	93.388	1.222	0.510	0.906	0.313	0.042	0.217	96.599
	90.076	1.243	0.751	0.835	0.100	0.243	0.054	93.301
	92.310	1.044	1.508	2.541	0.238	0.036	0.000	97.677
	95.084	1.433	0.340	0.839	0.234	0.000	0.000	97.930
	30.097	4.523	7.018	0.444	0.288	0.161	0.986	43.516
	93.999	1.245	0.455	0.611	0.167	0.308	0.000	96.783
	94.347	0.989	0.601	1.193	0.147	0.149	0.000	97.426
	91.077	1.203	0.477	0.661	0.095	0.028	0.180	93.722
	93.870	0.923	0.522	1.283	0.123	0.058	0.000	96.779
	95.184	1.171	0.226	0.611	0.087	0.000	0.054	97.333
	52.515	1.266	0.948	0.660	0.162	0.163	0.037	55.751
	94.040	1.048	1.292	0.993	0.255	0.036	0.000	97.664
	94.929	1.010	0.363	0.943	0.046	0.000	0.000	97.291
	90.883	0.295	0.331	0.784	0.125	0.149	0.513	93.180
	96.469	0.885	0.273	1.172	0.085	0.000	0.000	98.883
	93.376	0.247	1.971	1.580	0.131	0.157	0.180	97.642
	93.135	0.320	2.095	1.734	0.111	0.077	0.000	97.472
	94.656	0.452	2.117	1.392	0.061	0.028	0.197	98.903
	91.482	0.469	2.412	1.701	0.131	0.050	0.017	96.263
	92.078	0.475	2.196	1.523	0.076	0.000	0.234	96.582
	92.046	0.801	3.091	2.371	0.185	0.000	0.000	98.495
	96.237	0.126	1.338	1.142	0.081	0.000	0.000	98.924
	94.554	0.253	1.948	2.064	0.036	0.000	0.000	98.855
	92.585	0.349	2.769	2.457	0.050	0.263	0.000	98.472
	52.083	29.030	15.353	3.263	0.083	0.084	0.000	99.896
	51.177	28.344	15.676	3.712	0.074	0.035	0.000	99.017
	51.509	27.664	16.998	3.672	0.000	0.035	0.413	100.290
	50.791	27.496	16.321	3.706	0.094	0.041	0.000	98.449
	51.153	38.764	4.056	1.027	0.057	0.000	0.000	95.057
	52.822	40.481	2.998	1.027	0.048	0.000	0.000	97.377
	53.706	41.293	1.108	0.781	0.145	0.014	0.000	97.047
	48.849	38.433	1.614	0.760	0.154	0.000	0.000	89.810
	47.016	36.730	2.653	1.126	0.064	0.120	0.000	87.709
	41.914	32.984	2.150	0.616	0.181	0.000	0.000	77.843
	36.488	25.821	2.662	1.543	0.104	0.057	0.000	66.674
	51.120	39.818	2.021	1.029	0.135	0.091	0.000	94.214
	52.055	33.848	8.884	2.617	0.058	0.076	0.236	97.773
	40.388	30.500	1.942	0.802	0.036	0.022	0.000	73.689
	44.741	33.937	4.025	1.415	0.043	0.041	0.000	84.202
	41.273	31.938	5.649	0.979	0.073	0.000	0.037	79.948
	50.713	39.759	2.443	0.891	0.067	0.099	0.000	93.972
	51.198	37.176	5.346	1.701	0.127	0.077	0.000	95.625

	CaCO3	MgCO3	FeCO3	MnCO3	SrCO3	BaCO3	ZnCO3
	mol% end member						
	98.375	0.383	0.000	1.082	0.084	0.076	0.000
	97.018	1.334	0.453	0.907	0.158	0.000	0.130
	97.309	1.092	0.449	0.970	0.037	0.038	0.105
	96.073	1.724	0.889	0.871	0.129	0.106	0.209
	23.507	30.891	20.515	0.000	17.802	0.985	6.300
	98.105	0.316	0.100	1.270	0.034	0.073	0.102
	97.311	1.167	0.310	1.017	0.060	0.074	0.059
	97.232	1.800	0.122	0.647	0.141	0.058	0.000
	97.595	1.453	0.191	0.434	0.203	0.000	0.123
	96.340	1.464	0.499	1.037	0.099	0.196	0.366
	97.170	1.261	0.264	1.059	0.110	0.022	0.115
	96.866	1.613	0.359	0.974	0.167	0.000	0.000
	97.306	1.410	0.233	0.733	0.231	0.000	0.089
	97.501	1.327	0.285	0.789	0.060	0.038	0.000
	95.879	2.155	0.505	0.983	0.134	0.126	0.219
	95.733	1.892	0.780	0.997	0.329	0.069	0.201
	96.801	1.503	0.456	0.818	0.220	0.022	0.180
	96.689	1.583	0.697	0.780	0.073	0.132	0.046
	94.926	1.274	1.339	2.275	0.166	0.019	0.000
	97.056	1.736	0.300	0.746	0.162	0.000	0.000
	70.027	12.492	14.106	0.900	0.454	0.190	1.831
	97.237	1.528	0.406	0.550	0.117	0.161	0.000
	97.010	1.208	0.534	1.068	0.102	0.078	0.000
	97.184	1.524	0.440	0.614	0.069	0.015	0.154
	97.127	1.133	0.467	1.156	0.086	0.030	0.000
	97.721	1.428	0.200	0.546	0.060	0.000	0.044
	94.395	2.701	1.472	1.032	0.198	0.149	0.053
	96.495	1.277	1.145	0.887	0.177	0.019	0.000
	97.569	1.233	0.322	0.844	0.032	0.000	0.000
	97.880	0.377	0.308	0.735	0.092	0.082	0.527
	97.608	1.063	0.238	1.032	0.059	0.000	0.000
	96.205	0.302	1.754	1.417	0.092	0.082	0.148
	96.066	0.392	1.867	1.557	0.078	0.040	0.000
	96.149	0.545	1.858	1.231	0.042	0.015	0.160
	95.561	0.581	2.177	1.548	0.093	0.027	0.014
	95.811	0.587	1.974	1.380	0.053	0.000	0.195
	94.061	0.972	2.729	2.109	0.128	0.000	0.000
	97.611	0.151	1.173	1.009	0.056	0.000	0.000
	96.131	0.305	1.711	1.828	0.025	0.000	0.000
	94.767	0.424	2.448	2.189	0.035	0.136	0.000
	50.690	33.539	12.909	2.766	0.055	0.041	0.000
	50.338	33.095	13.320	3.180	0.049	0.017	0.000
	50.214	32.014	14.316	3.117	0.000	0.017	0.321
	50.367	32.368	13.982	3.200	0.063	0.021	0.000
	50.345	45.289	3.448	0.880	0.038	0.000	0.000
	50.599	46.032	2.481	0.857	0.031	0.000	0.000
	51.409	45.922	0.916	0.651	0.094	0.007	0.000
	50.551	47.213	1.443	0.685	0.108	0.000	0.000
	50.020	46.388	2.438	1.043	0.046	0.065	0.000
	50.145	46.845	2.222	0.641	0.147	0.000	0.000
	51.477	43.243	3.245	1.895	0.099	0.041	0.000
	50.530	46.723	1.725	0.886	0.091	0.046	0.000
	50.808	39.218	7.491	2.224	0.039	0.038	0.184
	51.120	45.828	2.123	0.884	0.031	0.014	0.000
	49.830	44.870	3.873	1.372	0.032	0.023	0.000
	48.558	44.605	5.741	1.003	0.058	0.000	0.035
	50.264	46.780	2.092	0.769	0.045	0.050	0.000
	50.415	43.456	4.547	1.459	0.085	0.039	0.000

	CaO	MgO	FeO	MnO	SrO	BaO	ZnO	SO4	Total
	wt%	wt%	wt%	wt%	wt%	wt%	wt%	wt%	wt%
535 Scan	29.085	19.087	1.393	0.649	0.180	0.104	0.000	0.092	50.591
535 Scan	28.324	19.202	1.678	0.615	0.028	0.000	0.000	0.799	50.645
535 Scan	29.362	19.707	0.998	0.405	0.007	0.060	0.213	0.135	50.888
535 Scan	19.193	11.955	3.288	0.794	0.000	0.104	0.000	0.050	35.384
535 Scan	20.484	11.372	3.605	1.349	0.080	0.055	0.036	1.236	38.217
535 Scan	29.547	19.527	1.324	0.553	0.045	0.022	0.000	0.127	51.145
535 Scan	5.842	4.034	1.871	0.462	0.276	0.269	0.000	0.494	13.268
535 Scan	26.705	17.862	1.342	0.365	0.000	0.049	0.000	0.235	46.558
535 Scan	0.043	0.035	0.000	0.000	0.032	0.000	0.112	0.017	0.240
535 Scan	5.447	4.222	38.380	0.129	0.057	0.079	0.365	57.533	106.211
535 Scan	27.679	18.717	1.424	0.482	0.129	0.000	0.036	0.252	48.719
535 Scan	29.635	19.752	0.906	0.536	0.066	0.153	0.012	0.117	51.178
535 Scan	28.902	19.162	1.409	0.433	0.000	0.126	0.000	0.142	50.173
535 Scan	30.268	20.019	0.786	0.399	0.050	0.060	0.047	0.067	51.696
535 Scan	26.998	17.784	1.891	0.684	0.096	0.055	0.095	0.287	47.889
535 Scan	29.902	20.298	1.527	0.591	0.060	0.198	0.000	0.042	52.619

	BaO	CaO	SrO	PbO	SO3	SeO3	Total
	wt%	wt%	wt%	wt%	wt%	wt%	wt%
BA141-02	63.81	0.04	1.17	0.00	33.63	0.00	98.65
BA141-05	62.75	0.44	0.36	0.00	32.45	0.00	96.00
BA141-03	63.58	0.06	0.94	0.00	33.45	0.00	98.03
BA284-08	65.21	0.06	0.22	0.00	34.13	0.00	99.62
BA284-07	66.22	0.03	0.29	0.00	34.19	0.00	100.73
BA284-01	65.55	0.02	0.20	0.00	34.26	0.00	100.03
BA141-06	64.61	0.02	0.23	0.00	33.40	0.00	98.26
BA284-02	65.26	0.05	0.19	0.00	33.19	0.00	98.69
BA284-10	65.45	0.02	0.12	0.00	32.70	0.00	98.29
BA284-03	65.25	0.05	0.09	0.00	33.42	0.00	98.81
BA284-11	65.26	0.05	0.07	0.00	33.01	0.00	98.39
BA284-09	65.55	0.00	0.13	0.00	32.73	0.00	98.41
BA207-07	63.99	0.07	1.81	0.00	34.07	0.00	99.94
BA137-01	63.75	0.07	0.98	0.00	34.10	0.00	98.90
BA137-02	63.68	0.03	0.86	0.00	33.35	0.00	97.92
BA146-03	65.39	0.02	0.81	0.00	33.23	0.00	99.45
BA207-09	65.38	0.01	0.64	0.00	33.73	0.00	99.76
BA137-03	65.23	0.05	0.32	0.00	33.26	0.00	98.86
BA146-02	65.11	0.00	0.29	0.00	34.72	0.00	100.12
BA207-08	65.38	0.08	0.08	0.00	35.69	0.00	101.23
BA146-01	65.19	0.00	0.19	0.00	33.73	0.00	99.11

	CaCO3	MgCO3	FeCO3	MnCO3	SrCO3	BaCO3	ZnCO3	Total
	wt% end member							
535 Scan	51.910	39.929	2.246	1.052	0.256	0.134	0.000	95.527
535 Scan	50.552	40.159	2.706	0.997	0.040	0.000	0.000	94.464
535 Scan	52.405	41.226	1.609	0.656	0.010	0.077	0.328	96.311
535 Scan	34.255	25.009	5.302	1.287	0.000	0.134	0.000	65.987
535 Scan	36.559	23.789	5.813	2.186	0.114	0.071	0.055	68.588
535 Scan	52.735	40.849	2.135	0.896	0.064	0.028	0.000	96.708
535 Scan	10.427	8.439	3.017	0.749	0.393	0.372	0.000	23.396
535 Scan	47.662	37.366	2.164	0.591	0.000	0.063	0.000	87.847
535 Scan	0.077	0.073	0.000	0.000	0.046	0.000	0.173	0.368
535 Scan	9.722	8.832	61.890	0.209	0.031	0.102	0.562	81.398
535 Scan	49.401	39.155	2.296	0.781	0.184	0.000	0.055	91.872
535 Scan	52.892	41.320	1.461	0.869	0.094	0.197	0.018	96.851
535 Scan	51.584	40.086	2.272	0.702	0.000	0.162	0.000	94.805
535 Scan	54.022	41.878	1.267	0.647	0.071	0.077	0.072	98.035
535 Scan	48.185	37.203	3.049	1.108	0.137	0.071	0.146	89.900
535 Scan	53.368	42.462	2.462	0.958	0.085	0.255	0.000	99.591

	BaSO4	CaSO4	SrSO4	PbSO4
	wt% end member			
BA141-02	97.12	0.11	2.09	0.00
BA141-05	95.48	1.06	0.68	0.00
BA141-03	96.75	0.17	1.70	0.00
BA284-08	99.22	0.12	0.39	0.00
BA284-07	100.76	0.06	0.47	0.00
BA284-01	99.79	0.06	0.39	0.00
BA141-06	98.35	0.06	0.38	0.00
BA284-02	99.31	0.11	0.31	0.00
BA284-10	99.59	0.06	0.23	0.00
BA284-03	99.27	0.11	0.15	0.00
BA284-11	99.34	0.11	0.15	0.00
BA284-09	99.76	0.00	0.23	0.00
BA207-07	97.43	0.17	3.22	0.00
BA137-01	97.07	0.17	1.72	0.00
BA137-02	96.90	0.06	1.54	0.00
BA146-03	99.49	0.06	1.47	0.00
BA207-09	99.49	0.06	1.17	0.00
BA137-03	99.32	0.11	0.54	0.00
BA146-02	99.14	0.00	0.56	0.00
BA207-08	99.53	0.18	0.16	0.00
BA146-01	99.25	0.00	0.31	0.00

	CaCO3	MgCO3	FeCO3	MnCO3	SrCO3	BaCO3	ZnCO3
	mol% end member						
535 Scan	50.690	46.285	1.895	0.894	0.170	0.066	0.000
535 Scan	49.820	46.994	2.304	0.855	0.027	0.000	0.000
535 Scan	50.577	47.232	1.342	0.552	0.007	0.038	0.253
535 Scan	49.138	42.587	6.571	1.607	0.000	0.097	0.000
535 Scan	50.860	39.287	6.987	2.648	0.108	0.050	0.062
535 Scan	50.751	46.668	1.775	0.751	0.042	0.014	0.000
535 Scan	43.160	41.468	10.789	2.698	1.104	0.781	0.000
535 Scan	50.471	46.971	1.980	0.545	0.000	0.034	0.000
535 Scan	23.094	26.154	0.000	0.000	9.301	0.000	41.451
535 Scan	13.065	14.090	71.854	0.245	0.074	0.069	0.603
535 Scan	50.044	47.086	2.010	0.689	0.126	0.000	0.045
535 Scan	50.789	47.101	1.212	0.726	0.061	0.096	0.014
535 Scan	50.659	46.733	1.928	0.600	0.000	0.081	0.000
535 Scan	51.187	47.105	1.038	0.533	0.046	0.037	0.055
535 Scan	50.092	45.911	2.739	1.003	0.096	0.037	0.121
535 Scan	49.913	47.143	1.990	0.780	0.054	0.121	0.000

	BaSO4	CaSO4	SrSO4	PbSO4
	mol% end member			
BA141-02	97.14	0.20	2.66	0.00
BA141-05	97.28	1.85	0.88	0.00
BA141-03	97.53	0.30	2.17	0.00
BA284-08	99.30	0.20	0.50	0.00
BA284-07	99.31	0.10	0.59	0.00
BA284-01	99.40	0.10	0.50	0.00
BA141-06	99.41	0.10	0.49	0.00
BA284-02	99.41	0.20	0.39	0.00
BA284-10	99.61	0.10	0.29	0.00
BA284-03	99.61	0.20	0.20	0.00
BA284-11	99.61	0.19	0.19	0.00
BA284-09	99.71	0.00	0.29	0.00
BA207-07	95.68	0.29	4.02	0.00
BA137-01	97.50	0.30	2.20	0.00
BA137-02	97.93	0.10	1.97	0.00
BA146-03	98.07	0.10	1.84	0.00
BA207-09	98.43	0.10	1.47	0.00
BA137-03	99.12	0.20	0.68	0.00
BA146-02	99.29	0.00	0.71	0.00
BA207-08	99.49	0.31	0.21	0.00
BA146-01	99.60	0.00	0.40	0.00

Pyrite/Marcasite

SAMPLE	Cu wt%	Hg wt%	Ag wt%	Au wt%	Fe wt%	As wt%	Zn wt%	Sb wt%	Se wt%	In wt%	Cd wt%	Ge wt%	Pb wt%	Bi wt%	Te wt%	V wt%	Mn wt%	S wt%	TOTAL wt%
MC114-01	0.028	0.000	0.383	0.087	45.015	0.318	0.004	0.000	0.025	0.000	0.000	0.000	0.000	0.042	0.030	0.021	0.032	52.195	98.180
MC114-02	0.123	0.173	0.265	0.056	45.593	0.461	0.050	0.000	0.086	0.000	0.015	0.000	0.000	0.256	0.036	0.013	0.000	52.012	99.139
MC114-03	0.181	0.000	0.081	0.000	45.428	0.862	0.000	0.000	0.009	0.000	0.035	0.000	0.000	0.292	0.000	0.000	0.004	52.415	99.307
MC178-07	0.000	0.146	0.039	0.000	45.415	0.020	0.000	0.000	0.044	0.020	0.000	0.062	0.000	0.077	0.053	0.000	0.165	53.697	99.738
MC178-08	0.047	0.000	0.000	0.049	45.928	0.072	0.016	0.013	0.000	0.024	0.000	0.000	0.000	0.221	0.000	0.026	0.059	53.895	100.350
MC178-09	0.000	0.000	0.044	0.025	46.095	0.056	0.018	0.044	0.053	0.049	0.046	0.000	0.000	0.098	0.044	0.030	0.024	53.542	100.168
MC207-01	0.000	0.000	0.031	0.031	45.969	0.118	0.008	0.007	0.037	0.000	0.000	0.000	0.000	0.094	0.000	0.009	0.053	51.955	98.312
MC207-02	0.000	0.025	0.000	0.000	45.691	0.058	0.000	0.028	0.048	0.000	0.000	0.000	0.000	0.317	0.000	0.000	0.072	52.523	98.762
MC207-03	0.000	0.191	0.059	0.025	46.805	0.028	0.000	0.000	0.000	0.000	0.000	0.000	0.000	0.136	0.000	0.018	0.138	52.722	100.122
MC207-04	0.000	0.074	0.064	0.037	46.153	0.077	0.000	0.000	0.080	0.014	0.054	0.000	0.000	0.214	0.053	0.000	0.136	52.812	99.768
MC207-05	0.000	0.043	0.000	0.000	46.605	0.091	0.060	0.000	0.024	0.022	0.000	0.000	0.000	0.229	0.000	0.000	0.094	52.962	100.130
MC207-06	0.043	0.012	0.000	0.025	44.371	0.134	0.037	0.054	0.000	0.000	0.000	0.000	0.000	0.229	0.000	0.012	0.701	51.727	97.345
MC207-08	0.000	0.099	0.000	0.069	46.235	0.456	0.013	0.000	0.043	0.000	0.000	0.000	0.000	0.178	0.071	0.003	0.242	52.504	99.913
MC207-09	0.010	0.076	0.000	0.000	41.271	4.255	0.000	0.000	0.037	0.024	0.035	0.000	0.000	0.277	0.017	0.000	0.450	44.788	91.240
MC207-10	0.000	0.000	0.020	0.000	44.984	1.539	0.009	0.028	0.016	0.038	0.000	0.000	0.000	0.241	0.130	0.000	0.119	51.341	98.465
PY114-07	0.000	0.000	0.011	0.013	44.482	2.218	0.000	0.000	0.084	0.020	0.000	0.000	0.000	0.063	0.000	0.005	0.004	51.313	98.213
PY114-08	0.000	0.000	0.014	0.063	44.644	2.099	0.000	0.000	0.077	0.010	0.000	0.000	0.000	0.000	0.020	0.000	0.028	50.864	97.819
PY114-09	0.000	0.000	0.064	0.063	44.587	1.482	0.001	0.000	0.034	0.057	0.004	0.000	0.000	0.178	0.024	0.024	0.000	51.286	97.804
PY114-10	0.000	0.118	0.053	0.050	45.525	1.567	0.108	0.008	0.000	0.000	0.000	0.000	0.000	0.079	0.000	0.000	0.010	51.856	99.374
PY114-11	0.000	0.000	0.131	0.063	45.493	1.585	0.021	0.000	0.000	0.069	0.000	0.000	0.000	0.215	0.027	0.000	0.000	51.854	99.458
PY114-12	0.000	0.019	0.089	0.132	45.944	1.342	0.004	0.036	0.040	0.040	0.151	0.000	0.000	0.272	0.000	0.027	0.009	52.337	100.442
PY114-13	0.000	0.000	0.000	0.000	44.642	1.966	0.032	0.000	0.013	0.069	0.000	0.000	0.000	0.131	0.005	0.000	0.137	50.345	97.340
PY114-14	0.000	0.194	0.000	0.076	44.632	2.463	0.047	0.065	0.000	0.020	0.031	0.000	0.000	0.074	0.041	0.029	0.087	50.514	98.273
PY114-15	0.000	0.025	0.022	0.000	45.357	2.009	0.000	0.000	0.003	0.061	0.066	0.000	0.000	0.157	0.024	0.000	0.047	51.470	99.241
PY160-05	0.000	0.000	0.102	0.138	43.200	4.227	0.000	0.049	0.017	0.000	0.000	0.000	0.000	0.230	0.014	0.012	0.010	51.146	99.145
PY160-06	0.000	0.019	0.066	0.032	42.883	5.899	0.000	0.034	0.035	0.000	0.000	0.000	0.000	0.195	0.064	0.016	0.015	50.483	99.741
PY160-07	0.000	0.000	0.025	0.025	46.166	0.236	0.004	0.008	0.000	0.057	0.000	0.000	0.000	0.088	0.000	0.012	0.000	53.616	100.237
PY160-08	0.000	0.024	0.044	0.000	45.750	0.384	0.012	0.013	0.042	0.000	0.058	0.000	0.000	0.051	0.008	0.000	0.000	53.924	100.313
PY160-09	0.000	0.000	0.036	0.062	45.497	1.013	0.000	0.000	0.005	0.010	0.000	0.000	0.000	0.000	0.072	0.020	0.004	53.516	100.235
PY160-10	0.022	0.049	0.097	0.000	44.337	0.592	0.000	0.039	0.000	0.000	0.054	0.000	0.000	0.211	0.000	0.003	0.083	52.281	97.768
PY160-11	0.000	0.006	0.144	0.106	44.519	2.414	0.126	0.000	0.000	0.000	0.058	0.000	0.000	0.021	0.000	0.000	0.154	51.966	99.514
PY160-12	0.000	0.000	0.017	0.000	45.241	1.757	0.034	0.000	0.091	0.049	0.011	0.000	0.000	0.182	0.081	0.000	0.200	51.521	99.184
PY160-13	0.000	0.000	0.000	0.105	45.235	1.516	0.034	0.013	0.036	0.104	0.000	0.000	0.000	0.197	0.000	0.000	0.011	53.113	100.364
PY160-14	0.000	0.000	0.083	0.000	45.818	0.514	0.000	0.000	0.000	0.000	0.000	0.000	0.000	0.330	0.039	0.000	0.000	53.633	100.417
PY160-15	0.000	0.031	0.061	0.142	46.229	0.327	0.056	0.000	0.012	0.000	0.042	0.000	0.000	0.077	0.000	0.030	0.004	53.654	100.565
PY160-4	0.000	0.176	0.207	0.133	42.691	5.122	0.039	0.000	0.065	0.000	0.000	0.000	0.000	0.105	0.029	0.000	0.000	49.712	98.279
PY178-04	0.474	0.019	0.063	0.000	42.807	6.671	0.072	0.000	0.047	0.000	0.073	0.000	0.000	0.074	0.036	0.037	0.000	49.701	100.074
PY178-05	0.362	0.000	0.149	0.051	43.506	4.424	0.129	0.006	0.016	0.006	0.077	0.000	0.000	0.058	0.109	0.000	0.004	50.670	99.567
PY178-06	0.000	0.000	0.061	0.123	46.101	0.091	0.076	0.000	0.018	0.065	0.000	0.000	0.000	0.000	0.028	0.012	0.000	53.630	100.205
PY178-10	0.022	0.055	0.000	0.000	45.075	0.119	0.000	0.000	0.000	0.000	0.081	0.000	0.000	0.088	0.000	0.013	0.512	52.914	98.879
PY178-11	0.014	0.031	0.000	0.000	45.260	0.094	0.033	0.000	0.014	0.067	0.000	0.000	0.000	0.216	0.044	0.013	0.340	53.151	99.277
PY178-12	0.002	0.116	0.011	0.012	44.853	0.131	0.000	0.018	0.078	0.035	0.000	0.000	0.000	0.304	0.000	0.034	0.191	53.146	98.931
PY193-04	7.246	0.000	0.260	0.000	36.569	6.496	0.396	0.000	0.084	0.000	0.036	0.000	0.000	0.107	0.000	0.041	0.074	47.296	98.607
PY193-05	19.330	0.067	0.090	0.000	25.615	9.715	1.589	0.336	0.076	0.000	0.004	0.000	0.000	0.100	0.000	0.017	0.006	41.837	98.790
PY193-06	0.501	0.137	0.000	0.000	42.970	3.687	0.057	0.045	0.037	0.000	0.062	0.000	0.000	0.000	0.000	0.007	0.000	51.907	99.410
PY193-07	4.672	0.000	0.237	0.000	37.649	6.223	0.323	0.000	0.067	0.086	0.000	0.000	0.000	0.101	0.084	0.034	0.020	48.183	97.679
PY193-08	4.792	0.000	0.149	0.026	36.398	7.063	0.406	0.039	0.079	0.016	0.000	0.000	0.000	0.160	0.000	0.019	0.014	46.863	96.024
PY193-12	9.481	0.000	0.248	0.035	26.513	13.433	0.889	0.040	0.142	0.000	0.052	0.000	0.000	0.174	0.061	0.000	0.226	35.010	86.304
PY193-13	0.080	0.000	0.072	0.000	44.347	1.292	0.058	0.047	0.039	0.065	0.000	0.016	0.000	0.155	0.014	0.019	0.016	52.384	98.604
PY193-14	0.456	0.000	0.072	0.000	42.367	3.808	0.123	0.029	0.019	0.000	0.000	0.000	0.000	0.105	0.000	0.000	0.000	49.249	96.228
PY193-15	11.053	0.000	0.181	0.000	25.318	13.677	1.683	0.180	0.153	0.036	0.011	0.000	0.000	0.216	0.000	0.000	0.158	31.105	83.771
PY207-11	0.000	0.019	0.000	0.062	45.415	0.095	0.004	0.000	0.103	0.000	0.082	0.000	0.000	0.115	0.000	0.002	1.008	53.391	100.296
PY207-12	0.000	0.006	0.000	0.000	46.018	0.000	0.073	0.000	0.000	0.040	0.000	0.000	0.000	0.265	0.022	0.006	0.183	53.320	99.933
PY207-13	0.000	0.056	0.050	0.000	45.565	0.079	0.000	0.000	0.038	0.018	0.000	0.000	0.000	0.161	0.039	0.000	0.240	52.206	98.452
PY207-14	0.076	0.000	0.039	0.000	45.637	0.040	0.049	0.077	0.034	0.000	0.062	0.000	0.000	0.166	0.009	0.003	0.206	53.017	99.415
PY207-15	0.000	0.000	0.006	0.012	45.973	0.003	0.000	0.000	0.026	0.050	0.050	0.012	0.000	0.208	0.008	0.016	0.246	52.706	99.316
PY360-01	0.000	0.019	0.020	0.050	44.860	0.110	0.021	0.000	0.086	0.000	0.000	0.000	0.000	0.125	0.042	0.001	0.274	51.696	97.304
PY360-02	0.000	0.000	0.031	0.044	43.022	0.058	0.000	0.000	0.035	0.000	0.000	0.008	0.000	0.213	0.000	0.032	0.419	49.984	93.846
PY360-03	0.059	0.074	0.103	0.000	44.410	0.036	0.065	0.000	0.000	0.004	0.000	0.000	0.000	0.151	0.009	0.049	0.470	51.022	96.472
PY360-04	0.056	0.000	0.109	0.000	43.979	0.106	0.000	0.114	0.008	0.000	0.015	0.000	0.000	0.094	0.000	0.039	1.132	51.497	97.149
PY360-06	0.055	0.000	0.033	0.044	39.955	0.075	0.000	0.026	0.066	0.000	0.042	0.000	0.000	0.047	0.000	0.017	1.393	43.655	85.553

Pyrite/Marcasite

SAMPLE	Cu at%	Hg at%	Ag at%	Au at%	Fe at%	As at%	Zn at%	Sb at%	Se at%	In at%	Cd at%	Ge at%	Pb at%	Bi at%	Te at%	V at%	Mn at%	S at%
MC114-01	0.018	0.000	0.145	0.018	32.973	0.174	0.003	0.000	0.013	0.000	0.000	0.000	0.000	0.008	0.010	0.017	0.024	66.598
MC114-02	0.079	0.035	0.100	0.012	33.266	0.251	0.031	0.000	0.044	0.000	0.005	0.000	0.000	0.050	0.011	0.010	0.000	66.105
MC114-03	0.116	0.000	0.030	0.000	32.995	0.467	0.000	0.000	0.005	0.000	0.013	0.000	0.000	0.057	0.000	0.000	0.003	66.316
MC178-07	0.000	0.029	0.014	0.000	32.596	0.011	0.000	0.000	0.022	0.007	0.000	0.034	0.000	0.015	0.017	0.000	0.120	67.135
MC178-08	0.029	0.000	0.000	0.010	32.783	0.038	0.010	0.004	0.000	0.008	0.000	0.000	0.000	0.042	0.000	0.020	0.043	67.012
MC178-09	0.000	0.000	0.016	0.005	33.006	0.030	0.011	0.014	0.027	0.017	0.016	0.000	0.000	0.019	0.014	0.024	0.017	66.783
MC207-01	0.000	0.000	0.012	0.006	33.625	0.064	0.005	0.002	0.019	0.000	0.000	0.000	0.000	0.018	0.000	0.007	0.039	66.201
MC207-02	0.000	0.005	0.000	0.000	33.245	0.031	0.000	0.009	0.025	0.000	0.000	0.000	0.000	0.062	0.000	0.000	0.053	66.570
MC207-03	0.000	0.038	0.022	0.005	33.684	0.015	0.000	0.000	0.000	0.000	0.000	0.000	0.000	0.026	0.000	0.014	0.101	66.094
MC207-04	0.000	0.015	0.024	0.008	33.304	0.041	0.000	0.000	0.041	0.005	0.019	0.000	0.000	0.041	0.017	0.000	0.100	66.385
MC207-05	0.000	0.009	0.000	0.000	33.486	0.049	0.037	0.000	0.012	0.008	0.000	0.000	0.000	0.044	0.000	0.000	0.069	66.287
MC207-06	0.028	0.002	0.000	0.005	32.754	0.074	0.023	0.018	0.000	0.000	0.000	0.000	0.000	0.045	0.000	0.010	0.526	66.514
MC207-08	0.000	0.020	0.000	0.014	33.394	0.246	0.008	0.000	0.022	0.000	0.000	0.000	0.000	0.034	0.022	0.002	0.178	66.059
MC207-09	0.007	0.017	0.000	0.000	33.530	2.577	0.000	0.000	0.021	0.009	0.014	0.000	0.000	0.060	0.006	0.000	0.372	63.386
MC207-10	0.000	0.000	0.008	0.000	33.109	0.844	0.006	0.009	0.008	0.014	0.000	0.000	0.000	0.047	0.042	0.000	0.089	65.824
PY114-07	0.000	0.000	0.004	0.003	32.798	1.219	0.000	0.000	0.044	0.007	0.000	0.000	0.000	0.012	0.000	0.004	0.003	65.906
PY114-08	0.000	0.000	0.005	0.013	33.086	1.160	0.000	0.000	0.040	0.004	0.000	0.000	0.000	0.000	0.006	0.000	0.021	65.664
PY114-09	0.000	0.000	0.025	0.013	32.974	0.817	0.001	0.000	0.018	0.021	0.001	0.000	0.000	0.035	0.008	0.019	0.000	66.069
PY114-10	0.000	0.024	0.020	0.010	33.175	0.851	0.067	0.003	0.000	0.000	0.000	0.000	0.000	0.015	0.000	0.000	0.007	65.827
PY114-11	0.000	0.000	0.049	0.013	33.156	0.861	0.013	0.000	0.000	0.024	0.000	0.000	0.000	0.042	0.009	0.000	0.000	65.832
PY114-12	0.000	0.004	0.033	0.027	33.183	0.722	0.002	0.012	0.020	0.014	0.054	0.000	0.000	0.052	0.000	0.021	0.007	65.847
PY114-13	0.000	0.000	0.000	0.000	33.302	1.093	0.020	0.000	0.007	0.025	0.000	0.000	0.000	0.026	0.002	0.000	0.104	65.421
PY114-14	0.000	0.040	0.000	0.016	33.112	1.362	0.030	0.022	0.000	0.007	0.011	0.000	0.000	0.015	0.013	0.024	0.066	65.282
PY114-15	0.000	0.005	0.008	0.000	33.181	1.096	0.000	0.000	0.002	0.022	0.024	0.000	0.000	0.031	0.008	0.000	0.035	65.590
PY160-05	0.000	0.000	0.039	0.029	31.844	2.323	0.000	0.017	0.009	0.000	0.000	0.000	0.000	0.045	0.005	0.010	0.007	65.673
PY160-06	0.000	0.004	0.025	0.007	31.666	3.247	0.000	0.012	0.018	0.000	0.000	0.000	0.000	0.038	0.021	0.013	0.011	64.938
PY160-07	0.000	0.000	0.009	0.005	33.016	0.126	0.002	0.003	0.000	0.020	0.000	0.000	0.000	0.017	0.000	0.009	0.000	66.793
PY160-08	0.000	0.005	0.016	0.000	32.657	0.204	0.007	0.005	0.021	0.000	0.021	0.000	0.000	0.010	0.002	0.000	0.000	67.051
PY160-09	0.000	0.000	0.013	0.013	32.596	0.541	0.000	0.000	0.003	0.003	0.000	0.000	0.000	0.000	0.023	0.016	0.003	66.789
PY160-10	0.014	0.010	0.037	0.000	32.572	0.324	0.000	0.013	0.000	0.000	0.020	0.000	0.000	0.041	0.000	0.002	0.062	66.904
PY160-11	0.000	0.001	0.054	0.022	32.437	1.311	0.078	0.000	0.000	0.000	0.021	0.000	0.000	0.004	0.000	0.000	0.114	65.956
PY160-12	0.000	0.000	0.006	0.000	33.091	0.958	0.021	0.000	0.047	0.017	0.004	0.000	0.000	0.036	0.026	0.000	0.149	65.645
PY160-13	0.000	0.000	0.000	0.021	32.522	0.812	0.021	0.004	0.018	0.036	0.000	0.000	0.000	0.038	0.000	0.000	0.008	66.518
PY160-14	0.000	0.000	0.031	0.000	32.780	0.274	0.000	0.000	0.000	0.000	0.000	0.000	0.000	0.063	0.012	0.000	0.000	66.840
PY160-15	0.000	0.006	0.023	0.029	32.985	0.174	0.034	0.000	0.006	0.000	0.015	0.000	0.000	0.015	0.000	0.023	0.003	66.687
PY160-4	0.000	0.037	0.080	0.028	31.998	2.862	0.025	0.000	0.034	0.000	0.000	0.000	0.000	0.021	0.010	0.000	0.000	64.905
PY178-04	0.309	0.004	0.024	0.000	31.705	3.683	0.046	0.000	0.025	0.000	0.027	0.000	0.000	0.015	0.012	0.030	0.000	64.122
PY178-05	0.234	0.000	0.057	0.011	32.058	2.430	0.081	0.002	0.008	0.002	0.028	0.000	0.000	0.011	0.035	0.000	0.003	65.039
PY178-06	0.000	0.000	0.023	0.025	32.979	0.049	0.046	0.000	0.009	0.023	0.000	0.000	0.000	0.000	0.009	0.009	0.000	66.829
PY178-10	0.014	0.011	0.000	0.000	32.670	0.064	0.000	0.000	0.000	0.000	0.029	0.000	0.000	0.017	0.000	0.010	0.377	66.807
PY178-11	0.009	0.006	0.000	0.000	32.692	0.051	0.020	0.000	0.007	0.024	0.000	0.000	0.000	0.042	0.014	0.010	0.250	66.876
PY178-12	0.001	0.023	0.004	0.002	32.510	0.071	0.000	0.006	0.040	0.012	0.000	0.000	0.000	0.059	0.000	0.027	0.141	67.103
PY193-04	4.866	0.000	0.103	0.000	27.944	3.700	0.258	0.000	0.045	0.000	0.014	0.000	0.000	0.022	0.000	0.034	0.057	62.955
PY193-05	13.655	0.015	0.041	0.000	20.589	5.821	1.091	0.124	0.043	0.000	0.002	0.000	0.000	0.021	0.000	0.015	0.005	58.579
PY193-06	0.322	0.028	0.000	0.000	31.422	2.010	0.036	0.015	0.019	0.000	0.023	0.000	0.000	0.000	0.000	0.006	0.000	66.120
PY193-07	3.136	0.000	0.094	0.000	28.754	3.543	0.211	0.000	0.036	0.032	0.000	0.000	0.000	0.021	0.028	0.028	0.016	64.102
PY193-08	3.288	0.000	0.060	0.006	28.414	4.110	0.271	0.014	0.044	0.006	0.000	0.000	0.000	0.033	0.000	0.016	0.011	63.727
PY193-12	7.773	0.000	0.120	0.009	24.735	9.341	0.708	0.017	0.094	0.000	0.024	0.000	0.000	0.043	0.025	0.000	0.214	56.895
PY193-13	0.051	0.000	0.027	0.000	32.395	0.704	0.036	0.016	0.020	0.023	0.000	0.009	0.000	0.030	0.004	0.015	0.012	66.657
PY193-14	0.305	0.000	0.028	0.000	32.196	2.157	0.080	0.010	0.010	0.000	0.000	0.000	0.000	0.021	0.000	0.000	0.000	65.193
PY193-15	9.582	0.000	0.092	0.000	24.975	10.057	1.418	0.081	0.107	0.017	0.005	0.000	0.000	0.057	0.000	0.000	0.158	53.449
PY207-11	0.000	0.004	0.000	0.013	32.512	0.051	0.002	0.000	0.052	0.000	0.029	0.000	0.000	0.022	0.000	0.002	0.734	66.580
PY207-12	0.000	0.001	0.000	0.000	33.046	0.000	0.045	0.000	0.000	0.014	0.000	0.000	0.000	0.051	0.007	0.005	0.134	66.698
PY207-13	0.000	0.011	0.019	0.000	33.272	0.043	0.000	0.000	0.020	0.006	0.000	0.000	0.000	0.031	0.012	0.000	0.178	66.406
PY207-14	0.048	0.000	0.015	0.000	32.951	0.022	0.030	0.026	0.017	0.000	0.022	0.000	0.000	0.032	0.003	0.002	0.151	66.681
PY207-15	0.000	0.000	0.002	0.002	33.266	0.002	0.000	0.000	0.013	0.018	0.018	0.007	0.000	0.040	0.003	0.013	0.181	66.435
PY360-01	0.000	0.004	0.008	0.010	33.123	0.061	0.013	0.000	0.045	0.000	0.000	0.000	0.000	0.025	0.014	0.001	0.206	66.491
PY360-02	0.000	0.000	0.012	0.010	32.913	0.033	0.000	0.000	0.019	0.000	0.000	0.000	0.005	0.000	0.044	0.000	0.027	0.326	66.612
PY360-03	0.039	0.015	0.040	0.000	33.119	0.020	0.054	0.000	0.000	0.011	0.000	0.000	0.000	0.030	0.003	0.040	0.356	66.282
PY360-04	0.036	0.000	0.042	0.000	32.540	0.058	0.000	0.039	0.004	0.000	0.006	0.000	0.000	0.019	0.000	0.032	0.851	66.373
PY360-06	0.000	0.000	0.014	0.011	33.872	0.047	0.000	0.010	0.040	0.000	0.018	0.000	0.000	0.011	0.000	0.016	1.200	64.762

Chalcopyrite

	Cu wt%	Hg wt%	Ag wt%	Au wt%	Fe wt%	Zn wt%	Sb wt%	As wt%	Se wt%	In wt%	Cd wt%	Ge wt%	Pb wt%	Bi wt%	Te wt%	V wt%	Mn wt%	S wt%	Total wt%
CP240	44.877	0.000	0.426	0.000	3.415	3.025	0.244	20.145	0.194	0.043	0.058	0.000	0.000	0.000	0.000	0.000	0.032	27.501	99.960
CP114-04	33.615	0.055	0.016	0.000	29.596	0.029	0.000	0.156	0.000	0.004	0.000	0.090	0.000	0.073	0.031	0.011	0.002	34.667	98.345
CP114-05	33.782	0.253	0.082	0.000	28.850	0.090	0.000	0.267	0.045	0.032	0.059	0.492	0.000	0.107	0.018	0.014	0.023	34.168	98.282
CP114-06	33.960	0.000	0.000	0.014	28.590	0.068	0.017	0.147	0.086	0.000	0.084	0.851	0.000	0.242	0.000	0.027	0.006	34.533	98.625

	Cu at%	Hg at%	Ag at%	Au at%	Fe at%	Zn at%	Sb at%	As at%	Se at%	In at%	Cd at%	Ge at%	Pb at%	Bi at%	Te at%	V at%	Mn at%	S at%
CP240	36.212	0.000	0.203	0.000	3.136	2.372	0.103	13.787	0.126	0.019	0.026	0.000	0.000	0.000	0.000	0.000	0.030	43.985
CP114-04	24.658	0.013	0.007	0.000	24.703	0.021	0.000	0.097	0.000	0.002	0.000	0.058	0.000	0.016	0.011	0.010	0.002	50.404
CP114-05	24.954	0.059	0.036	0.000	24.248	0.065	0.000	0.167	0.027	0.013	0.025	0.318	0.000	0.024	0.007	0.013	0.020	50.026
CP114-06	24.949	0.000	0.000	0.003	23.899	0.049	0.007	0.092	0.051	0.000	0.035	0.547	0.000	0.054	0.000	0.025	0.005	50.285

Sphalerite

	Cu wt%	Hg wt%	Ag wt%	Au wt%	Fe wt%	Zn wt%	Sb wt%	As wt%	Se wt%	In wt%	Cd wt%	Ge wt%	Pb wt%	Bi wt%	Te wt%	V wt%	Mn wt%	S wt%	Total wt%
5160	0.000	0.054	0.117	0.078	0.045	67.089	0.070	0.000	0.094	0.026	0.093	0.000	0.000	0.265	0.038	0.010	0.000	33.312	101.291
SP147-01	0.000	0.075	0.000	0.000	0.057	65.901	0.051	0.000	0.040	0.000	0.246	0.037	0.000	0.043	0.057	0.000	0.012	32.[illegible]	99.181
SP147-02	0.000	0.000	0.066	0.103	0.082	58.081	0.041	0.011	0.000	0.053	0.159	0.000	11.745	0.000	0.000	0.011	0.023	30.[illegible]	100.501
SP147-03	0.043	0.218	0.131	0.039	0.093	66.224	0.027	0.023	0.034	0.019	0.219	0.000	0.000	0.043	0.034	0.007	0.000	32.991	100.145
SP147-03	0.000	0.195	0.000	0.000	0.159	66.032	0.000	0.021	0.000	0.005	0.174	0.000	0.000	0.255	0.000	0.000	0.040	33.244	100.126
SP147-03	0.000	0.000	0.019	0.054	0.287	65.855	0.038	0.141	0.064	0.000	0.034	0.000	0.000	0.073	0.069	0.004	0.015	32.834	99.487
SP147 05	0.000	0.248	0.000	0.054	0.092	65.754	0.000	0.063	0.000	0.027	0.155	0.000	0.000	0.000	0.046	0.000	0.002	32.866	99.307
SP147-06	0.000	0.000	0.098	0.085	0.317	65.042	0.000	0.014	0.080	0.077	0.261	0.000	0.000	0.000	0.002	0.004	0.000	33.250	99.230
SP147-07	0.047	0.000	0.134	0.000	0.999	60.481	0.061	0.135	0.000	0.088	0.259	0.000	2.872	0.269	0.000	0.000	0.032	32.065	97.442
SP147-08	0.103	0.000	0.150	0.000	0.464	64.588	0.008	0.175	0.108	0.000	0.083	0.040	0.000	0.158	0.000	0.000	0.019	33.094	98.990
SP147-09	0.000	0.022	0.000	0.092	0.101	65.342	0.000	0.113	0.057	0.000	0.049	0.000	0.000	0.102	0.042	0.000	0.000	32.983	98.903
SP160-01	0.000	0.018	0.009	0.043	0.118	21.180	0.002	0.000	0.000	0.000	0.085	0.000	60.286	0.010	0.083	0.017	0.016	19.591	101.458
SP160-02	0.045	0.000	0.143	0.000	0.354	62.572	0.000	0.126	0.000	0.000	0.052	0.000	0.341	0.173	0.035	0.005	0.006	32.108	95.960
SP160-03	0.040	0.000	0.134	0.000	0.420	64.290	0.040	0.099	0.042	0.054	0.129	0.000	0.000	0.018	0.000	0.015	0.060	32.266	97.607
SP355-01	0.061	0.045	0.200	0.000	0.254	64.493	0.000	0.138	0.000	0.000	0.038	0.000	0.000	0.000	0.000	0.007	0.000	32.914	98.150
SP355-02	0.000	0.150	0.085	0.000	0.237	64.108	0.037	0.000	0.000	0.015	0.083	0.000	0.000	0.273	0.017	0.003	0.000	32.074	97.082
SP355-03	0.186	0.172	0.469	0.000	0.258	63.680	0.102	0.124	0.034	0.062	0.231	0.000	0.000	0.067	0.051	0.003	0.021	32.472	97.932
SP355-04	0.000	0.000	0.049	0.116	0.265	63.730	0.034	0.049	0.062	0.000	0.205	0.123	0.000	0.182	0.000	0.000	0.000	32.328	97.143
SP355-05	0.085	0.000	0.038	0.000	0.200	63.051	0.003	0.068	0.068	0.039	0.170	0.000	0.000	0.164	0.000	0.000	0.013	31.242	95.141
SP355-06	0.000	0.113	0.093	0.093	0.094	64.581	0.019	0.000	0.000	0.000	0.045	0.000	0.000	0.000	0.000	0.013	0.024	32.596	97.671
SP355-07	0.000	0.000	0.000	0.000	0.027	64.941	0.010	0.000	0.022	0.000	0.227	0.000	0.000	0.194	0.071	0.000	0.000	32.802	98.294
SP355-08	0.005	0.083	0.025	0.000	0.088	64.684	0.051	0.145	0.008	0.000	0.125	0.000	0.000	0.085	0.000	0.000	0.027	32.606	97.932
SP355-09																			

	Cu at%	Hg at%	Ag at%	Au at%	Fe at%	Zn at%	Sb at%	As at%	Se at%	In at%	Cd at%	Ge at%	Pb at%	Bi at%	Te at%	V at%	Mn at%	S at%
5160	0.000	0.013	0.052	0.019	0.039	49.516	0.028	0.000	0.057	0.011	0.040	0.000	0.000	0.061	0.014	0.009	0.000	50.139
SP147-01	0.000	0.018	0.000	0.000	0.050	49.589	0.021	0.000	0.025	0.000	0.108	0.025	0.000	0.010	0.022	0.000	0.011	50.121
SP147-02	0.000	0.000	0.032	0.028	0.078	46.995	0.018	0.008	0.000	0.024	0.075	0.000	2.999	0.000	0.000	0.011	0.022	49.710
SP147-03	0.033	0.053	0.059	0.010	0.081	49.399	0.011	0.015	0.021	0.008	0.095	0.000	0.000	0.010	0.013	0.007	0.000	50.185
SP147-03	0.000	0.047	0.000	0.000	0.139	49.158	0.000	0.014	0.000	0.003	0.075	0.000	0.000	0.059	0.000	0.000	0.035	50.470
SP147-03	0.000	0.000	0.009	0.013	0.252	49.338	0.015	0.092	0.040	0.000	0.015	0.000	0.000	0.017	0.026	0.004	0.013	50.165
SP147-05	0.000	0.051	0.000	0.013	0.081	49.376	0.000	0.041	0.000	0.012	0.068	0.000	0.0[illegible]	0.000	0.018	0.000	0.002	50.329
SP147-06	0.000	0.000	0.044	0.021	0.278	48.689	0.000	0.009	0.050	0.033	0.114	0.000	0.000	0.000	0.001	0.004	0.000	50.758
SP147-07	0.038	0.000	0.063	0.000	0.910	47.049	0.025	0.092	0.000	0.039	0.117	0.000	0.705	0.065	0.000	0.000	0.030	50.867
SP147-08	0.080	0.000	0.068	0.000	0.408	48.482	0.003	0.115	0.067	0.000	0.036	0.027	0.000	0.037	0.000	0.000	0.017	50.660
SP147-09	0.000	0.005	0.000	0.023	0.089	49.134	0.000	0.074	0.035	0.000	0.021	0.000	0.000	0.024	0.016	0.000	0.000	50.578
SP160-01	0.000	0.007	0.007	0.018	0.172	26.325	0.001	0.000	0.000	0.000	0.061	0.000	23.644	0.004	0.053	0.027	0.024	49.657
SP160-02	0.036	0.000	0.067	0.000	0.321	48.531	0.000	0.085	0.000	0.000	0.023	0.000	0.083	0.042	0.014	0.005	0.006	50.785
SP160-03	0.031	0.000	0.062	0.000	0.375	49.058	0.016	0.066	0.027	0.023	0.057	0.000	0.000	0.004	0.000	0.015	0.054	50.210
SP355-01	0.047	0.011	0.092	0.000	0.225	48.762	0.000	0.091	0.000	0.000	0.017	0.000	0.000	0.000	0.000	0.007	0.000	50.749
SP355-02	0.000	0.038	0.040	0.000	0.213	49.288	0.015	0.000	0.000	0.007	0.037	0.000	0.000	0.066	0.007	0.003	0.000	50.288
SP355-03	0.146	0.043	0.217	0.000	0.230	48.547	0.042	0.082	0.021	0.027	0.102	0.000	0.000	0.016	0.020	0.003	0.019	50.484
SP355-04	0.000	0.000	0.023	0.030	0.238	48.860	0.014	0.033	0.039	0.000	0.091	0.085	0.000	0.044	0.000	0.000	0.000	50.544
SP355-05	0.069	0.000	0.018	0.000	0.184	49.486	0.001	0.047	0.044	0.017	0.078	0.000	0.000	0.040	0.000	0.000	0.012	50.004
SP355-06	0.000	0.028	0.043	0.023	0.084	49.160	0.008	0.000	0.000	0.000	0.020	0.000	0.000	0.000	0.000	0.013	0.022	50.600
SP355-07	0.000	0.000	0.00[illegible]	0.000	0.024	49.154	0.004	0.000	0.014	0.000	0.100	0.000	0.000	0.046	0.028	0.000	0.000	50.631
SP355-08	0.004	0.021	0.012	0.000	0.078	49.145	0.021	0.096	0.005	0.000	0.055	0.000	0.000	0.020	0.000	0.000	0.024	50.519
SP355-09																		

Tennantite

	Cu wt%	Hg wt%	Ag wt%	Au wt%	Fe wt%	Zn wt%	Sb wt%	As wt%	Se wt%	In wt%	Cd wt%	Ge wt%	Pb wt%	Bi wt%	Te wt%	V wt%	Mn wt%	S wt%	Total wt%
TN178-01	43.487	0.000	0.150	0.047	3.654	3.872	0.305	20.115	0.145	0.071	0.015	0.000	0.000	0.060	0.075	0.000	0.018	28.467	100.481
TN178-02	43.722	0.023	0.247	0.000	4.472	3.064	0.232	20.439	0.162	0.000	0.000	0.031	0.000	0.024	0.000	0.000	0.000	28.670	101.086
TN178-03	43.313	0.067	0.121	0.015	4.126	3.646	0.408	20.205	0.125	0.024	0.160	0.000	0.000	0.145	0.064	0.024	0.000	28.734	101.177
TN193-01	44.405	0.000	0.042	0.077	4.571	1.809	0.069	20.325	0.134	0.011	0.000	0.000	0.000	0.060	0.000	0.000	0.010	28.917	100.430
TN193-02	44.111	0.157	0.187	0.000	4.648	1.874	0.054	20.386	0.012	0.034	0.000	0.000	0.000	0.000	0.000	0.007	0.000	28.568	100.038
TN193-03	44.126	0.000	0.058	0.000	4.722	1.958	0.043	20.743	0.158	0.024	0.095	0.000	0.000	0.078	0.000	0.010	0.000	28.802	100.817
TN193-09	43.127	0.060	0.105	0.000	4.754	3.351	0.160	19.923	0.117	0.073	0.000	0.000	0.000	0.145	0.043	0.006	0.000	28.763	100.627
TN193-10	43.904	0.037	0.155	0.000	3.986	3.214	0.122	20.335	0.086	0.026	0.110	0.000	0.000	0.151	0.000	0.015	0.034	28.873	101.048
TN193-11	43.907	0.000	0.071	0.000	4.043	2.992	0.105	20.462	0.121	0.000	0.153	0.000	0.000	0.127	0.019	0.004	0.046	28.570	100.620
5193	44.298	0.000	0.018	0.087	4.379	1.953	0.005	21.038	0.093	0.000	0.055	0.000	0.000	0.096	0.035	0.008	0.016	28.667	100.748
5193	44.293	0.041	0.031	0.087	4.413	2.498	0.000	20.584	0.092	0.000	0.084	0.023	0.000	0.193	0.000	0.006	0.038	28.928	101.311
5193	44.489	0.130	0.164	0.065	4.313	2.227	0.095	20.932	0.102	0.007	0.000	0.000	0.000	0.119	0.059	0.027	0.068	28.736	101.535
5193	44.410	0.000	0.232	0.000	4.081	2.645	3.041	18.596	0.047	0.047	0.069	0.009	0.000	0.107	0.003	0.000	0.028	28.508	101.823
5160	35.358	0.000	5.920	0.000	3.839	8.265	0.059	19.981	0.043	0.000	0.004	0.000	0.000	0.039	0.116	0.012	0.040	28.884	102.560

	Cu at. %	Hg at. %	Ag at. %	Au at. %	Fe at. %	Zn at. %	Sb at. %	As at. %	Se at. %	In at. %	Cd at. %	Ge at. %	Pb at. %	Bi at. %	Te at. %	V at. %	Mn at. %	S at. %
TN178-01	34.679	0.000	0.070	0.012	3.316	3.001	0.127	13.605	0.093	0.031	0.007	0.000	0.000	0.015	0.030	0.000	0.017	44.997
TN178-02	34.593	0.006	0.115	0.000	4.026	2.356	0.096	13.716	0.103	0.000	0.000	0.021	0.000	0.006	0.000	0.000	0.000	44.962
TN178-03	34.304	0.017	0.056	0.004	3.718	2.807	0.169	13.573	0.080	0.011	0.072	0.000	0.000	0.035	0.025	0.024	0.000	45.107
TN193-01	35.200	0.000	0.020	0.020	4.123	1.394	0.029	13.666	0.085	0.005	0.000	0.000	0.000	0.014	0.000	0.000	0.009	45.435
TN193-02	35.187	0.040	0.088	0.000	4.219	1.453	0.022	13.793	0.008	0.015	0.000	0.000	0.000	0.000	0.000	0.007	0.000	45.169
TN193-03	34.918	0.000	0.027	0.000	4.252	1.506	0.018	13.922	0.101	0.011	0.042	0.000	0.000	0.019	0.000	0.010	0.000	45.175
TN193-09	34.208	0.015	0.049	0.000	4.291	2.583	0.066	13.403	0.075	0.032	0.000	0.000	0.000	0.035	0.017	0.006	0.000	45.220
TN193-10	34.719	0.009	0.072	0.000	3.587	2.470	0.050	13.639	0.055	0.011	0.049	0.000	0.000	0.036	0.000	0.015	0.031	45.256
TN193-11	34.906	0.000	0.033	0.000	3.657	2.312	0.044	13.797	0.077	0.000	0.069	0.000	0.000	0.031	0.008	0.004	0.042	45.020
5193	35.139	0.000	0.008	0.022	3.952	1.506	0.002	14.154	0.059	0.000	0.025	0.000	0.000	0.023	0.014	0.008	0.015	45.072
5193	34.918	0.010	0.014	0.022	3.959	1.914	0.000	13.763	0.058	0.000	0.037	0.016	0.000	0.046	0.000	0.006	0.035	45.201
5193	35.100	0.032	0.076	0.017	3.872	1.708	0.039	14.007	0.065	0.003	0.000	0.000	0.000	0.029	0.023	0.027	0.062	44.941
5193	35.301	0.000	0.109	0.000	3.691	2.044	1.262	12.537	0.030	0.021	0.031	0.006	0.000	0.026	0.001	0.000	0.026	44.916
5160	28.142	0.000	2.776	0.000	3.477	6.394	0.025	13.488	0.028	0.000	0.002	0.000	0.000	0.009	0.046	0.012	0.037	45.566

Rammelsbergite

	Fe	S	Co	As	Ni	Sb	Se	Total
	wt%	wt%	wt%	wt%	wt%	wt%	wt%	wt%
5193-1	0.964	2.094	0.763	69.769	26.986	0.026	0.322	100.924
5193-2	0.876	5.706	2.964	64.144	25.873	0.053	0.228	99.826
5193-3	0.718	2.417	0.846	68.622	27.121	0.000	0.251	99.975
5193-4	2.336	7.631	2.406	60.628	25.223	0.059	0.073	98.356
5193-5	0.842	4.177	1.922	66.117	26.549	0.000	0.240	99.847
5193-6	0.382	4.236	1.915	65.769	26.300	0.000	0.195	98.797

	Fe	S	Co	As	Ni	Sb	Se
	at.%	at.%	at.%	at.%	at.%	at.%	at.%
5193-1	1.158	4.382	0.869	62.469	30.835	0.014	0.274
5193-2	1.016	11.527	3.238	55.458	28.546	0.028	0.187
5193-3	0.867	5.081	0.967	61.734	31.136	0.000	0.214
5193-4	2.679	15.248	2.616	51.842	27.524	0.031	0.060
5193-5	0.995	8.595	2.152	58.223	29.834	0.000	0.201
5193-6	0.456	8.808	2.167	58.533	29.870	0.000	0.165